iScience

CellPress
OPEN ACCESS

Article

[Pd(NHC)(μ-Cl)Cl]$_2$: Versatile and Highly Reactive Complexes for Cross-Coupling Reactions that Avoid Formation of Inactive Pd(I) Off-Cycle Products

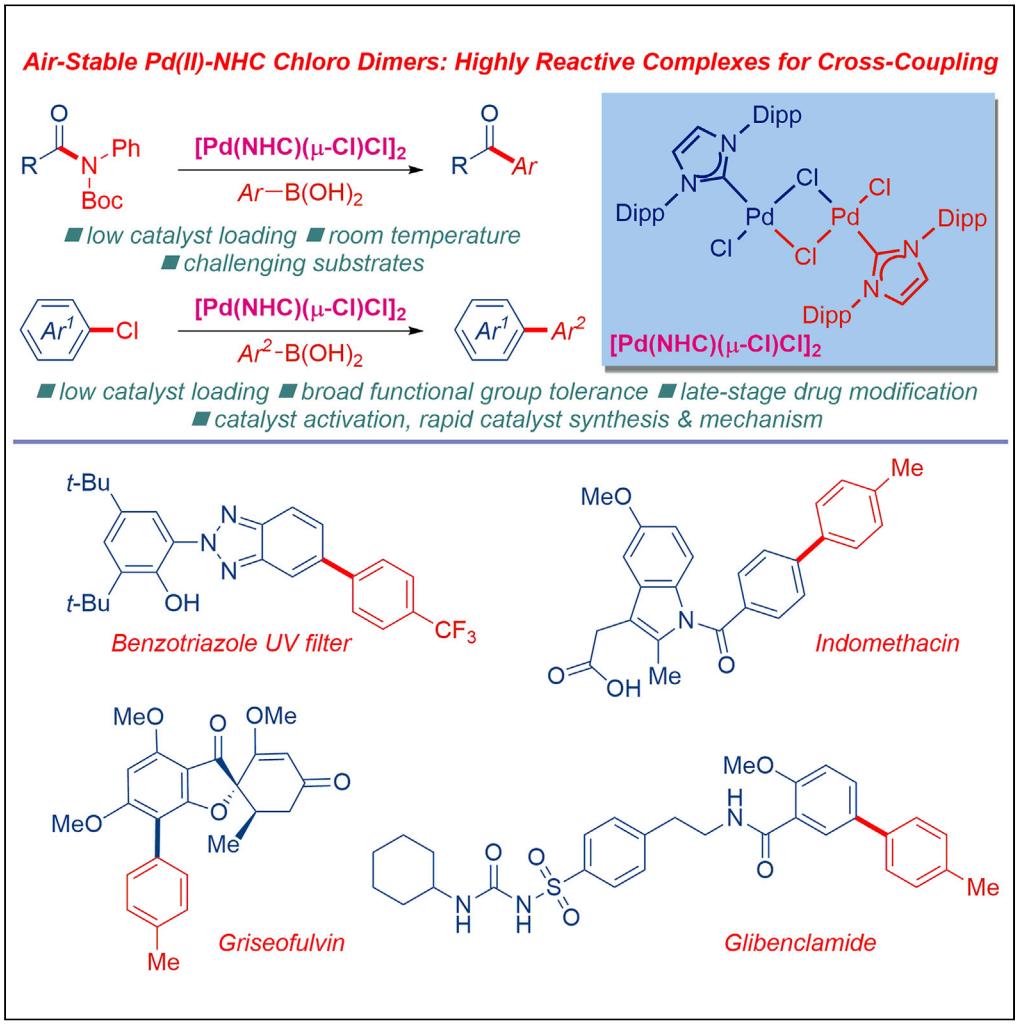

Tongliang Zhou, Siyue Ma, Fady Nahra, ..., Catherine S.J. Cazin, Steven P. Nolan, Michal Szostak

albert.poater@udg.edu (A.P.)
steven.nolan@ugent.be (S.P.N.)
michal.szostak@rutgers.edu (M.S.)

HIGHLIGHTS

Highly reactive, air-stable Pd^{II}–NHC chloro-dimer catalysts for cross-coupling reactions

Broad substrate scope, excellent functional group tolerance, and chemoselectivity

Rapid one-step catalyst synthesis and facile catalyst activation

DFT studies provide key insights into Pd^{II}–NHC chloro-dimer activation pathway

Zhou et al., iScience *23*, 101377
August 21, 2020
https://doi.org/10.1016/j.isci.2020.101377

iScience

CellPress
OPEN ACCESS

Article

[Pd(NHC)(μ-Cl)Cl]$_2$: Versatile and Highly Reactive Complexes for Cross-Coupling Reactions that Avoid Formation of Inactive Pd(I) Off-Cycle Products

Tongliang Zhou,[1] Siyue Ma,[1] Fady Nahra,[2,3] Alan M.C. Obled,[4] Albert Poater,[5,*] Luigi Cavallo,[6] Catherine S.J. Cazin,[2] Steven P. Nolan,[2,*] and Michal Szostak[1,7,*]

SUMMARY

The development of more reactive, general, easily accessible, and readily available Pd(II)–NHC precatalysts remains a key challenge in homogeneous catalysis. In this study, we establish air-stable NHC–Pd(II) chloro-dimers, [Pd(NHC)(μ-Cl)Cl]$_2$, as the most reactive Pd(II)–NHC catalysts developed to date. Most crucially, compared with [Pd(NHC)(allyl)Cl] complexes, replacement of the allyl throw-away ligand with chloride allows for a more facile activation step, while effectively preventing the formation of off-cycle [Pd$_2$(μ-allyl)(μ-Cl)(NHC)$_2$] products. The utility is demonstrated via broad compatibility with amide cross-coupling, Suzuki cross-coupling, and the direct, late-stage functionalization of pharmaceuticals. Computational studies provide key insight into the NHC–Pd(II) chloro-dimer activation pathway. A facile synthesis of NHC–Pd(II) chloro-dimers in one-pot from NHC salts is reported. Considering the tremendous utility of Pd-catalyzed cross-coupling reactions and the overwhelming success of [Pd(NHC)(allyl)Cl] precatalysts, we believe that NHC–Pd(II) chloro-dimers, [Pd(NHC)(μ-Cl)Cl]$_2$, should be considered as go-to precatalysts of choice in cross-coupling processes.

INTRODUCTION

Palladium-catalyzed cross-coupling reactions are among the most powerful molecular assembly tools in chemistry by enabling facile construction of C–C and C–heteroatom bonds (Molander et al., 2013; Colacot, 2015; Diez-Gonzalez et al., 2009). Tremendous advances have been achieved through the discovery of tailor-made ligands that facilitate challenging oxidative addition and reductive elimination elementary steps (Fortman and Nolan, 2011; Martin and Buchwald, 2008). The Pd-catalyzed Suzuki-Miyaura reaction now ranks as the most frequently executed catalytic transformation in production of pharmaceuticals, with numerous commercial syntheses of drugs singularly relying on this bond forming technology (Blakemore et al., 2018). Mechanistically, it is now established that achieving high activity of Pd catalysts involves the formation of monoligated Pd(0) species (Christmann and Vilar, 2005). As a result, the development of well-defined Pd(0) and Pd(II) precatalysts, wherein Pd and ligand are in a 1:1 ratio, represents a major direction in catalyst design (Molander et al., 2013; Colacot, 2015; Diez-Gonzalez et al., 2009; Fortman and Nolan, 2011; Martin and Buchwald, 2008). In this context, commercially available [Pd(NHC)(allyl)Cl] (NHC = N-heterocyclic carbene) complexes developed by one of us (S.P.N.) are among the most powerful and widely used Pd catalysts for various cross-coupling reactions worldwide (Marion et al., 2006; Hopkinson et al., 2014; Nolan and Cazin, 2017); however, their reactivity is limited by the formation of off-cycle Pd(I) allyl products (Figures 1A and 1B) (Hruszkewycz et al., 2014; Melvin et al., 2015; Johansson Seechurn et al., 2017).

The [Pd(NHC)(allyl)Cl] complexes were first introduced in 2002 (Marion et al., 2006; Viciu et al., 2002a, 2002b). The proposed activation pathway involved a nucleophilic addition to the allyl or the halide displacement with an alkoxide and reductive elimination to give the active NHC–Pd(0) species. In 2006, it was established that addition of bulky substituents at the 1-position of the allyl ligands, such as cinnamyl or prenyl, resulted in a dramatic increase of catalyst efficiency (Marion et al., 2006). In the meantime, [Pd(NHC)(cin)Cl] (cin = cinnamyl) complexes complexes have become a commercially available class of

[1]Department of Chemistry, Rutgers University, 73 Warren Street, Newark, NJ 07102, USA

[2]Department of Chemistry and Center for Sustainable Chemistry, Ghent University, Krijgslaan 281, S-3, 9000 Ghent, Belgium

[3]Separation and Conversion Technology Unit, VITO (Flemish Institute for Technological Research), Boeretang 200, 2400 Mol, Belgium

[4]EaStCHEM School of Chemistry, University of St Andrews, St Andrews, KY16 9ST, UK

[5]Institut de Química Computacional i Catàlisi and Departament de Química, Universitat de Girona, c/ Maria Aurèlia Capmany 69, Campus Montilivi, 17003 Girona, Catalonia, Spain

[6]King Abdullah University of Science & Technology, KAUST Catalysis Center (KCC), 23955-6900 Thuwal, Saudi Arabia

[7]Lead Contact

*Correspondence: albert.poater@udg.edu (A.P.), steven.nolan@ugent.be (S.P.N.), michal.szostak@rutgers.edu (M.S.)

https://doi.org/10.1016/j.isci.2020.101377

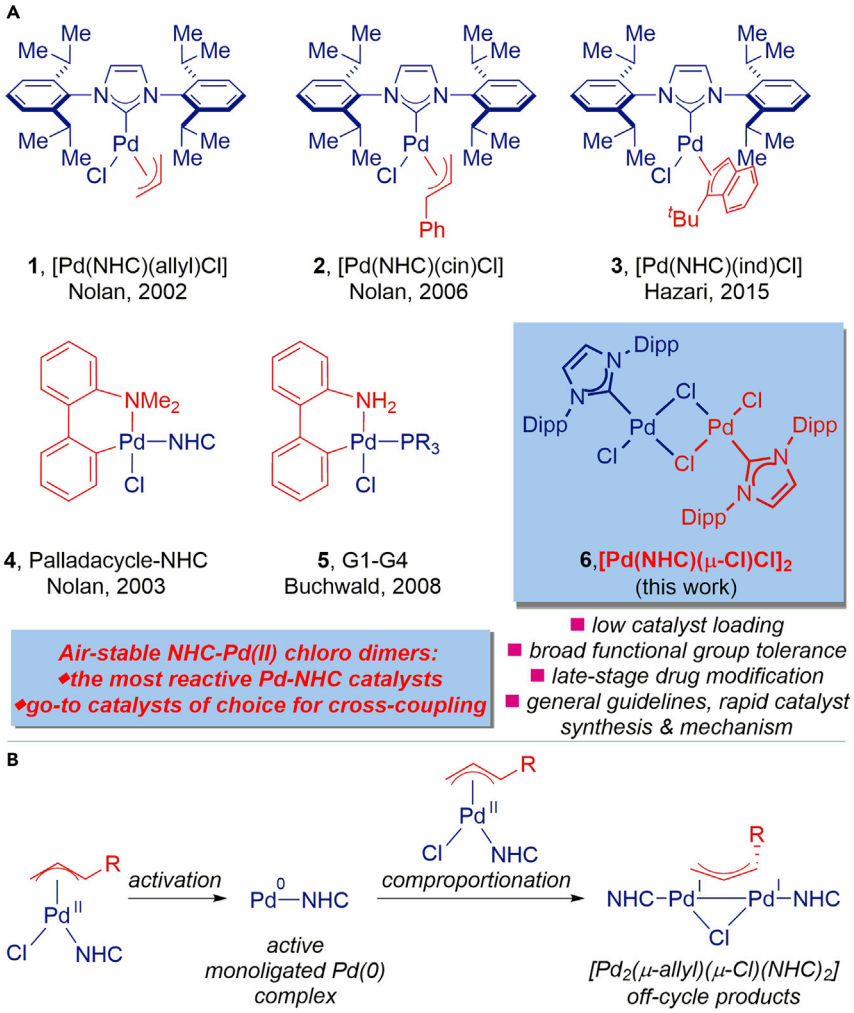

Figure 1. Pd–NHC Complexes in Cross-Coupling

(A) Structures of well-defined Pd(II) precatalysts.

(B) Comproportionation mechanism.

Pd catalysts of choice for cross-coupling reactions. The use of NHC ancillary ligands expedites the reaction development owing to the strong σ-donating properties of NHC ligands cf. phosphines (Martin and Buchwald, 2008; Marion et al., 2006; Hopkinson et al., 2014; Nolan and Cazin, 2017). These [Pd(NHC)(allyl)Cl] catalysts are now available in several forms from various suppliers, facilitating challenging C–C and C–heteroatom cross-couplings worldwide. It should also be noted that, in addition to Pd(II)–NHC precatalysts bearing highly effective allyl-type or palladacycle-type throw-away ligands (Figure 1A), heteroatom donors, including the PEPPSI-class of catalysts, have attracted considerable attention (Chart 1) (Nolan and Cazin, 2017; O'Brien et al., 2006).

In 2014, it was identified that the formation of inactive [Pd_2(μ-allyl)(μ-Cl)$(NHC)_2$] dimers during the activation of [Pd(NHC)(allyl)Cl] complexes takes place (Figure 1B) (Hruszkewycz et al., 2014). It was established that the monoligated NHC–Pd(0) species undergoes comproportionation with [Pd(NHC)(allyl)Cl] monomers to give the inactive allyl-bridged Pd(I) dimers, [Pd_2(μ-allyl)(μ-Cl)$(NHC)_2$]. The extent of formation of this inactive dipalladium complex is dependent on the presence of substituents at the allylic terminal position. Thus, allyl-type complexes bearing sterically bulky *t*-Bu-indenyl ligand, [Pd(NHC)(1-*t*-Bu-ind)Cl], showed high reactivity by suppressing the formation of the inactive Pd(I) allyl products (Melvin et al., 2015). However, this class of catalysts still relies on catalyst activation by allyl displacement (cf. dissociation),

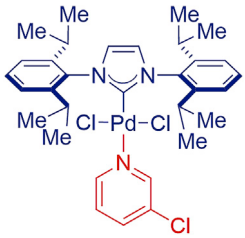

Chart 1. Structure of Pd-PEPPSI-IPr (10)

multi-step synthesis, and the introduction of waste-generating throw-away allyl ligand, which is less than desirable from the activation-, reactivity-, atom-, step-, and cost-economy perspective.

Over the past years, we have introduced Pd–NHC complexes for the cross-coupling of amides through oxidative addition of N–C(O) bonds, which is also instrumental for the cross-coupling of bench-stable esters via acyl-metals from common amides and esters (Shi et al., 2018). In the context, we have studied Pd–NHC complexes with various throw-away ligands (M.S.) (Lei et al., 2017).

In this study, we establish air-stable NHC–Pd(II) chloro dimers, $[Pd(NHC)(\mu\text{-}Cl)Cl]_2$, as the most reactive Pd(II)–NHC catalysts developed to date. Most crucially, compared with [Pd(NHC)(allyl)Cl] complexes, replacement of the allyl throw-away ligand with chloride allows for a more facile activation step, while effectively preventing the formation of off-cycle $[Pd_2(\mu\text{-allyl})(\mu\text{-}Cl)(NHC)_2]$ products. These catalysts are highly reactive, easy to prepare, readily activated to Pd(0)–NHC by dimer dissociation (cf. allyl displacement), and avoid cost- and waste-generating allyl ligands. The utility of this class of catalysts is demonstrated via broad compatibility with privileged biaryls and the direct, late-stage functionalization of common pharmaceuticals. Extensive computational studies provide key insight into the NHC–Pd(II) chloro dimer activation pathway. With the goal of providing increasingly practical technologies, a facile synthesis of NHC–Pd(II) chloro dimers in one-pot from NHC salts is reported. Considering the tremendous utility of Pd-catalyzed cross-coupling reactions in chemical synthesis and the overwhelming success of [Pd(NHC)(allyl)Cl] precatalysts, we believe that NHC–Pd(II) chloro dimers, $[Pd(NHC)(\mu\text{-}Cl)Cl]_2$, should be considered as go-to precatalysts of choice in cross-coupling processes.

Results and Discussion

Catalytic Studies

Our investigation of the reactivity of NHC–Pd(II) chloro dimers, $[Pd(NHC)(\mu\text{-}Cl)Cl]_2$, was initiated by evaluating the reactivity of a model IPr-based catalyst (IPr = 1,3-bis(2,6-diisopropylphenyl)imidazol-2-ylidene) in the cross-coupling of amide **7** with boronic acids. Somewhat ironically, it is worth noting that the $[Pd(IPr)(\mu\text{-}Cl)Cl]_2$ catalyst was first reported by one of us (S.P.N.) in 2002; however, at that point the focus was aimed at the seemingly more reactive [Pd(NHC)(allyl)Cl] complexes (Viciu et al., 2002a, 2002b; Navarro et al., 2003). Now, after nearly 20 years in catalyst development (Marion et al., 2006; Shi et al., 2018), we hypothesized that $[Pd(NHC)(\mu\text{-}Cl)Cl]_2$ complexes might be of great benefit in cross-coupling reactions owing to facile activation and elimination of the off-cycle products in the absence of problematic allyl throw-away ligands.

Selected optimization results are summarized in Table 1. Full optimization results are presented in the Supplemental Information. After preliminary experiments, we found that the desired cross-coupling occurred in >98% yield at 0.25 mol% catalyst loading under very mild room temperature conditions (Table 1, entry 3). Furthermore, the reaction could be successfully performed at 0.050–0.025 mol% catalyst loading (>95% conversion) by increasing the temperature to 40°C (Table 1, entries 7 and 8).

At this point, kinetic profiling studies were conducted to gain insight into the reaction and compare the reactivity of $[Pd(IPr)(\mu\text{-}Cl)Cl]_2$ with other classes of Pd(II)–NHC catalysts (Figure 2). Crucially, in kinetic profiling studies, we found that $[Pd(IPr)(\mu\text{-}Cl)Cl]_2$ (**6**) was a superior catalyst to [Pd(IPr)(cin)Cl] and [Pd(IPr)(1-*t*-Bu-ind)Cl] (Marion et al., 2006; Melvin et al., 2015), whereas the heterocycle-based Pd-PEPSI-IPr (**10**) (O'Brien et al., 2006) (Chart 1) showed the lowest reactivity. It is well known that activation of Pd-PEPPSI-type catalysts is slow (Hopkinson et al., 2014). However, it should also be noted that, in specific cases, the rate of catalyst activation might differ between substrates, including cases when substrate

Entry	Catalyst (mol%)	Boronic Acid (equiv)	Base (equiv)	H_2O (equiv)	Yield[a] (%)
1	1.5	1.2	2.0	0	56
2	1.5	1.2	2.0	5	>98
3	0.25	1.05	1.1	5	>98
4	0.05	1.05	1.1	5	32
5[b]	0.05	2.0	1.1	5	74
6[b,c]	0.05	2.0	3.0	5	85
7[b,d]	0.05	2.0	3.0	5	>98
8[b,d]	0.025	2.0	3.0	5	96

Table 1. Optimization of Pd-Catalyzed Suzuki-Miyaura Cross-Coupling of Amides

Conditions: amide **7a**, PhC(O)–NPh/Boc, (1.0 equiv), catalyst ([Pd(IPr)(μ-Cl)Cl]$_2$) (x mol%), 4-Tol-B(OH)$_2$ (1.05–2.0 equiv), K_2CO_3 (1.1–3.0 equiv), H_2O (0–5 equiv), THF (0.25 M), 23°C, 12 h.

[a]GC/^{1}H NMR yields.

[b]0.50 M.

[c]Toluene.

[d]40°C. See Transparent Methods for full details. IPr, 1,3-bis(2,6-diisopropylphenyl)imidazol-2-ylidene.

activation by nucleophilic addition takes place (Shi et al., 2018). The reaction of amide **7** gave 89% conversion after 4 h using **6** as catalyst, which can be compared with 42% and 25% conversion when using [Pd(IPr)(-cin)Cl] and [Pd(IPr)(1-*t*-Bu-ind)Cl] catalysts. Crucially, initial rates revealed that the NHC–Pd(II) chloro dimer [Pd(IPr)(μ-Cl)Cl]$_2$ catalyst gives 3.1 and 4.2 times faster reaction than the cinnamyl- and *t*-Bu-indenyl-based catalysts.

Our preliminary studies indicate that sterically hindered imidazolylidene and saturated imidazolinylidene ligands perform well as ancillary ligands in [Pd(NHC)(μ-Cl)Cl]$_2$ complexes. As such, two other chloro dimers [Pd(NHC)(μ-Cl)Cl]$_2$ based on SIPr and IPr* NHC ancillary ligands were prepared and evaluated in the cross-coupling of amide **7** with 4-Tol-B(OH)$_2$ (see Scheme S1). The reactivity of saturated imidazolinylidene-based catalyst SIPr (SIPr = 1,3-bis(2,6-diisopropylphenyl)imidazolidin-2-ylidene) (74% yield) and sterically hindered IPr* (IPr* = 1,3-bis(2,6- bis(diphenylmethyl)4-methylphenyl)imidazol-2-ylidene) (Izquierdo et al., 2014) (24% yield) at 0.050 mol% loading was identified as promising but provided lower yields than **6**. Our ongoing studies are focused on the development of NHC ligands that can be broadly utilized as supporting ligands in cross-coupling reactions.

The substrate scope of amide bond cross-coupling using the NHC–Pd(II) chloro dimer [Pd(IPr)(μ-Cl)Cl]$_2$ **6** was briefly investigated (Scheme 1). As such, the cross-coupling of electronically varied amides and boronic acids, including electrophilic functional groups (**9e**), alkyl amides (**9d**), and deactivated substrates (**9c, 9b'**), could be achieved at room temperature at low catalyst loading in excellent yields. Furthermore, a turnover number (TON) of 14,800 was calculated for the cross-coupling of amide **7a** ([Pd(IPr)(μ-Cl)Cl]$_2$ (**6**), 25 ppm, 4-Tol-B(OH)$_2$, 120°C, 2-MeTHF). The use of 2-MeTHF is preferred for TON determination owing to much better solubility of the base in this solvent (see Scheme S3).

At this stage, we turned our attention to the more synthetically significant biaryl Suzuki-Miayura cross-coupling. Beyond doubt, the biaryl Suzuki-Miyaura synthesis ranks as the most important and powerful C–C bond forming cross-coupling reaction discovered to date (Fyfe and Watson, 2017). The impact of the biaryl Suzuki-Miyaura cross-coupling is clearly illustrated by the change of the shape of bioactive pharmacophores that are now prepared as medicines and scaffolds in drug discovery enabled by the emergence of this cross-coupling technology (Yet, 2018).

Our initial optimization focused on two standard conditions that are routinely applied in the development of Suzuki-Miyaura cross-coupling, namely, the much preferred conditions using weak base (K_2CO_3) and the alternative conditions using strong base (KO*t*-Bu) (see Table S1). Crucially, the NHC–Pd(II) chloro dimer [Pd(IPr)(μ-Cl)Cl]$_2$ **6** promoted the model cross-coupling of 4-chlorotoluene with Ph–B(OH)$_2$ in quantitative yield under both conditions in EtOH as a solvent.

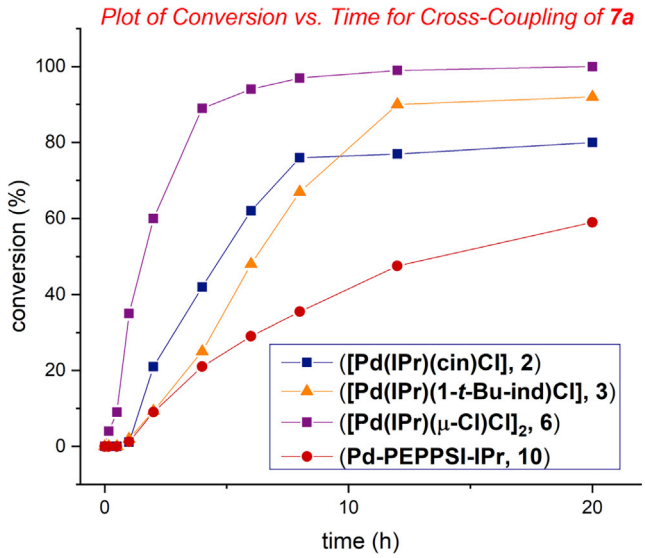

Figure 2. Kinetic Profile of Suzuki-Miyaura Cross-Coupling of Amides

Conditions: **7a** (PhCONBocPh), 4-Tol-B(OH)$_2$ (2.0 equiv), catalyst ([Pd(IPr)(μ-Cl)Cl]$_2$, 0.05 mol%; other catalysts, 0.10 mol %), K_2CO_3 (3.0 equiv), H_2O (5 equiv), toluene (0.50 M), 23°C, 0–20 h.

Next, kinetic profiling studies revealed the NHC–Pd(II) chloro dimer [Pd(IPr)(μ-Cl)Cl]$_2$ **6** is a superior catalyst to [Pd(IPr)(1-*t*-Bu-ind)Cl] under the much preferred mild base conditions using K_2CO_3 (orange triangles versus red triangles, Figure 3) consistent with facile activation by dimer dissociation. Interestingly, the reactivity of **6** is similar to [Pd(IPr)(1-*t*-Bu-ind)Cl] under KO*t*-Bu conditions (green squares versus blue squares, Figure 3). It is also worth noting that K_2CO_3 is the preferred base in case of selected substrates (see Schemes S5 and S6). We have further evaluated the comparative reactivity of the NHC–Pd(II) chloro dimer [Pd(IPr)(μ-Cl)Cl]$_2$ **6** and [Pd(IPr)(1-*t*-Bu-ind)Cl] in the cross-coupling of electron-rich and sterically hindered substrates, wherein **6** also showed better reactivity. Our preliminary studies indicate that [Pd(NHC)(μ-Cl)Cl]$_2$ catalysts are efficient in cross-coupling of sterically hindered 2,6-di-substituted aryl chlorides (see Scheme S6). Our future studies will focus on expanding the scope of reactions enabled by [Pd(NHC)(μ-Cl)Cl]$_2$ catalysts.

With the knowledge that the NHC–Pd(II) chloro dimer [Pd(IPr)(μ-Cl)Cl]$_2$ **6** is a highly effective catalyst operating under mild, synthetically useful conditions, we next investigated the synthetic scope of **6** with a focus on compatibility with privileged biaryls and the direct, late-stage functionalization of common drugs (Schemes 2, 3, and 4).

As outlined in Schemes 2 and 3, the NHC–Pd(II) chloro dimer [Pd(IPr)(μ-Cl)Cl]$_2$ **6** can be deployed successfully with a remarkably broad range of aryl chlorides and boronic acids (Afagh and Yudin, 2010). Most crucially, the highlighted functional groups are among the most commonly encountered in pharmaceuticals and allow for further functionalization by traditional or orthogonal cross-coupling methods (Blakemore et al., 2018). A variety of synthetically useful substituents is tolerated, including nitriles; unprotected hydroxyl; free amines; pyridines; esters; free indoles; triazines; benzofurazans; aldehydes; free carboxylic acids; dioxolanes; polyfluorinated substrates; Boc-protected amines; NH-benzamides; pyridazines; primary, secondary, tertiary amides; sulfonamides; 2,1,3-benzothiadiazoles; pyrazines; bis-heterocycles; pyrimidines; functionalized indoles; benzotriazoles; and pyrroles, enabling the synthesis of privileged biaryl motifs in excellent yields. When aryl chlorides gave lower conversion or are not easily available, aryl bromides could be used successfully.

Furthermore, the NHC–Pd(II) chloro dimer [Pd(IPr)(μ-Cl)Cl]$_2$ **6** could be readily deployed in the direct cross-coupling of densely functionalized pharmaceuticals (Scheme 4), such as Fenofibrate, Haloperidol, Indomethacin, Chlorpromazine, Glibenclamide, Griseofulvin, and Chloroquine, thus clearly demonstrating the potential impact on the synthesis and potential late-stage further derivatization of complex biaryls in

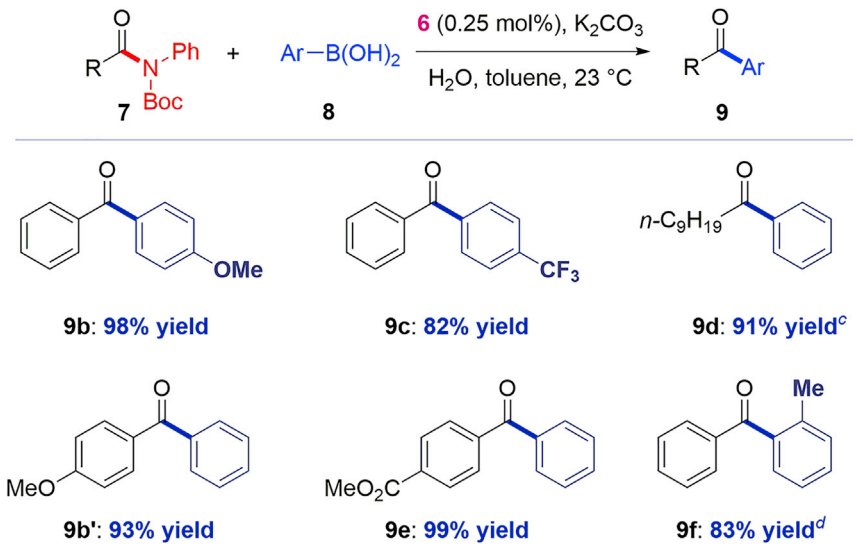

Scheme 1. Scope of Amide Suzuki-Miyaura Cross-Coupling

Conditions: amide (1.0 equiv), Ar-B(OH)$_2$ (2.0 equiv), [Pd(IPr)(μ-Cl)Cl]$_2$, 0.25 mol%, K_2CO_3 (3.0 equiv), H_2O (5 equiv), toluene (1.0 M), 23°C, 12 h. [a]Isolated yields. [b]0.50 mol%. [d][Pd(IPr*)(μ-Cl)Cl]$_2$, 0.25 mol%. See Transparent Methods for details.

pharmaceutical settings. The selected substrates further demonstrate the functional group tolerance with respect to privileged motifs that are broadly present in pharmaceutical development.

Preliminary studies using the NHC–Pd(II) chloro dimer [Pd(IPr)(μ-Cl)Cl]$_2$ **6** indicated that the cross-coupling at 25 ppm catalyst loading is also feasible using K_2CO_3 as a mild carbonate base (see Scheme S7). To our knowledge, these results establish the NHC–Pd(II) chloro dimer [Pd(IPr)(μ-Cl)Cl]$_2$ **6** as the most active Pd(II)–NHC catalysts discovered to date and a major improvement over the overwhelmingly successful [Pd(NHC)(allyl)Cl] catalysts. The use of the commonly available IPr ligand and the commercial availability on large scale (i.e., kg scale) surely make the NHC–Pd(II) chloro dimer [Pd(IPr)(μ-Cl)Cl]$_2$ **6** an attractive tool to be used in small- and larger-scale molecular assembly cross-coupling strategies.

Mechanism Studies

To gain further insight into the reactivity of the palladium halide dimer catalysts, [Pd(NHC)(μ-X)X]$_2$, we prepared the bromo- and iodo-based congeners, [Pd(IPr)(μ-Br)Br]$_2$ and [Pd(IPr)(μ-I)I]$_2$, and evaluated their reactivity in the model Suzuki cross-coupling (see Table S2). The bromo dimer showed slightly lower reactivity than the chloro relative, whereas the iodo dimer was completely unreactive across electronically and sterically differentiated substrates at room temperature; however, moderate conversion was observed at 60°C. This establishes the reactivity order of the halide dimer catalysts: Cl > Br > I, which is consistent with the activation of [Pd(NHC)(μ-X)X]$_2$ halide dimer catalysts to yield the active, monoligated NHC–Pd(0) complex (Fairlamb et al., 2006).

To further understand the high reactivity of **6**, we measured the activation rate to the monoligated IPr–Pd(0) (Scheme 5). The rate was measured in the presence of dvds (dvds = 1,3-divinyl-1,1,3,3-tetramethyldisiloxane) and base (Hruszkewycz et al., 2014). We found that, in a comparison between [Pd(IPr)(allyl)Cl], [Pd(IPr)(cin)Cl], and [Pd(IPr)(μ-Cl)Cl]$_2$ (**6**), the allyl complex is activated the fastest (k_{obs} = 1.1 * 10^{-3} s^{-1}), whereas the chloro dimer (k_{obs} = 7.0 * 10^{-4} s^{-1}) was activated faster than the cinnamyl complex (k_{obs} = 3.0 * 10^{-4} s^{-1}) (see Scheme S8). The absence of an allyl moiety in **6** obviously excludes a decomposition route leading to bridged-allyl dinuclear palladium complexes. The high activation rate of [Pd(IPr)(μ-Cl)Cl]$_2$ is consistent with the excellent activity of this catalyst in cross-coupling.

Computational Analysis of [(IPr)Pd(μ-Cl)Cl]$_2$ Activation

DFT studies (M06/Def2TZVP ~ SDD//BP86-d3(PCM,THF)/SVP ~ SDD) were conducted to gain insight into the exact activation pathway employed by **6** and compare it with those of other classes of air-stable Pd(II)

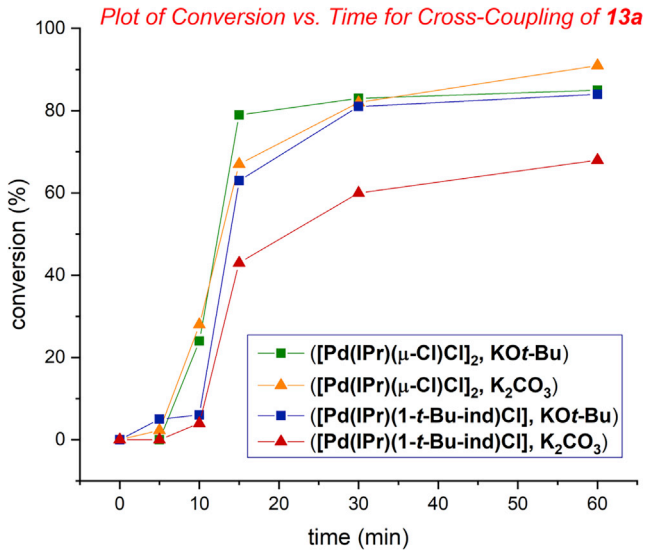

Figure 3. Kinetic Profile of Biaryl Suzuki-Miyaura Cross-Coupling of Aryl Chlorides

Conditions: **13a** (4-Tol-Cl), Ph-B(OH)$_2$ (1.05 equiv), catalyst ([Pd(IPr)(μ-Cl)Cl]$_2$, 0.50 mol%; [Pd(IPr)(1-*t*-Bu-ind)Cl], 1.0 mol%), KO*t*-Bu (1.1 equiv)/K_2CO_3 (2.2 equiv), EtOH (0.50 M), 23°C, 0–1 h.

precatalysts (Data S1, Cartesian coordinates and energies, related to Figure 4). From catalyst **6**, via a barrierless step (checked by a linear transit), the simple cleavage of the dimer requires 17.6 kcal/mol, thus affordable at room temperature. Analyzing the halide that holds together the dimer structure, calculations validated the results found in the reactivity order of the halide dimer catalysts (see Table S2), with higher thermodynamic cost for the dimer cleavage of 2.1 and 10.5 kcal/mol for Br and I, respectively. The latter value is in perfect agreement with experiments and confirms the activity at 60°C and the poorer results at rt. Second, the analysis moved to the different NHC ligands that occupy different space around the metal. The mechanism to activate catalysts **6**, **11**, and **12**, i.e., that leads to the active catalytic Pd(0) species, is included in Figure 4. The computed values for the barrierless dimer cleavage are 17.6 (IPr), 16.8 (SIPr), and 26.5 (IPr*) kcal/mol, thus becoming unfavored for larger NHC ligands (Falivene et al., 2016, 2019). The higher energy cost for the cleavage of **12** is in agreement with experimental results (see Scheme S1), explaining the poor performance of the sterically very encumbered **12** at rt, but much improved activity at more elevated temperatures.

Post dimer cleavage, we envisaged that Ph-B(OH)$_2$ together with the base K_2CO_3 must assist in the displacement/removal of one of the halides and deliver a phenyl ligand. This hypothesis is supported by results in Table 1 where better catalytic performance is obtained with an excess of boronic acid. After the first rearrangement caused by the entering K_2CO_3, the Ph-B(OH)$_2$ bonds to the ionic KCO_3 moiety, and the aryl group on boron is transferred to the palladium in the **e**→**f** step with an energetic cost of 21.7, 22.1, and 22.4 kcal/mol for **6**, **11**, and **12**, respectively, calculated not from intermediate **d**, but **c** as a reference. In the absence of base, the aryl transfer to the metal shows an increase in the energy barrier for **6** of 18.2 kcal/mol. Next, there is the favorable thermodynamic dissociation of the $K_2CO_3ClB(OH)_2$ moiety, followed by a second coordination of a base that in combination of a second Ph-B(OH)$_2$ moiety allows the aryl transfer from boron to palladium (see Figure 5). The kinetic requirement of the latter **j**→**k** step is 23.3, 24.6, and 23.6 kcal/mol for **6**, **11**, and **12**, respectively, calculated from intermediate **i**. In the precatalyst activation sequence, this latter step becomes the rate determining step (rds) for **6** and **11**, whereas for **12** this remains the halide bond cleavage of the dimer. Finally, once the $K_2CO_3ClB(OH)_2$ moiety is released, the two aryl groups bound to palladium eliminate and form biphenyl and yield a Pd(0) species. Alternatively, instead of involving a second equivalent of base, the release of chlorobenzene from the initially formed [Pd(NHC)(Ph)Cl] was studied. This reductive elimination was found to be not kinetically facile, with an energy barrier of 22.4 kcal/mol, together with a thermodynamic cost of 18.1 kcal/mol (see Figure S1). Using the Pd(0) species for the acyl Suzuki-Miyaura cross-coupling of amides by N–C(O) cleavage has been previously shown to involve upper energy barriers of 23.8 and 26.5 kcal/mol for catalysts **6** and **12** (Li et al., 2018), thus mirroring the same trend as in the pre-activation of the corresponding catalysts.

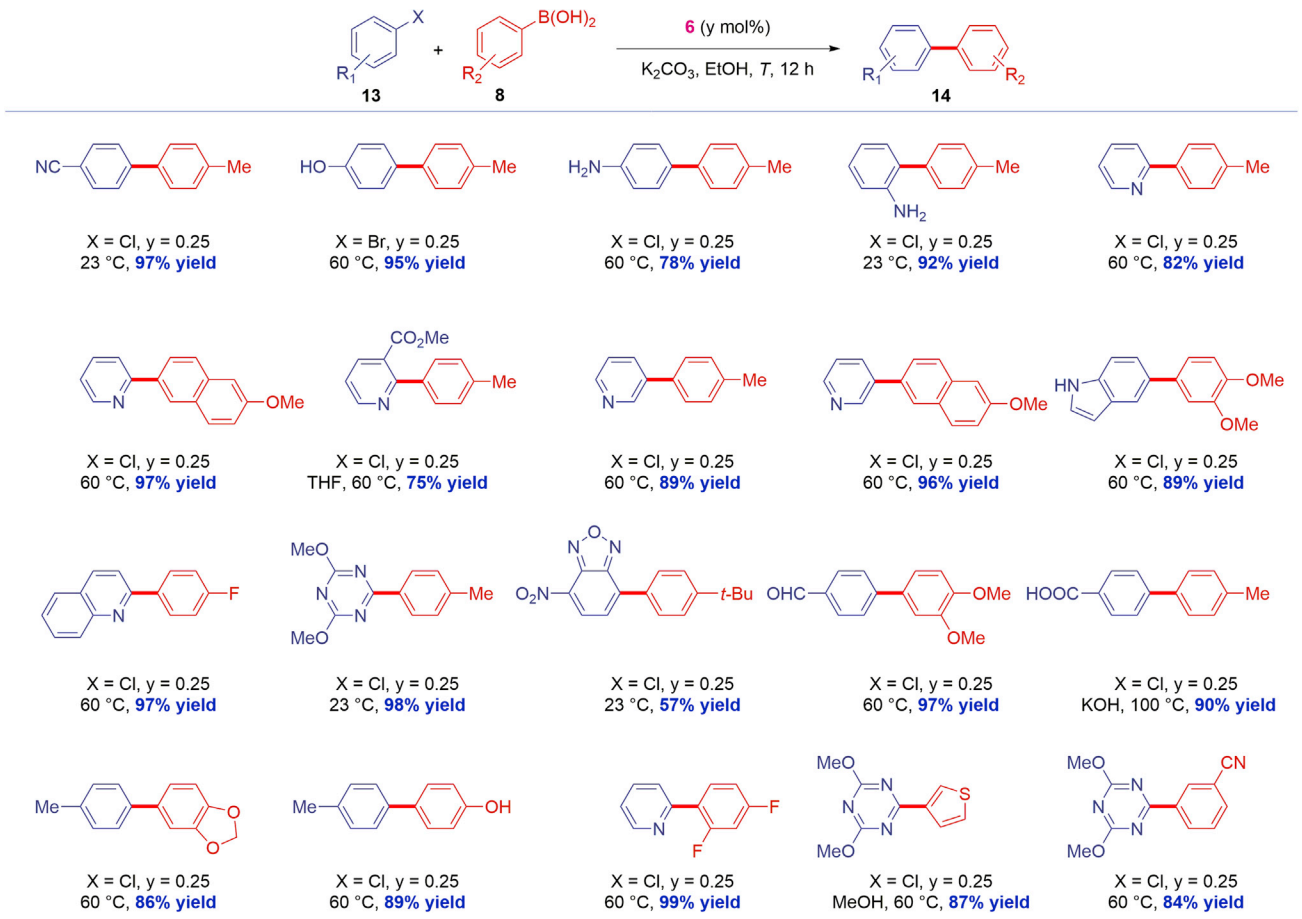

Scheme 2. Scope of Pd-Catalyzed Biaryl Suzuki-Miyaura Cross-Coupling

Conditions: Ar-X (1.0 equiv), Ar-$B(OH)_2$ (2.0 equiv), K_2CO_3 (3.0 equiv), $[Pd(IPr)(\mu\text{-}Cl)Cl]_2$ (**6**) (y mol %), EtOH (0.50 M), 12 h. Isolated yields. See Transparent Methods for details.

We also compared the energetics for the dimeric **6** with those for the monomeric **1** and **2** leading to the Pd(0) species (see Figure S2). Even though the kinetics require just 25.3 and 23.3 kcal/mol for **1** and **2**, respectively, generation of an active species is hindered by the starting metal catalyst since formation of a bridged allyl dipalladium is highly favored by 17.4 and 14.3 kcal/mol. And this forces a kinetic requirement of 30.9 and 27.2 kcal/mol to recover the Pd(0) species. Thus, the catalyst itself with the off-cycle intermediate blocks the formation of the catalytic active species Pd(0) at mild temperature, contrarily to what happens with simple halide bridged catalysts **6**, **11**, and even **12**, studied here. Not having any allyl or substituted allyl supporting ligand appears to represent the simplest solution to avoiding catalyst deactivation.

One-Pot Synthesis of $[Pd(IPr)(\mu\text{-}Cl)Cl]_2$

Our catalytic experiments clearly indicated the excellent activity of the NHC–Pd(II) chloro dimer $[Pd(IPr)(\mu\text{-}Cl)Cl]_2$ **6**. To provide practical synthetic technologies to practitioners, we developed a facile one-pot synthesis of NHC–Pd(II) chloro dimers from NHC salts (Scheme 6). As such, the air-stable NHC–Pd(II) chloro dimer $[Pd(IPr)(\mu\text{-}Cl)Cl]_2$ **6** could be readily prepared both on a small scale (0.11 mmol, ca. 60 mg) or on a preparative gram scale (3.7 mmol, 1.69 g) in 81% yield. The rapid availability of **6** compares very favorably with other Pd(II)–NHC precatalysts (*note that **6** is also already commercially available*) and should provide facile access to this class of catalysts for various cross-coupling technologies as well as for a plethora of other catalytic reactions that require monoligated Pd complexes, including C–H activation and hydrofunctionalization processes (Hopkinson et al., 2014; Nolan and Cazin, 2017).

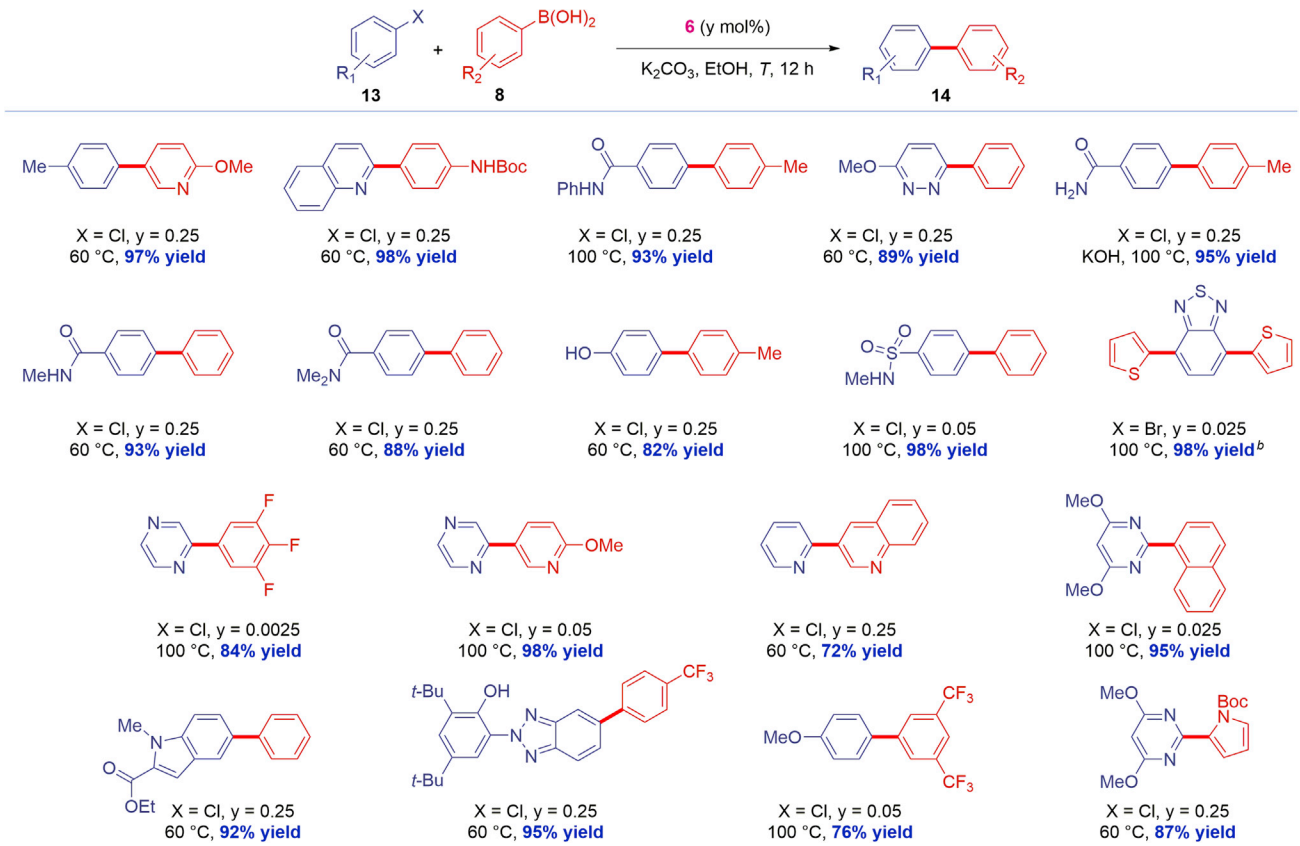

Scheme 3. Scope of Pd-Catalyzed Biaryl Suzuki-Miyaura Cross-Coupling

Conditions: Ar-X (1.0 equiv), Ar-B(OH)$_2$ (2.0 equiv), K_2CO_3 (3.0 equiv), [Pd(IPr)(μ-Cl)Cl]$_2$ (**6**) (y mol %), EtOH (0.50 M), 12 h. Isolated yields. [a]Ar-B(OH)$_2$ (3.0 equiv). See Transparent Methods for details.

Conclusions

In summary, we have established air-stable NHC–Pd(II) chloro dimers, [Pd(NHC)(μ-Cl)Cl]$_2$, as the most reactive Pd(II)–NHC catalysts developed to date. The key feature of this class of catalysts is that replacement of the allyl throw-away ligand from the overwhelmingly successful [Pd(NHC)(allyl)Cl] complexes by a bridging chloride imparts a facile activation by dissociation, prevents the formation of off-cycle allyl products, and eliminates synthetic and economic technological issues associated with allyl ligands. These catalysts are highly reactive, easy to prepare, readily activated to Pd(0)–NHC by dimer dissociation (cf. allyl displacement), and avoid cost- and waste-generating allyl ligands. The utility of this class of catalysts has been demonstrated in the synthesis of privileged biaryls and the direct, late-stage functionalization of pharmaceuticals, showing excellent functional group tolerance and chemoselectivity. Computational studies provided key insight into the NHC–Pd(II) chloro dimer activation pathway and rationalized the superior catalytic performance of the dimer catalysts compared with that of the allyl and substituted-allyl palladium catalysts. Crucially, a facile, one-pot synthesis of NHC–Pd(II) chloro dimers has been developed, thus enabling simple and scalable access to [Pd(NHC)(μ-Cl)Cl]$_2$ complexes. Overall, the scope of the reactions catalyzed by [Pd(NHC)(μ-Cl)Cl]$_2$ complexes supersedes other classes of Pd–NHC catalysts, including activation, rate of cross-coupling of model substrates in different reaction classes, and catalyst synthesis. Our future studies will be focused on expanding the range of transformations mediated by [Pd(NHC)(μ-Cl)Cl]$_2$ complexes.

Considering the tremendous impact of Pd-catalyzed cross-coupling reactions in chemical synthesis and the tremendous success of [Pd(NHC)(allyl)Cl] precatalysts by practitioners worldwide, we believe that NHC–Pd(II) chloro dimers, [Pd(NHC)(μ-Cl)Cl]$_2$, should be routinely considered as go-to precatalysts of choice in cross-

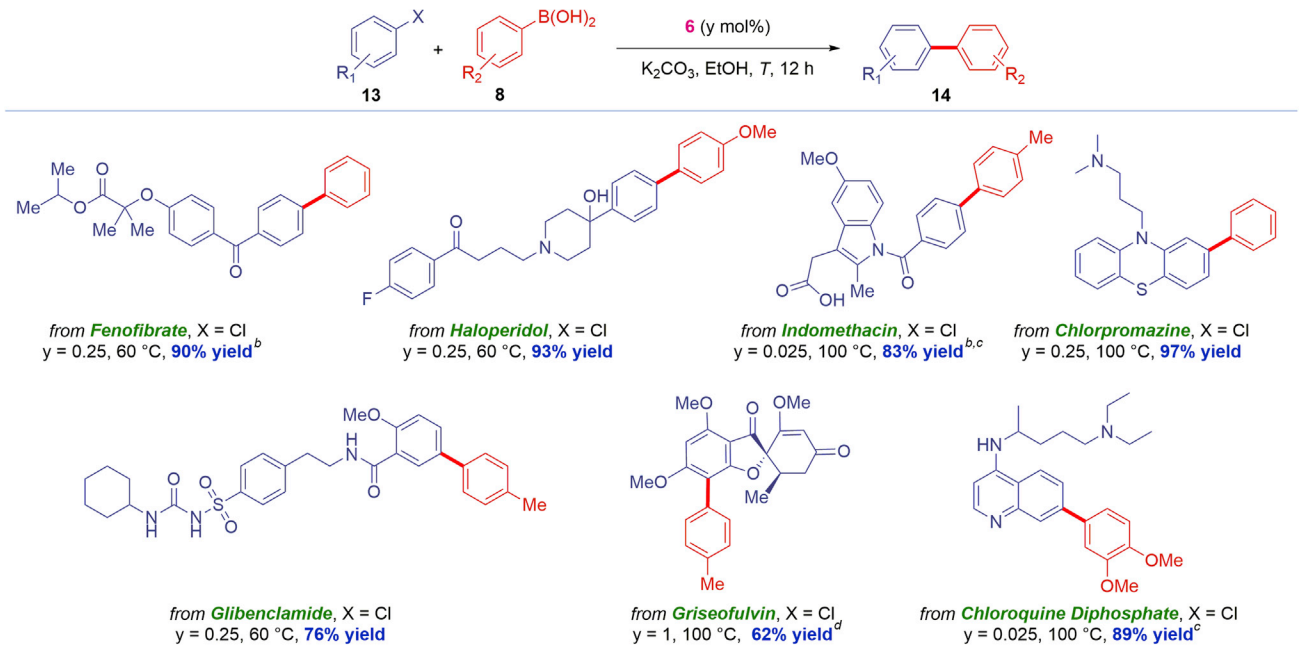

Scheme 4. Direct Cross-Coupling of Pharmaceuticals

Conditions: Ar-X (1.0 equiv), Ar-$B(OH)_2$ (2.0 equiv), K_2CO_3 (3.0 equiv), $[Pd(IPr)(\mu\text{-}Cl)Cl]_2$ (6) (y mol %), EtOH (0.50 M), 12 h. Isolated yields. [a] *i*PrOH. [b] K_2CO_3 (5 equiv). [c] *t*-BuOH. See Transparent Methods for details.

coupling processes. The exceptional performance of $[Pd(NHC)(\mu\text{-}Cl)Cl]_2$ catalysts provides a strong foundation to accelerate applications in the synthesis of medicines, organic molecules, and polymers.

Limitations of the Study

Limitations are typical to NHC-based catalyst systems and include lower efficiency for highly sterically hindered substrates using IPr ligand and high reaction temperature using ppm catalyst levels. Our future studies will focus on the development of more active ligands and catalysts to expand the scope of application of Pd–NHC catalysis.

Resource Availability

Lead Contact

Further information and requests for resources and reagents should be directed to and will be fulfilled by the Lead Contact, Michal Szostak (michal.szostak@rutgers.edu).

Materials Availability

This study did not generate new unique reagents.

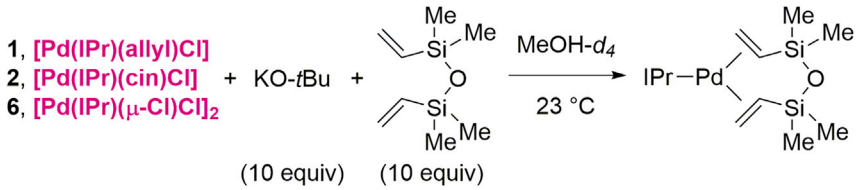

Scheme 5. Rates of Activation of Allyl, Cinnamyl and Chloro Dimer, $[(NHC)Pd(\mu\text{-}Cl)Cl]_2$, Complexes

Conditions: Pd–NHC (1.0 equiv), KO*t*-Bu (10 equiv), dvds (10 equiv), MeOH-d_4, 23°C, 0–3 h.

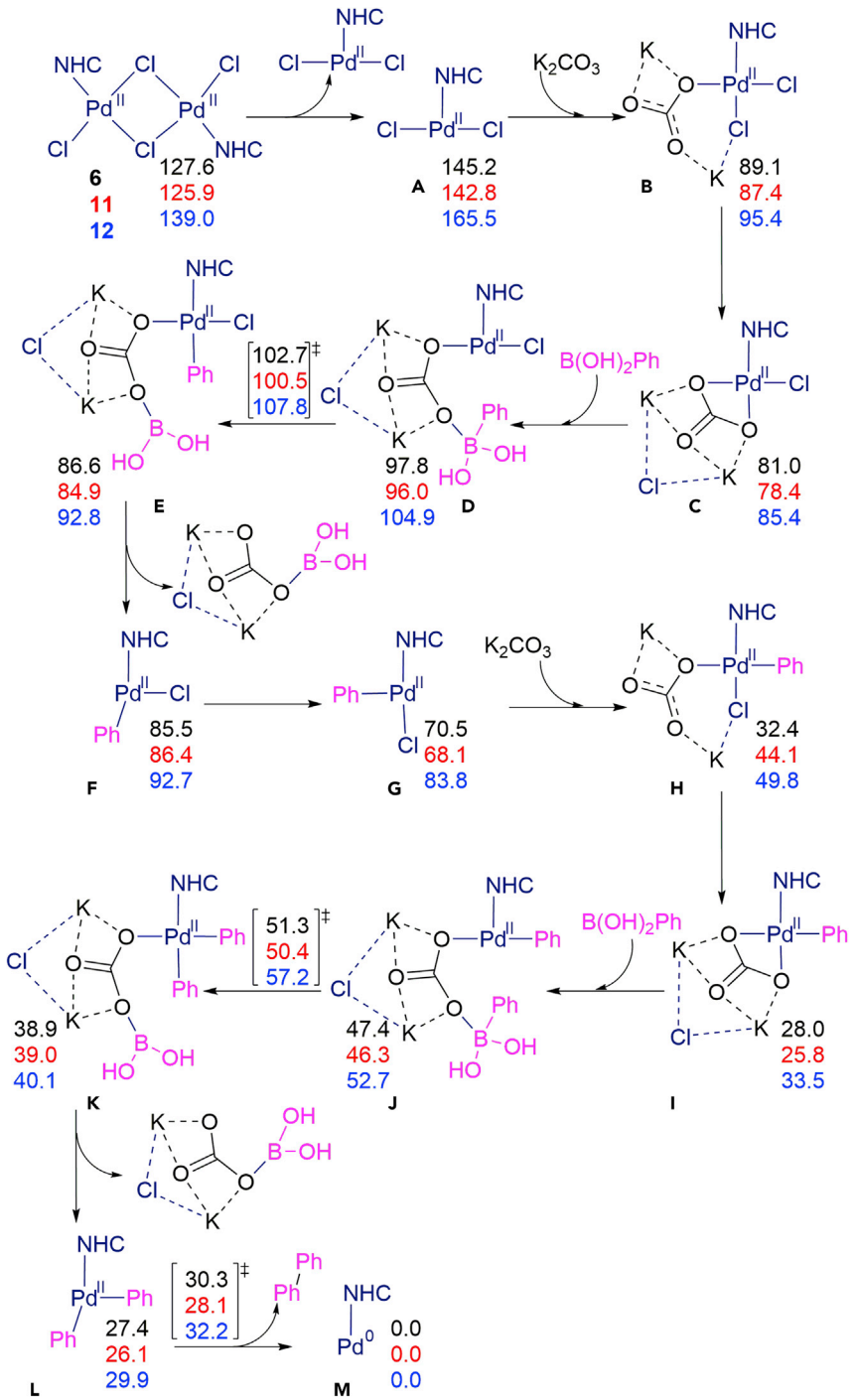

Figure 4. DFT-Optimized Pathway (Relative Energies to Pd(0) in kcal/mol) for the Activation of Catalysts 6 (black), 11 (red), and 12 (blue). 6 = IPr, 11 = SIPr, 12 = IPr*, $[Pd(NHC)(\mu\text{-}Cl)Cl]_2$

Data and Code Availability

The published article includes all data generated during this study.

METHODS

All methods can be found in the accompanying Transparent Methods supplemental file.

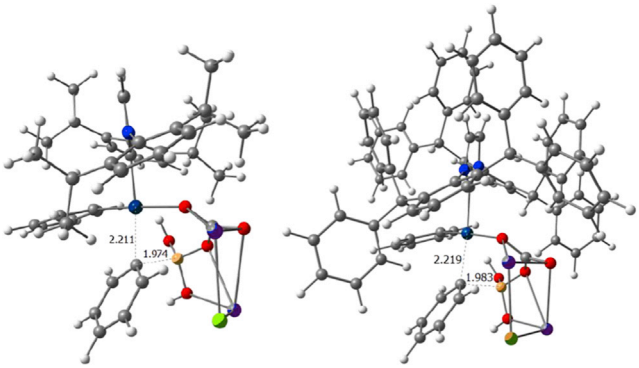

Figure 5. DFT-Optimized Transition State of the Second Aryl Transfer from Boron to Palladium for 6 (left) and 12 (right); Main Distances Are Given in Å

Scheme 6. Facile, One-Step Synthesis of 6

Conditions: IPrHCl (1.0 equiv, 3.7 mmol), $Pd(OAc)_2$ (1.2 equiv), K_2CO_3 (4 equiv), toluene, 80°C, followed by addition of HCl.

SUPPLEMENTAL INFORMATION

Supplemental Information can be found online at https://doi.org/10.1016/j.isci.2020.101377.

ACKNOWLEDGMENTS

We thank Rutgers University (M.S.), the NSF (CAREER CHE-1650766, M.S.), and the NIH (1R35GM133326, M.S.) for financial support. The Bruker 500 MHz spectrometer used in this study was supported by the NSF-MRI grant (CHE-1229030). For work conducted in Belgium, S.P.N. and C.S.J.C. wish to thank the UGent BOF (starter and senior research grants). Umicore AG is thanked for gifts of materials. A.P. is a Serra Húnter Fellow and ICREA Academia Prize 2019 holder. A.P. thanks the Spanish MICINN for project PGC2018-097722-B-I00.

AUTHOR CONTRIBUTIONS

T.Z., S.M., F.N., A.M.C.O., A.P., L.C., and C.S.J.C. performed the experiments. M.S., A.P., and S.P.N. wrote the manuscript and directed the project. All the authors discussed the results and commented on the manuscript.

DECLARATION OF INTERESTS

The authors declare no competing interests.

Received: May 30, 2020
Revised: June 25, 2020
Accepted: July 14, 2020
Published: August 21, 2020

REFERENCES

Afagh, N.A., and Yudin, A.K. (2010). Chemoselectivity and the curious reactivity preferences of functional groups. Angew. Chem. Int. Ed. *49*, 262–310.

Blakemore, D.C., Castro, L., Churcher, I., Rees, D.C., Thomas, A.W., Wilson, D.M., and Wood, A. (2018). Organic synthesis provides opportunities to transform drug discovery. Nat. Chem. *10*, 383–394.

Christmann, U., and Vilar, R. (2005). Monoligated palladium species as catalysts in cross-coupling reactions. Angew. Chem. Int. Ed. *44*, 366–374.

Colacot, T.J. (2015). New Trends in Cross-Coupling: Theory and Applications (RSC).

Diez-Gonzalez, S., Marion, N., and Nolan, S.P. (2009). N-heterocyclic carbenes in late transition metal catalysis. Chem. Rev. *109*, 3612–3676.

Fairlamb, I.J.S., Taylor, R.J.K., Serrano, J.L., and Sanchez, G. (2006). Halide and pseudohalide effects in Pd-catalyzed cross-coupling reactions. New J. Chem. *30*, 1695–1704.

Falivene, L., Credendino, R., Poater, A., Petta, A., Serra, L., Oliva, R., Scarano, V., and Cavallo, L. (2016). SambVca 2. A web tool for analyzing catalytic pockets with topographic steric maps. Organometallics *35*, 2286–2293.

Falivene, L., Cao, Z., Petta, A., Serra, L., Poater, A., Oliva, R., Scarano, V., and Cavallo, L. (2019). Towards the online computer-aided design of catalytic pockets. Nat. Chem. *11*, 872–879.

Fortman, G.C., and Nolan, S.P. (2011). N-heterocyclic carbene (NHC) ligands and palladium in homogeneous cross-coupling catalysis: a perfect union. Chem. Soc. Rev. *40*, 5151–5169.

Fyfe, J.W.B., and Watson, A.J.B. (2017). Recent developments in organoboron chemistry: old dogs, new tricks. Chem *3*, 31–55.

Hopkinson, M.N., Richter, C., Schedler, M., and Glorius, F. (2014). An overview of N-heterocyclic carbenes. Nature *510*, 485–496.

Hruszkewycz, D.P., Balcells, D., Guard, L.M., Hazari, N., and Tilset, M. (2014). Insight into the efficiency of cinnamyl-supported precatalysts for the Suzuki–Miyaura reaction: observation of Pd(I) dimers with bridging allyl ligands during catalysis. J. Am. Chem. Soc. *136*, 7300–7316.

Izquierdo, F., Manzini, S., and Nolan, S.P. (2014). The use of the sterically demanding IPr* and related ligands in catalysis. Chem. Commun. *50*, 14926–14937.

Johansson Seechurn, C.C.C., Sperger, T., Scrase, T.G., Schoenebeck, F., and Colacot, T.J. (2017). Understanding the unusual reduction mechanism of Pd(II) to Pd(I): uncovering hidden species and implications in catalytic cross-coupling reactions. J. Am. Chem. Soc. *139*, 5194–5200.

Lei, P., Meng, G., and Szostak, M. (2017). General method for the Suzuki-Miyaura cross-coupling of amides using commercially available, air- and moisture-stable palladium/NHC (NHC = N-heterocyclic carbene) complexes. ACS Catal. *7*, 1960–1965.

Li, G., Lei, P., Szostak, M., Casals-Cruañas, E., Poater, A., Cavallo, L., and Nolan, S.P. (2018). Mechanistic study of Suzuki–Miyaura cross-coupling reactions of amides mediated by [Pd(NHC)(allyl)Cl] precatalysts. ChemCatChem *10*, 3096–3106.

Marion, N., Navarro, O., Mei, J., Stevens, E.D., Scott, N.M., and Nolan, S.P. (2006). Modified (NHC)Pd(allyl)Cl (NHC = N-heterocyclic carbene) complexes for room-temperature Suzuki-Miyaura and Buchwald-Hartwig reactions. J. Am. Chem. Soc. *128*, 4101–4111.

Martin, R., and Buchwald, S.L. (2008). Palladium-catalyzed Suzuki−Miyaura cross-coupling reactions employing dialkylbiaryl phosphine ligands. Acc. Chem. Res. *41*, 1461–1473.

Melvin, P.R., Nova, A., Balcells, D., Dai, W., Hazari, N., Hruszkewycz, D.P., Shah, H.P., and Tudge, M.T. (2015). Design of a versatile and improved precatalyst scaffold for palladium-catalyzed cross-coupling: $(\eta^3\text{-1-}t\text{-Bu-indenyl})_2(\mu\text{-Cl})_2Pd_2$. ACS Catal. *5*, 5596–5606.

Molander, G.A., Wolfe, J.P., and Larhed, M. (2013). Science of Synthesis: Cross-Coupling and Heck-type Reactions (Thieme).

Navarro, O., Kelly, R.A., and Nolan, S.P. (2003). A general method for the Suzuki-Miyaura cross-coupling of sterically hindered aryl Chlorides: synthesis of di- and tri-ortho-substituted biaryls in 2-propanol at room temperature. J. Am. Chem. Soc. *125*, 16194–16195.

Nolan, S.P., and Cazin, C.S.J. (2017). Science of Synthesis: N-Heterocyclic Carbenes in Catalytic Organic Synthesis (Thieme).

O'Brien, C.J., Kantchev, E.A.B., Valente, C., Hadei, N., Chass, G.A., Lough, A., Hopkinson, A.C., and Organ, M.G. (2006). Easily prepared air- and moisture-stable Pd–NHC (NHC=N-heterocyclic carbene) complexes: a reliable, user-friendly, highly active palladium precatalyst for the Suzuki–Miyaura reaction. Chem. Eur. J. *12*, 4743–4748.

Shi, S., Nolan, S.P., and Szostak, M. (2018). Well-defined palladium(II)-NHC (NHC = N-heterocyclic carbene) precatalysts for cross-coupling reactions of amides and esters by selective acyl CO–X (X = N, O) cleavage. Acc. Chem. Res. *51*, 2589–2599.

Viciu, M.S., Germaneau, R.F., Navarro-Fernandez, O., Stevens, E.D., and Nolan, S.P. (2002a). Activation and reactivity of (NHC)Pd(allyl)Cl (NHC = N-heterocyclic carbene) complexes in cross-coupling reactions. Organometallics *21*, 5470–5472.

Viciu, M.S., Kissling, R.M., Stevens, E.D., and Nolan, S.P. (2002b). An air-stable palladium/N-heterocyclic carbene complex and its reactivity in aryl amination. Org. Lett. *4*, 2229–2231.

Yet, L. (2018). Privileged Structures in Drug Discovery: Medicinal Chemistry and Synthesis (Wiley).

iScience, Volume *23*

Supplemental Information

[Pd(NHC)(μ-Cl)Cl]$_2$: Versatile and Highly Reactive Complexes for Cross-Coupling Reactions that Avoid Formation of Inactive Pd(I) Off-Cycle Products

Tongliang Zhou, Siyue Ma, Fady Nahra, Alan M.C. Obled, Albert Poater, Luigi Cavallo, Catherine S.J. Cazin, Steven P. Nolan, and Michal Szostak

Figure S1. Full DFT-optimized pathway (relative energies to Pd(0) in kcal/mol) for the activation of catalysts **6** (black), **11** (red) and **12** (blue); including the release of PhCl and PhPh, Related to **Figure 4**.

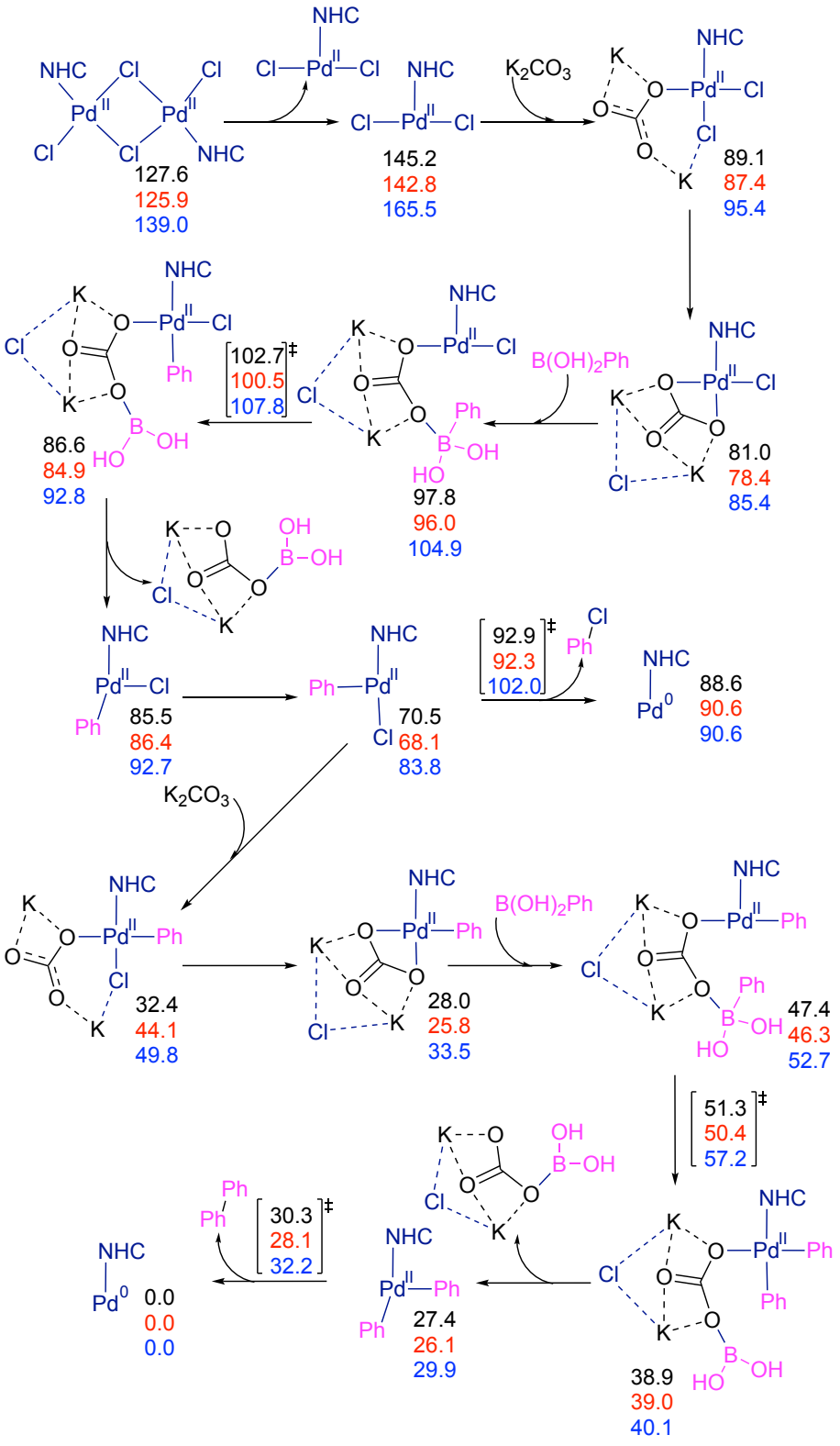

Figure S2. DFT-optimized pathway for the activation of catalysts **1** and **2** (relative energies to Pd(0) in kcal/mol), Related to **Figure 4**.

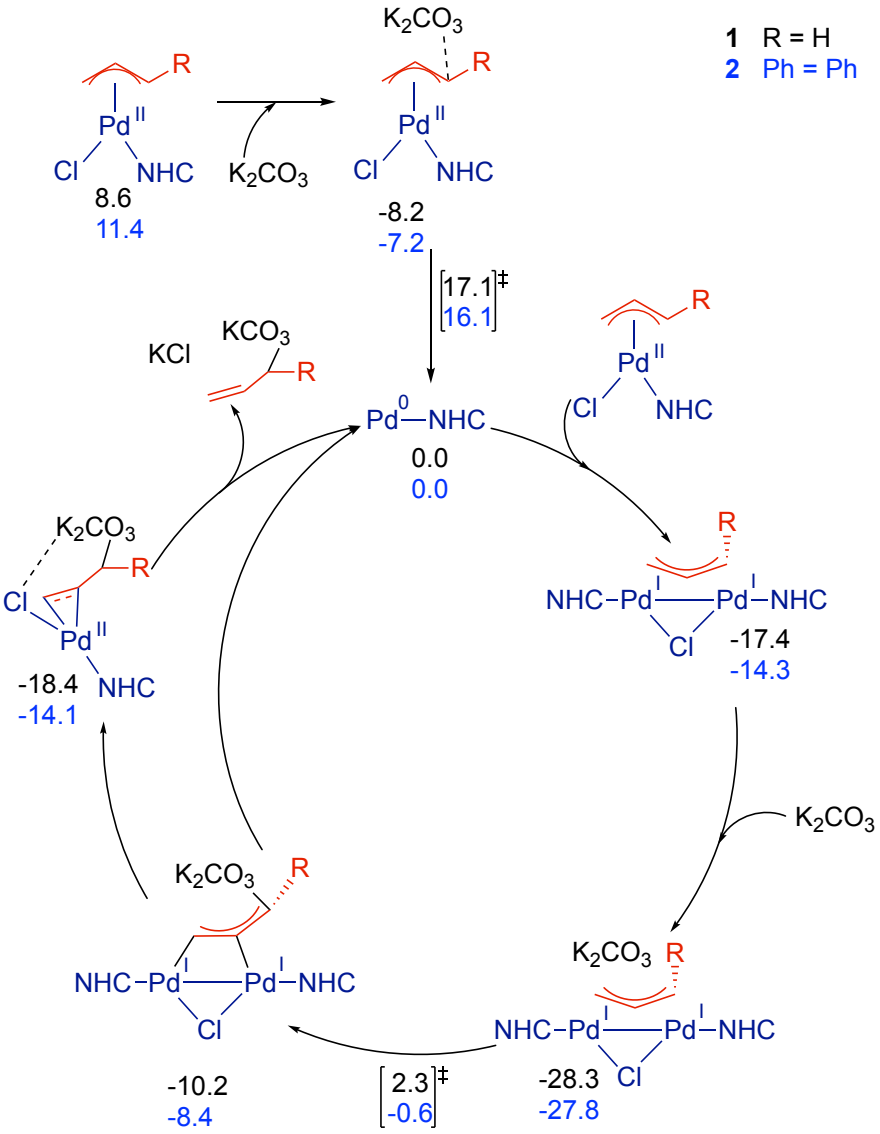

Figure S3. ^{1}H NMR spectrum of phenyl(*p*-tolyl)methanone, related to **Scheme 1**

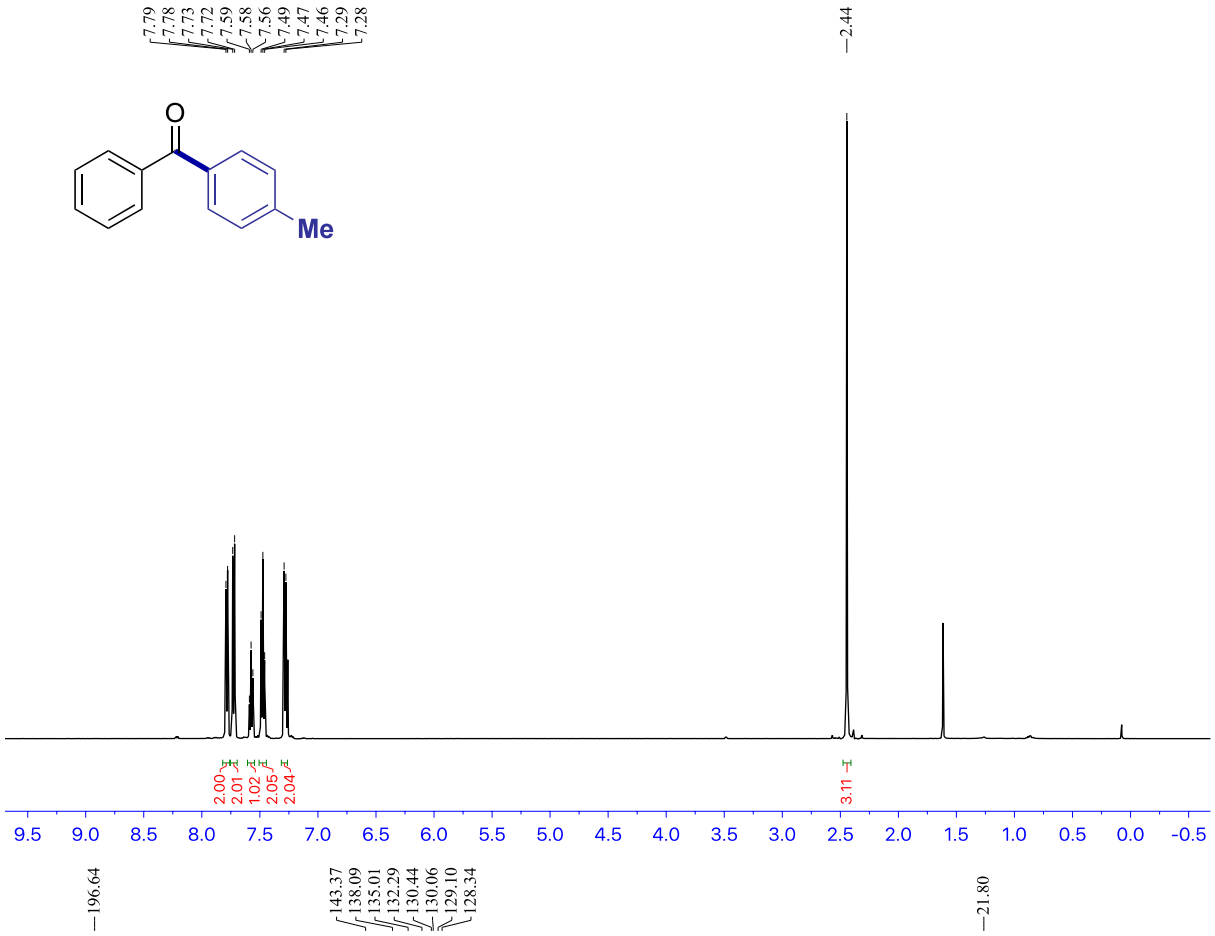

Figure S4. ^{13}C NMR spectrum of phenyl(*p*-tolyl)methanone, related to **Scheme 1**

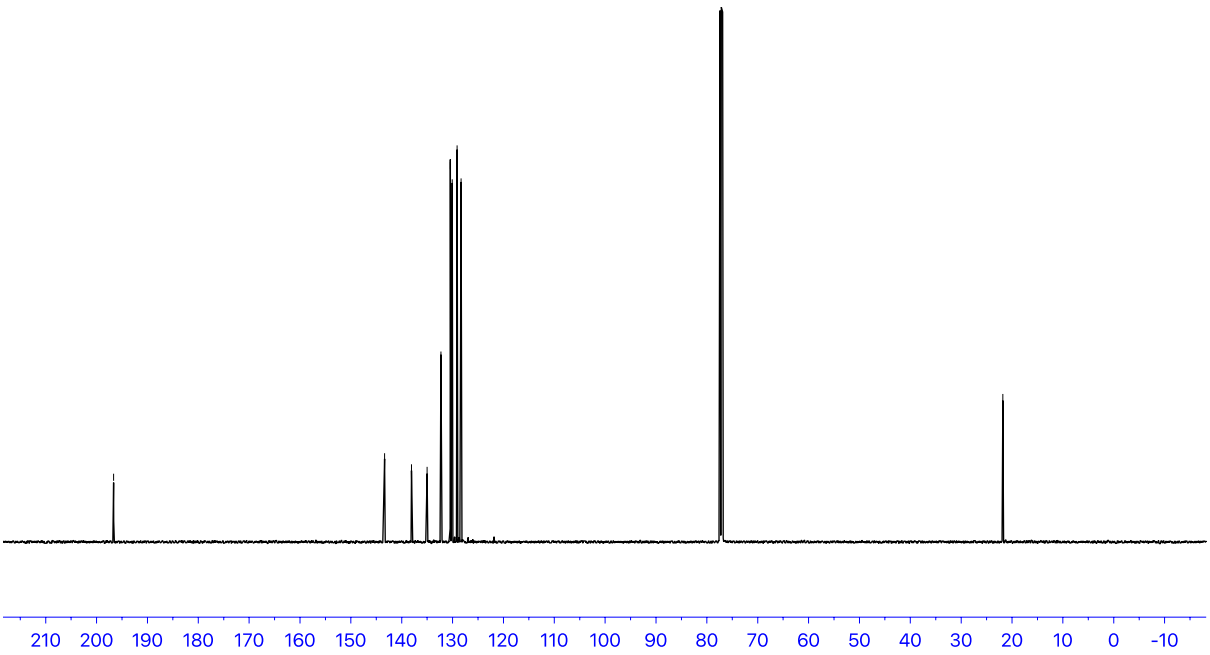

Figure S5. ^{1}H NMR spectrum of (4-methoxyphenyl)(phenyl)methanone, related to **Scheme 1**

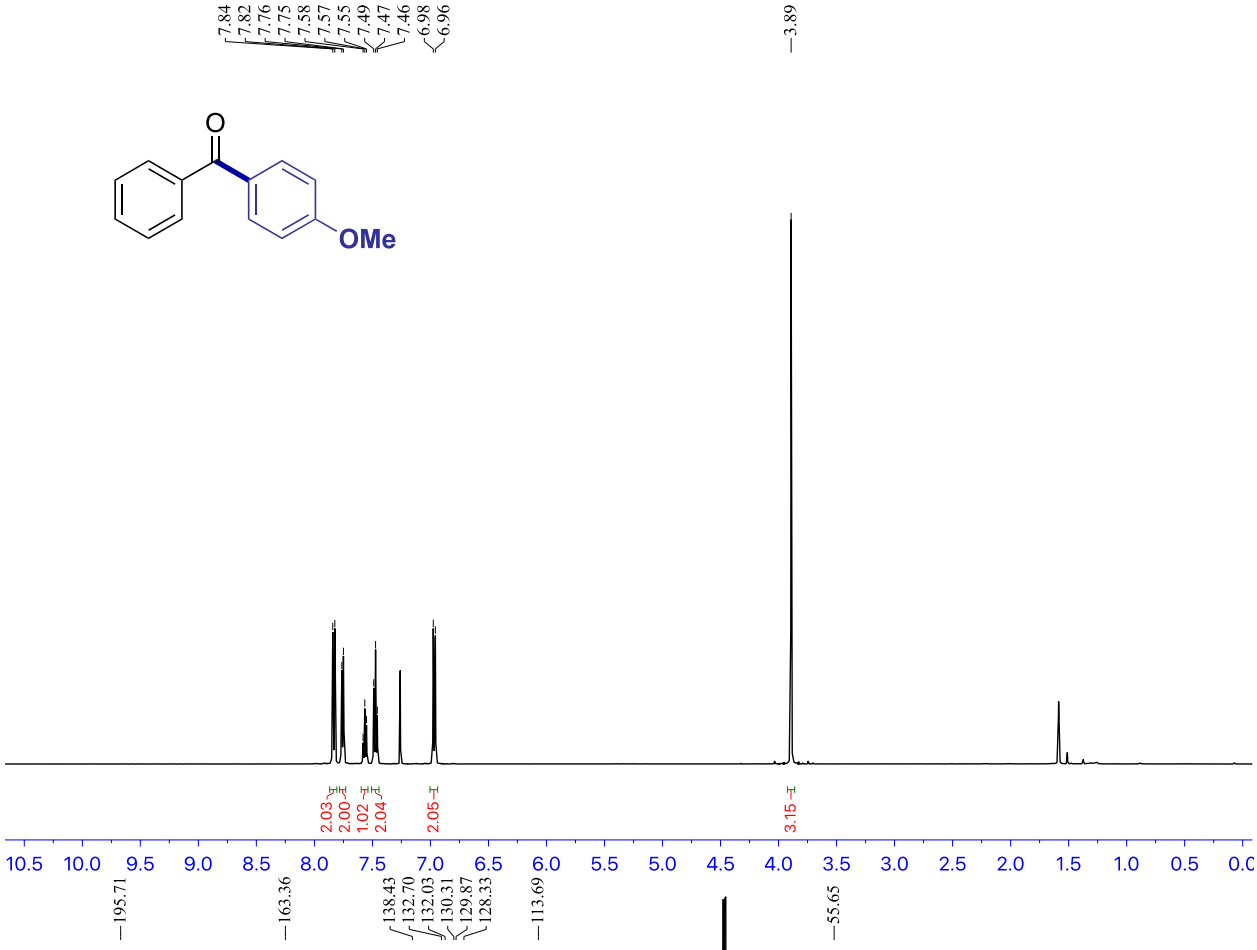

Figure S6. ^{13}C NMR spectrum of (4-methoxyphenyl)(phenyl)methanone, related to **Scheme 1**

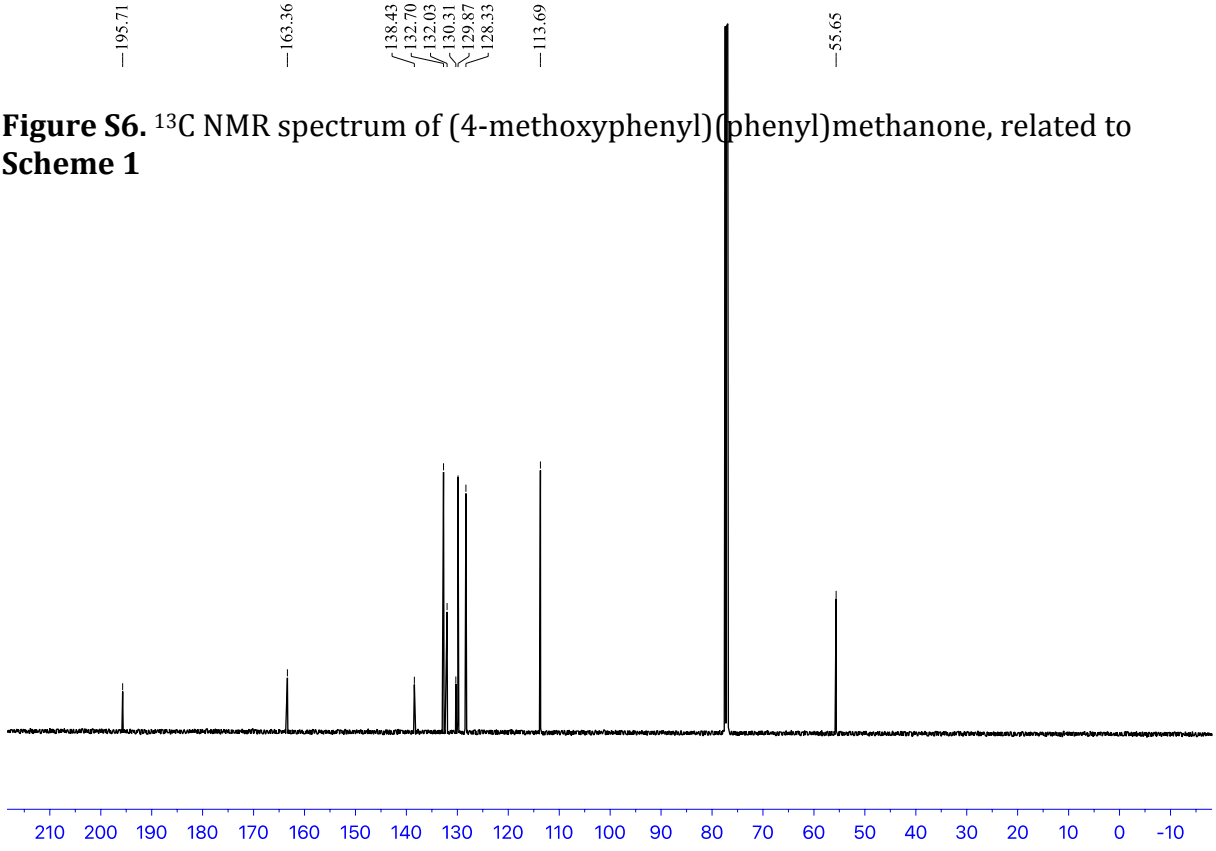

Figure S7. ^{1}H NMR spectrum of phenyl(4-(trifluoromethyl)phenyl)methanone, related to **Scheme 1**

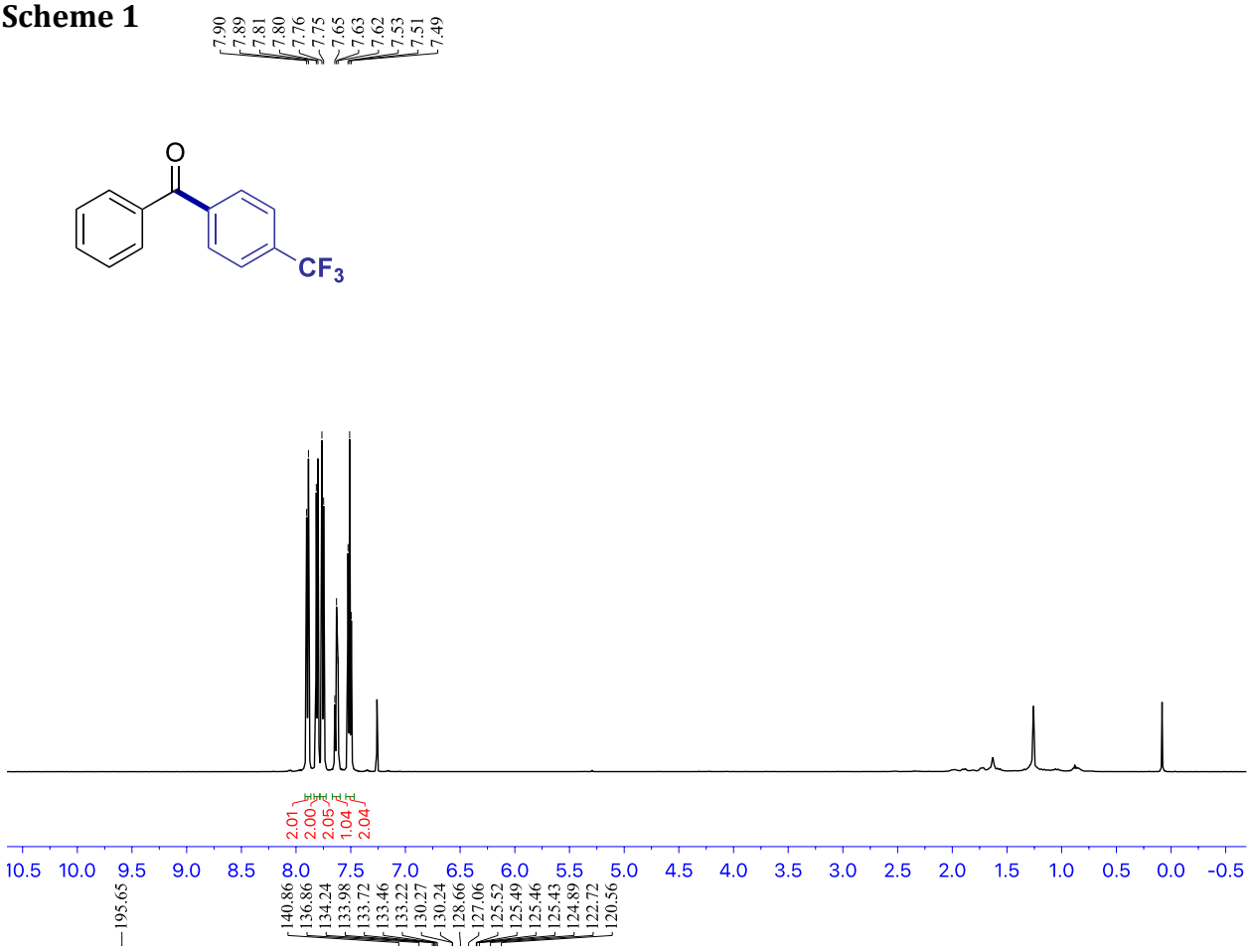

Figure S8. ^{13}C NMR spectrum of phenyl(4-(trifluoromethyl)phenyl)methanone, related to **Scheme 1**

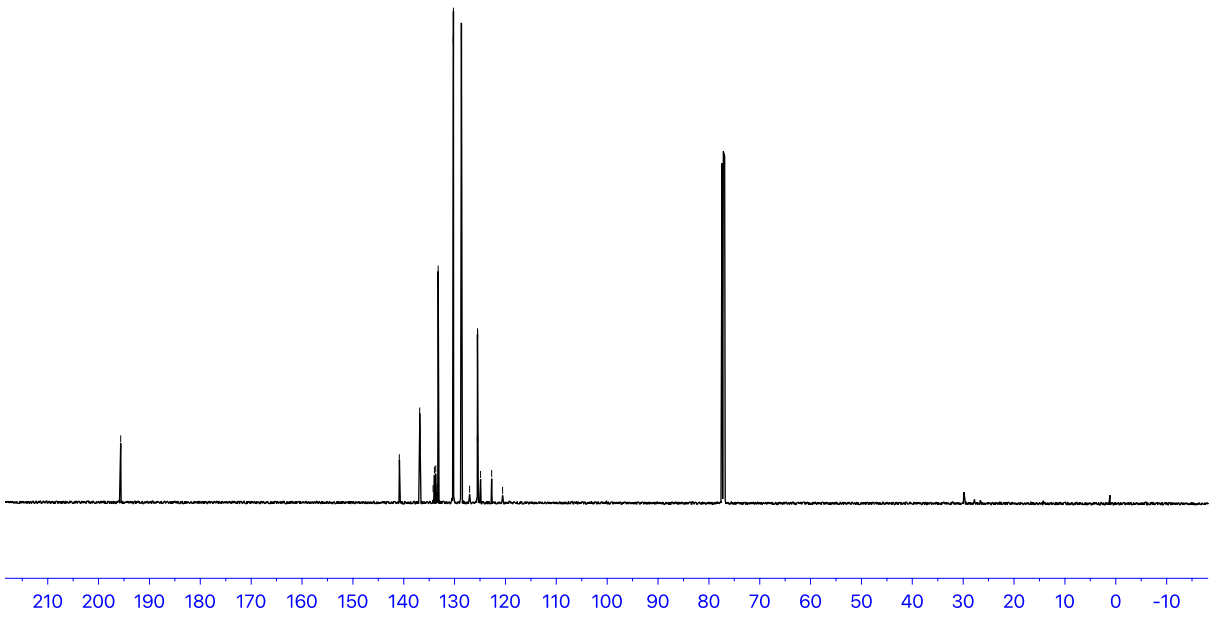

Figure S9. ^{19}F NMR spectrum of phenyl(4-(trifluoromethyl)phenyl)methanone, related to **Scheme 1**

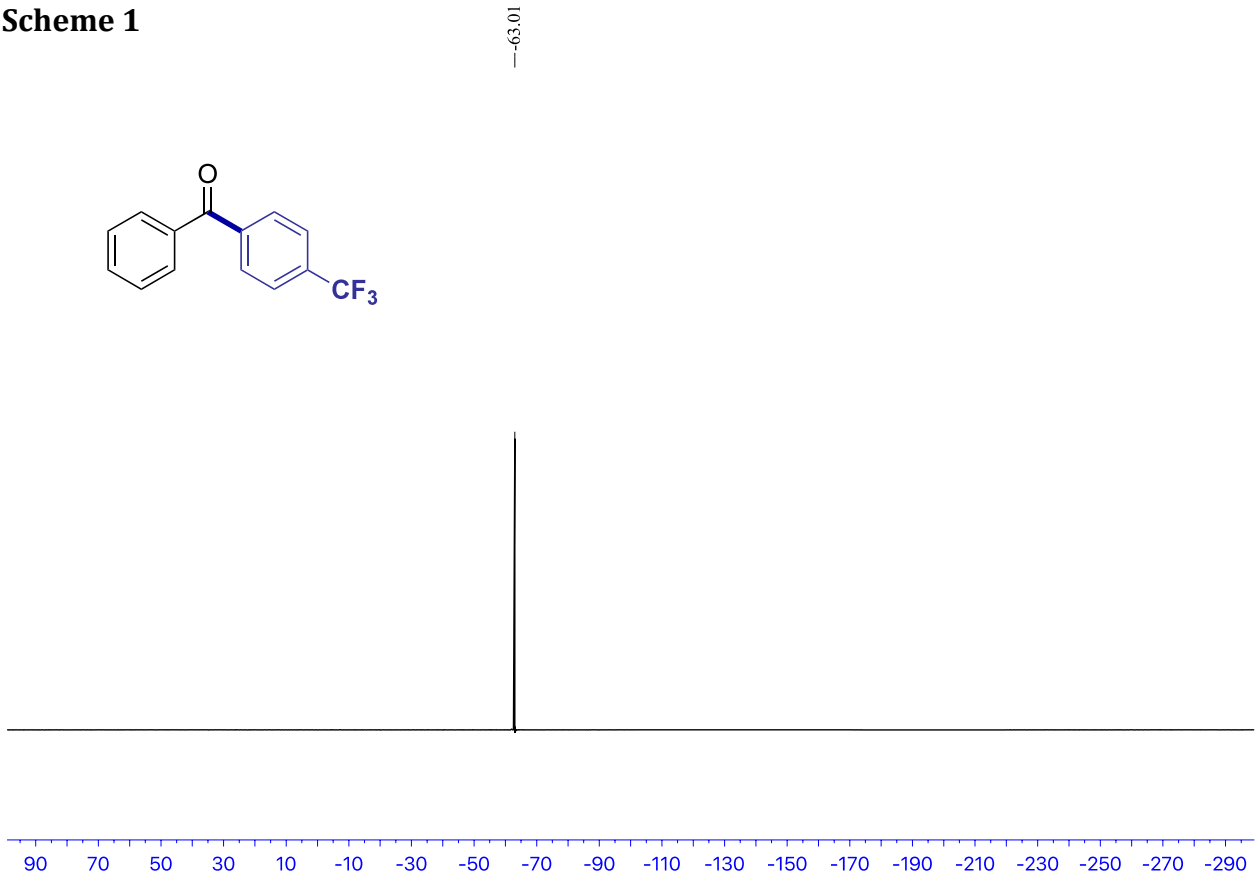

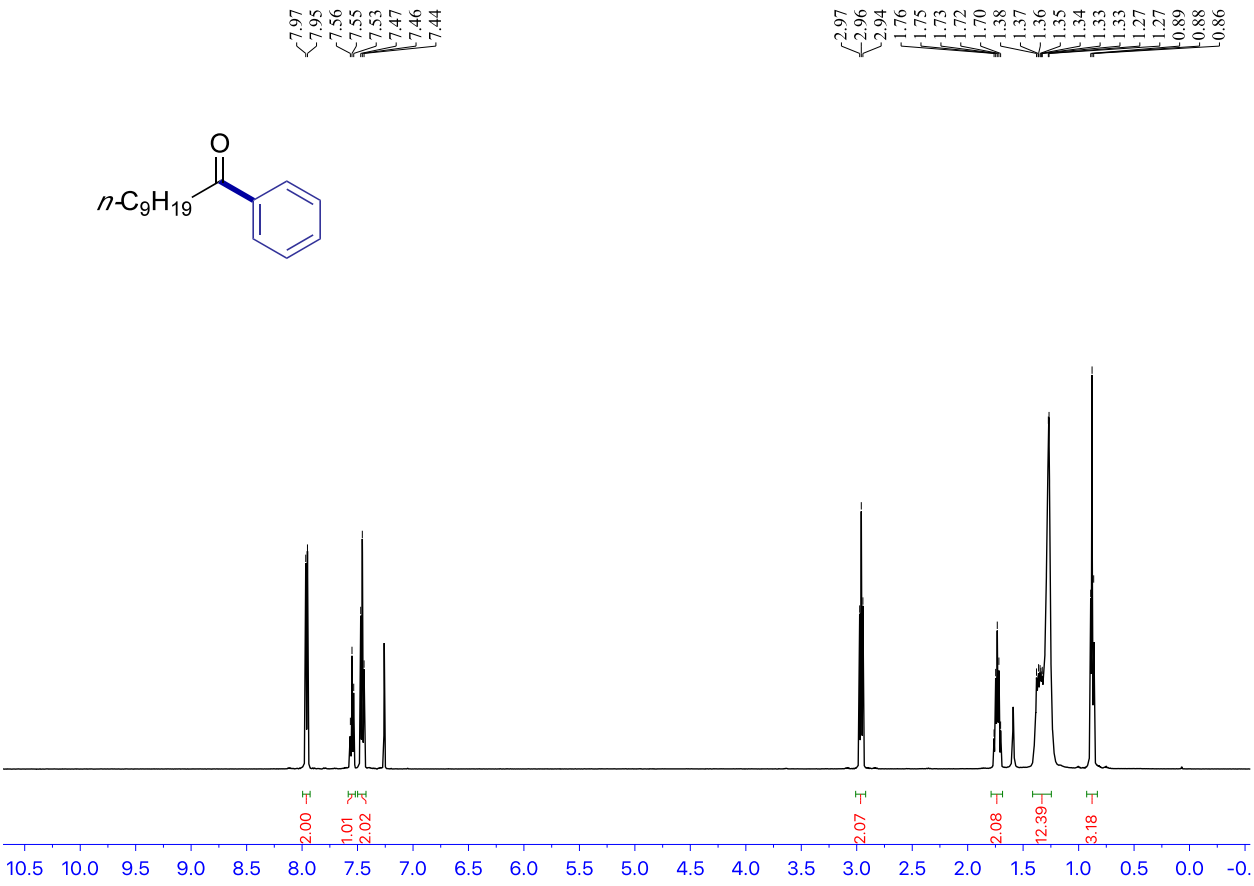
7.97
7.95
7.56
7.55
7.53
7.47
7.46
7.44
2.97
2.96
2.94
1.76
1.75
1.73
1.72
1.70
1.38
1.37
1.36
1.35
1.34
1.33
1.33
1.27
1.27
0.89
0.88
0.86
O
n-C9H19
2.00
1.01
2.02
2.07
2.08
12.39
3.18
10.5 10.0 9.5 9.0 8.5 8.0 7.5 7.0 6.5 6.0 5.5 5.0 4.5 4.0 3.5 3.0 2.5 2.0 1.5 1.0 0.5 0.0 -0.

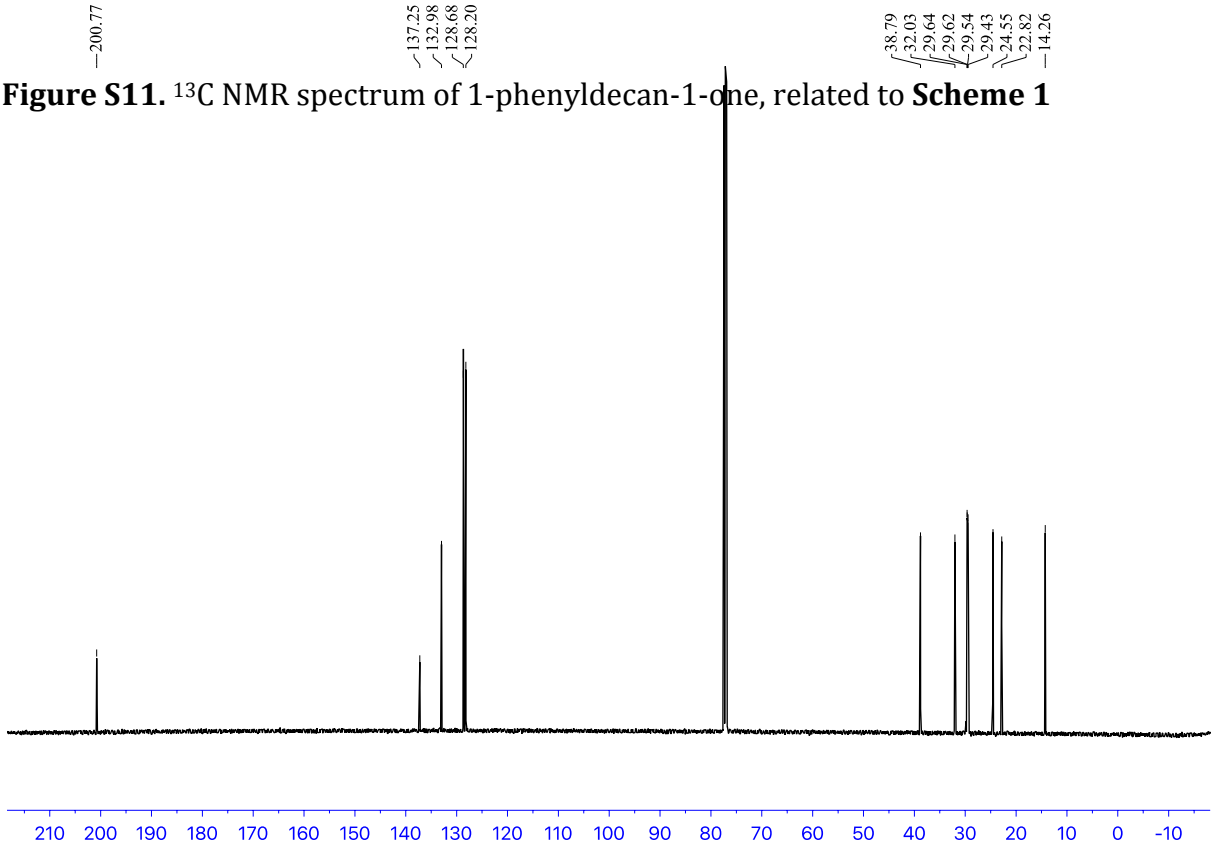

Figure S11. ^{13}C NMR spectrum of 1-phenyldecan-1-one, related to **Scheme 1**

Figure S12. ^{1}H NMR spectrum of methyl 4-benzoylbenzoate, related to **Scheme 1**

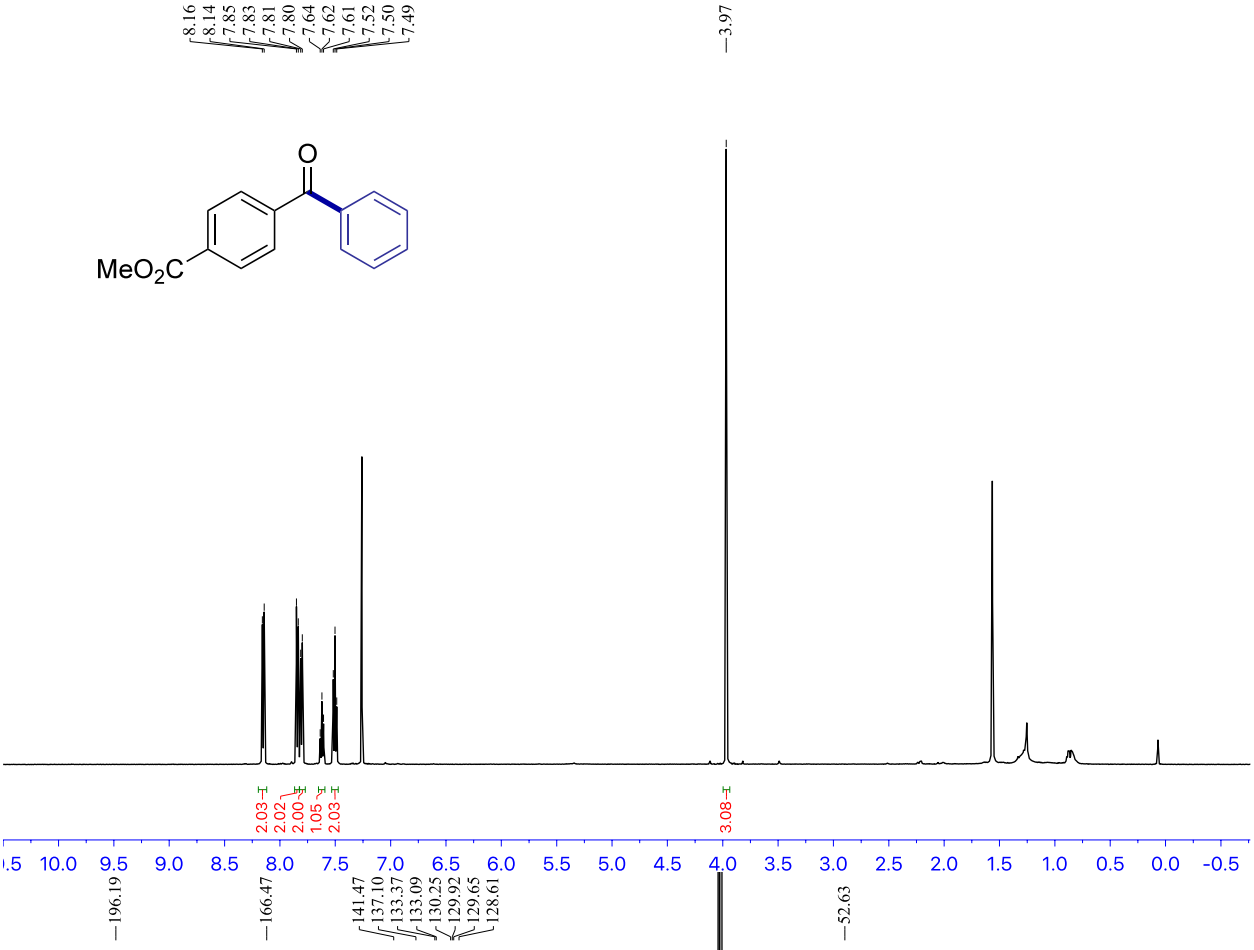

Figure S13. ^{13}C NMR spectrum of methyl 4-benzoylbenzoate, related to **Scheme 1**

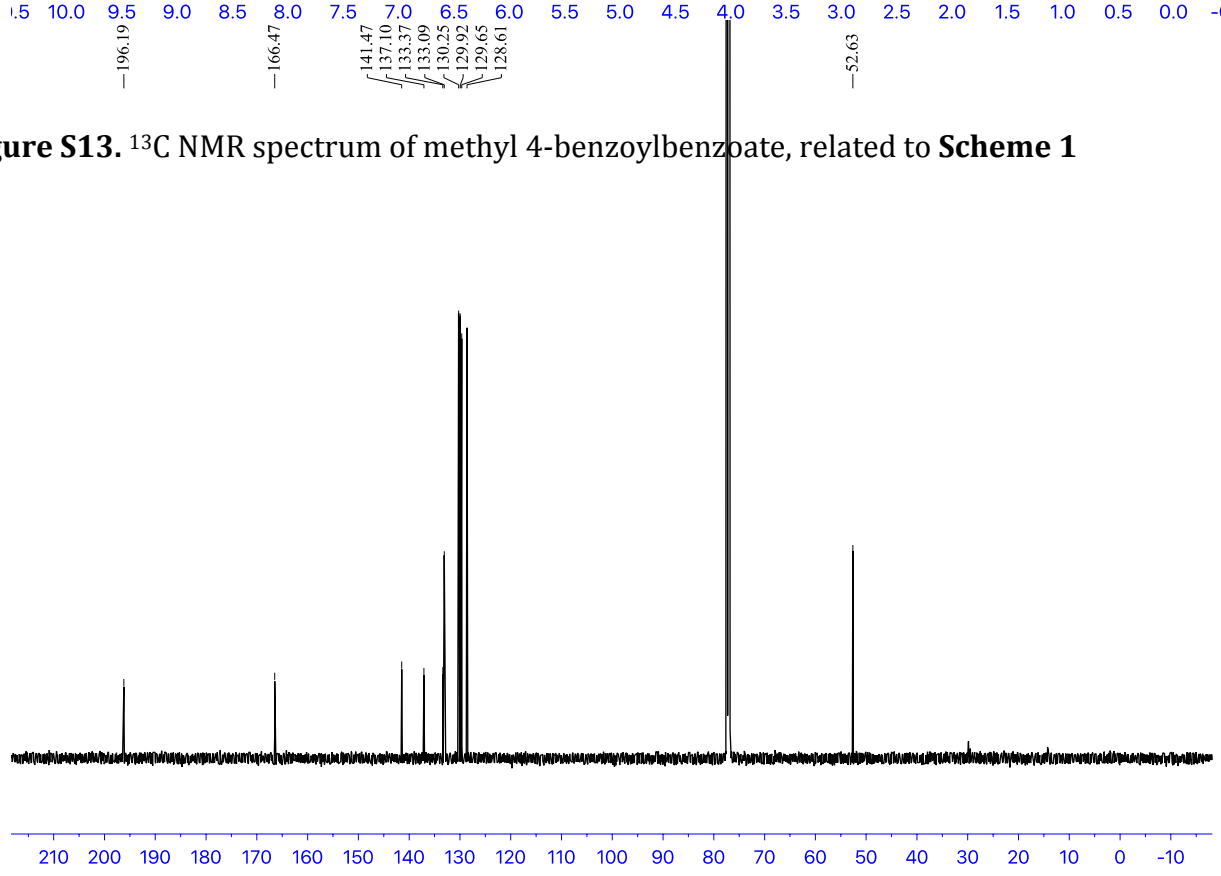

Figure S14. ^{1}H NMR spectrum of phenyl(*o*-tolyl)methanone, related to **Scheme 1**

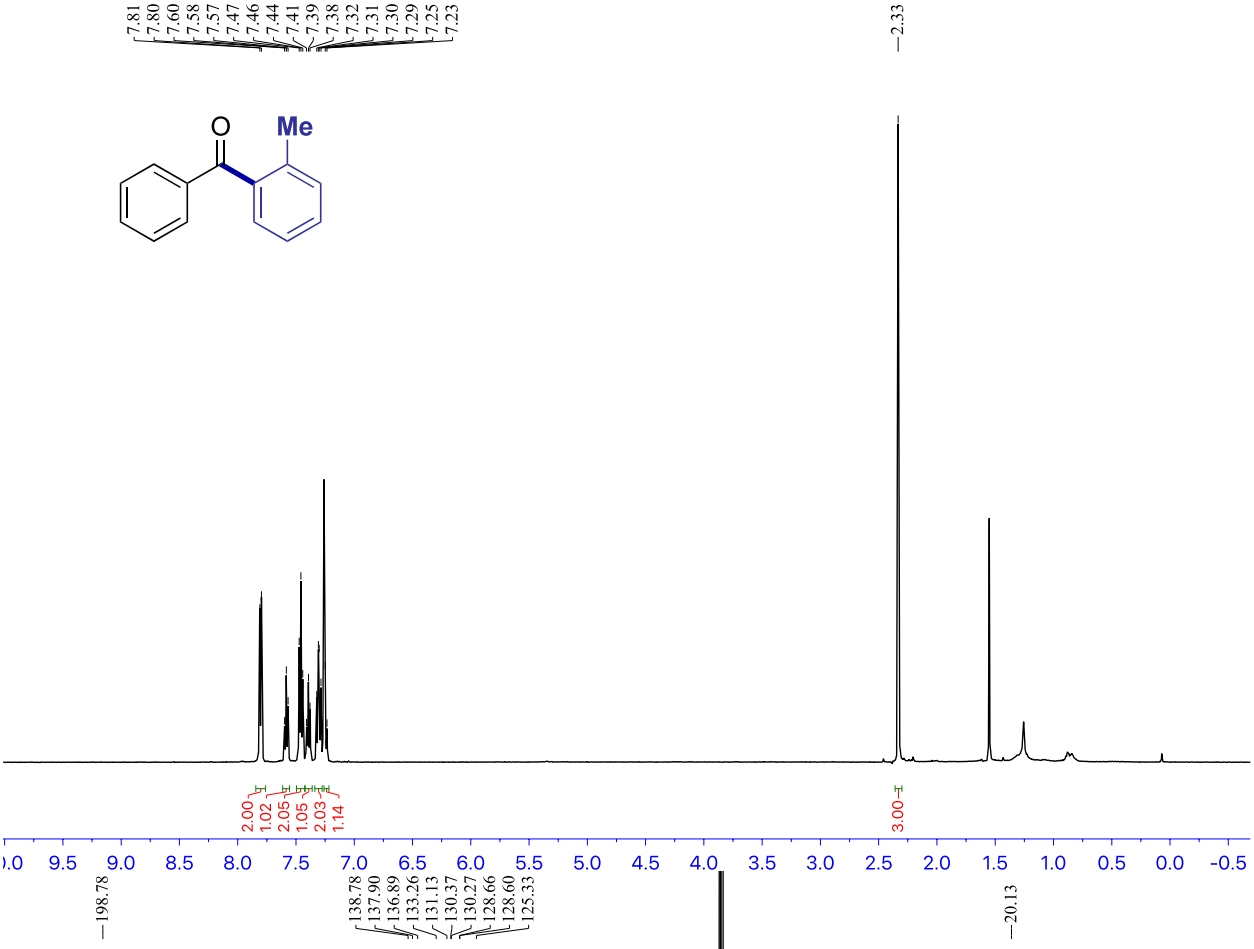

Figure S15. ^{13}C NMR spectrum of phenyl(*o*-tolyl)methanone, related to **Scheme 1**

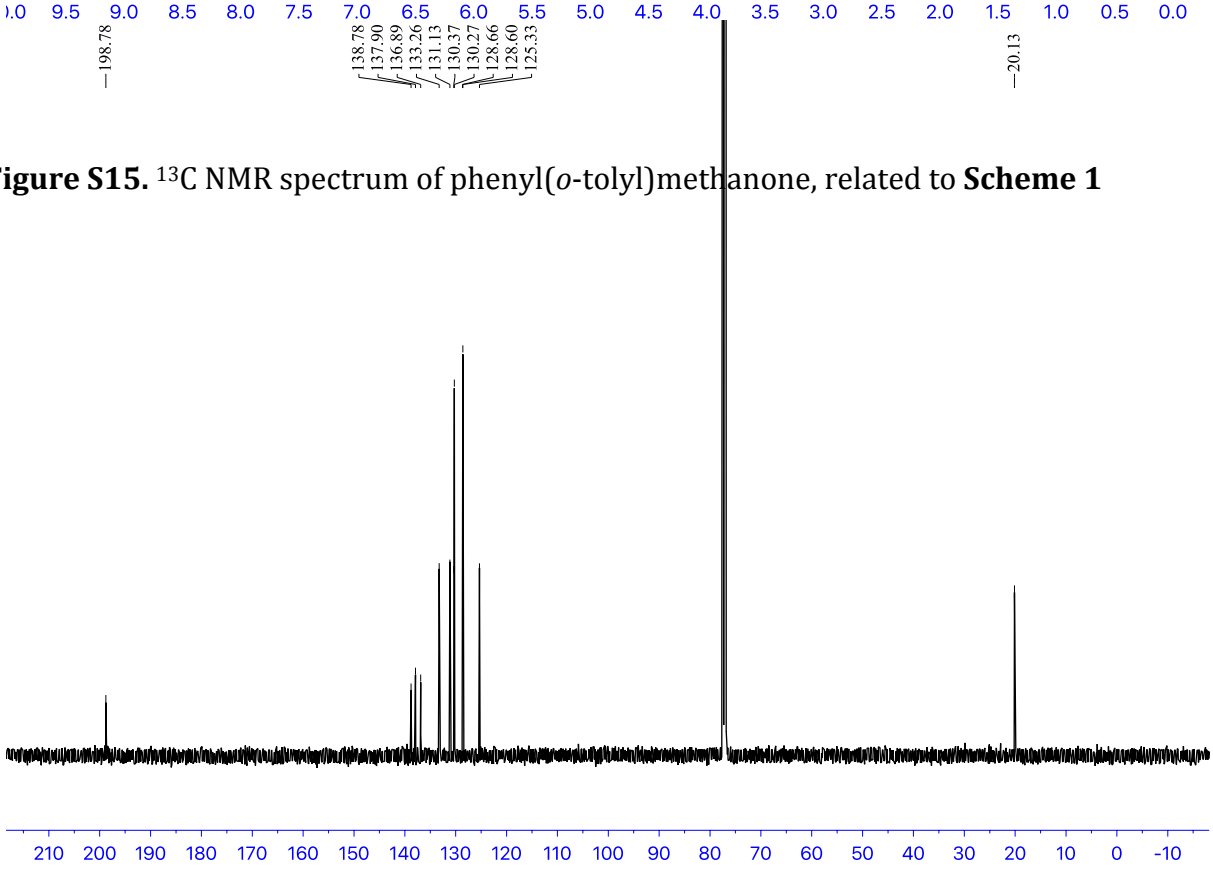

Figure S16. ^{1}H NMR spectrum of 4-methylbiphenyl, related to **Scheme 2**

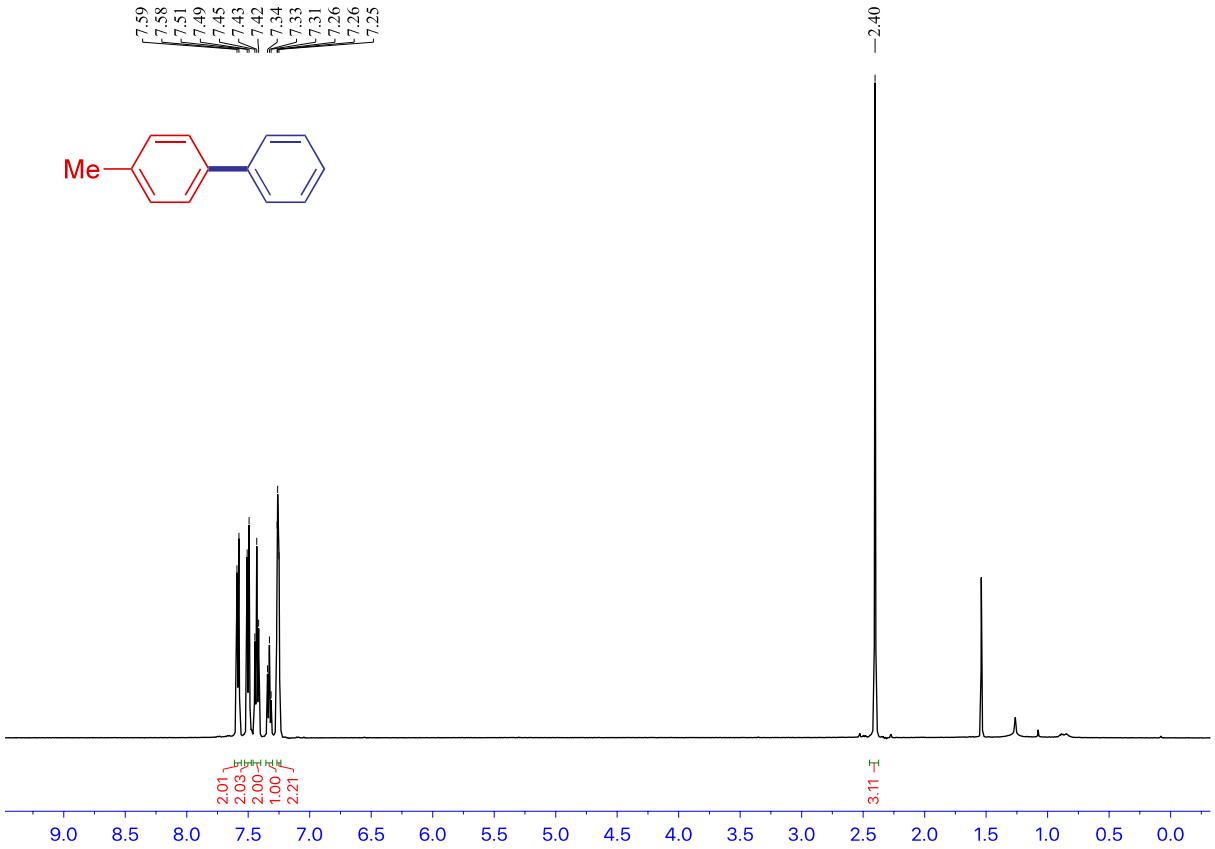

Figure S17. ^{13}C NMR spectrum of 4-methylbiphenyl, related to **Scheme 2**

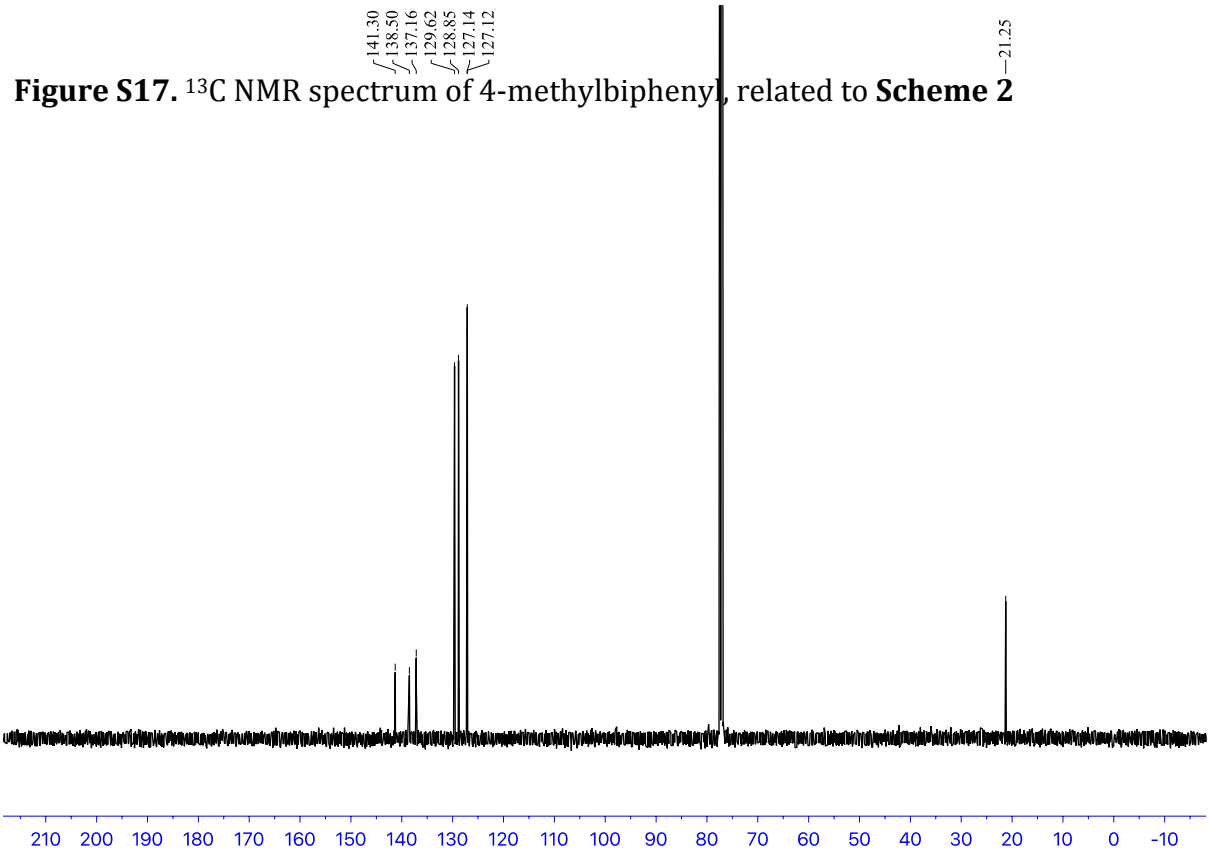

Figure S18. ^{1}H NMR spectrum of 4-methoxybiphenyl, related to **Scheme 2**

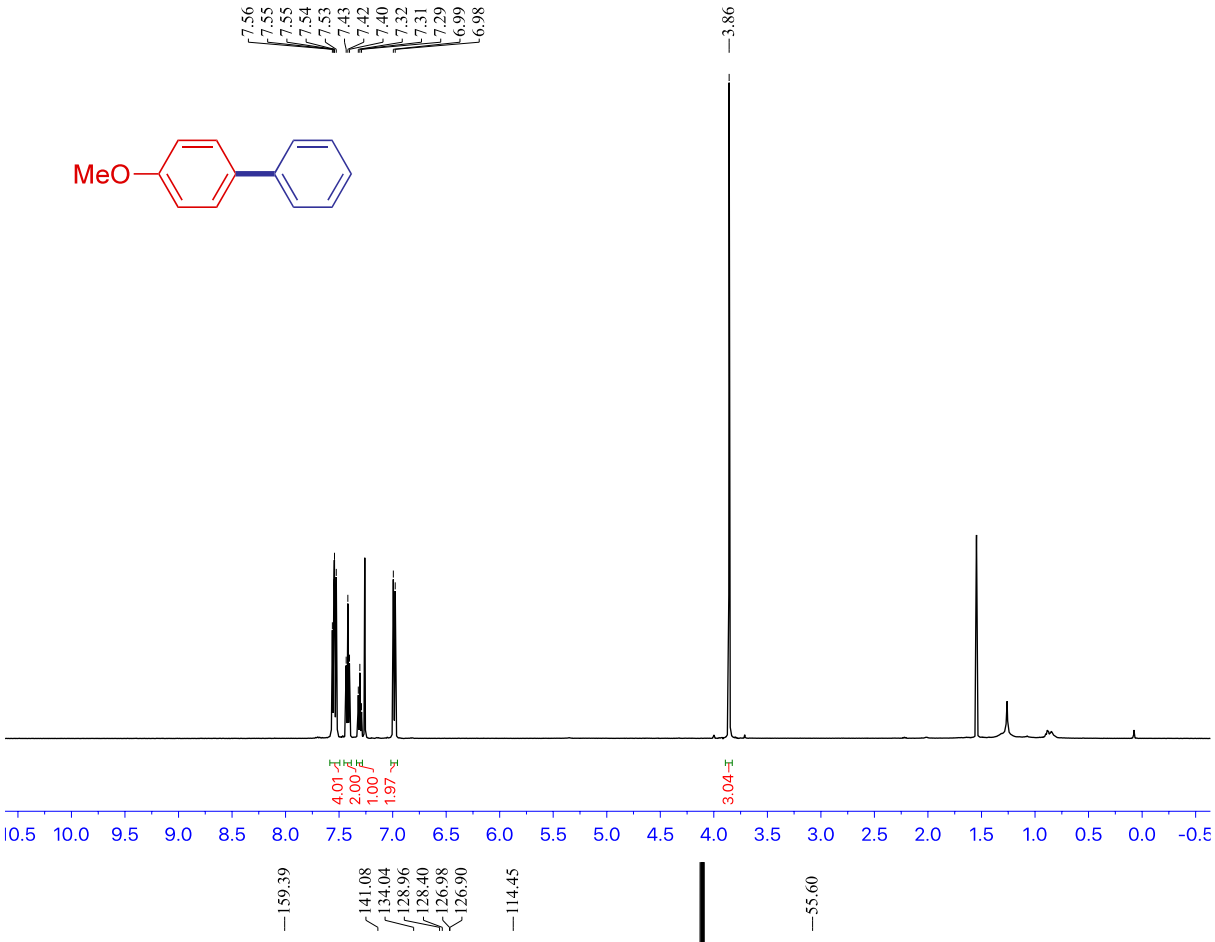

Figure S19. ^{13}C NMR spectrum of 4-methoxybiphenyl, related to **Scheme 2**

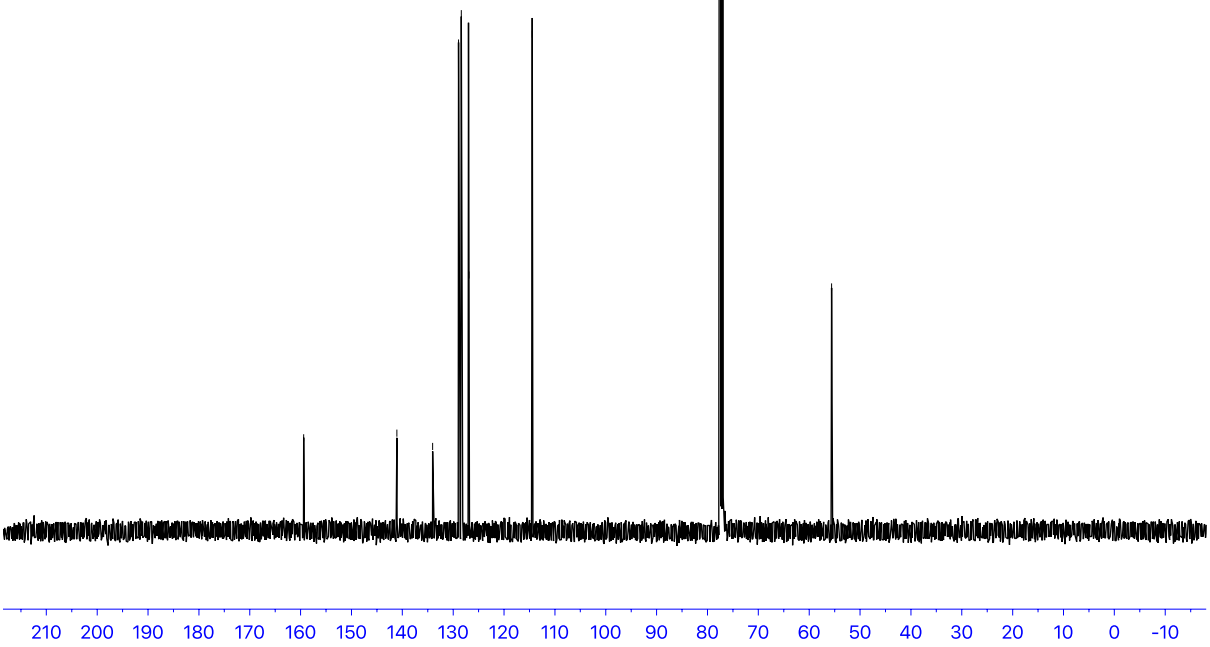

Figure S20. ^{1}H NMR spectrum of 4'-methoxy-2,6-dimethylbiphenyl, related to **Scheme 2**

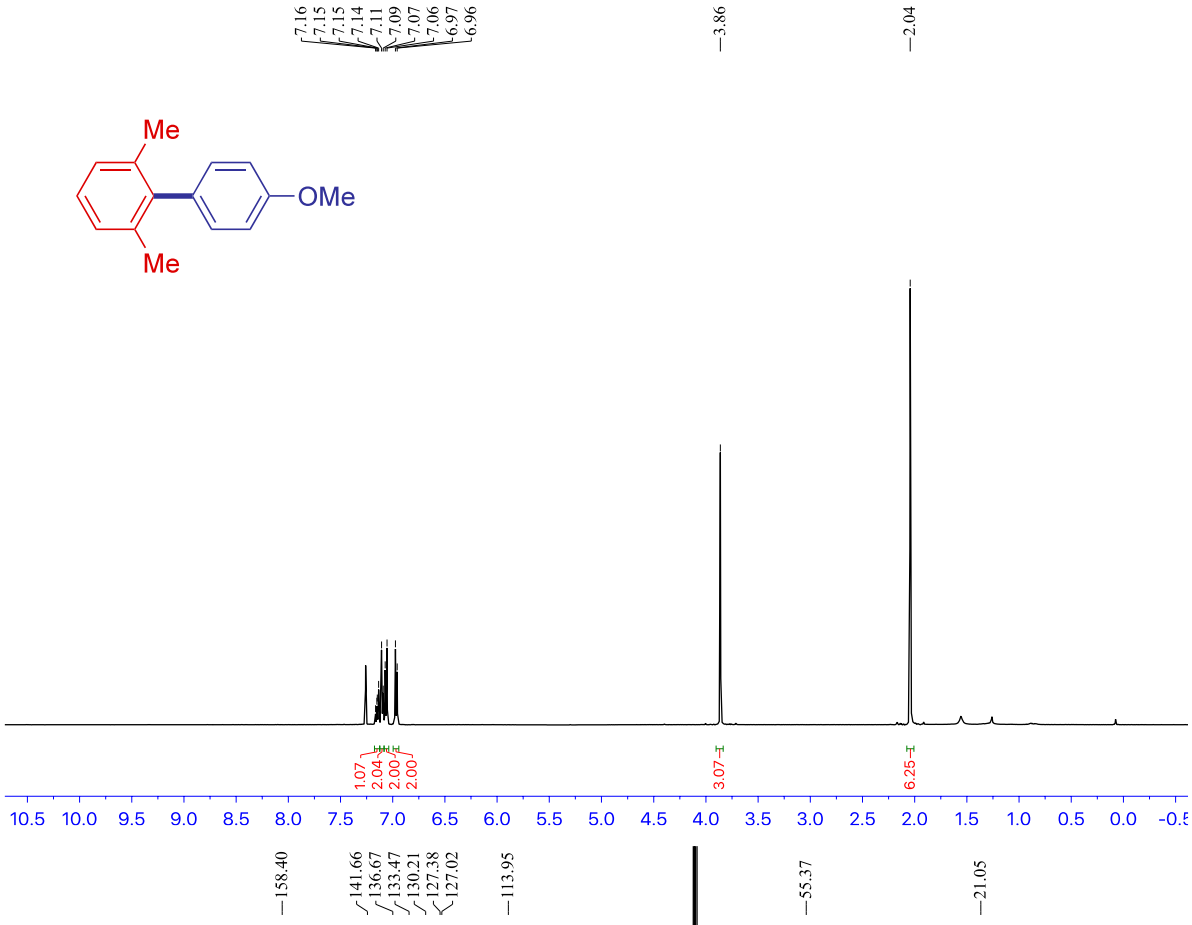

Figure S21. ^{13}C NMR spectrum of 4'-methoxy-2,6-dimethylbiphenyl, related to **Scheme 2**

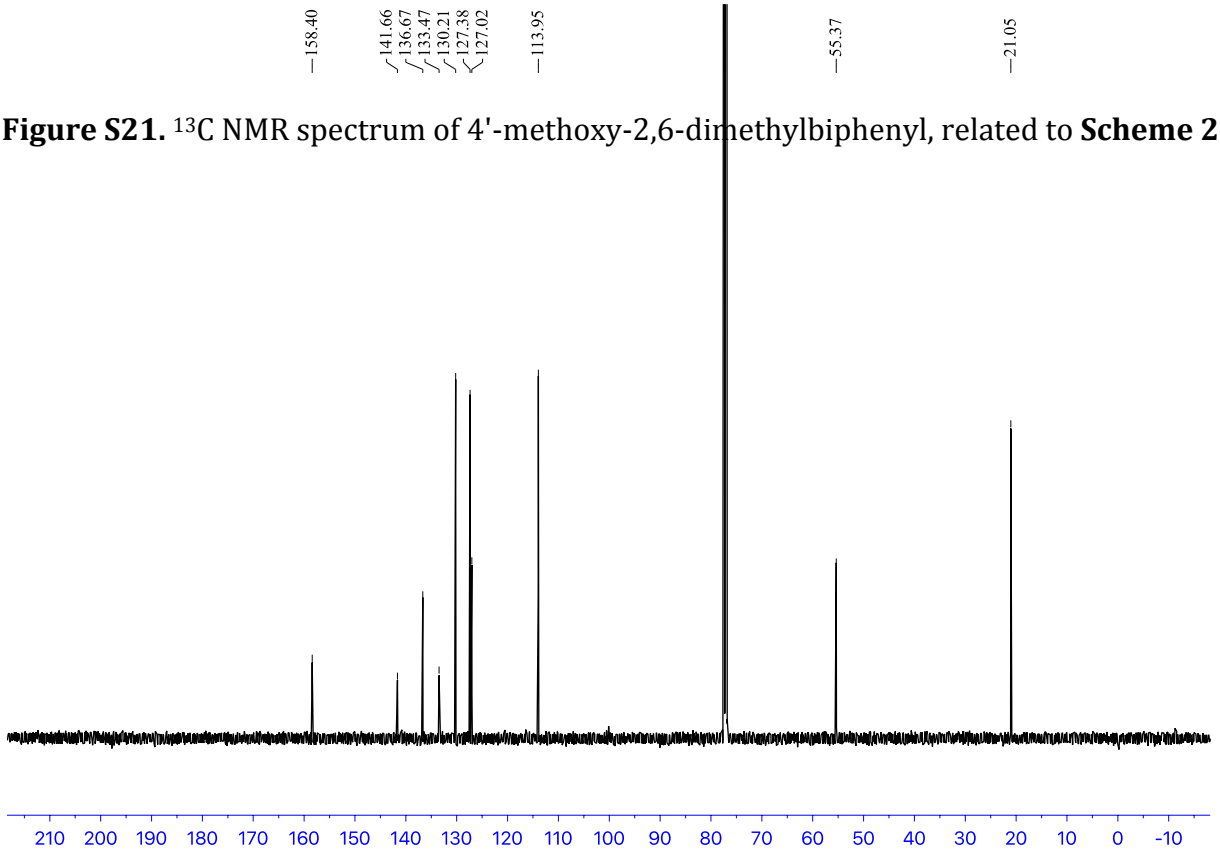

Figure S22. ^{1}H NMR spectrum of 4-cyano-4'-methylbiphenyl, related to **Scheme 2**

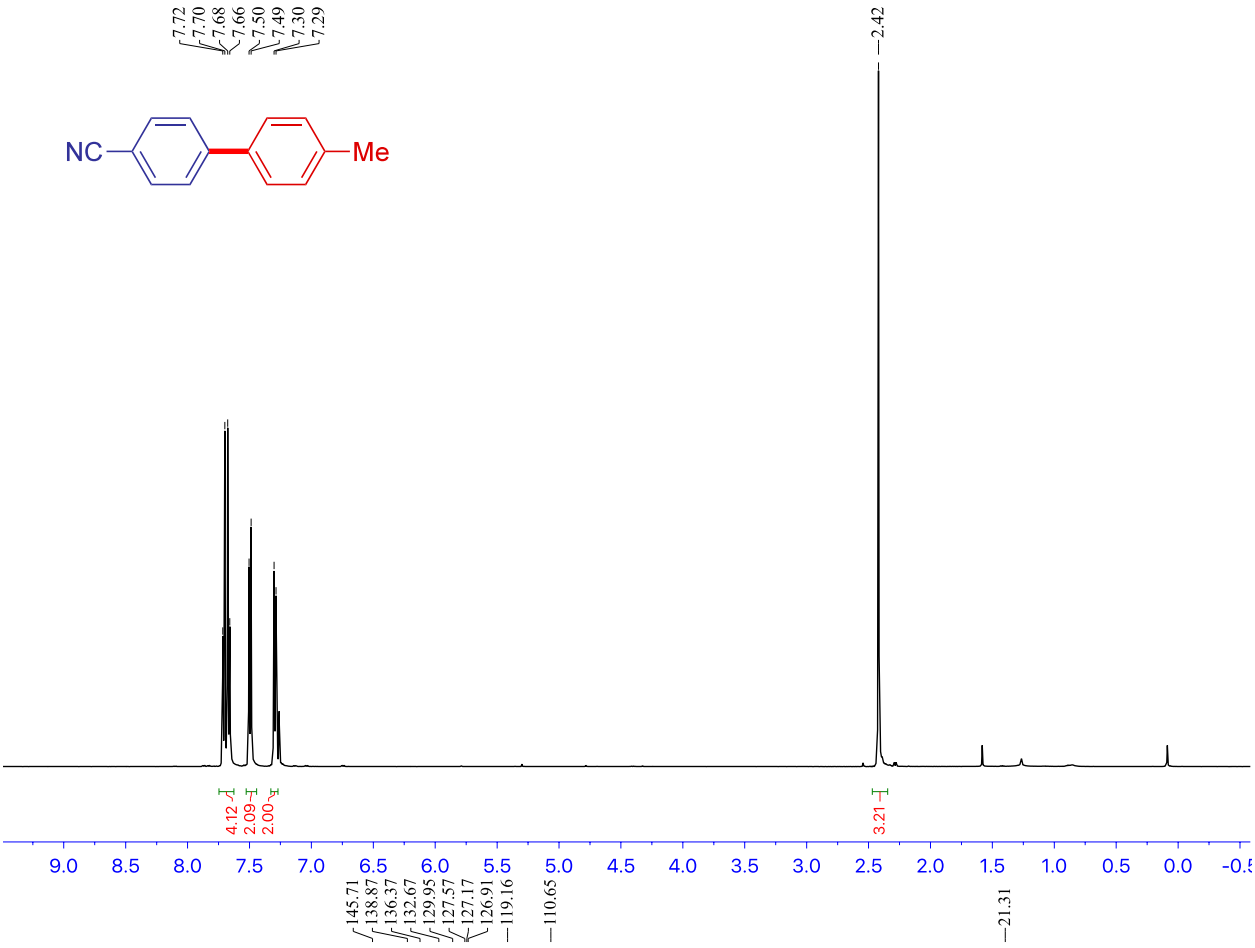

Figure S23. ^{13}C NMR spectrum of 4-cyano-4'-methylbiphenyl, related to **Scheme 2**

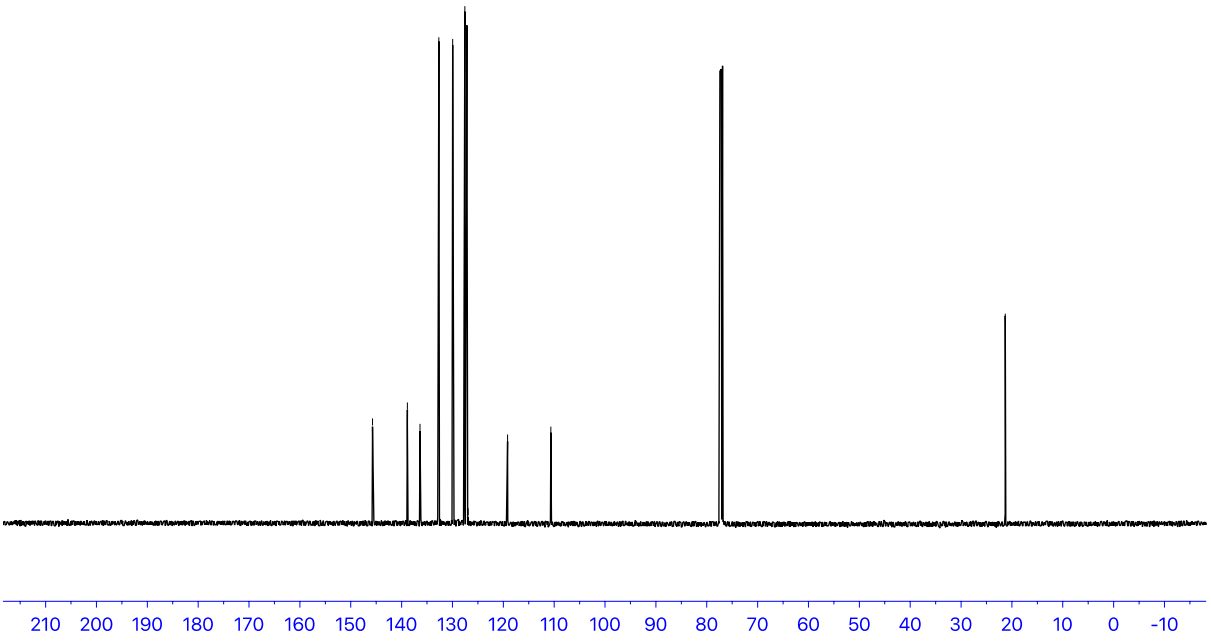

Figure S24. ^{1}H NMR spectrum of 4-hydroxy-4'-methylbiphenyl, related to **Scheme 2**

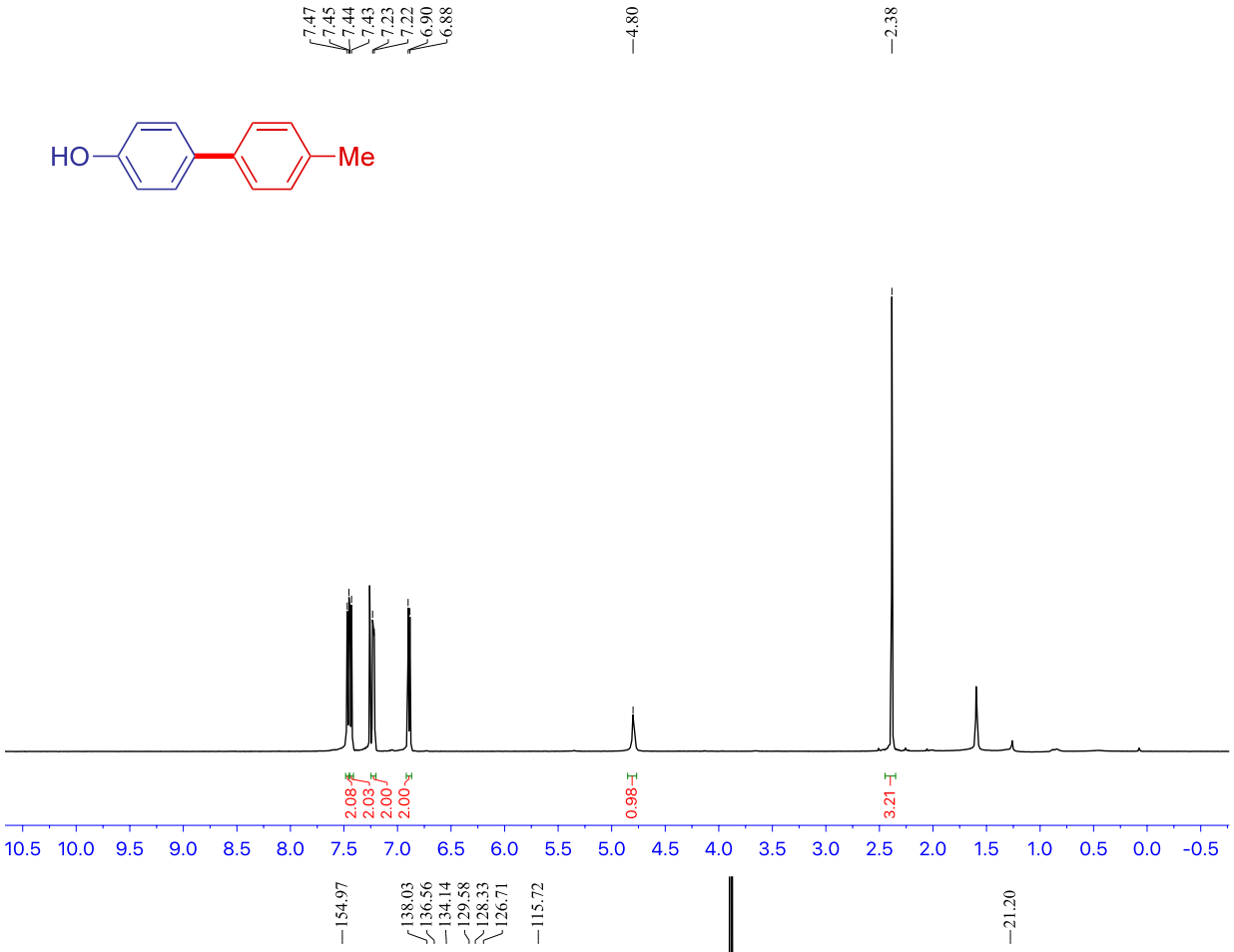

Figure S25. ^{13}C NMR spectrum of 4-hydroxy-4'-methylbiphenyl, related to **Scheme 2**

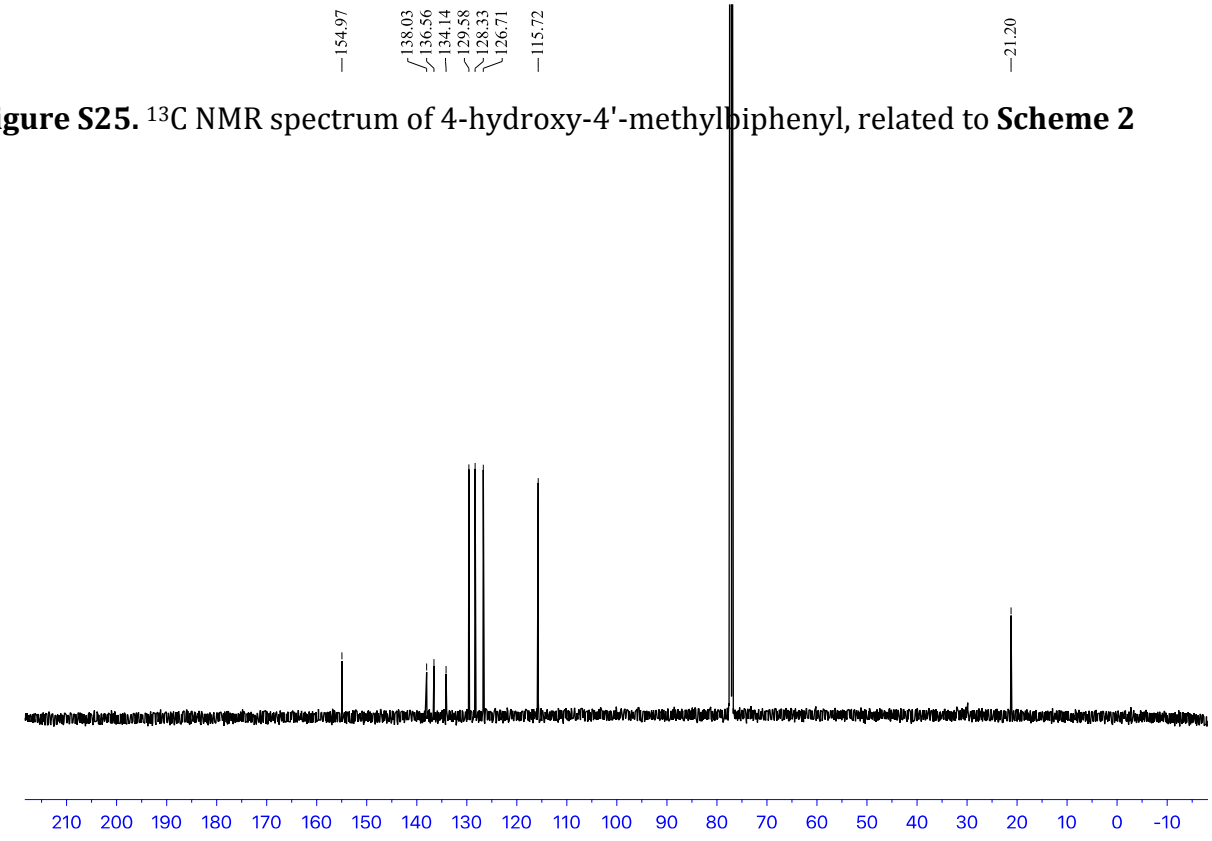

Figure S26. ^{1}H NMR spectrum of 4-amino-4'-methylbiphenyl, related to **Scheme 2**

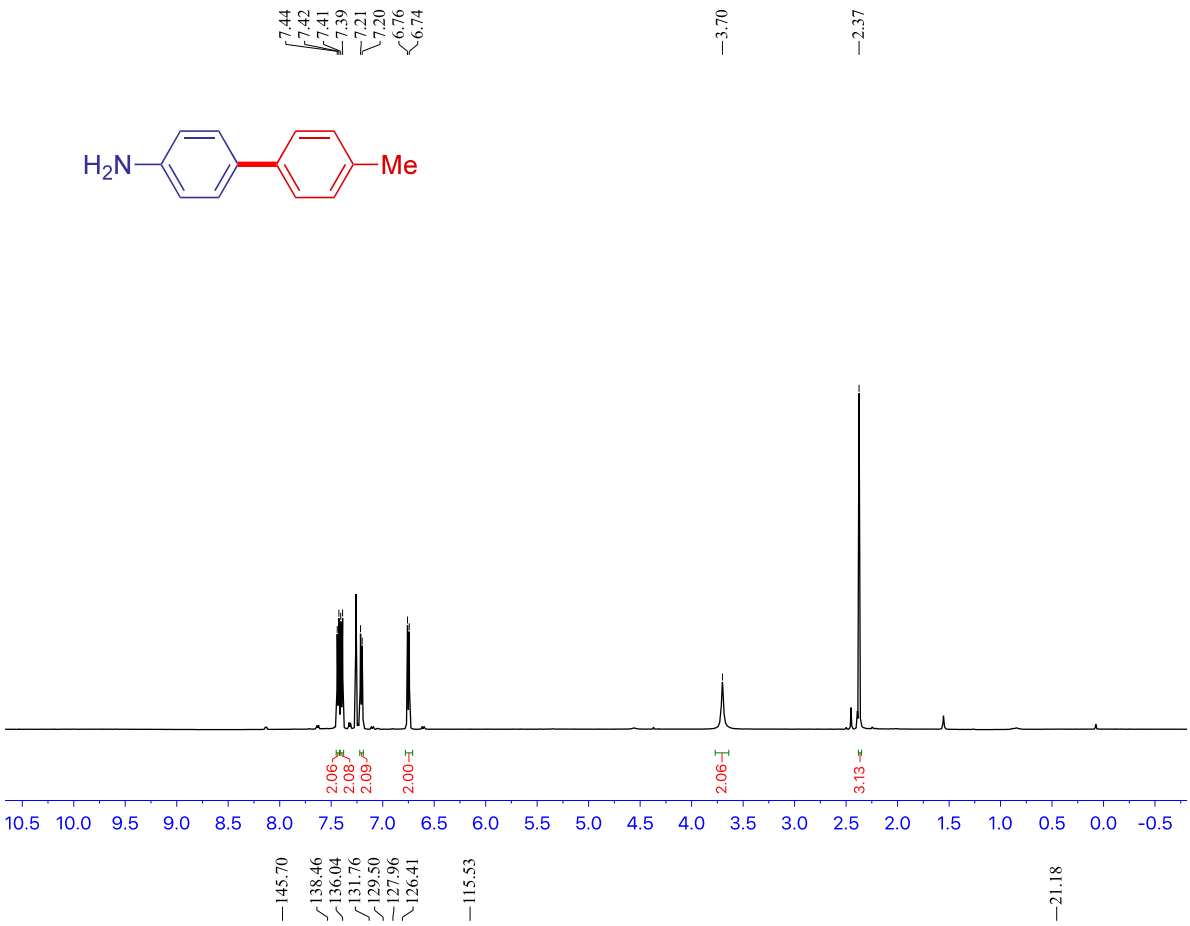

Figure S27. ^{13}C NMR spectrum of 4-amino-4'-methylbiphenyl, related to **Scheme 2**

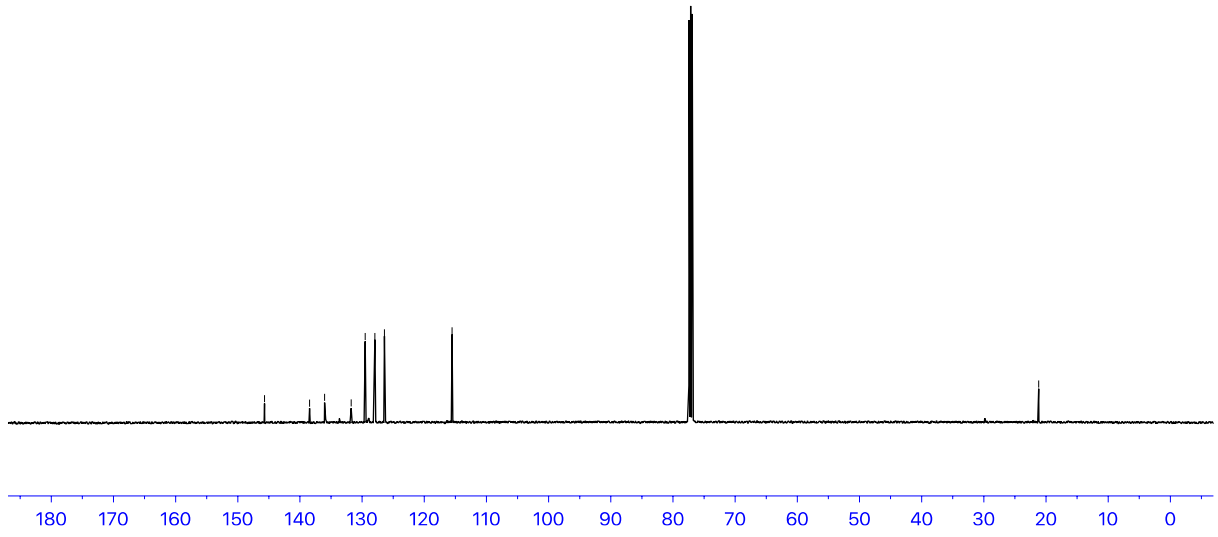

Figure S28. ^{1}H NMR spectrum of 2-amino-4'-methylbiphenyl, related to **Scheme 2**

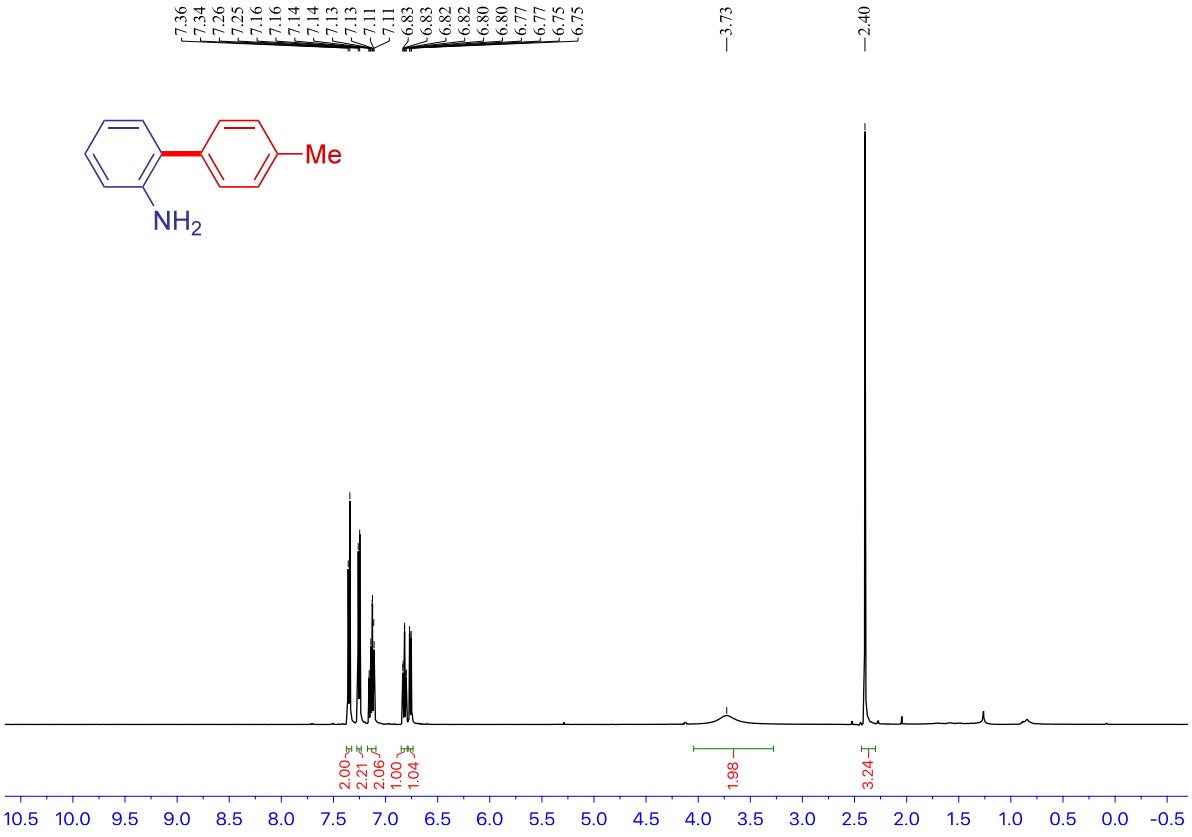

Figure S29. ^{13}C NMR spectrum of 2-amino-4'-methylbiphenyl, related to **Scheme 2**

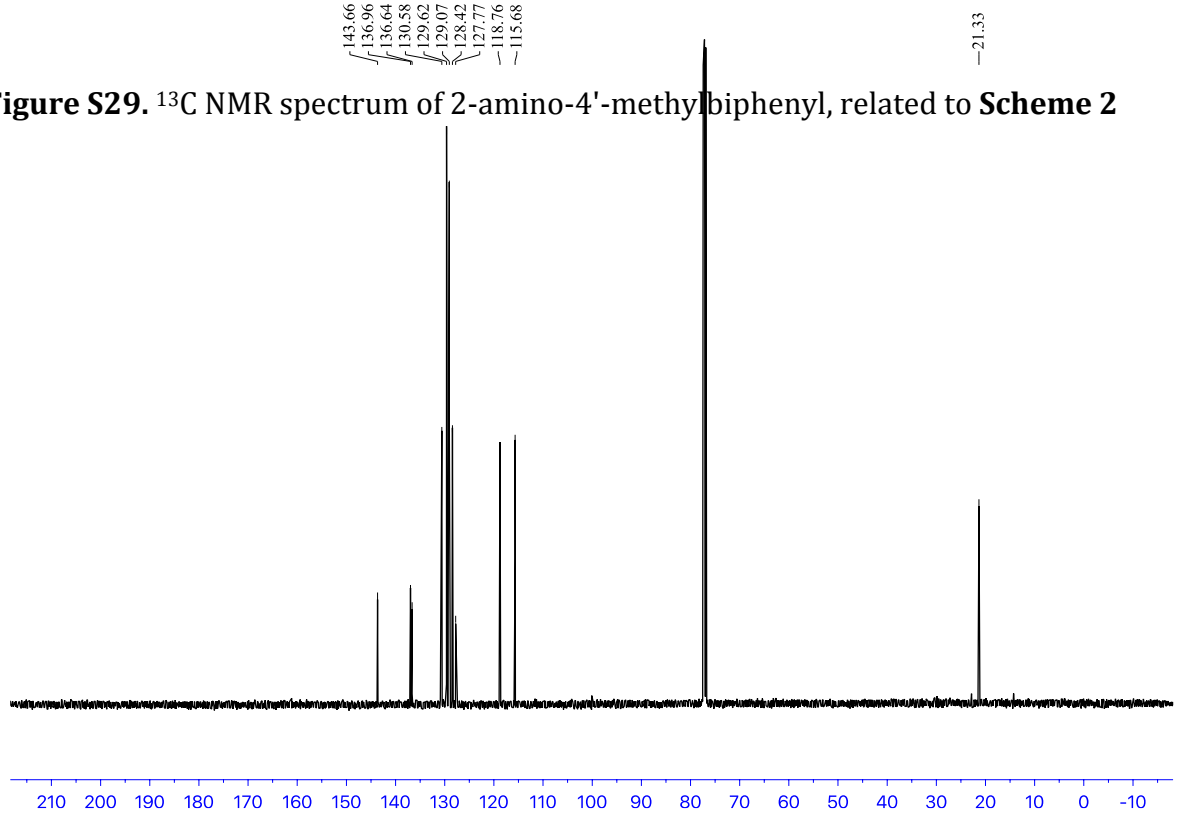

Figure S30. ^{1}H NMR spectrum of 2-(*p*-tolyl)pyridine, related to **Scheme 2**

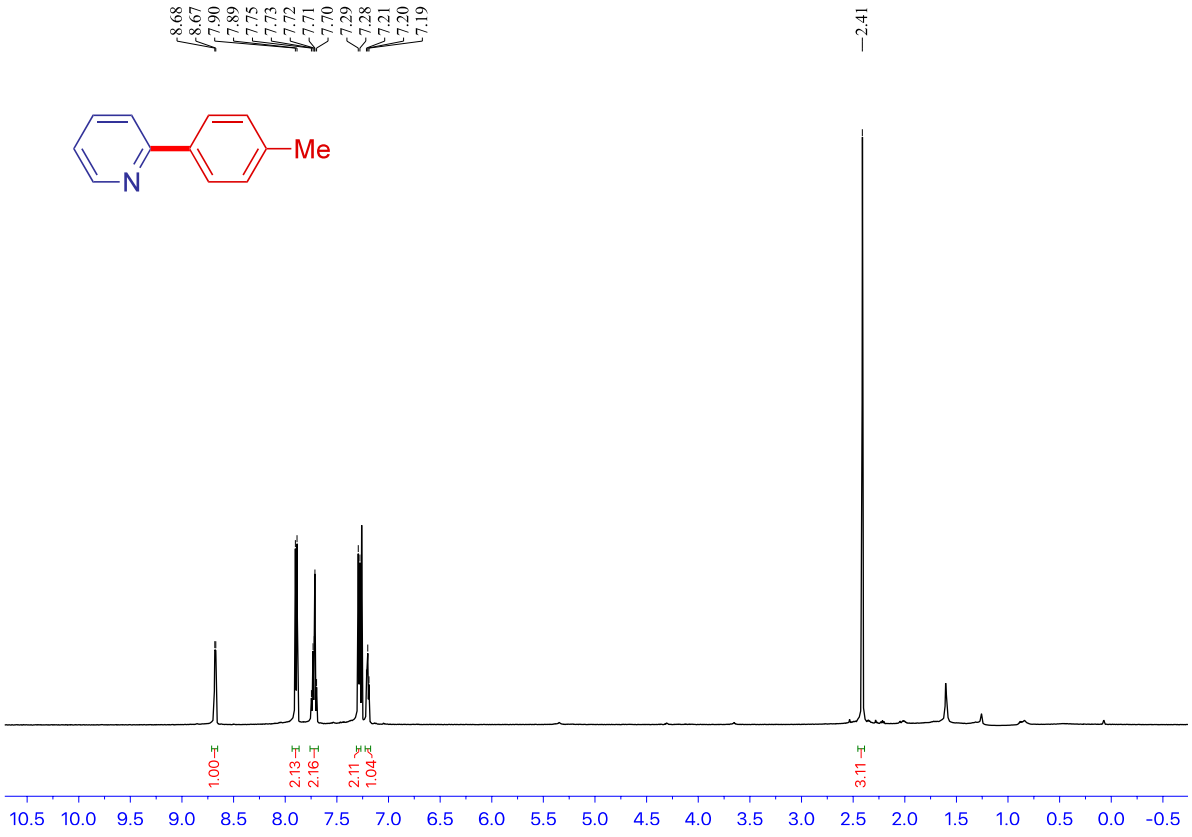

Figure S31. ^{13}C NMR spectrum of 2-(*p*-tolyl)pyridine, related to **Scheme 2**

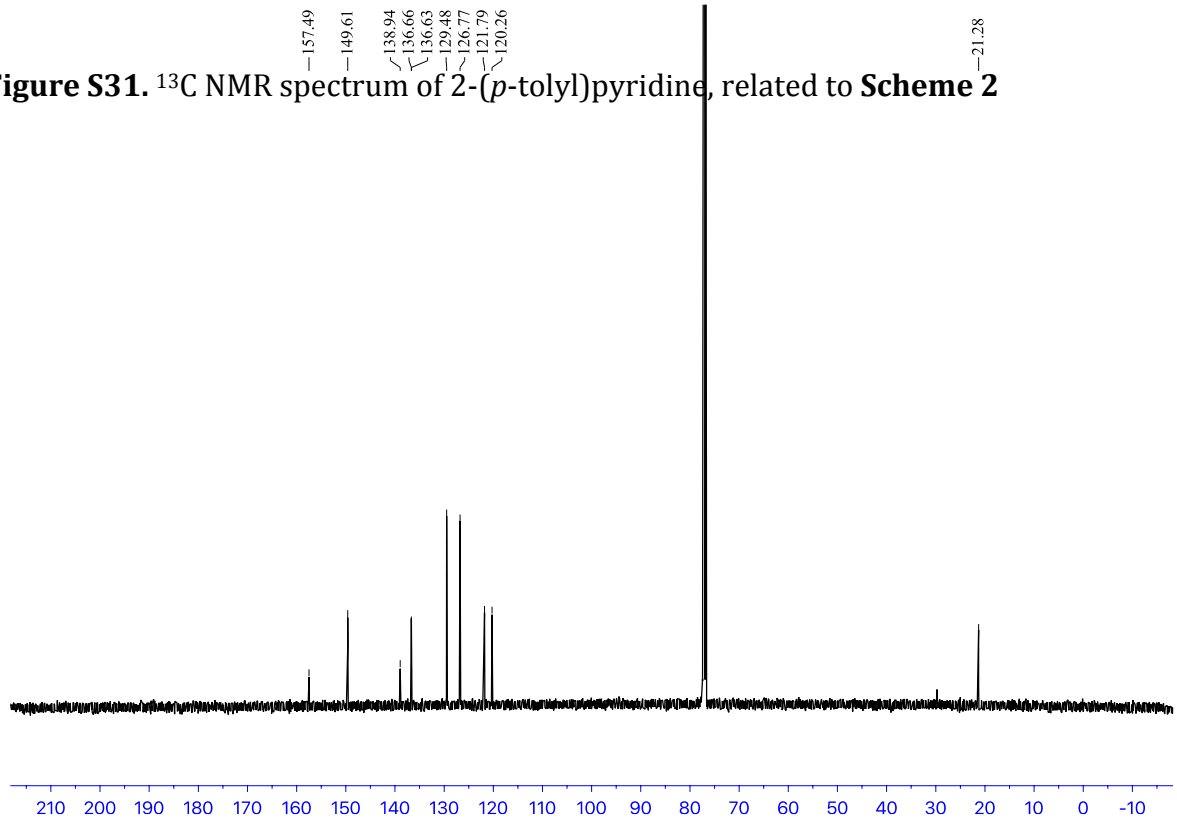

Figure S32. ^{1}H NMR spectrum of 3-(6-methoxynaphthalen-2-yl)pyridine, related to **Scheme 2**

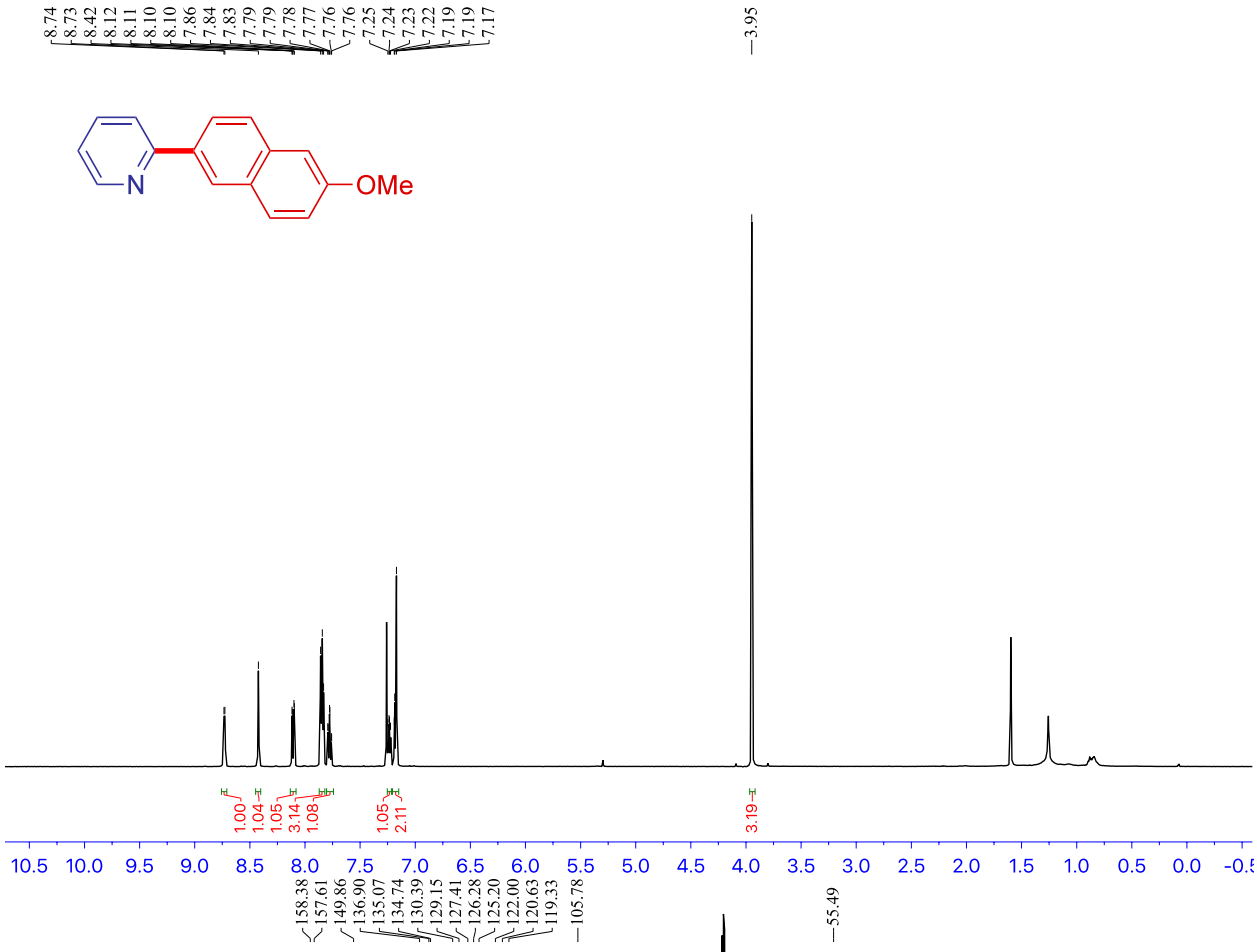

Figure S33. ^{13}C NMR spectrum of 3-(6-methoxynaphthalen-2-yl)pyridine, related to **Scheme 2**

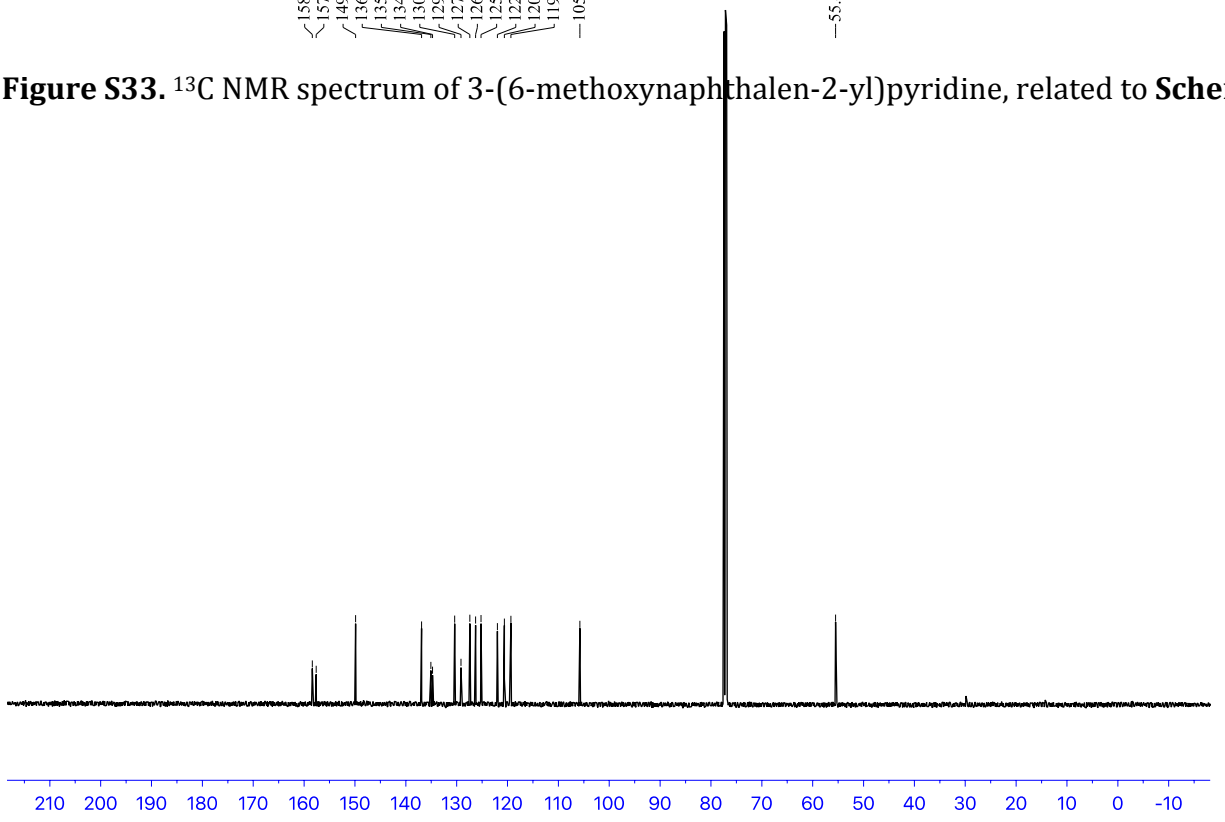

Figure S34. ^{1}H NMR spectrum of methyl 2-(*p*-tolyl)nicotinate, related to **Scheme 2**

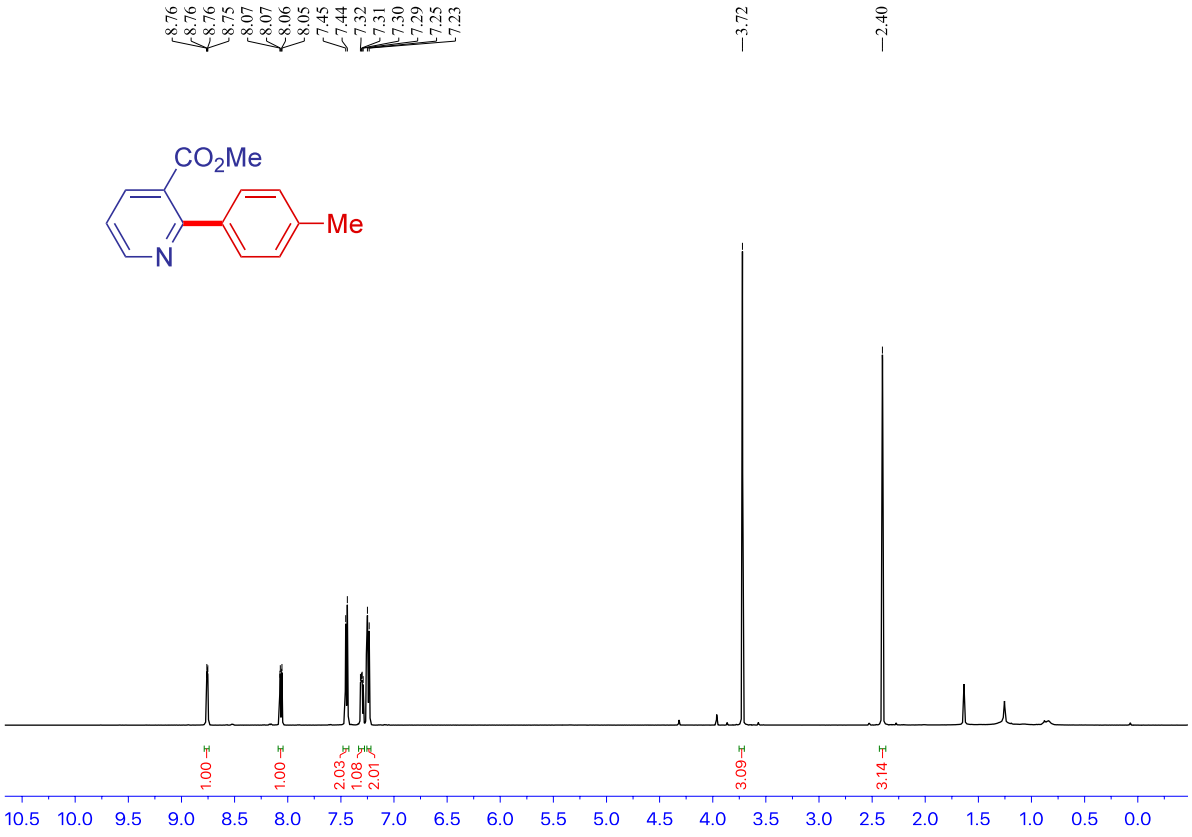

Figure S35. ^{13}C NMR spectrum of methyl 2-(*p*-tolyl)nicotinate, related to **Scheme 2**

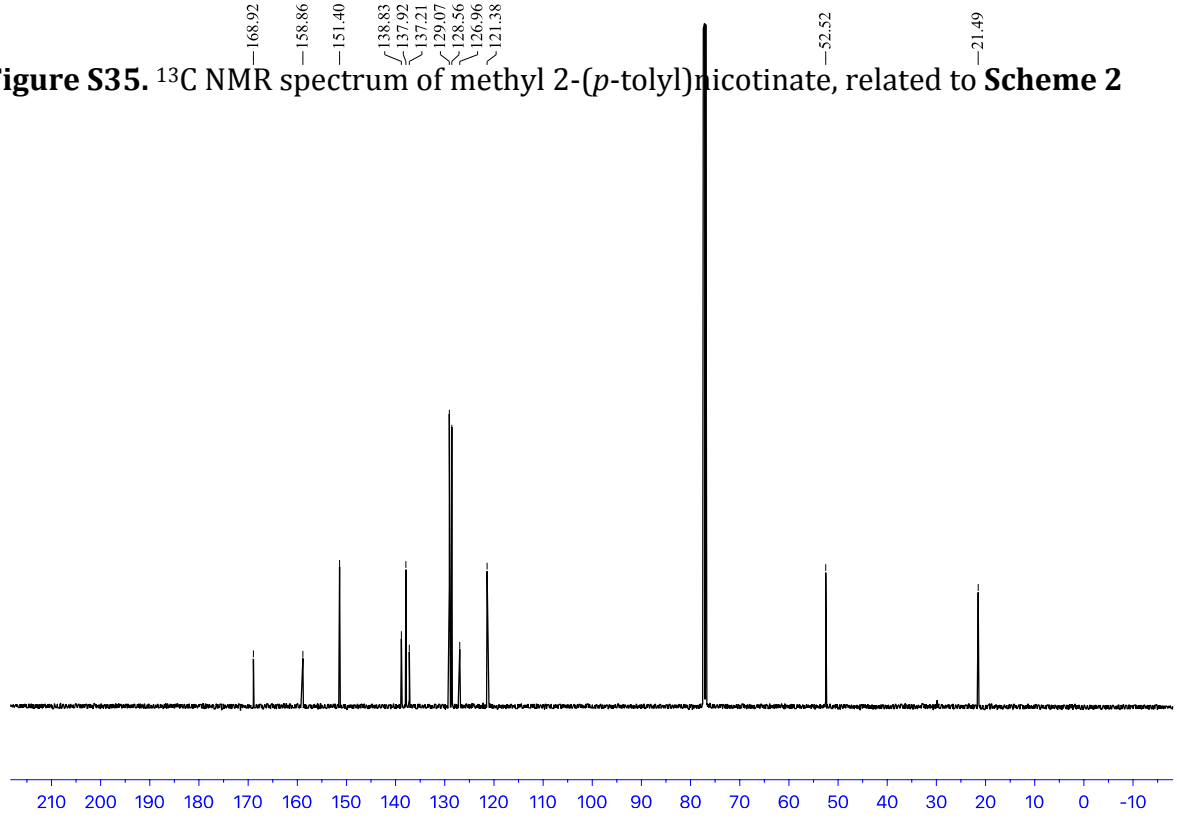

Figure S36. ^{1}H NMR spectrum of 3-(*p*-tolyl)pyridine, related to **Scheme 2**

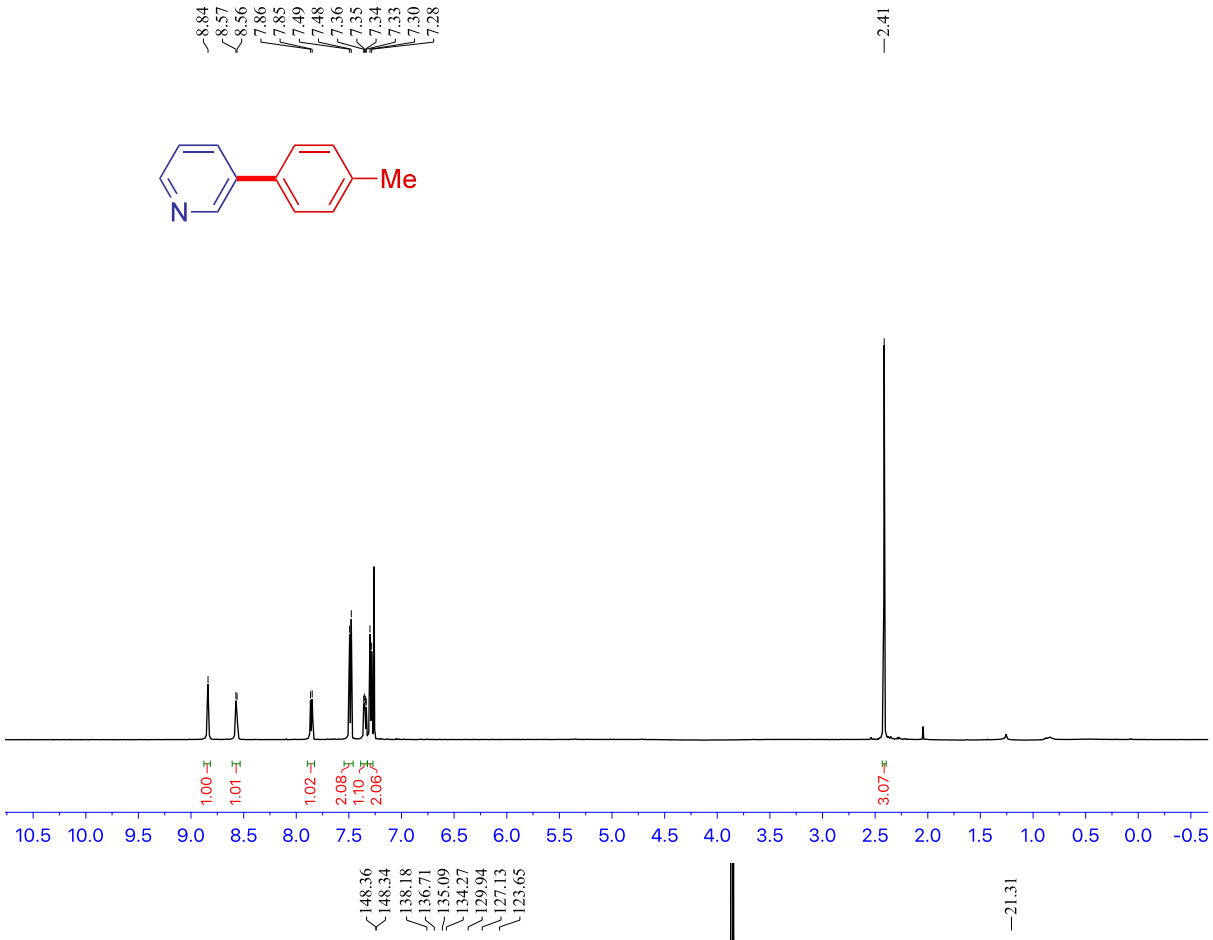

Figure S37. ^{13}C NMR spectrum of 3-(*p*-tolyl)pyridine, related to **Scheme 2**

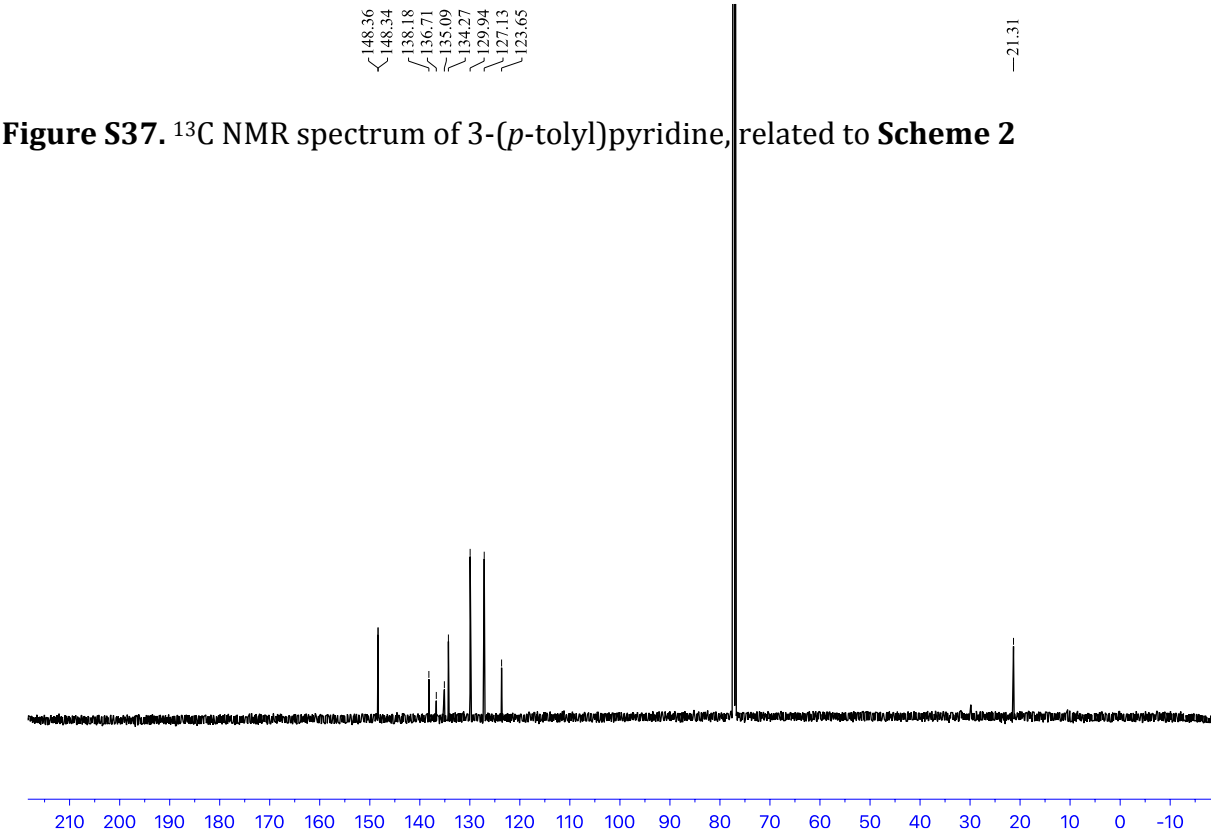

Figure S38. ^{1}H NMR spectrum of 3-(6-methoxynaphthalen-2-yl)pyridine, related to **Scheme 2**

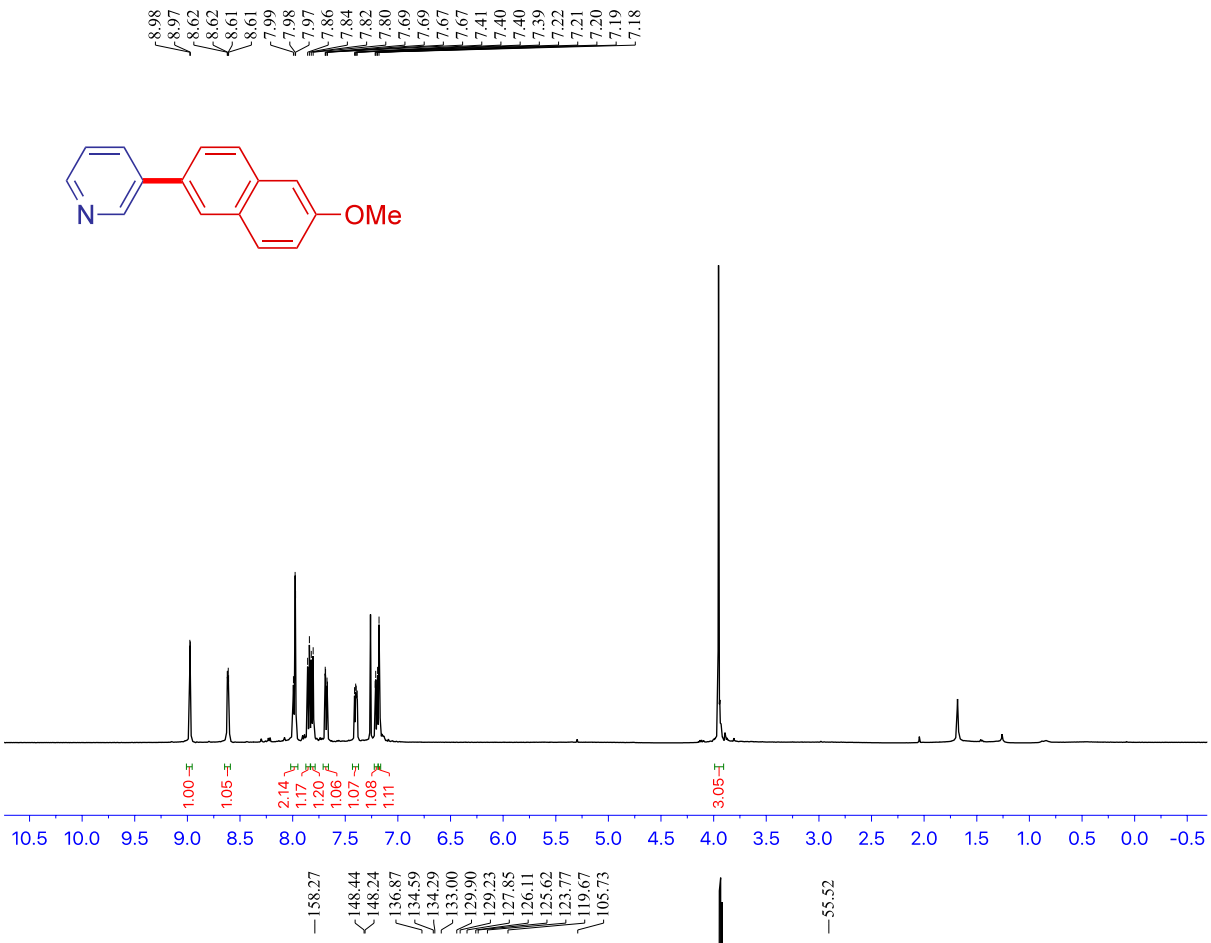

Figure S39. ^{13}C NMR spectrum of 3-(6-methoxynaphthalen-2-yl)pyridine, related to **Scheme 2**

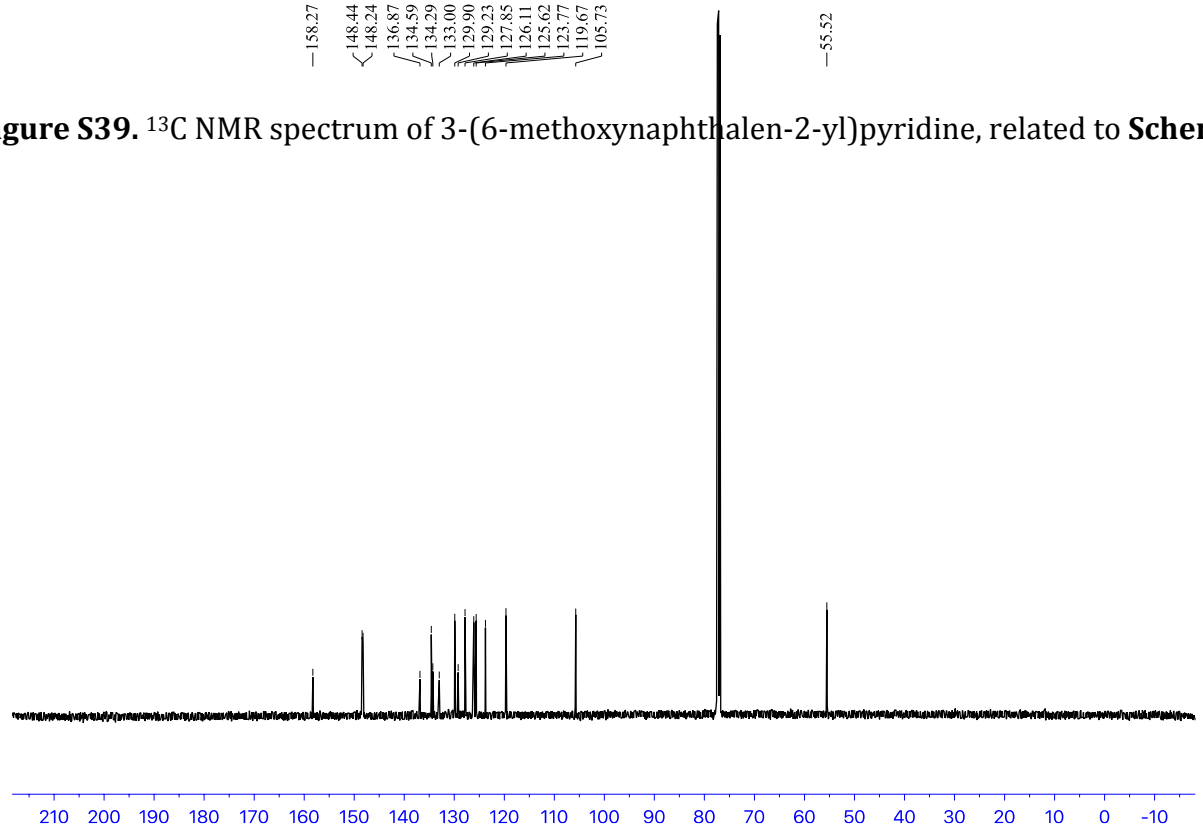

Figure S40. ^{1}H NMR spectrum of 5-(3,4-dimethoxyphenyl)-1*H*-indole, related to **Scheme 2**

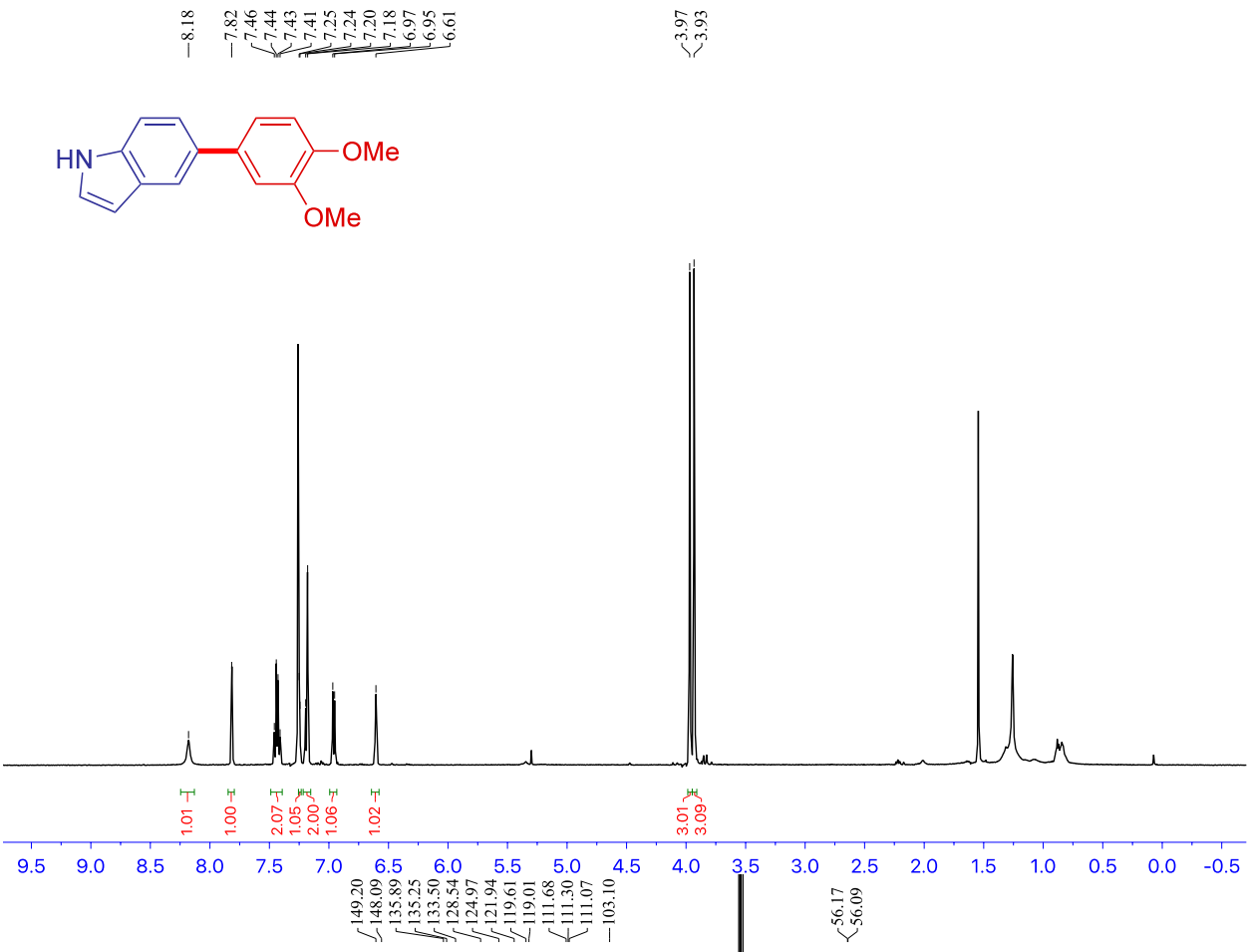

Figure S41. ^{13}C NMR spectrum of 5-(3,4-dimethoxyphenyl)-1*H*-indole, related to **Scheme 2**

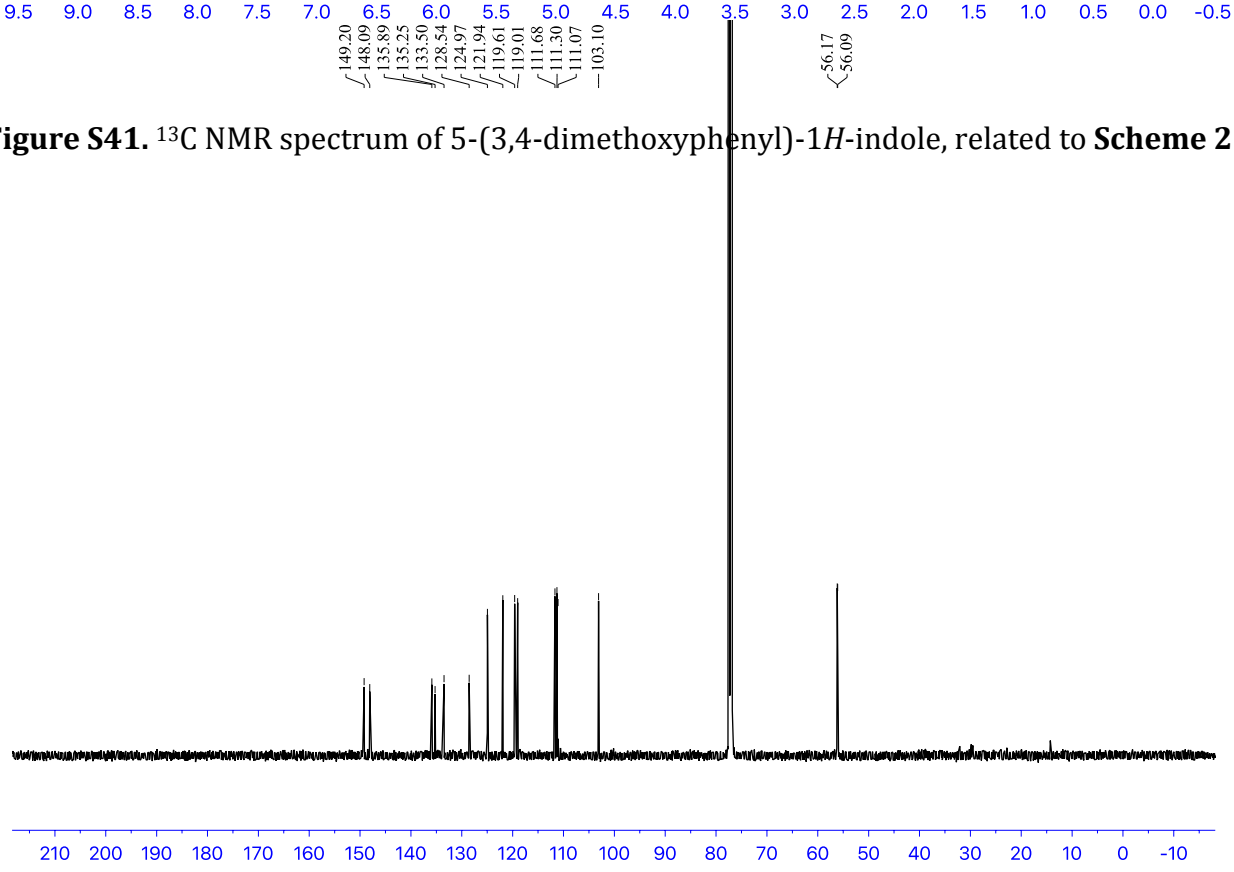

Figure S42. ^{1}H NMR spectrum of 2-(4-fluorophenyl)quinoline, related to **Scheme 2**

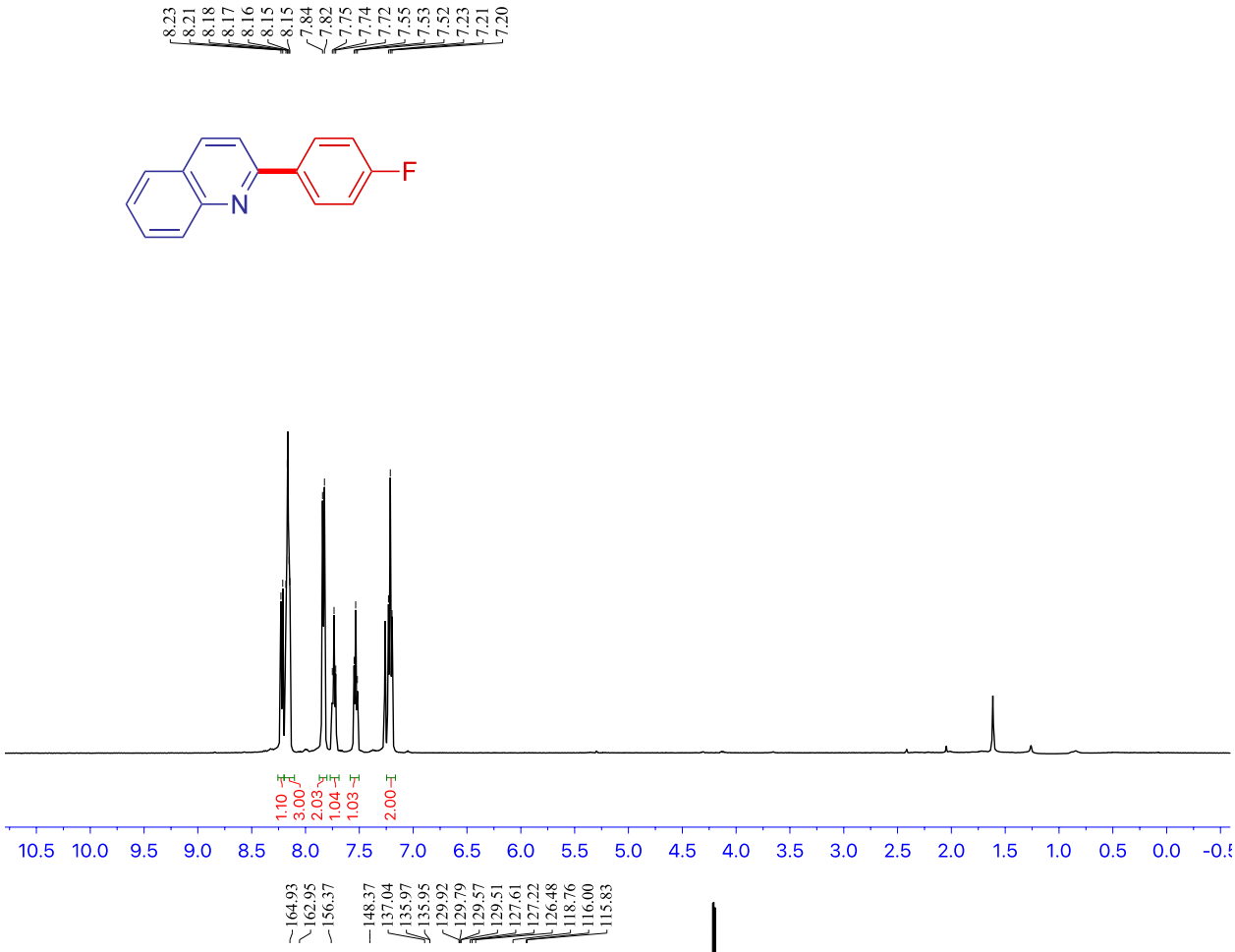

Figure S43. ^{13}C NMR spectrum of 2-(4-fluorophenyl)quinoline, related to **Scheme 2**

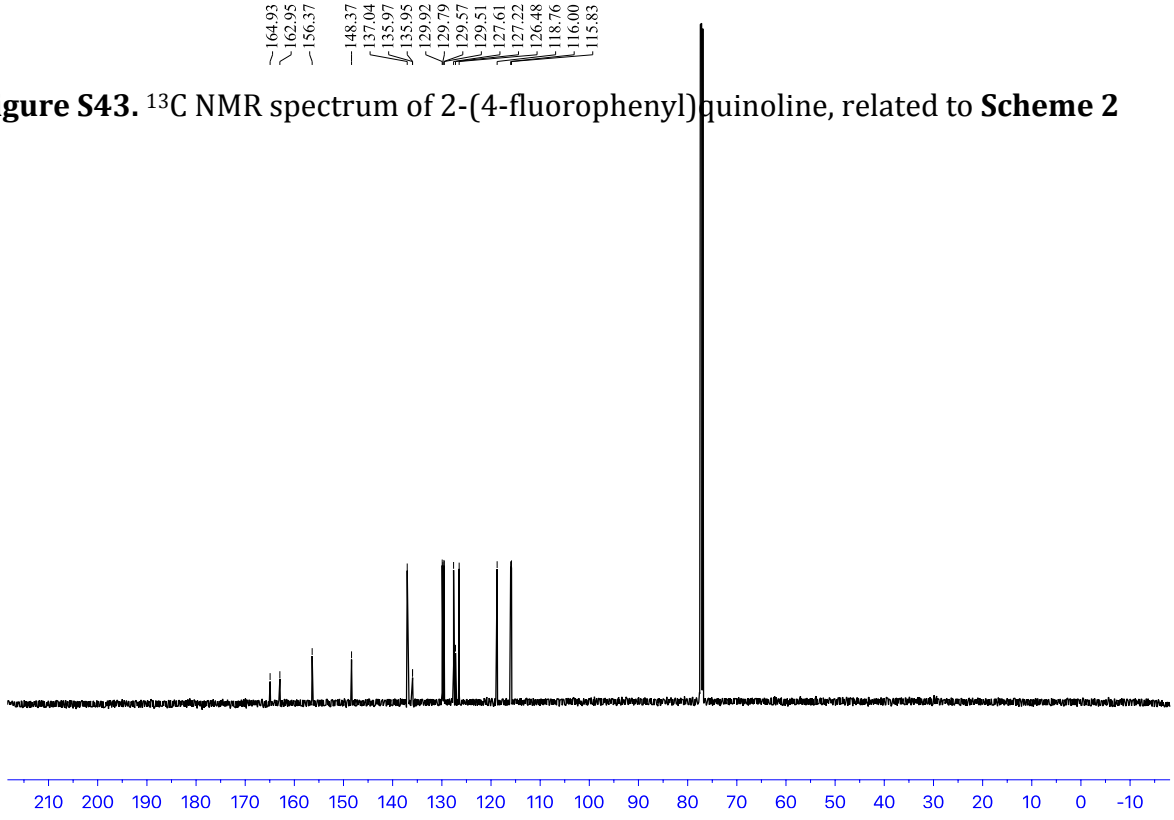

Figure S44. ^{19}F NMR spectrum of 2-(4-fluorophenyl)quinoline, related to **Scheme 2**

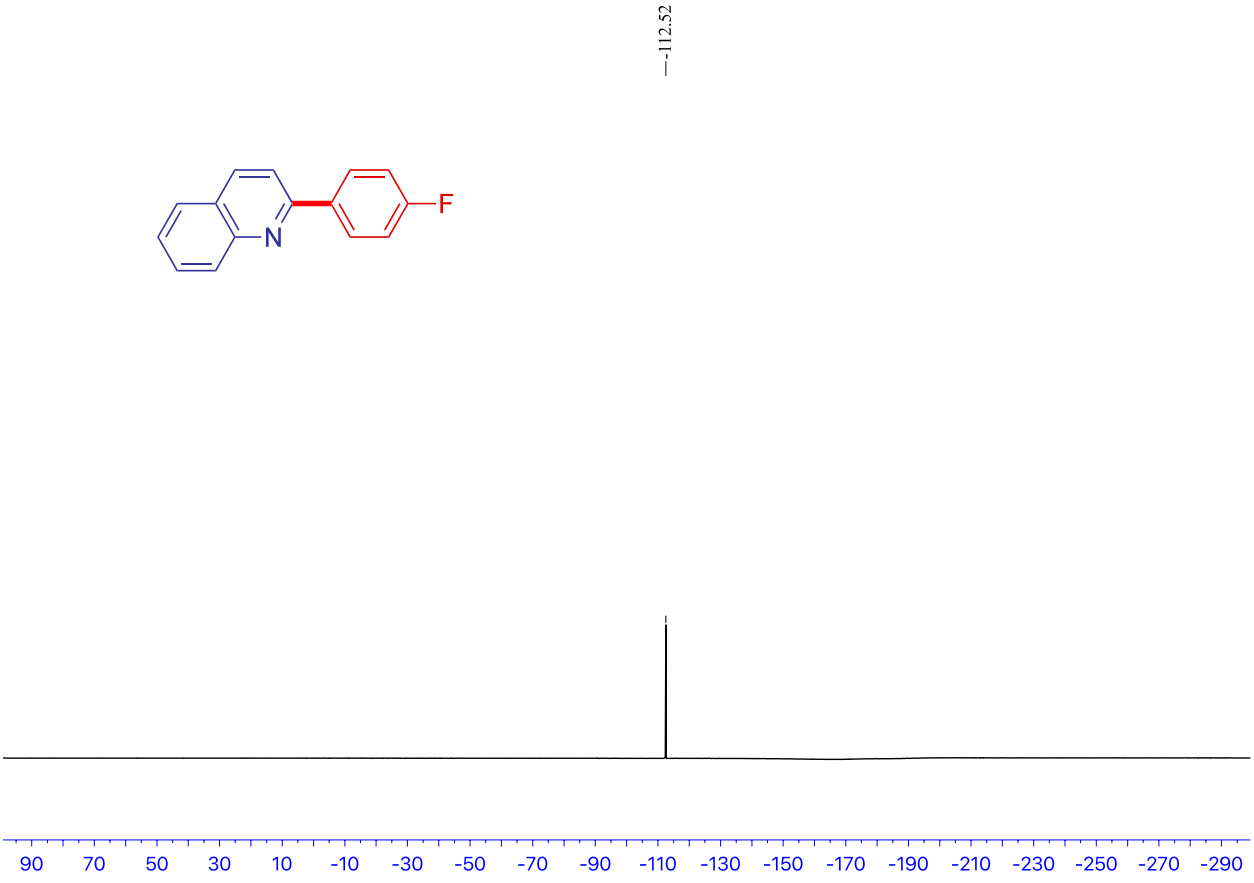

Figure S45. ^{1}H NMR spectrum of 2,4-dimethoxy-6-(*p*-tolyl)-1,3,5-triazine, related to **Scheme 2**

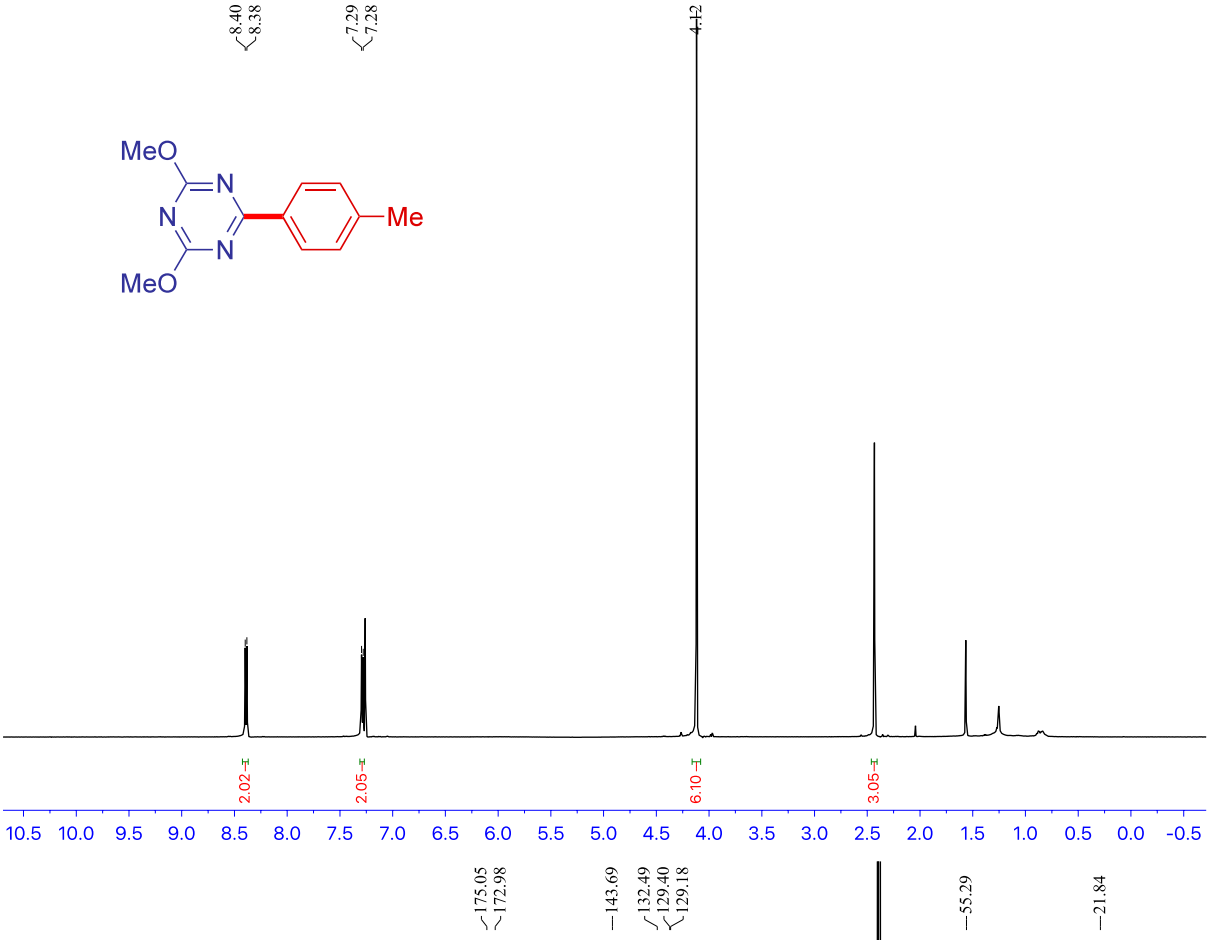

Figure S46. ^{13}C NMR spectrum of 2,4-dimethoxy-6-(*p*-tolyl)-1,3,5-triazine, related to **Scheme 2**

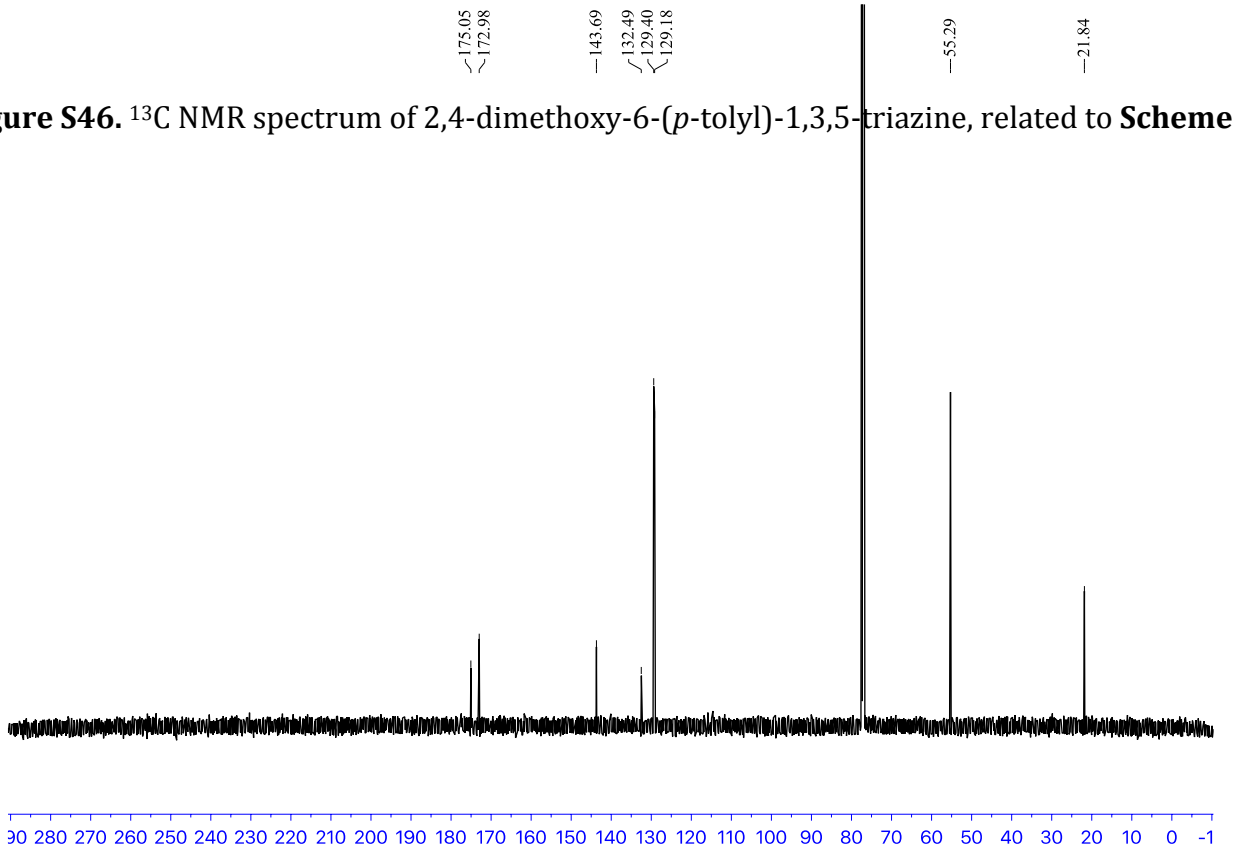

Figure S47. ^{1}H NMR spectrum of 4-(4-(*tert*-butyl)phenyl)-7-nitrobenzo[*c*][1,2,5]oxadiazole, related to **Scheme 2**

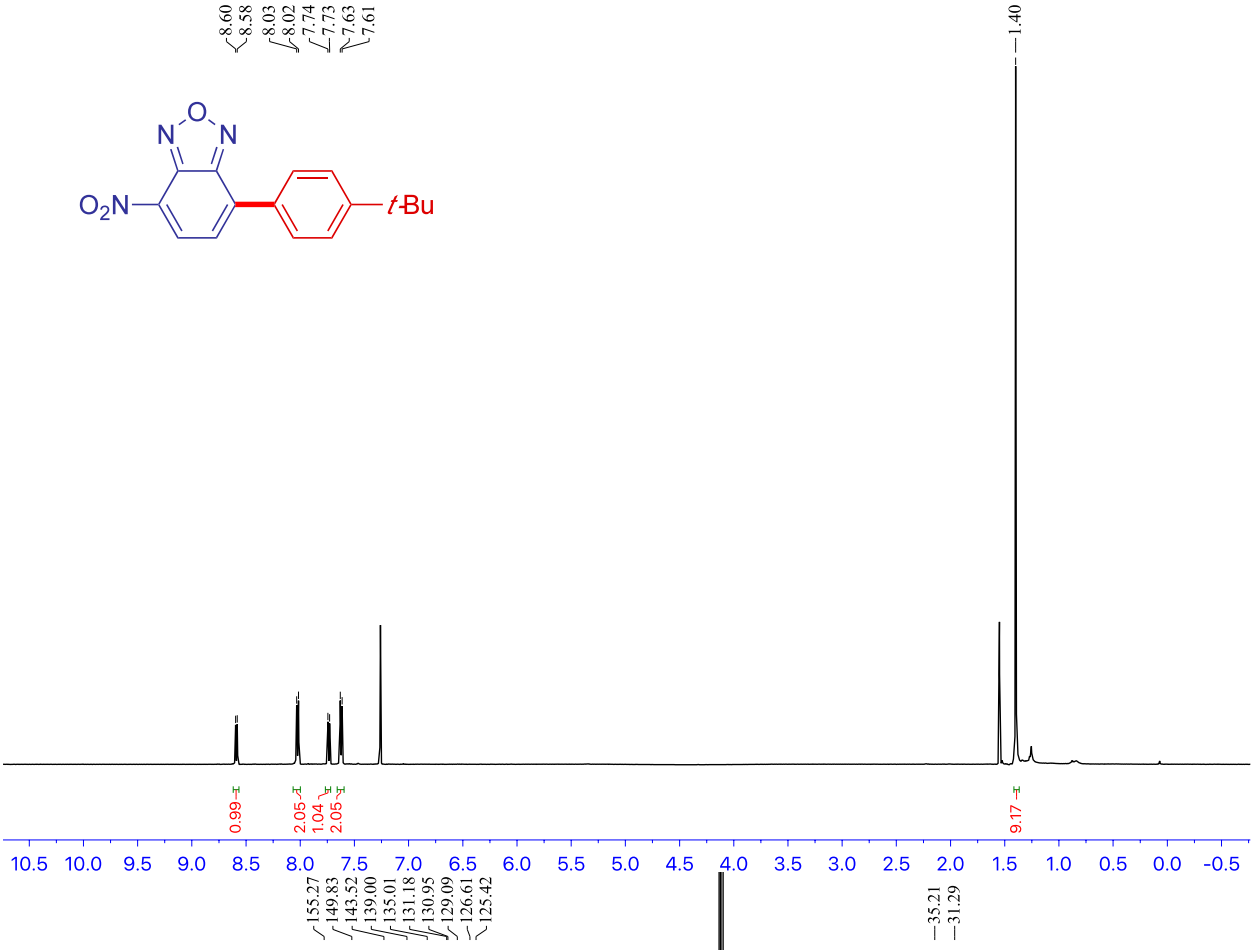

Figure S48. ^{13}C NMR spectrum of 4-(4-(*tert*-butyl)phenyl)-7-nitrobenzo[*c*][1,2,5]oxadiazole, related to **Scheme 2**

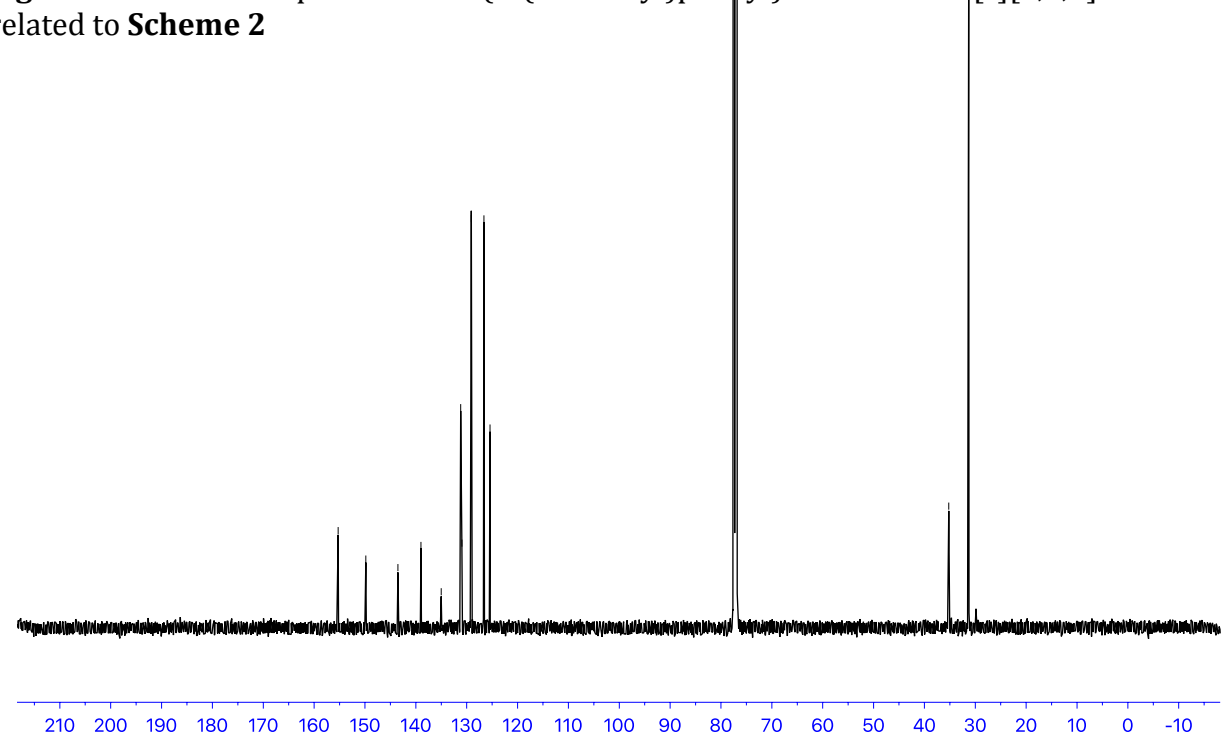

Figure S49. ^{1}H NMR spectrum of 3',4'-dimethoxy-4-formylbiphenyl, related to **Scheme 2**

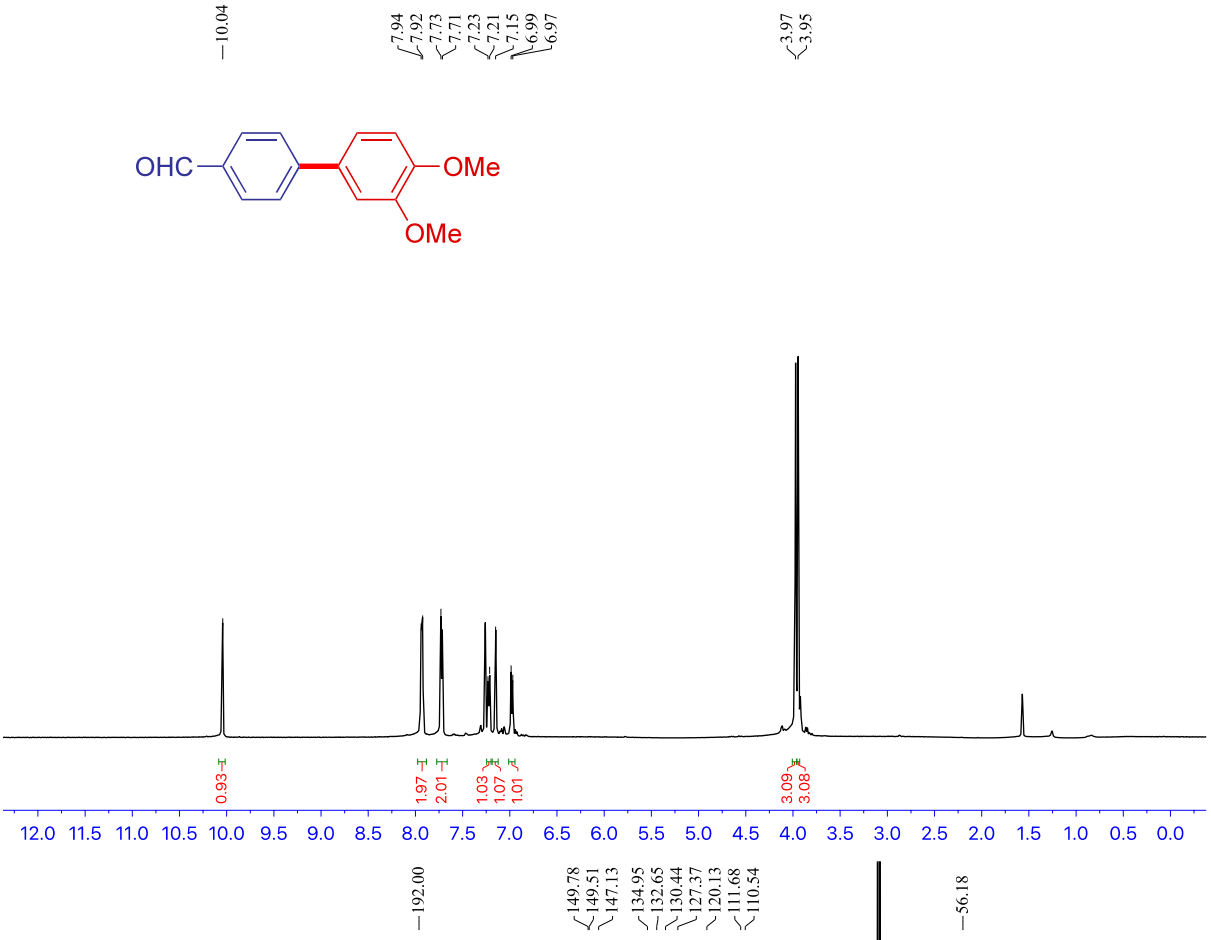

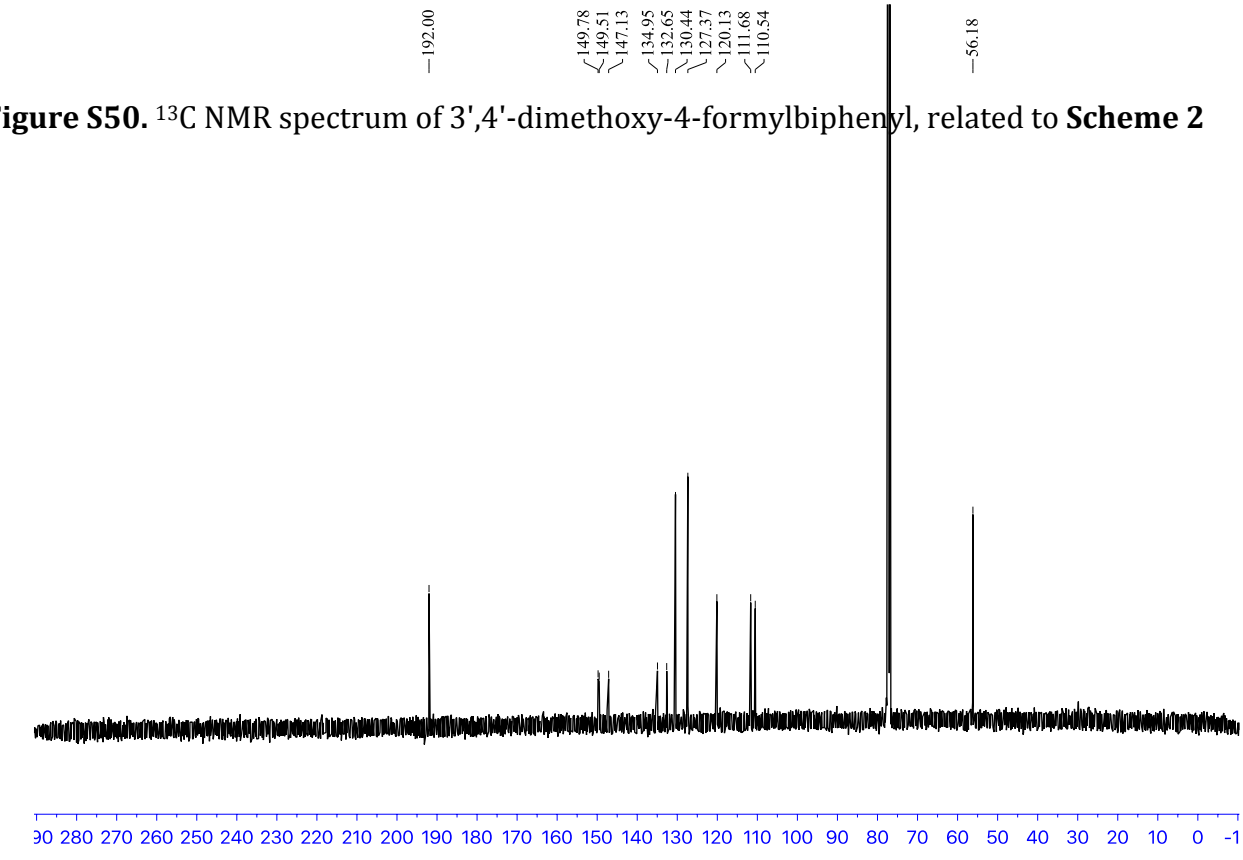

Figure S50. ^{13}C NMR spectrum of 3',4'-dimethoxy-4-formylbiphenyl, related to **Scheme 2**

Figure S51. [1]H NMR spectrum of 4'-methyl-[1,1'-biphenyl]-4-carboxylic acid, related to **Scheme 2**

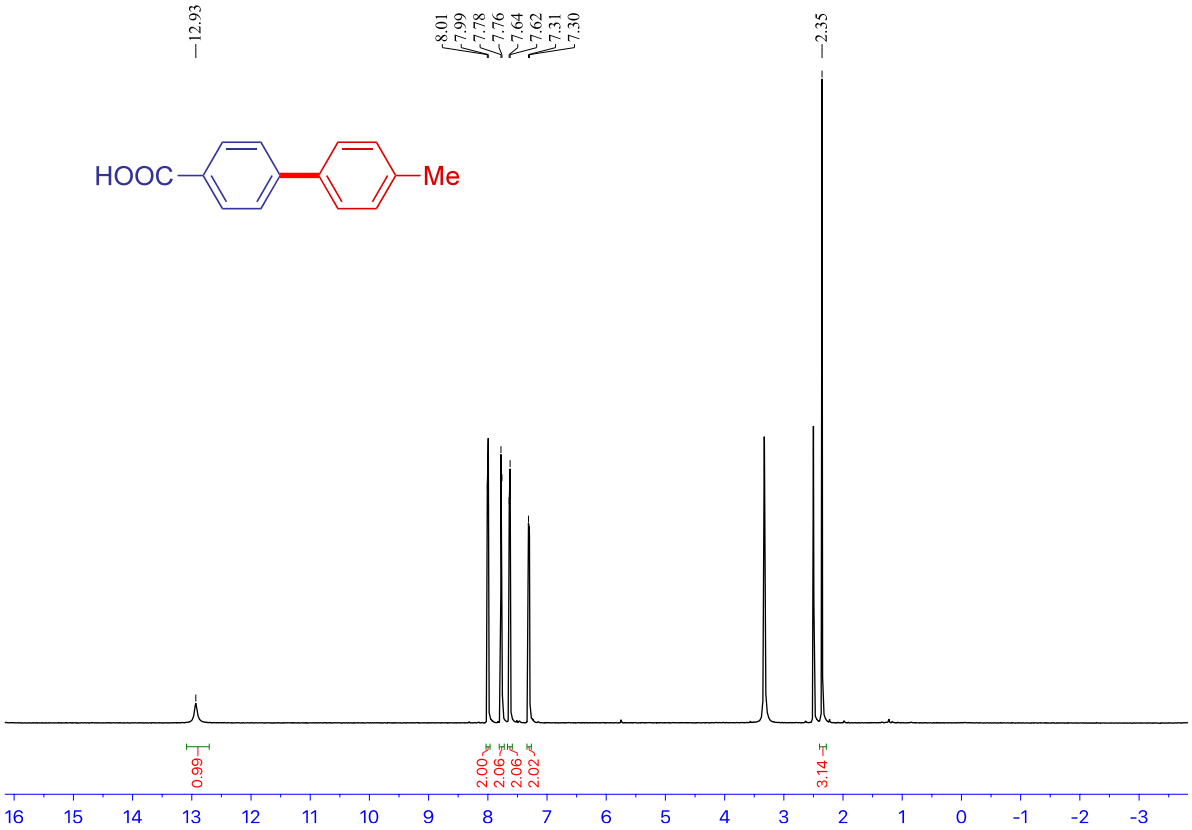

Figure S52. [13]C NMR spectrum of 4'-methyl-[1,1'-biphenyl]-4-carboxylic acid, related to **Scheme 2**

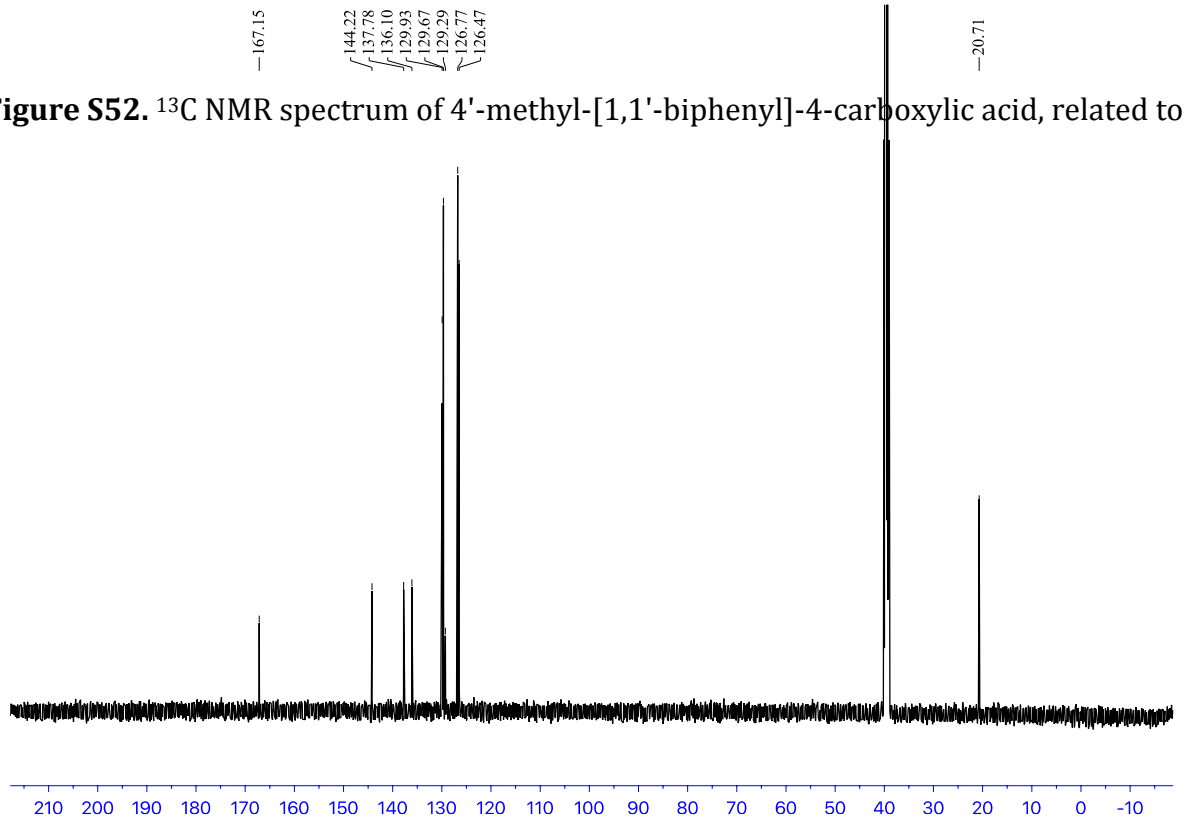

Figure S53. ^{1}H NMR spectrum of 5-(*p*-tolyl)benzo[*d*][1,3]dioxole, related to **Scheme 2**

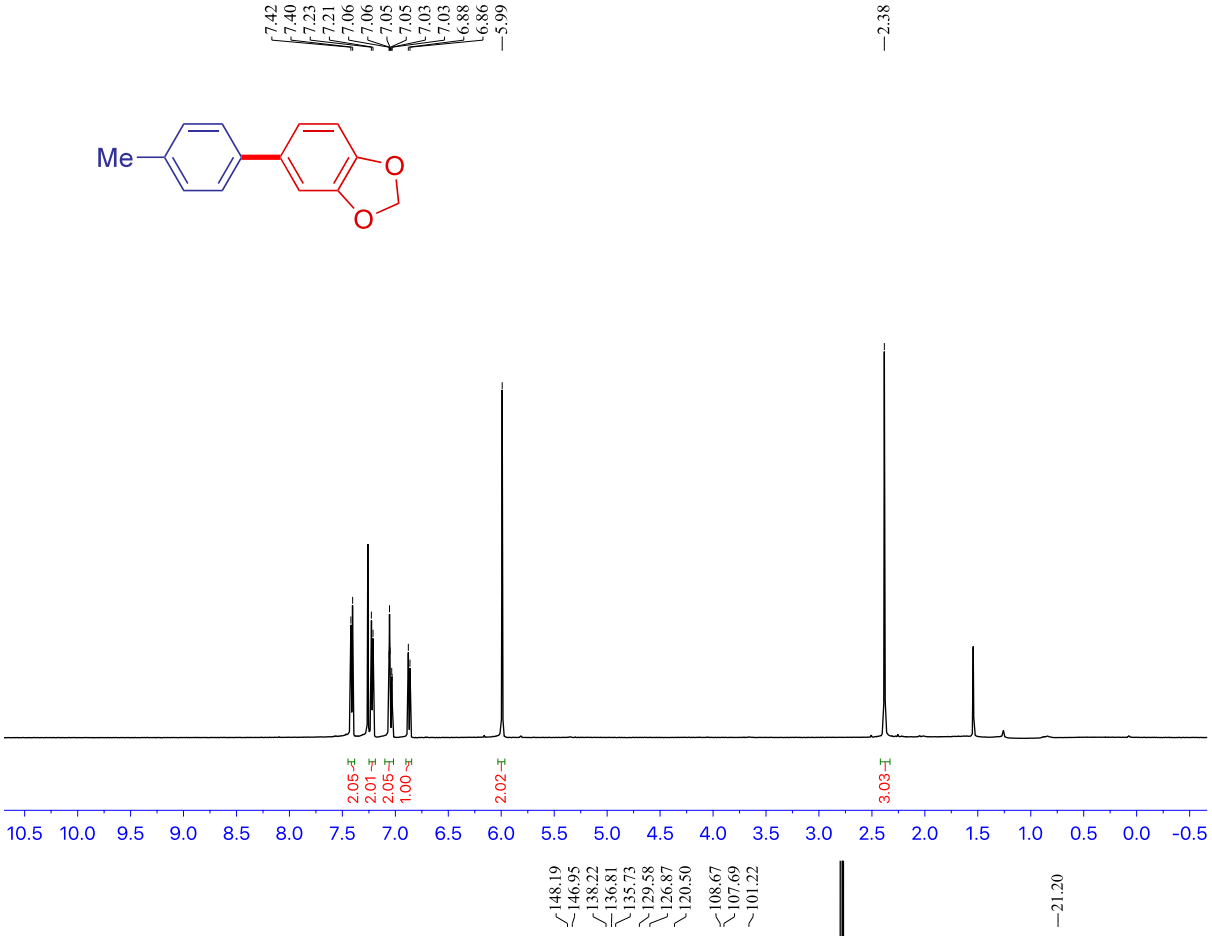

Figure S54. ^{13}C NMR spectrum of 5-(*p*-tolyl)benzo[*d*][1,3]dioxole, related to **Scheme 2**

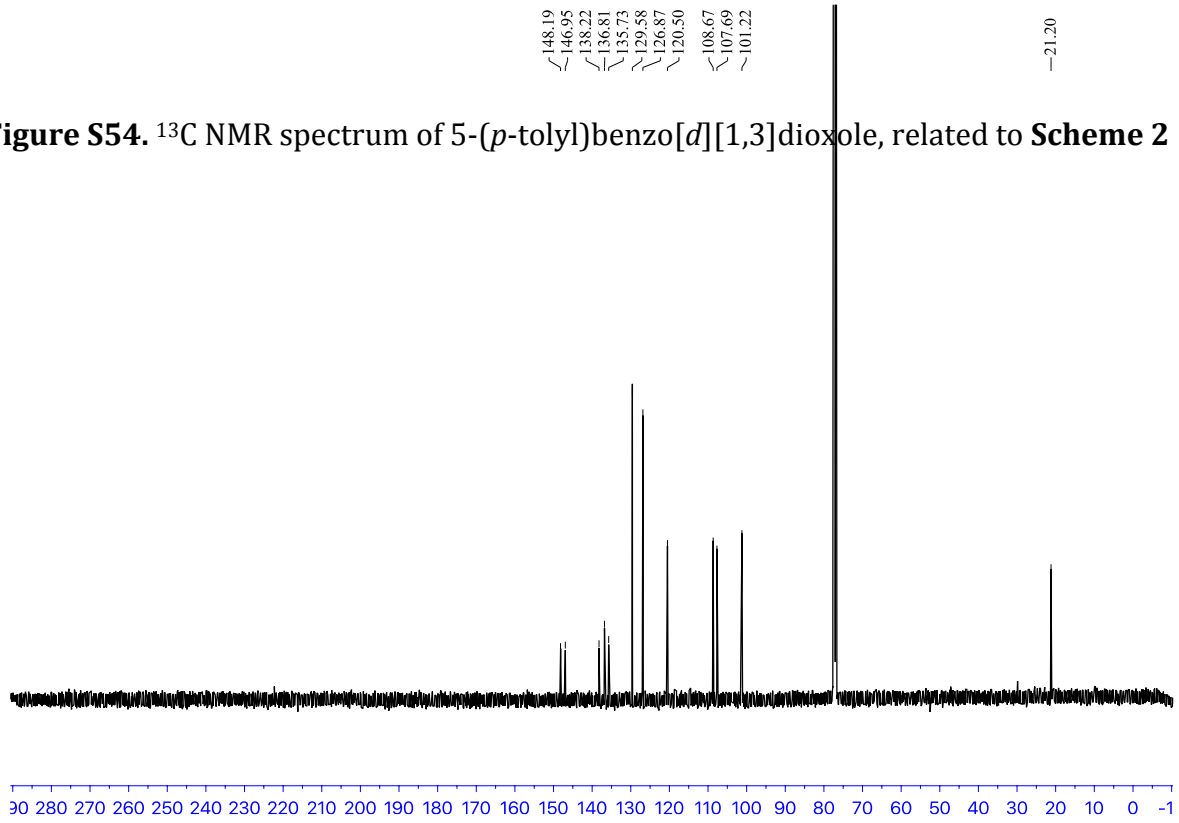

Figure S55. ^{1}H NMR spectrum of 2-(2,4-difluorophenyl)pyridine, related to **Scheme 2**

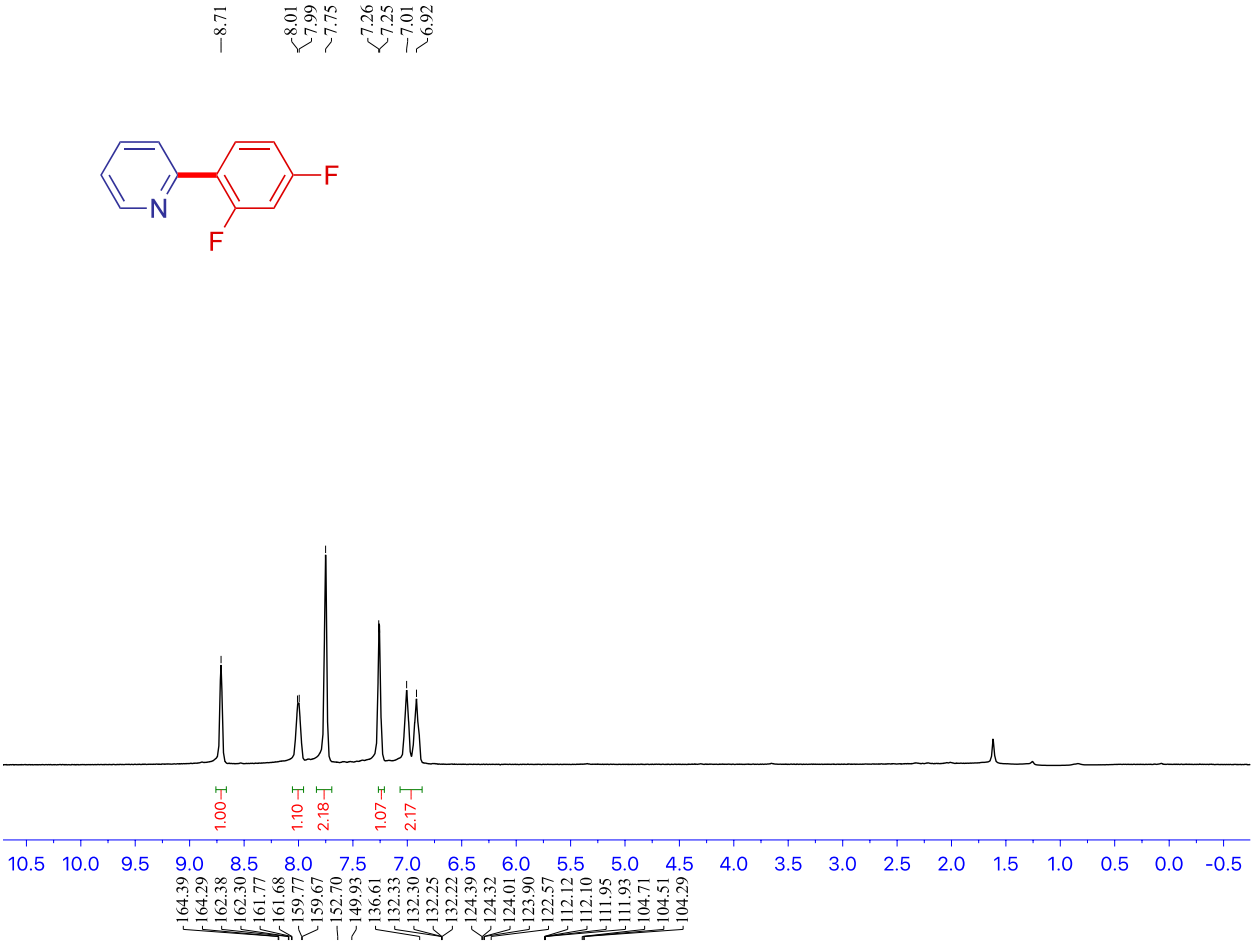

Figure S56. ^{13}C NMR spectrum of 2-(2,4-difluorophenyl)pyridine, related to **Scheme 2**

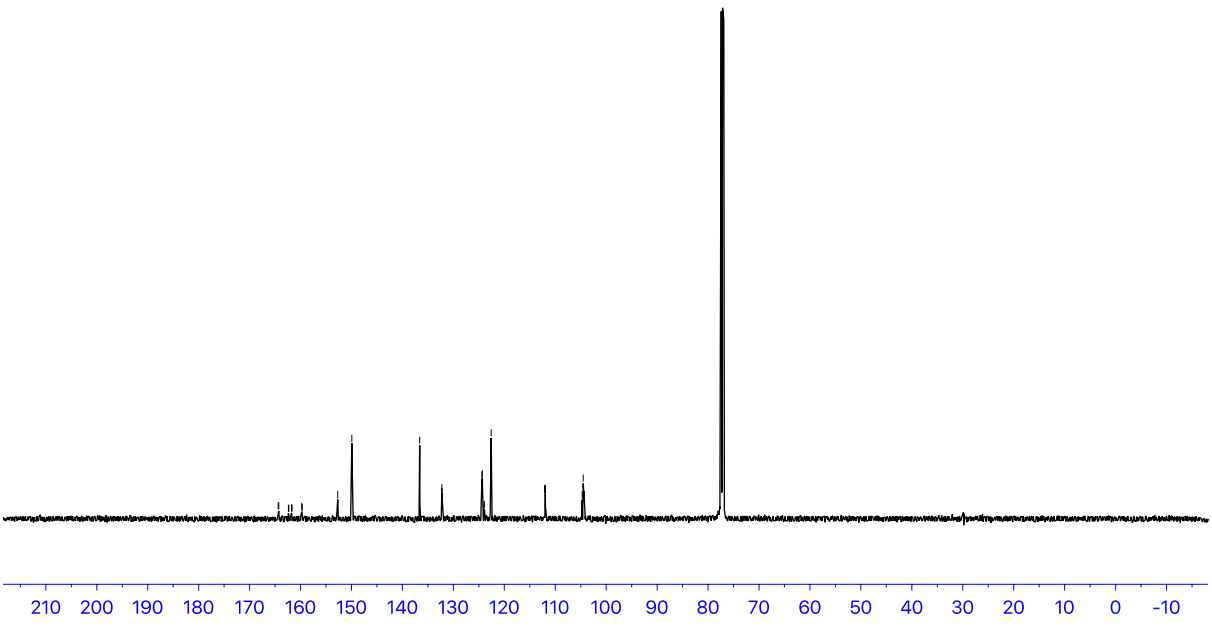

Figure S57. ^{19}F NMR spectrum of 2-(2,4-difluorophenyl)pyridine, related to **Scheme 2**

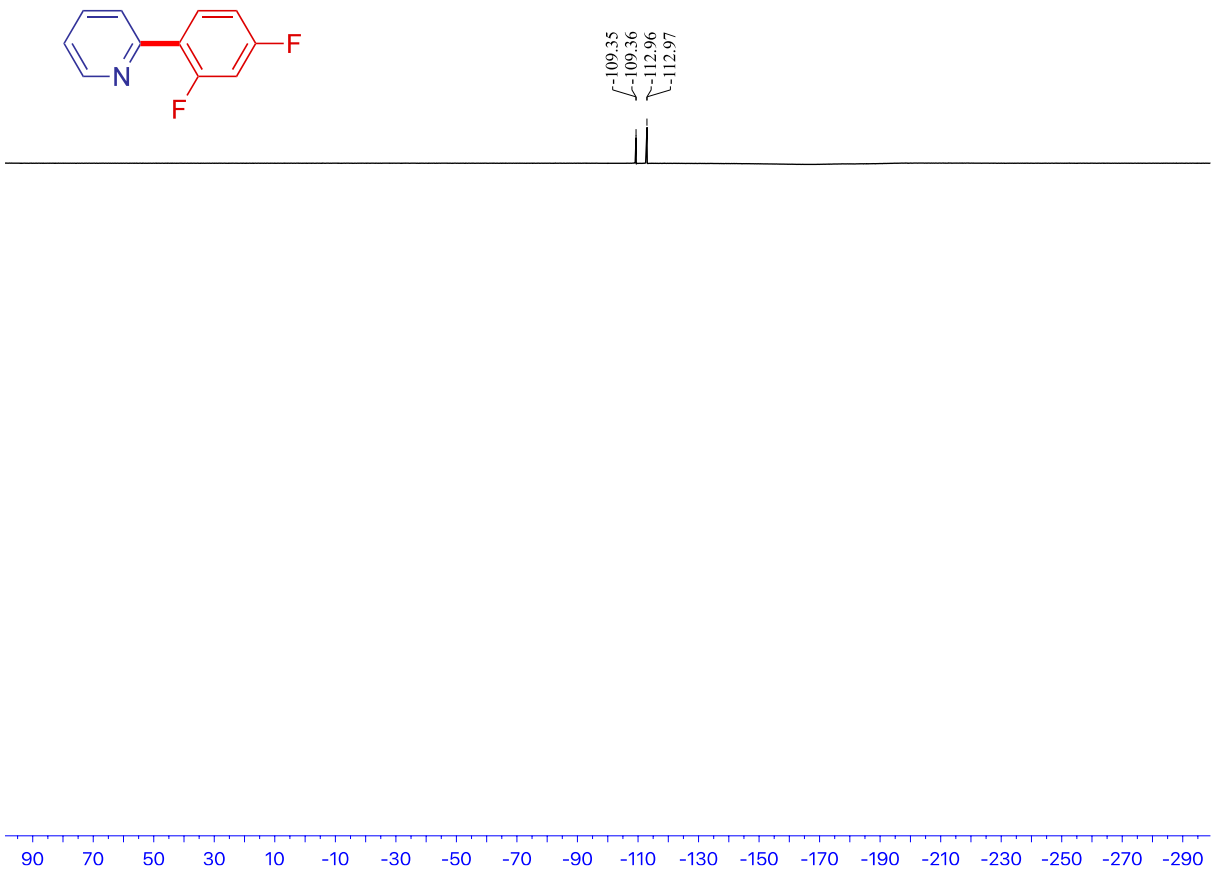

Figure S58. ^{1}H NMR spectrum of 2,4-dimethoxy-6-(thiophen-3-yl)-1,3,5-triazine, related to **Scheme 2**

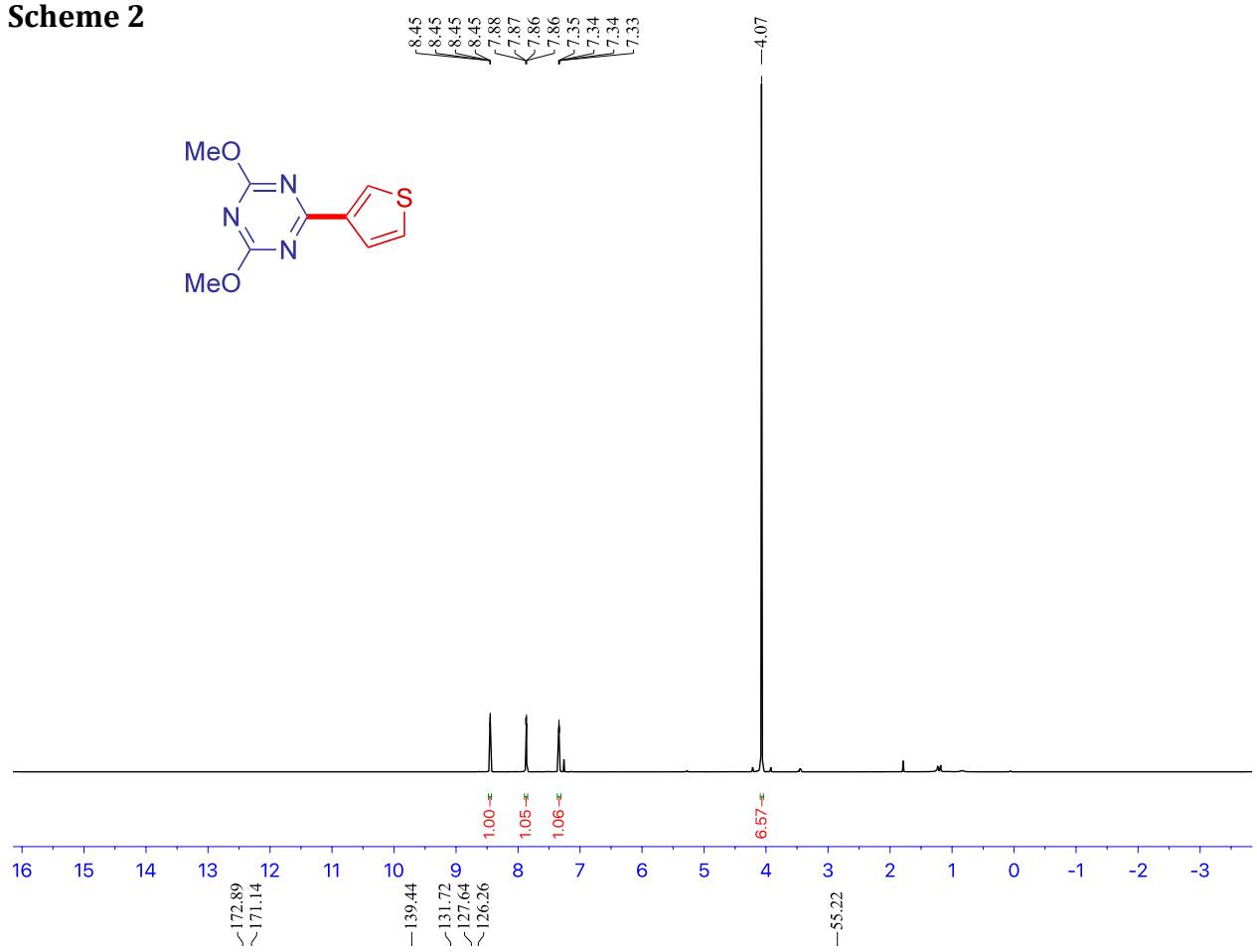

Figure S59. ^{13}C NMR spectrum of 2,4-dimethoxy-6-(thiophen-3-yl)-1,3,5-triazine, related to **Scheme 2**

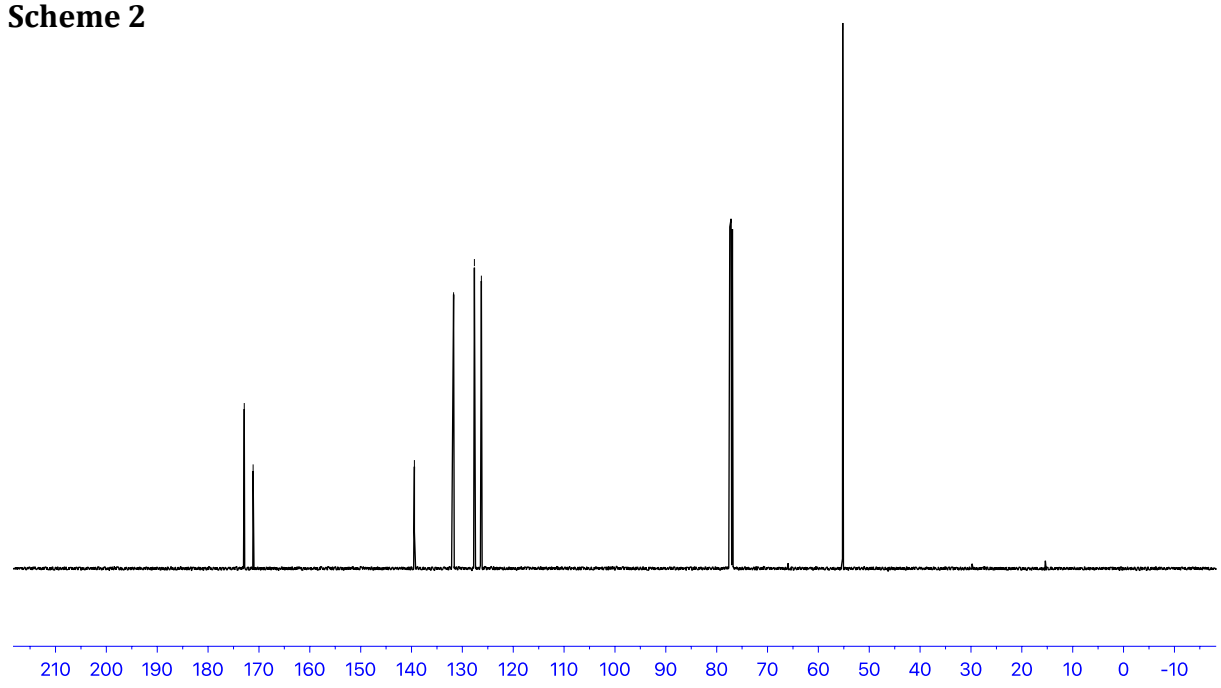

Figure S60. ^{1}H NMR spectrum of 3-(4,6-dimethoxy-1,3,5-triazin-2-yl)benzonitrile, related to **Scheme 2**

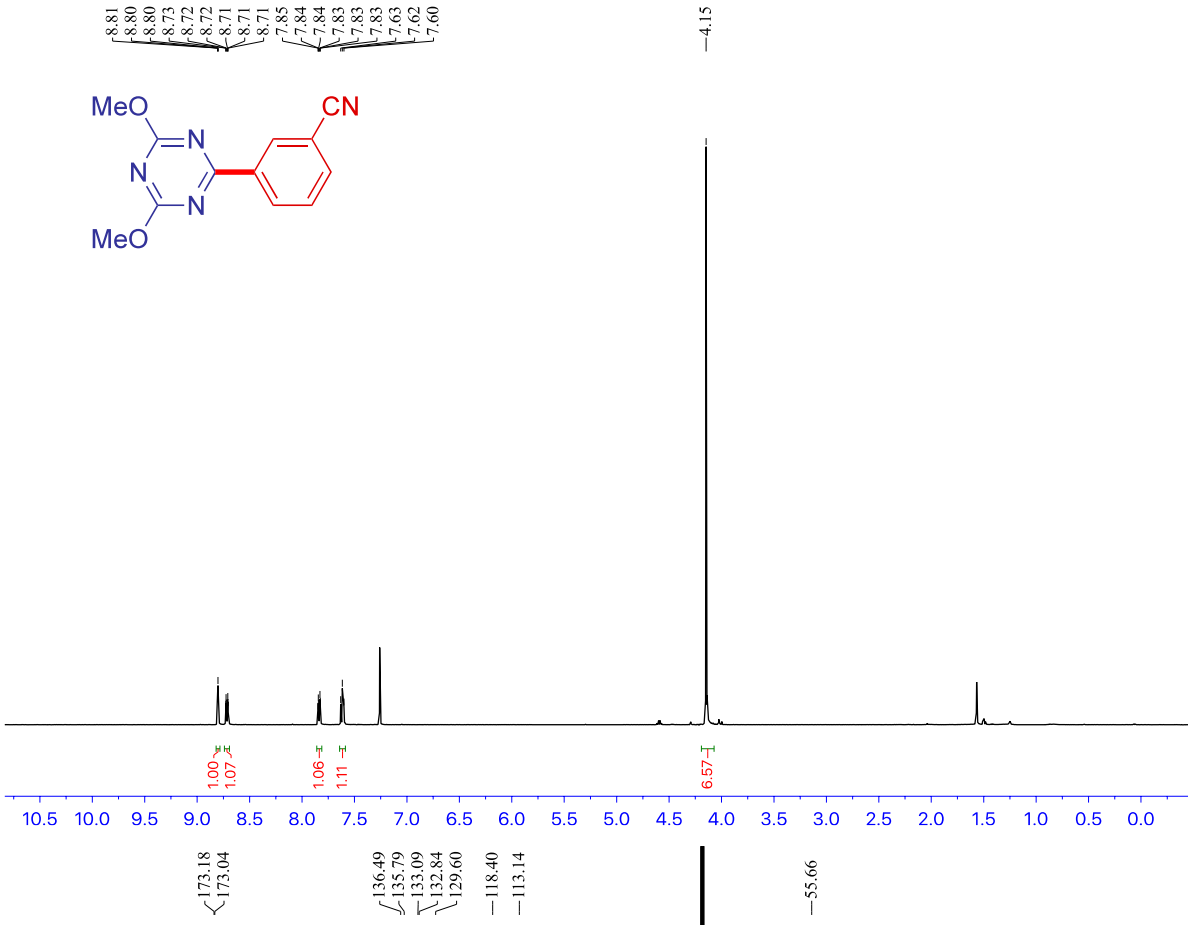

Figure S61. ^{13}C NMR spectrum of 3-(4,6-dimethoxy-1,3,5-triazin-2-yl)benzonitrile, related to **Scheme 2**

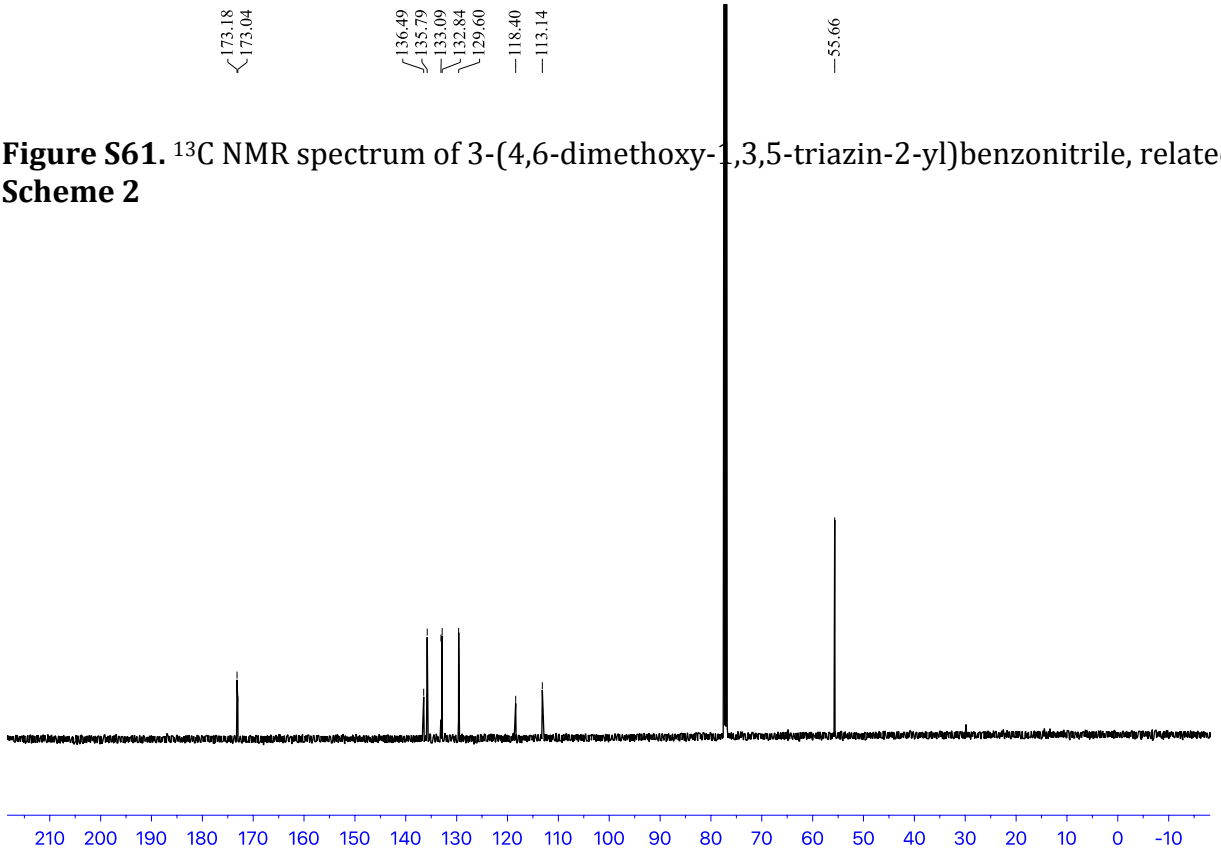

Figure S62. ^{1}H NMR spectrum of 2-methoxy-5-(*p*-tolyl)pyridine, related to **Scheme 3**

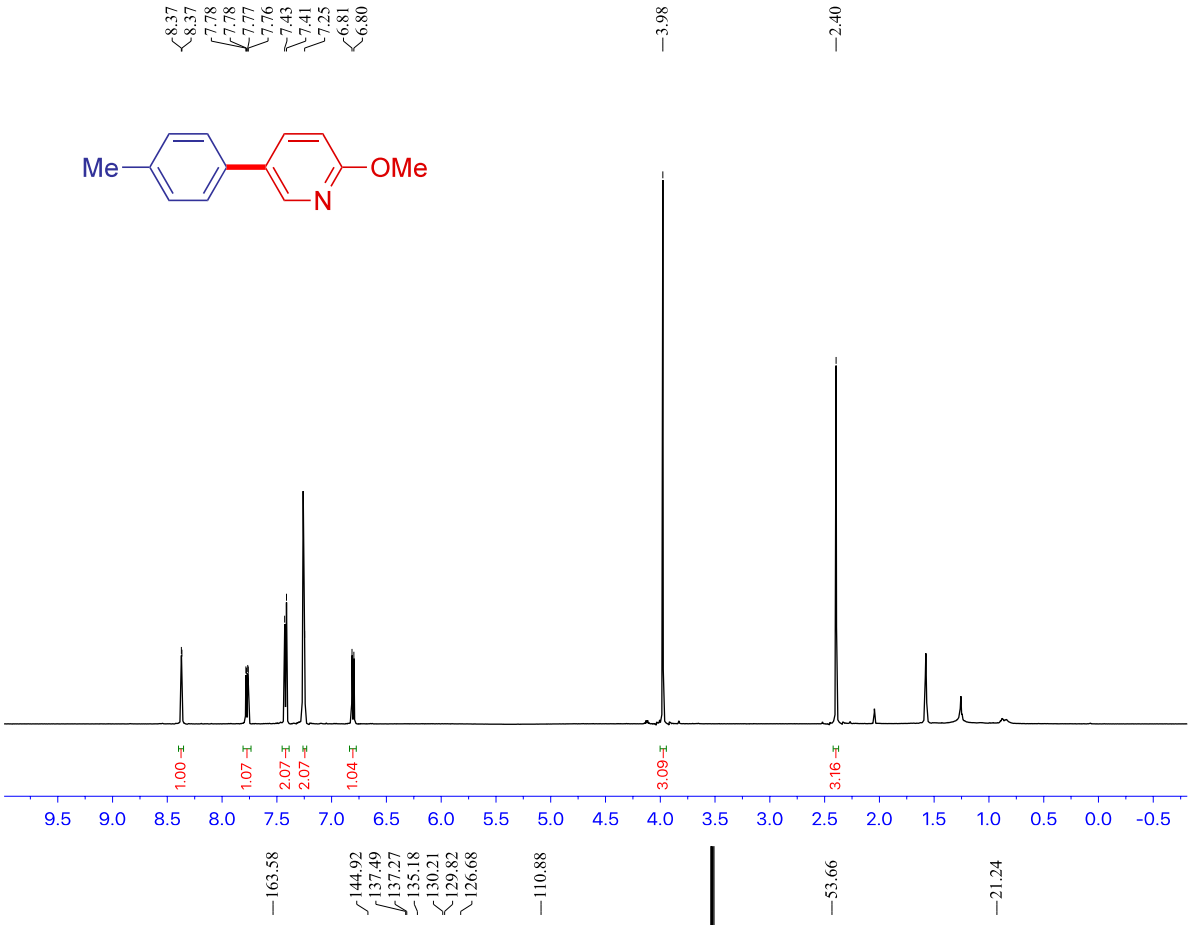

Figure S63. ^{13}C NMR spectrum of 2-methoxy-5-(*p*-tolyl)pyridine, related to **Scheme 3**

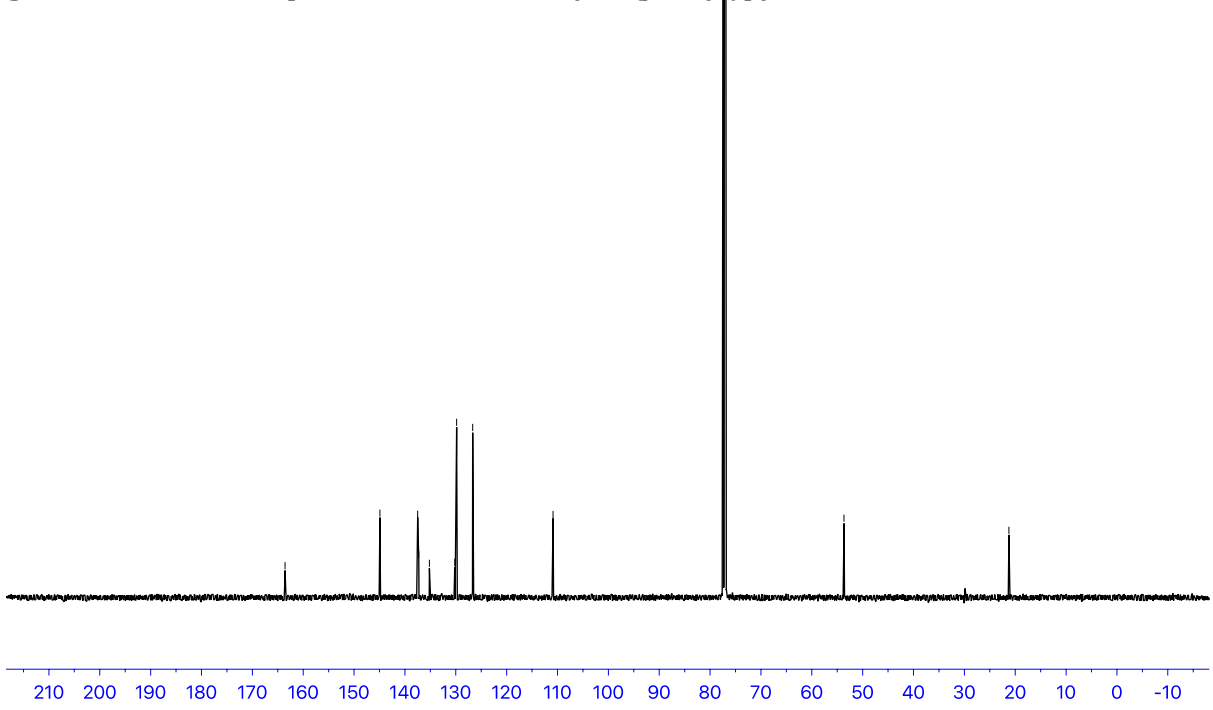

Figure S64. ^{1}H NMR spectrum of *tert*-butyl (4-(quinolin-2-yl)phenyl)carbamate, related to **Scheme 3**

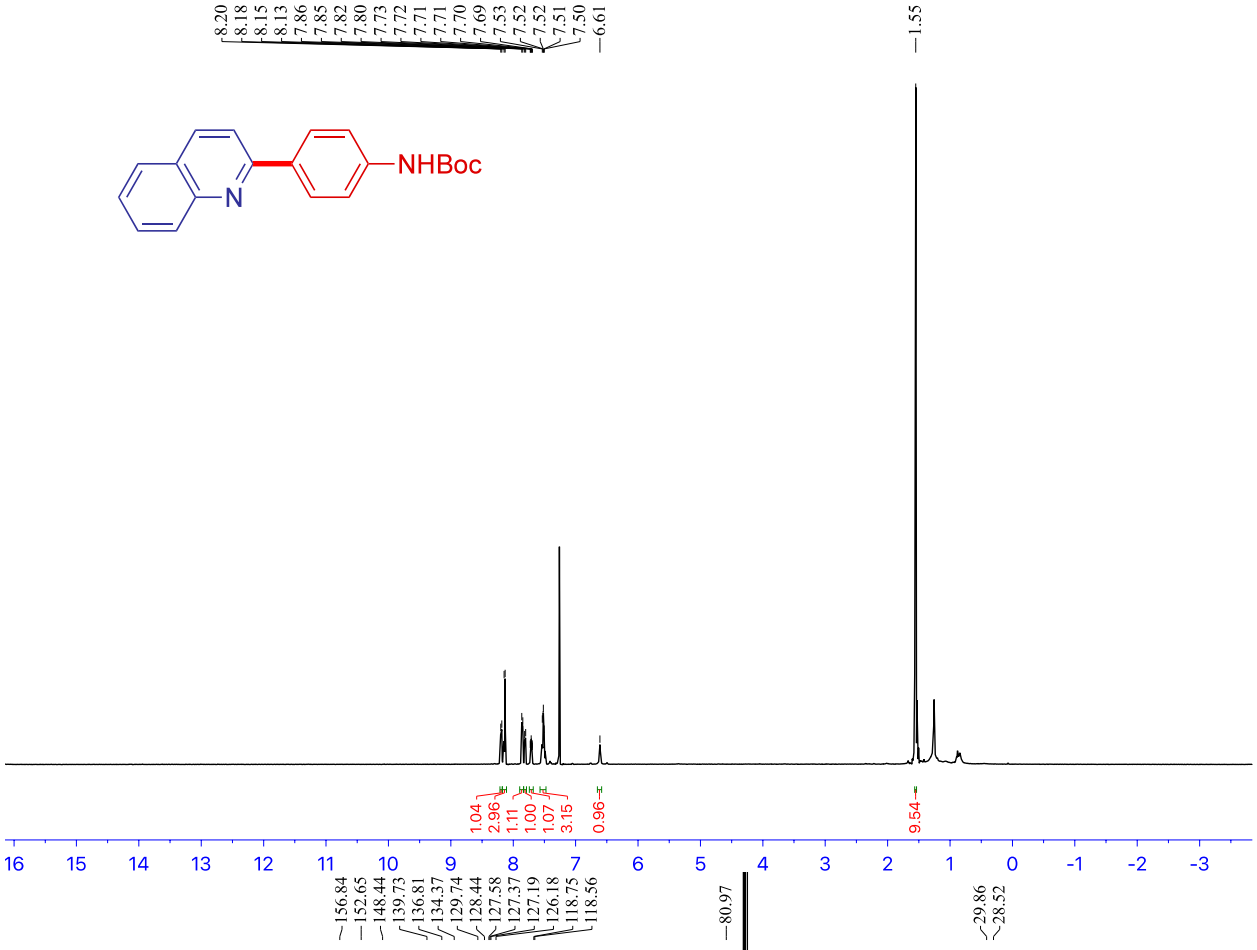

Figure S65. ^{13}C NMR spectrum of *tert*-butyl (4-(quinolin-2-yl)phenyl)carbamate, related to **Scheme 3**

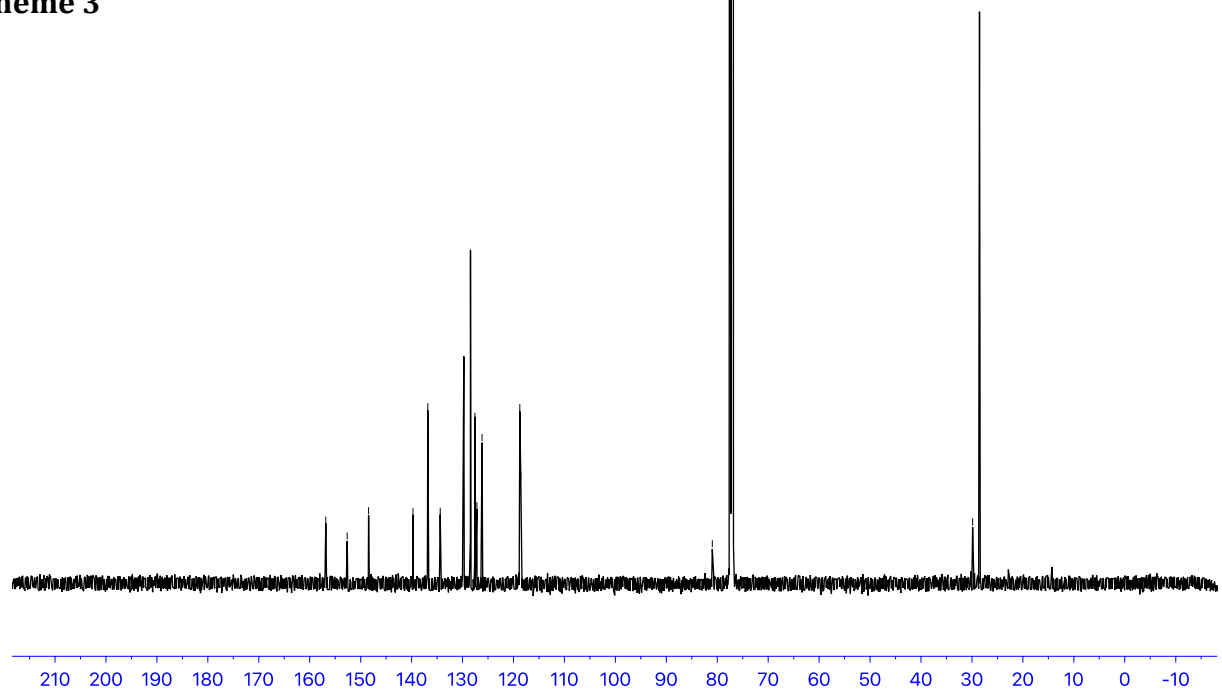

Figure S66. [1]H NMR spectrum of 4'-methyl-*N*-phenyl-[1,1'-biphenyl]-4-carboxamide, related to **Scheme 3**

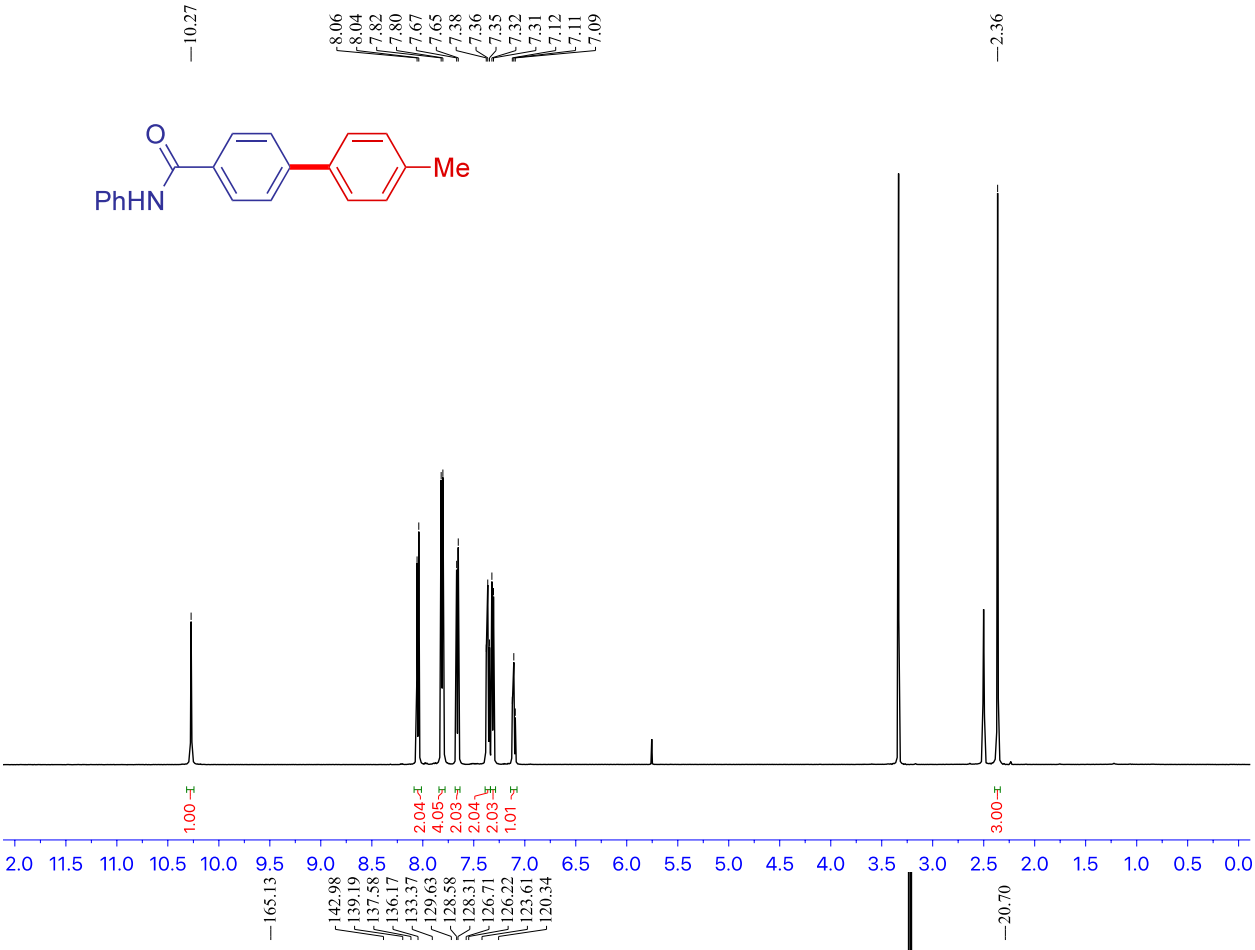

Figure S67. [13]C NMR spectrum of 4'-methyl-*N*-phenyl-[1,1'-biphenyl]-4-carboxamide, related to **Scheme 3**

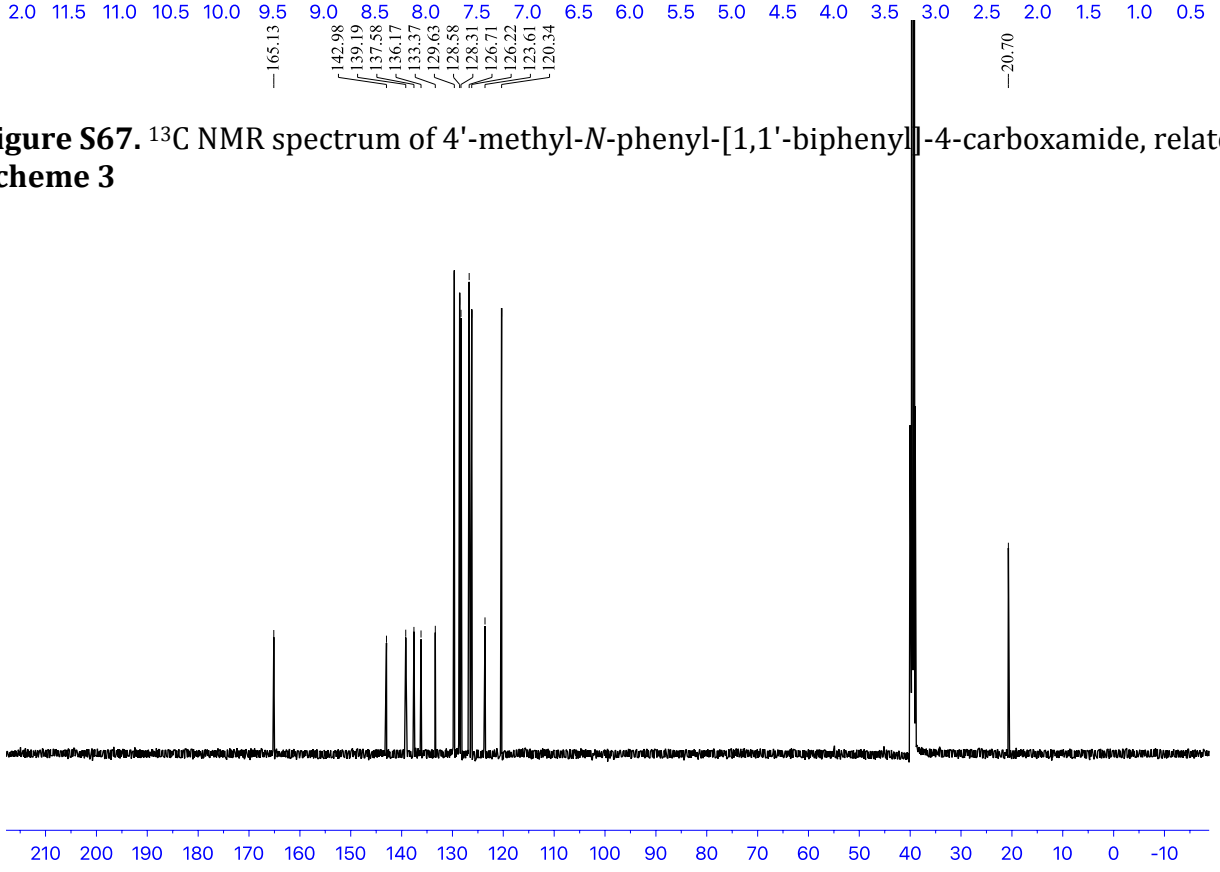

Figure S68. ^{1}H NMR spectrum of 3-methoxy-6-phenylpyridazine, related to **Scheme 3**

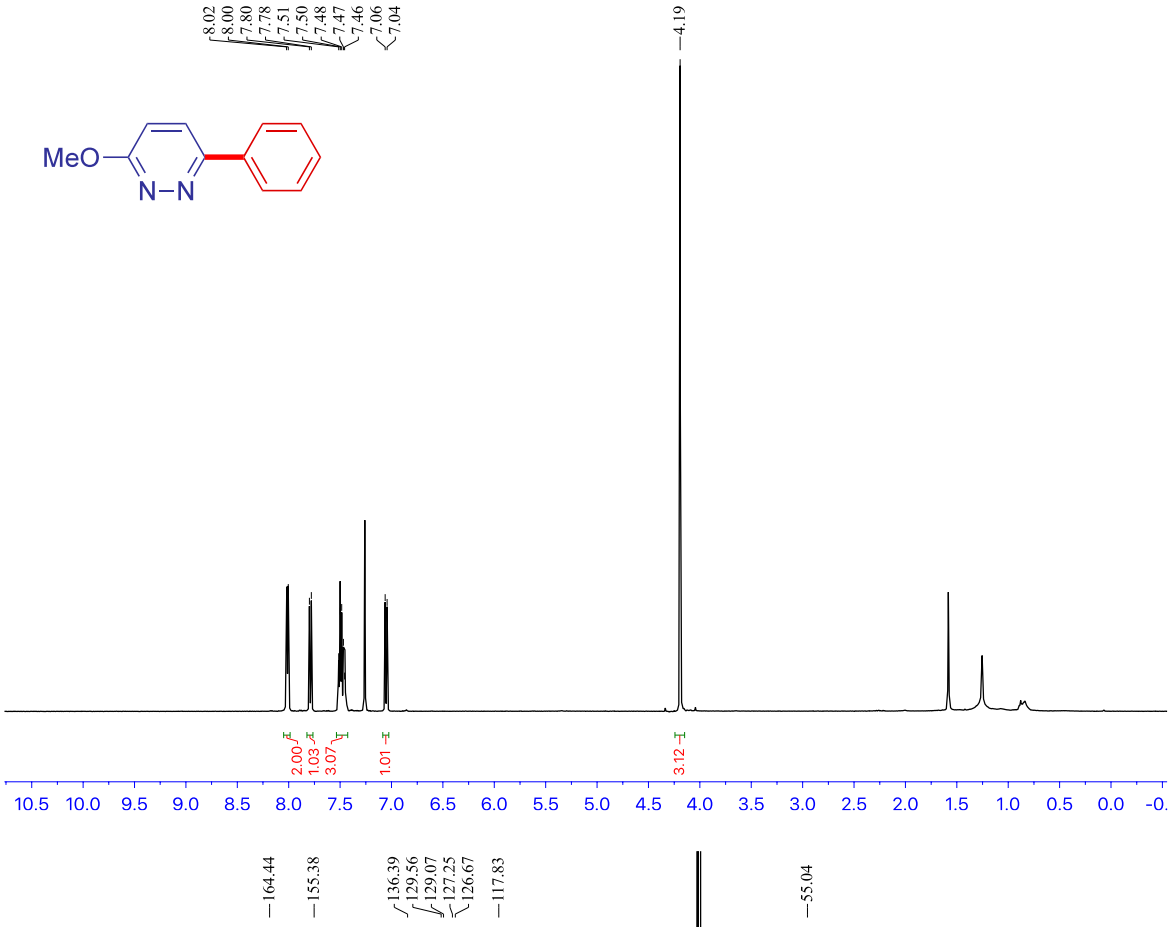

Figure S69. ^{13}C NMR spectrum of 3-methoxy-6-phenylpyridazine, related to **Scheme 3**

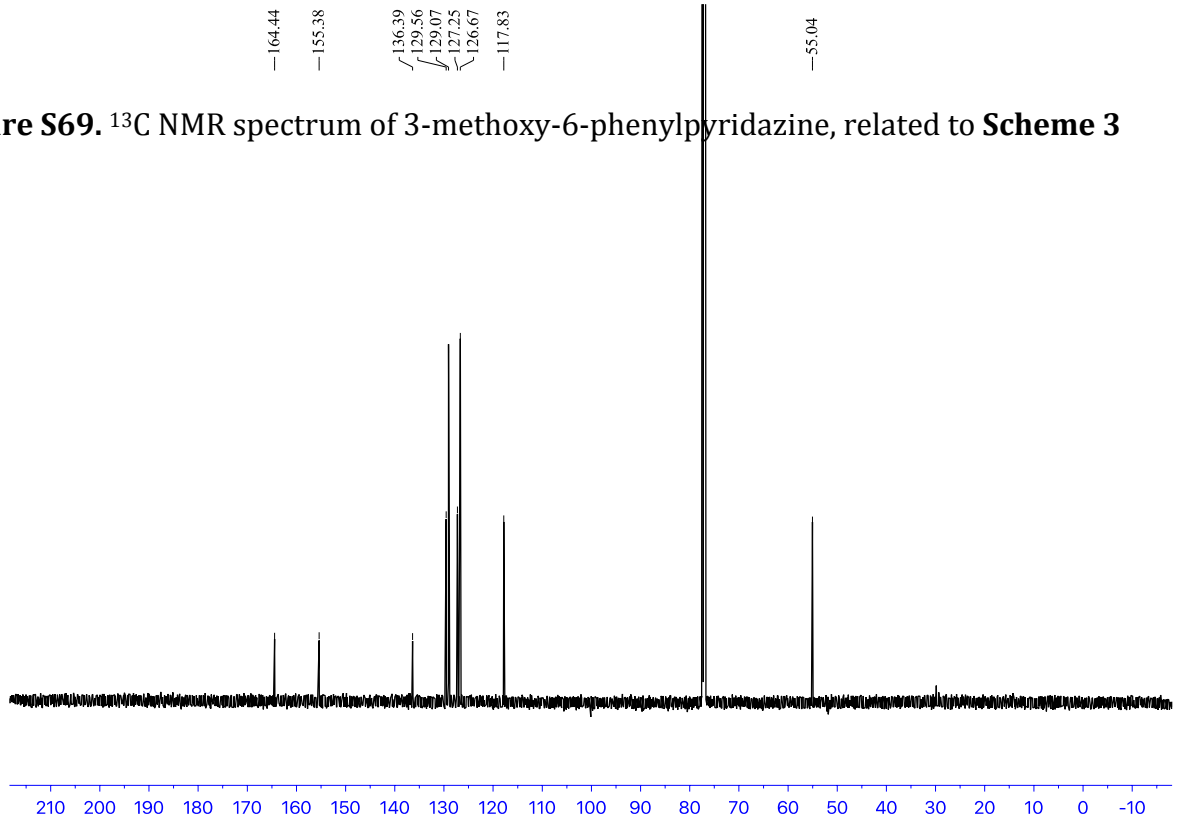

Figure S70. ^{1}H NMR spectrum of 4'-methyl-[1,1'-biphenyl]-4-carboxamide, related to **Scheme 3**

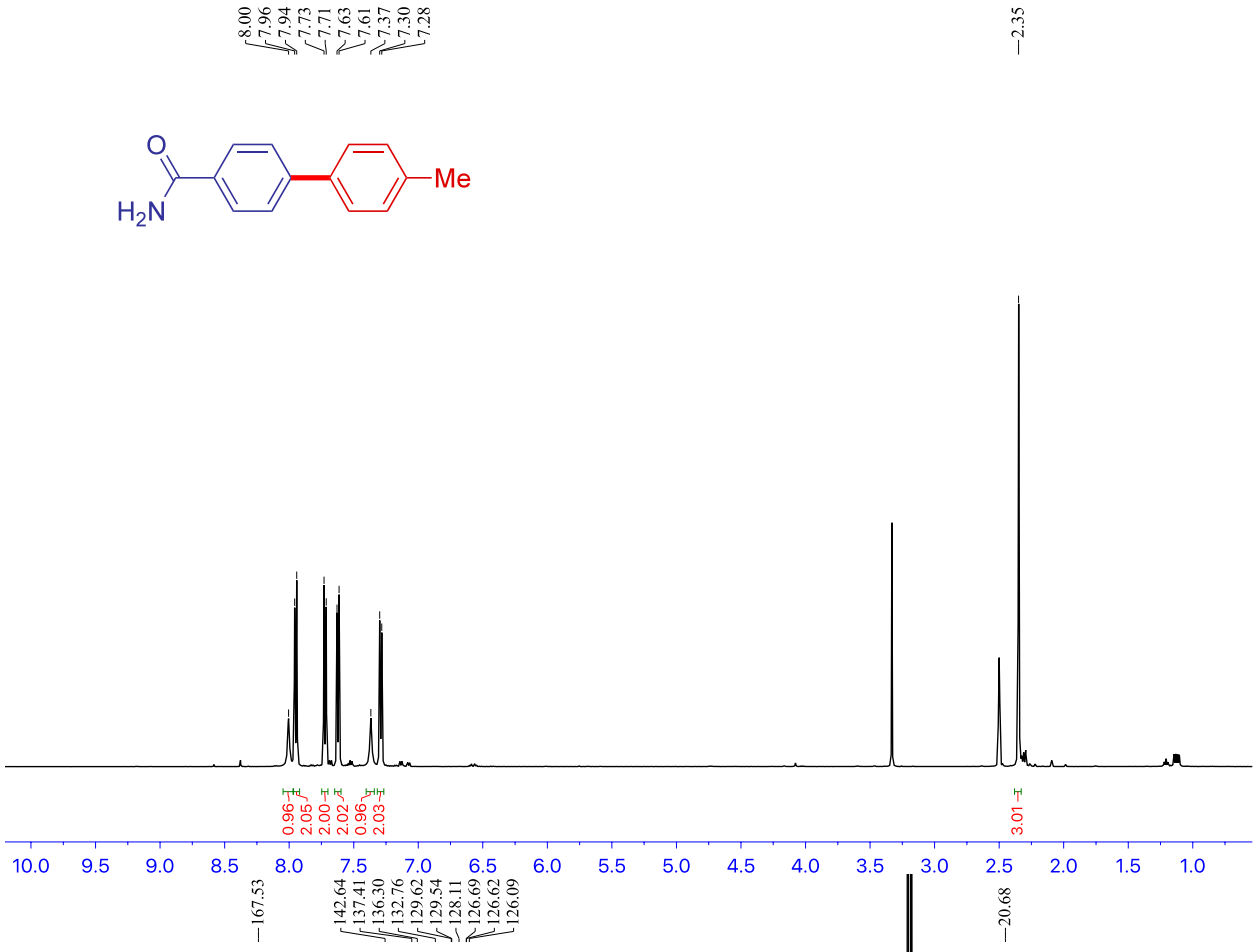

Figure S71. ^{13}C NMR spectrum of 4'-methyl-[1,1'-biphenyl]-4-carboxamide, related to **Scheme 3**

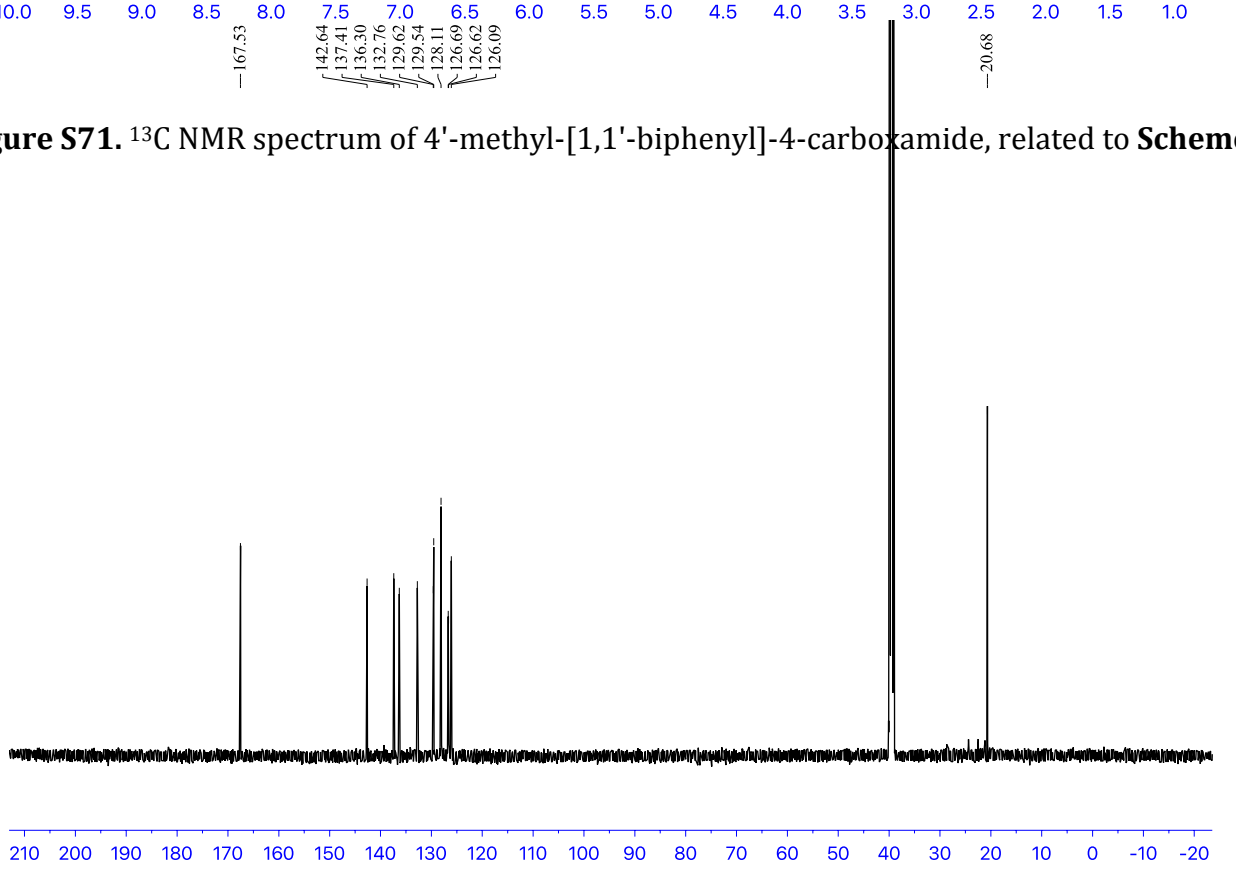

Figure S72. ^{1}H NMR spectrum of *N*-methyl-[1,1'-biphenyl]-4-carboxamide, related to **Scheme 3**

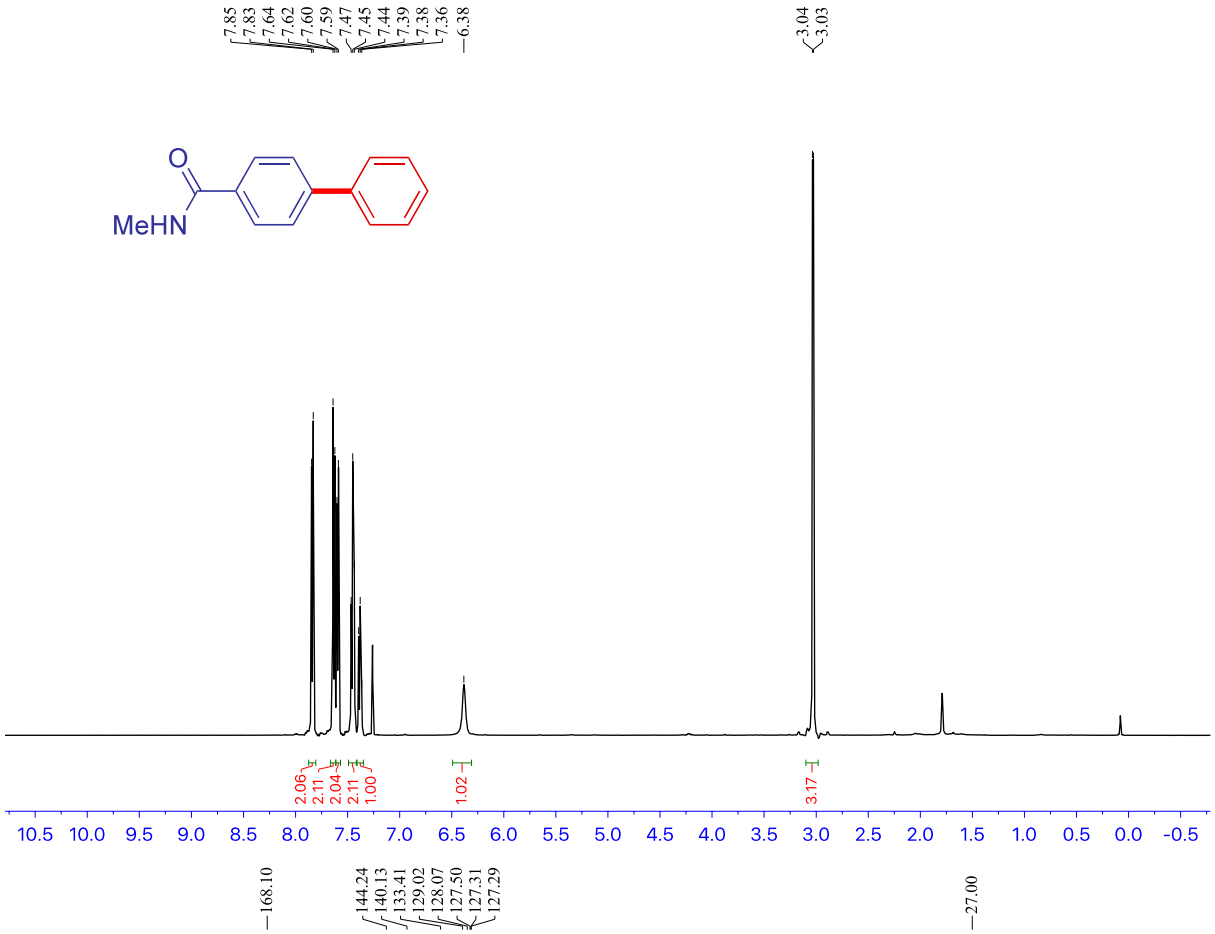

Figure S73. ^{13}C NMR spectrum of *N*-methyl-[1,1'-biphenyl]-4-carboxamide, related to **Scheme 3**

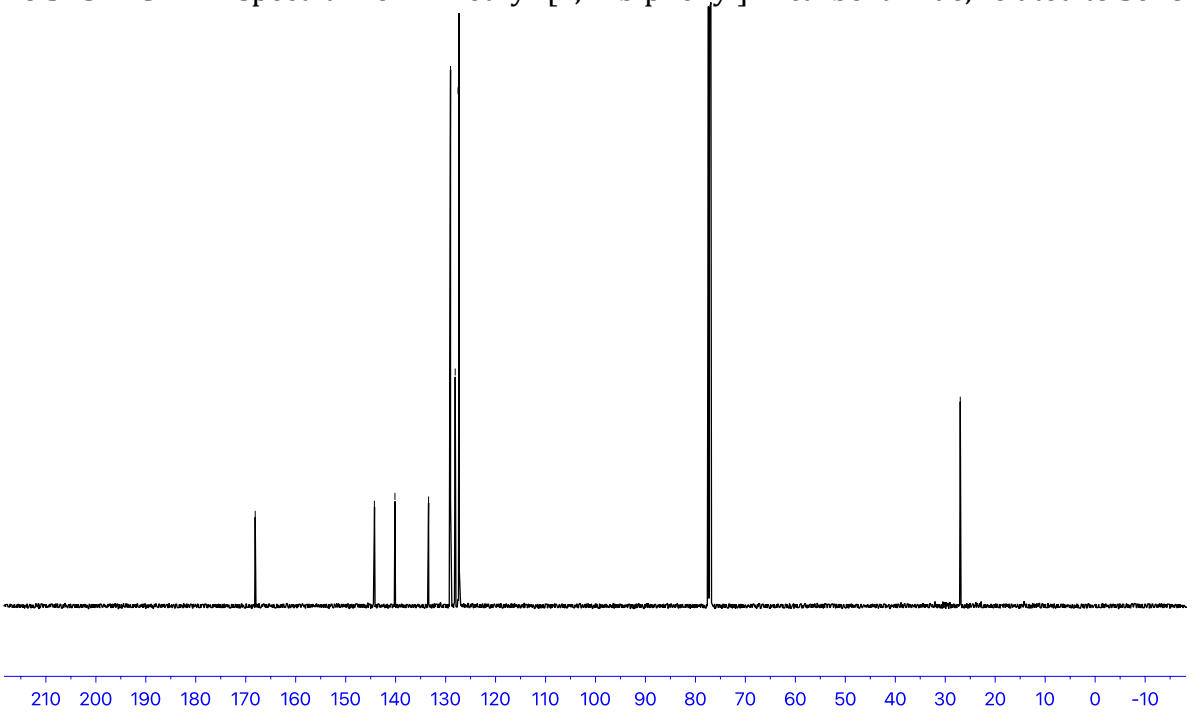

Figure S74. ^{1}H NMR spectrum of *N,N*-dimethyl-[1,1'-biphenyl]-4-carboxamide, related to **Scheme 3**

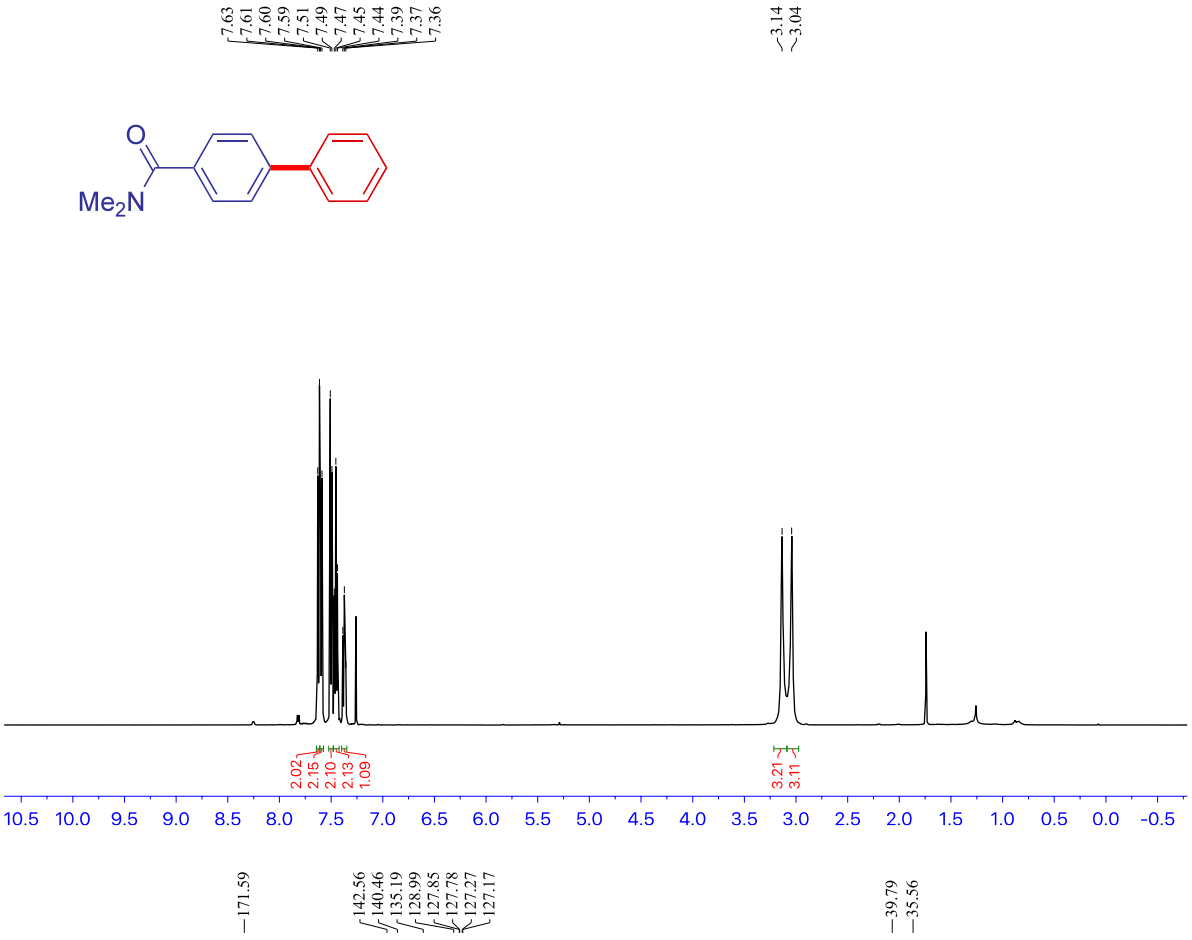

Figure S75. ^{13}C NMR spectrum of *N,N*-dimethyl-[1,1'-biphenyl]-4-carboxamide, related to **Scheme 3**

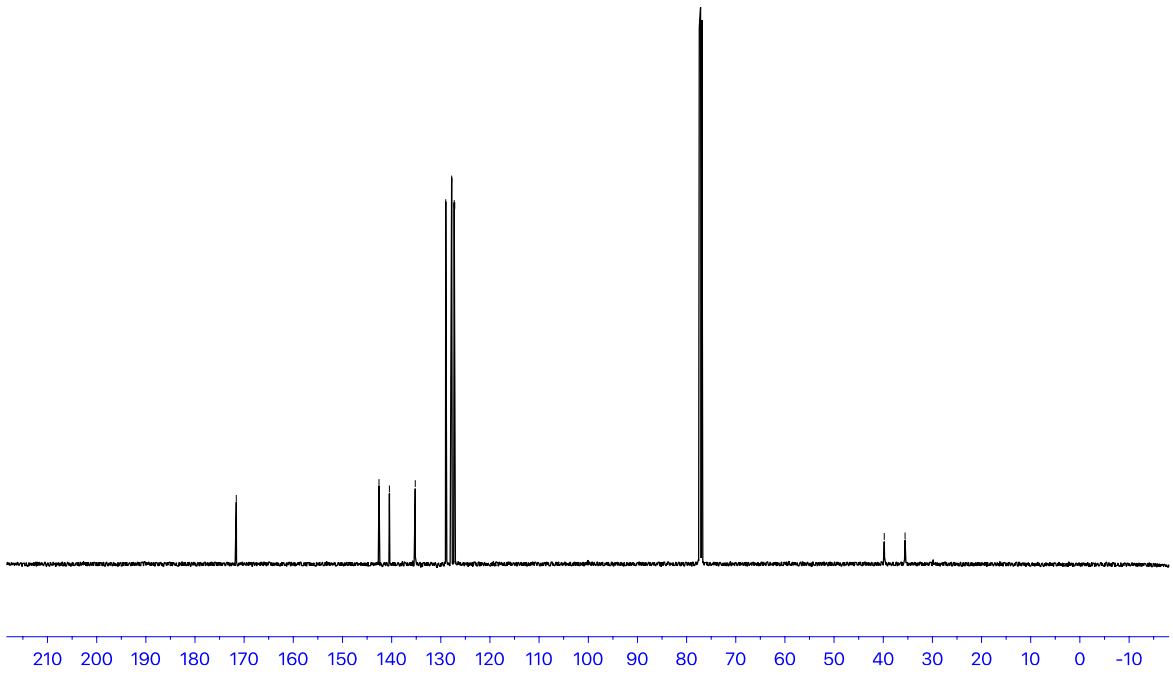

Figure S76. ^{1}H NMR spectrum of *N*-methyl-[1,1'-biphenyl]-4-sulfonamide, related to **Scheme 3**

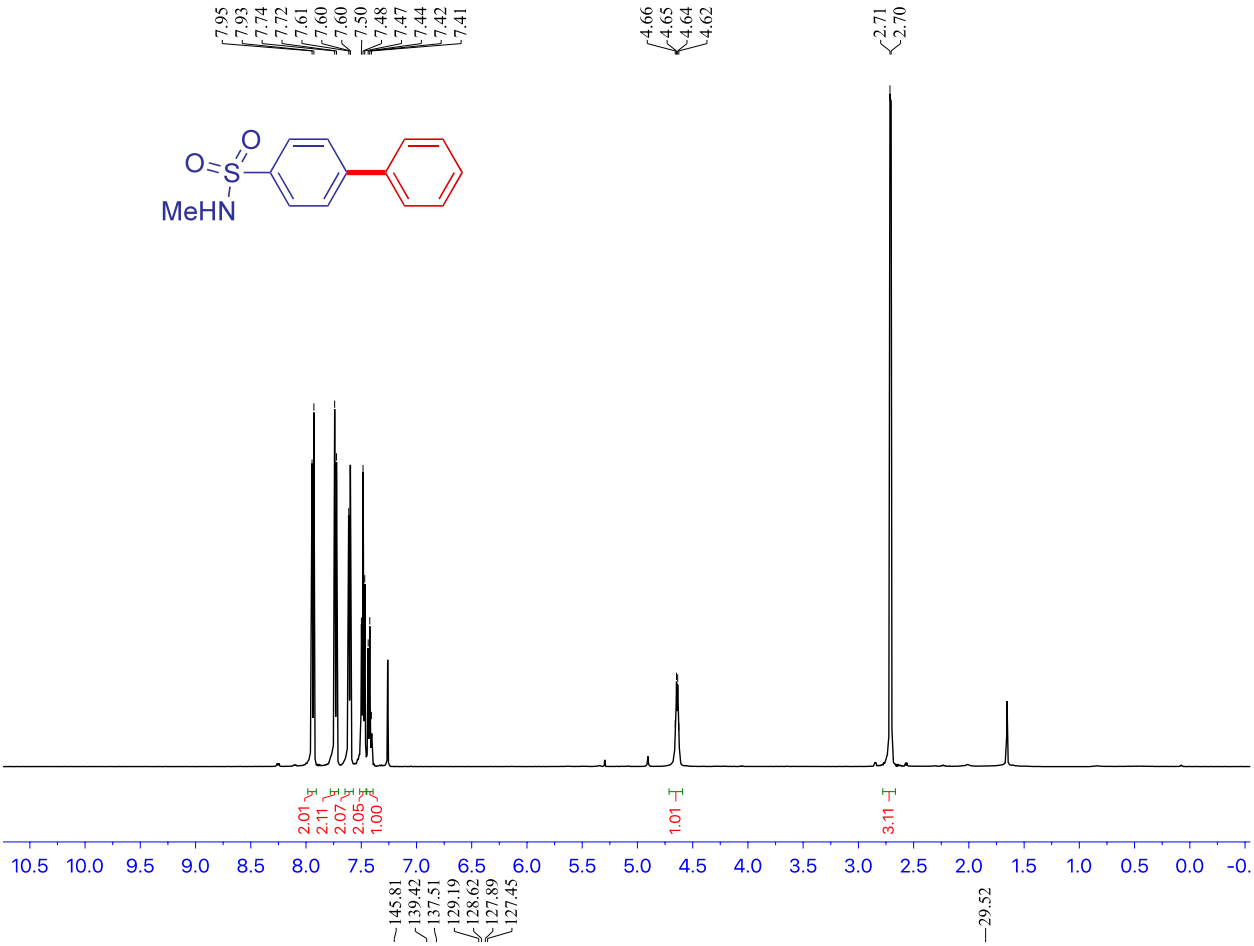

Figure S77. ^{13}C NMR spectrum of *N*-methyl-[1,1'-biphenyl]-4-sulfonamide, related to **Scheme 3**

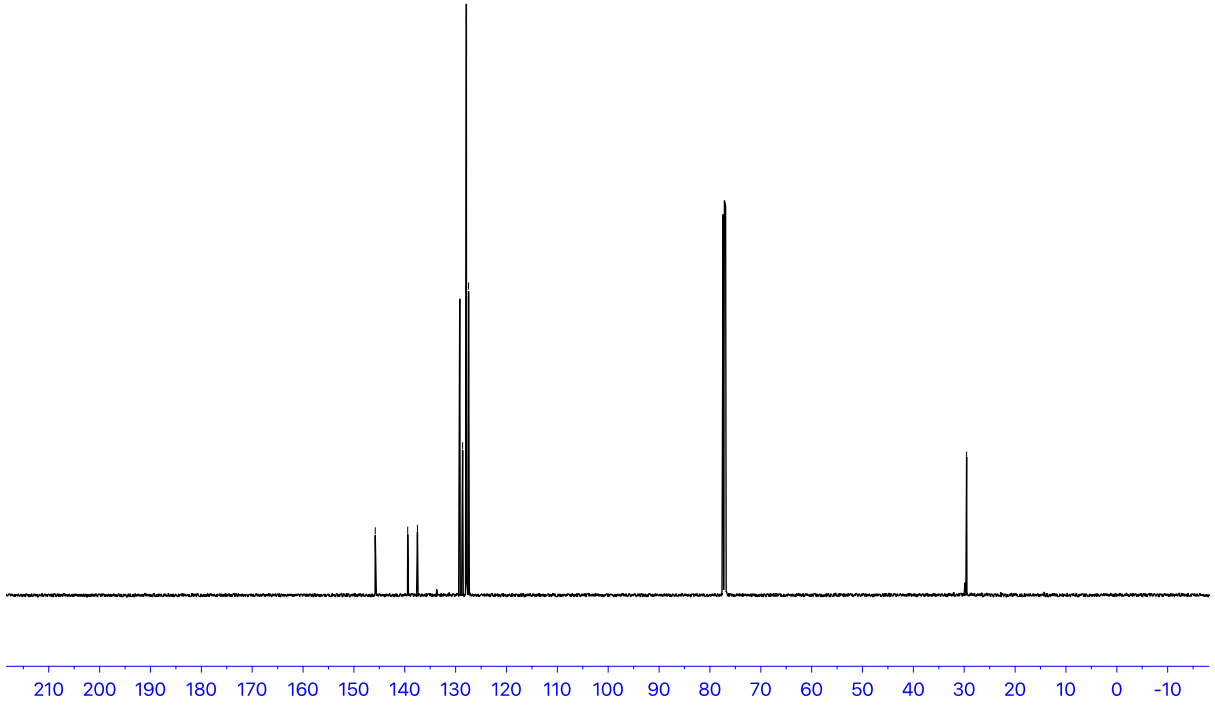

Figure S78. ^{1}H NMR spectrum of 4,7-di(thiophen-2-yl)benzo[*c*][1,2,5]thiadiazole, related to **Scheme 3**

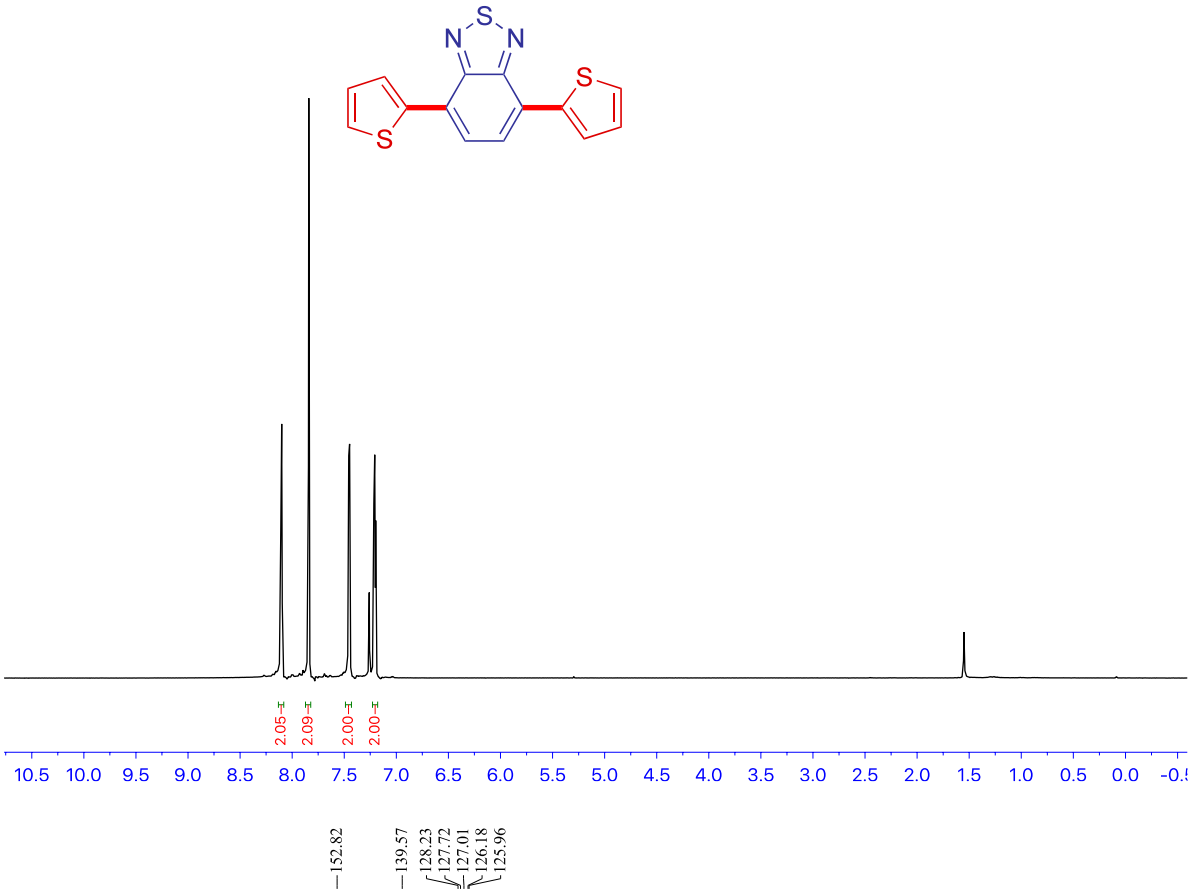

Figure S79. ^{13}C NMR spectrum of 4,7-di(thiophen-2-yl)benzo[*c*][1,2,5]thiadiazole, related to **Scheme 3**

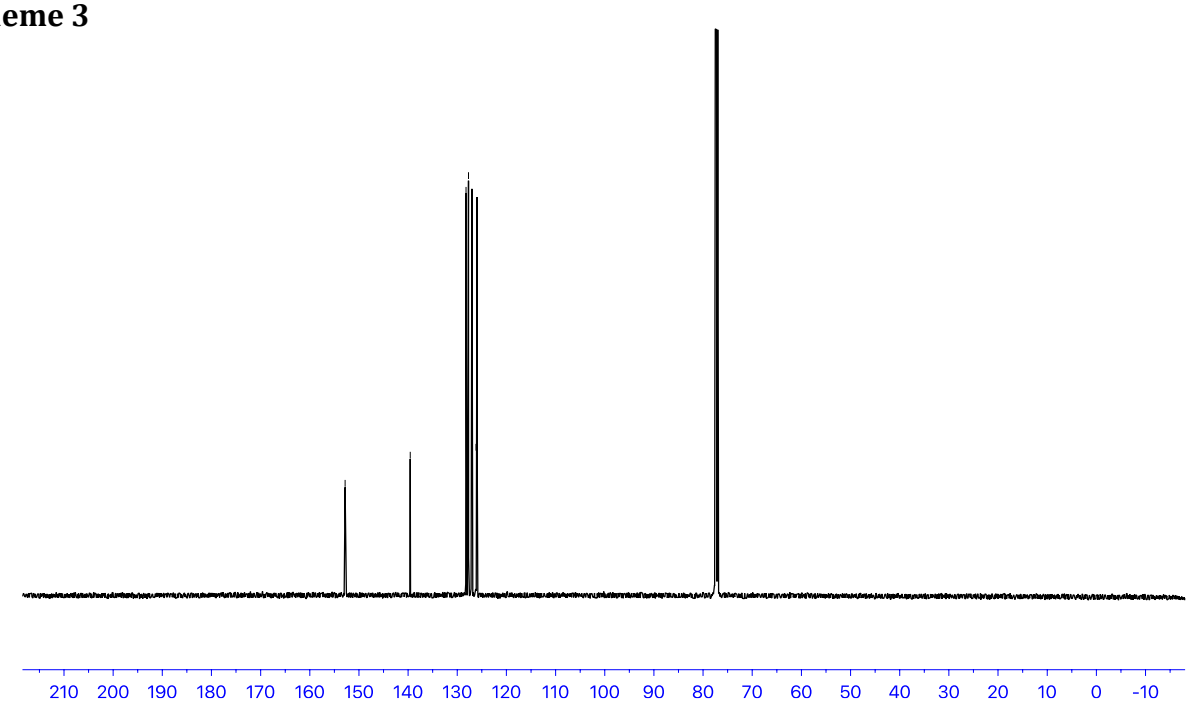

Figure S80. ^{1}H NMR spectrum of 2-(3,4,5-trifluorophenyl)pyrazine, related to **Scheme 3**

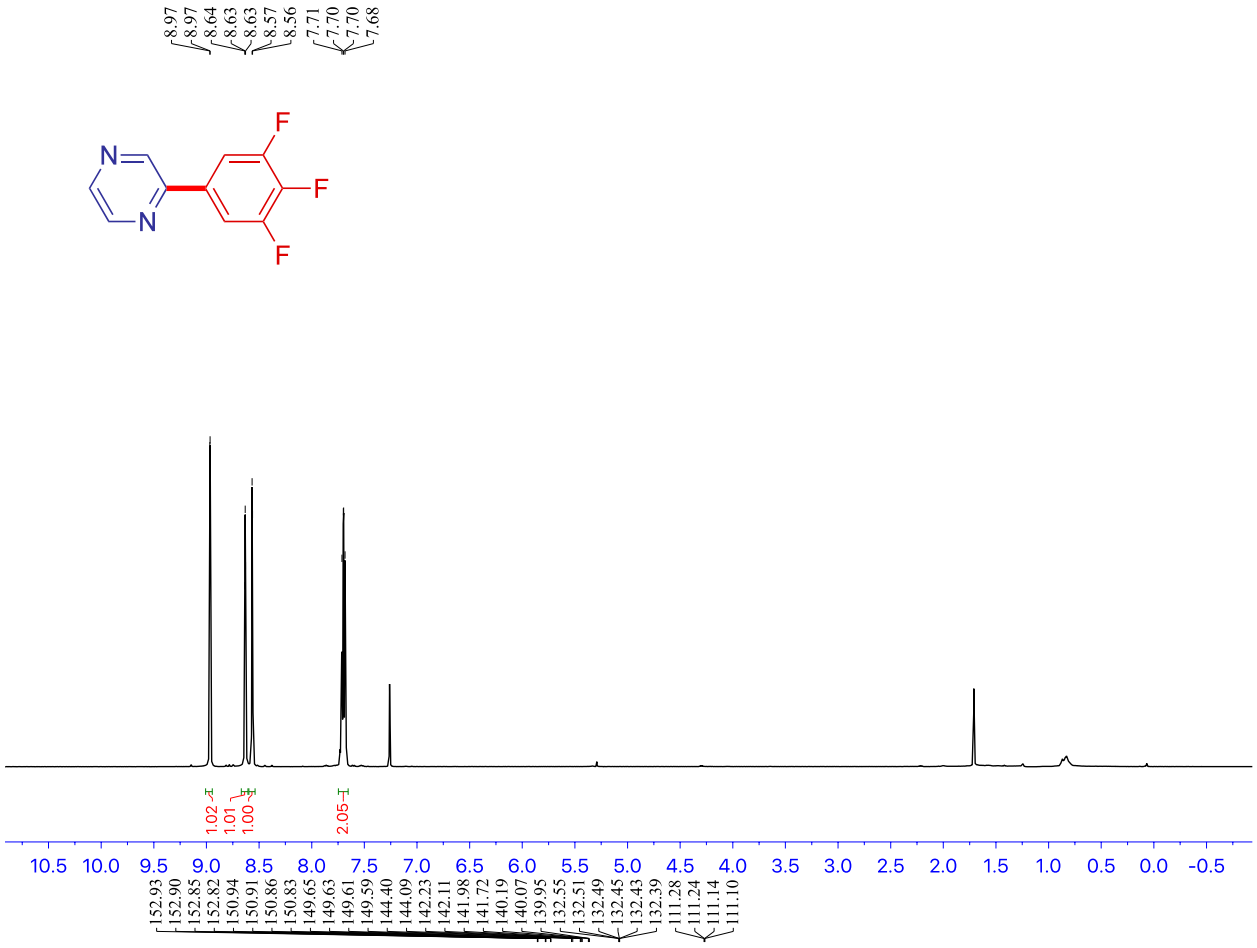

Figure S81. ^{13}C NMR spectrum of 2-(3,4,5-trifluorophenyl)pyrazine, related to **Scheme 3**

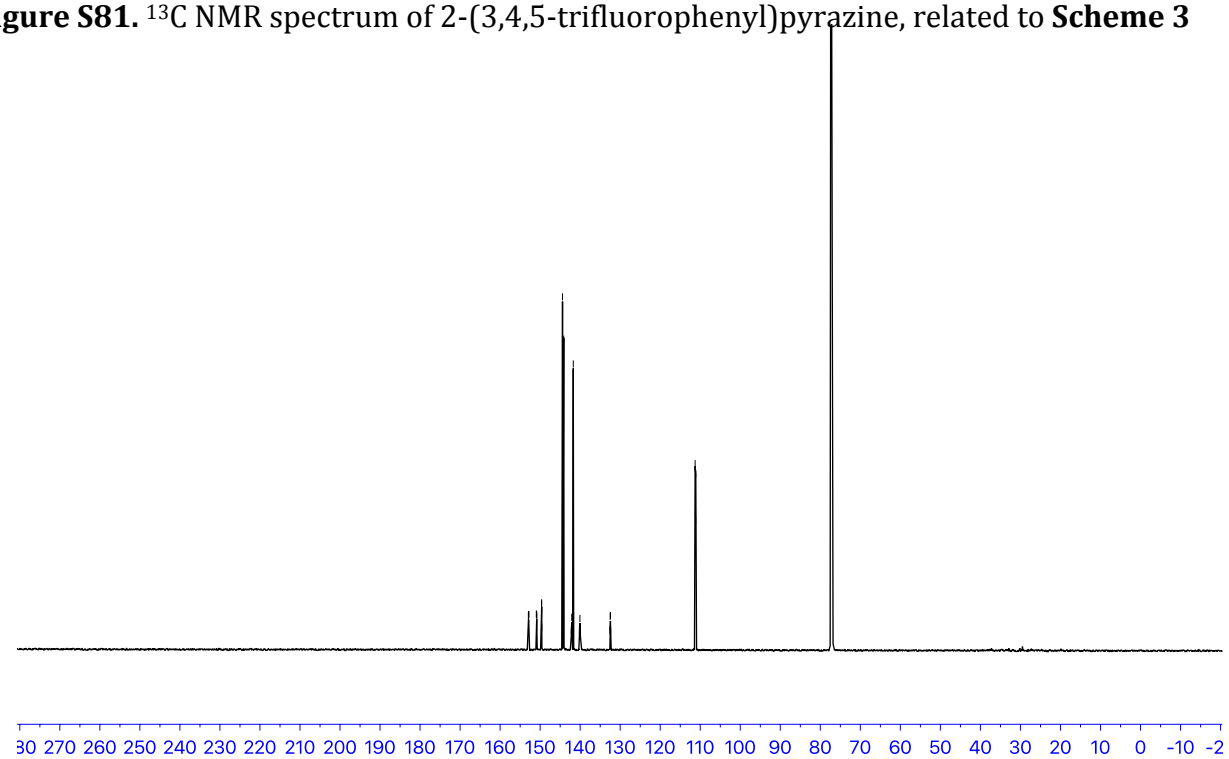

Figure S82. ^{19}F NMR spectrum of 2-(3,4,5-trifluorophenyl)pyrazine, related to **Scheme 3**

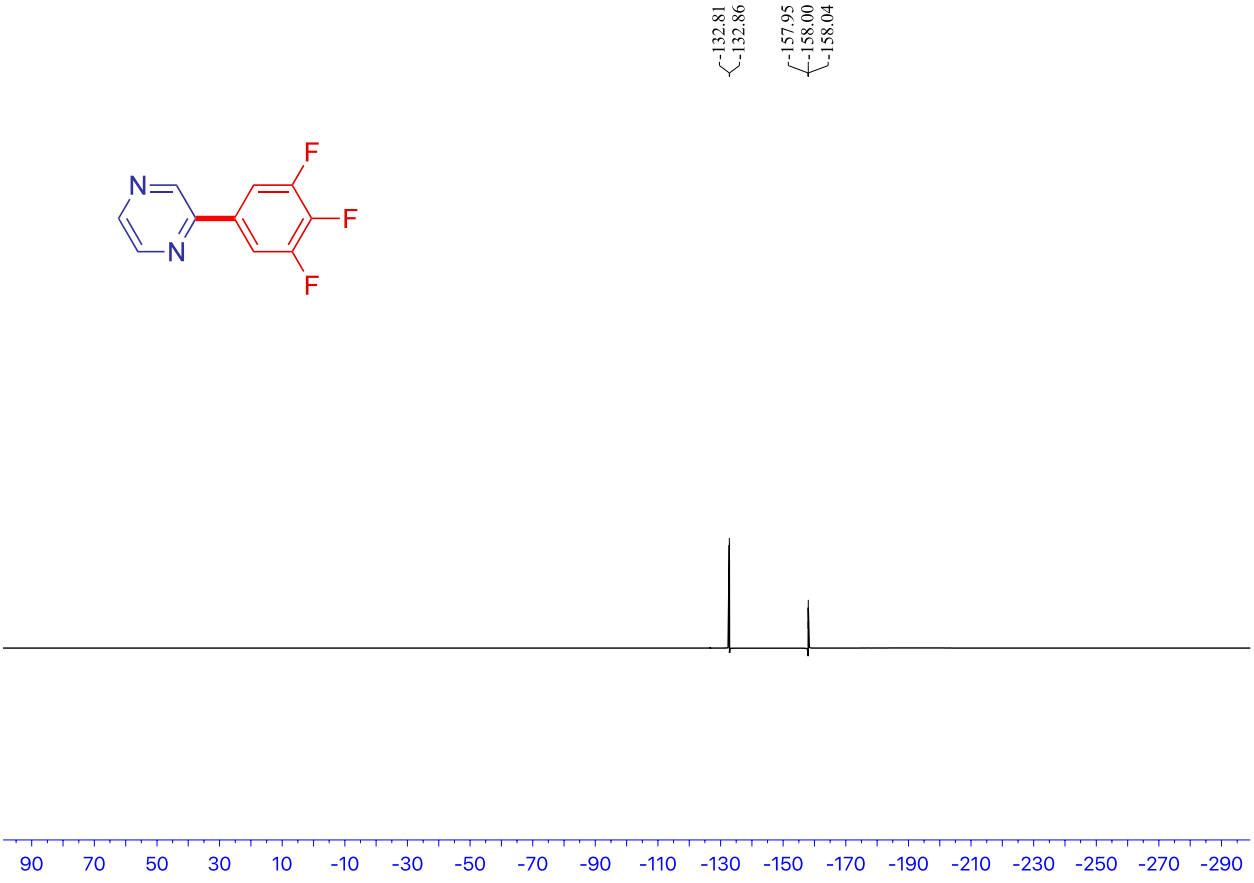

Figure S83. ^{1}H NMR spectrum of 2-(6-methoxypyridin-3-yl)pyrazine, related to **Scheme 3**

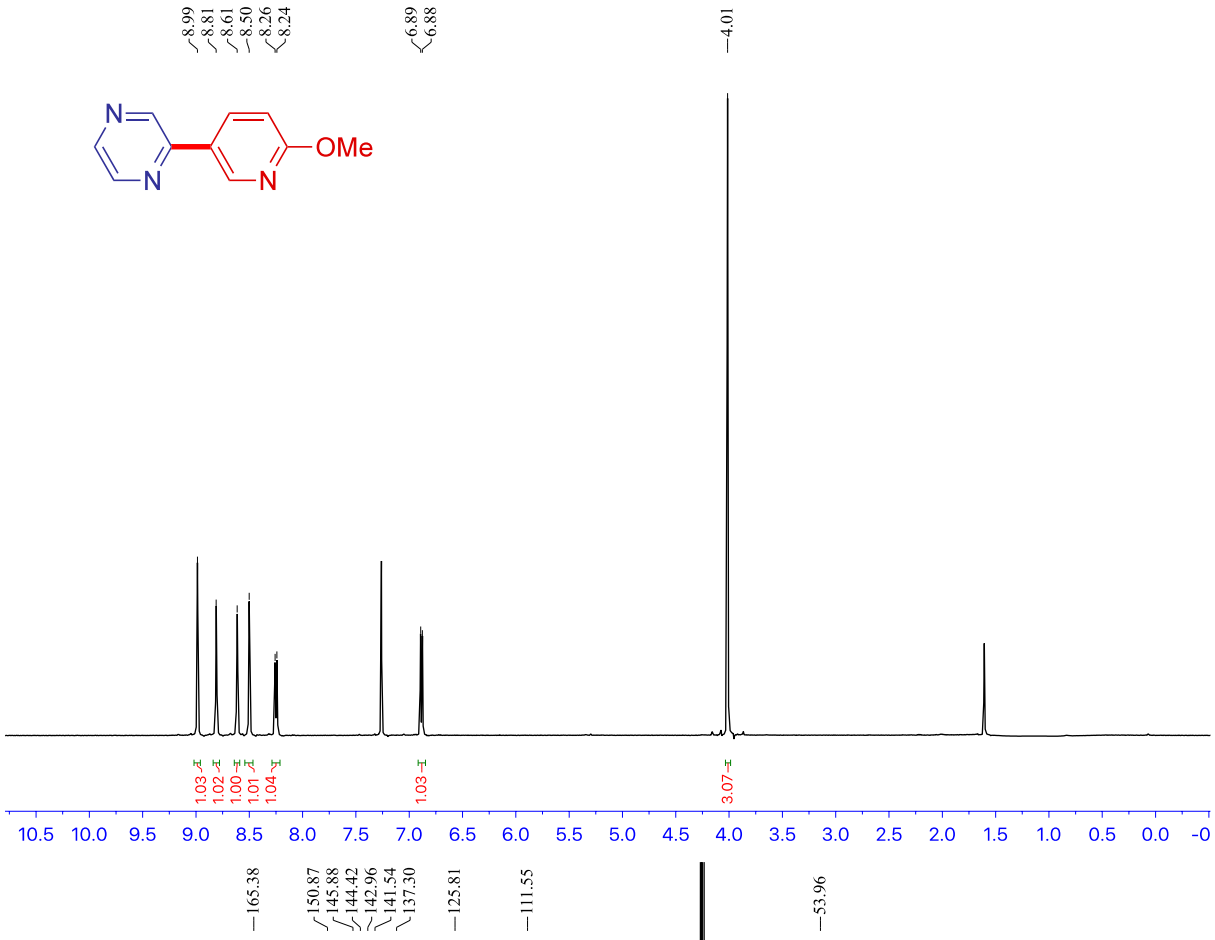

Figure S84. ^{13}C NMR spectrum of 2-(6-methoxypyridin-3-yl)pyrazine, related to **Scheme 3**

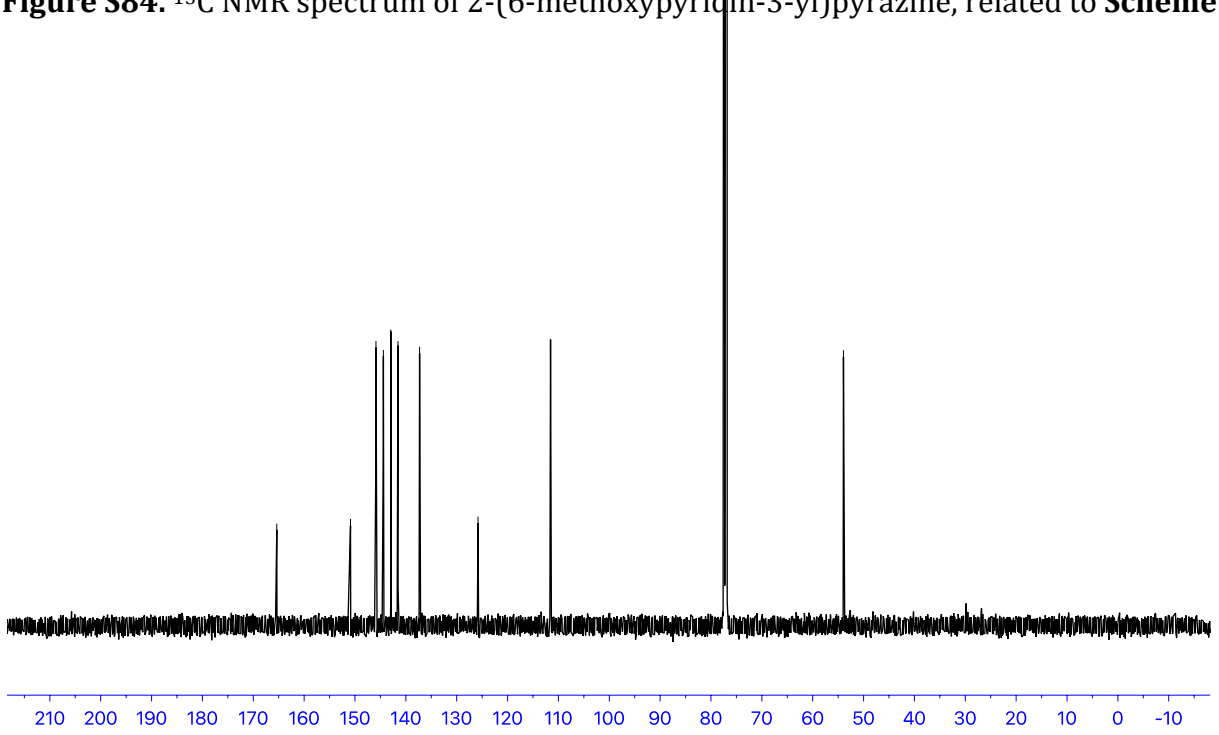

Figure S85. ^{1}H NMR spectrum of 3-(pyridin-2-yl)quinoline, related to **Scheme 3**

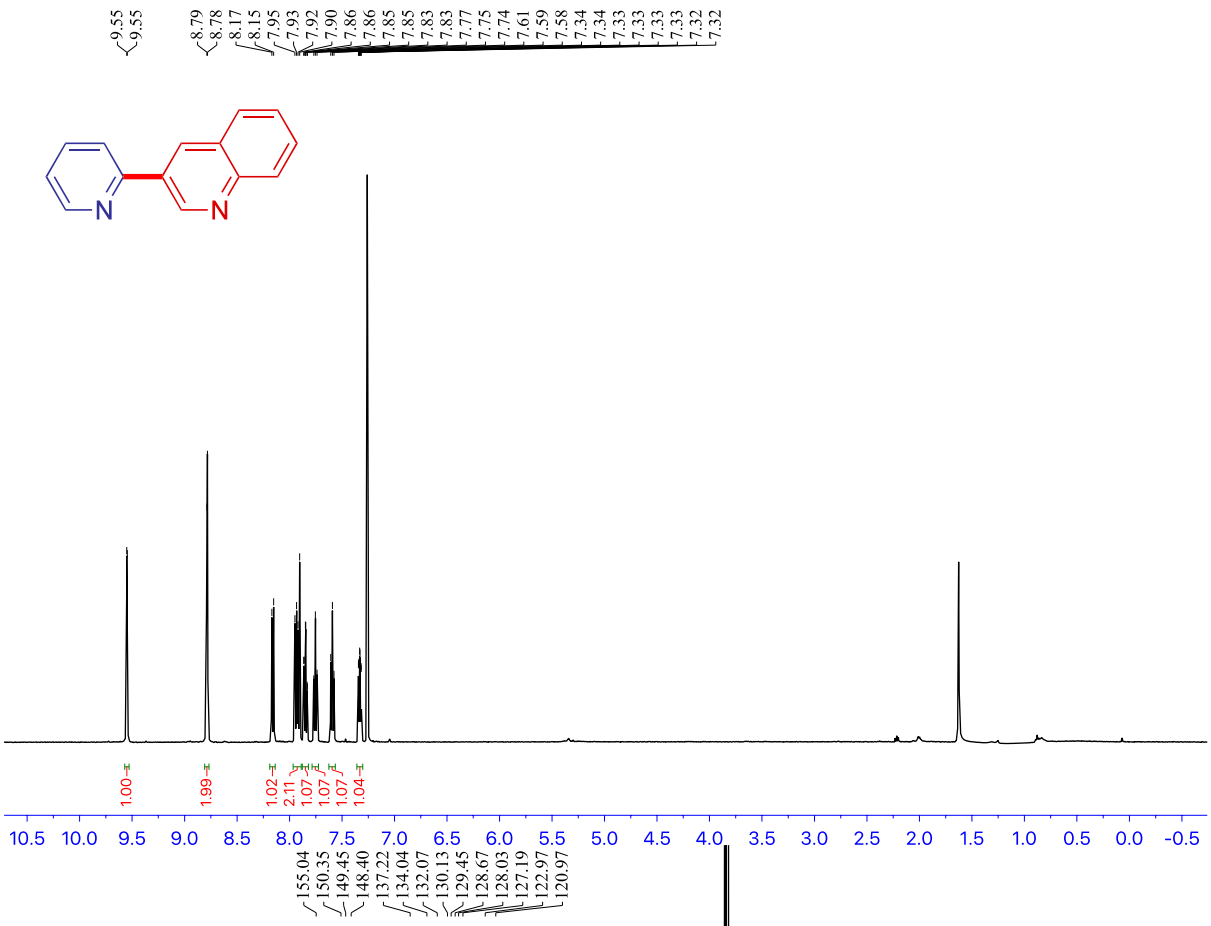

Figure S86. ^{13}C NMR spectrum of 3-(pyridin-2-yl)quinoline, related to **Scheme 3**

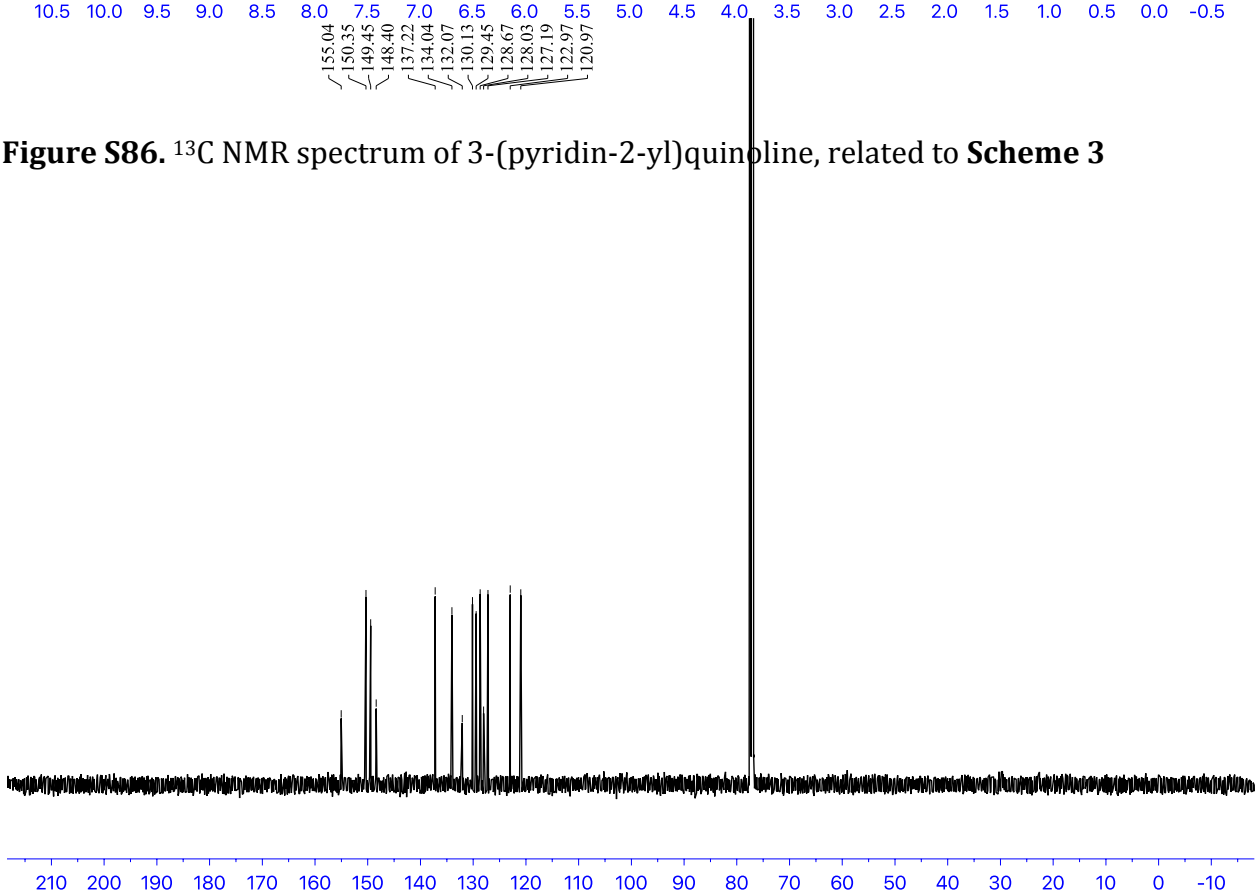

Figure S87. ^{1}H NMR spectrum of 4,6-dimethoxy-2-(naphthalen-1-yl)pyrimidine, related to **Scheme 3**

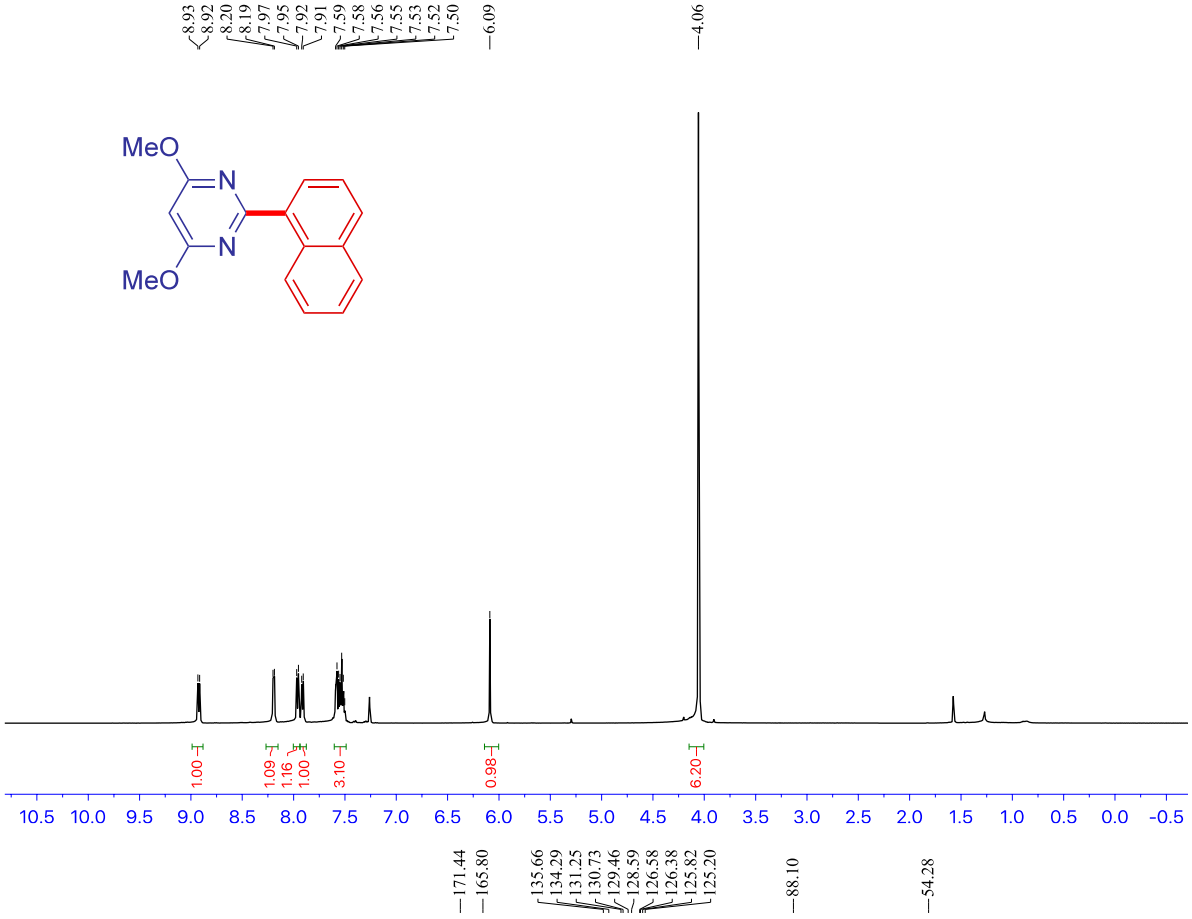

Figure S88. ^{13}C NMR spectrum of 4,6-dimethoxy-2-(naphthalen-1-yl)pyrimidine, related to **Scheme 3**

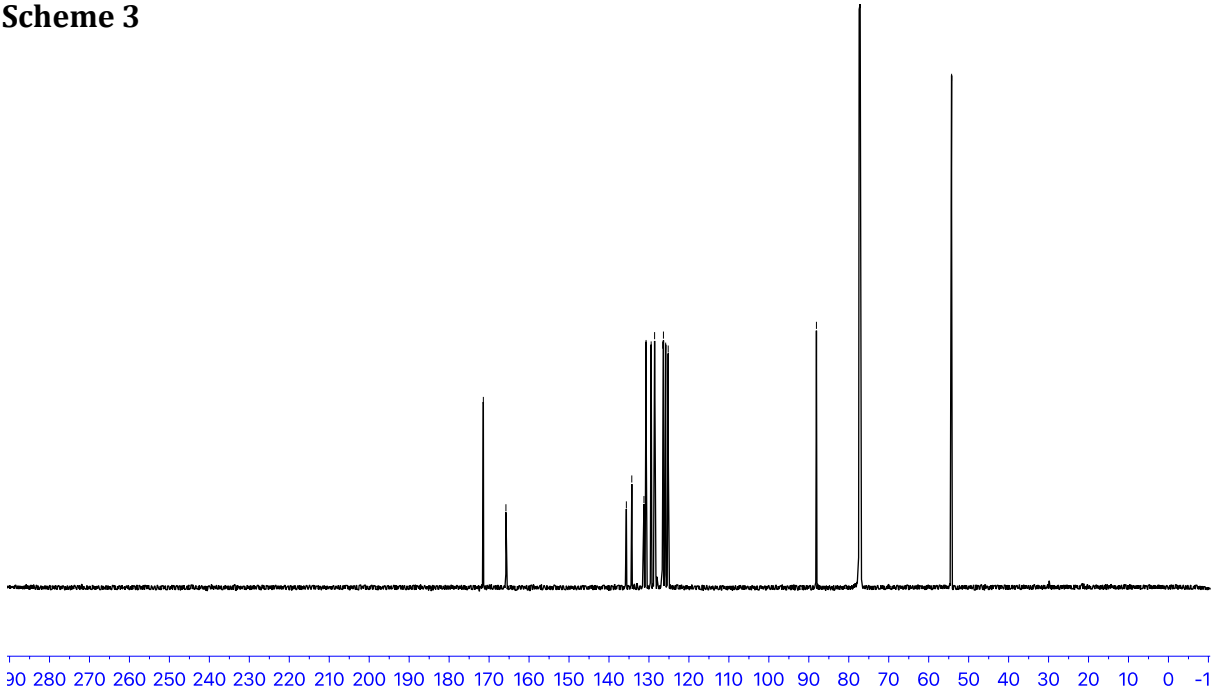

Figure S89. ^{1}H NMR spectrum of ethyl 1-methyl-5-phenyl-1*H*-indole-2-carboxylate, related to **Scheme 3**

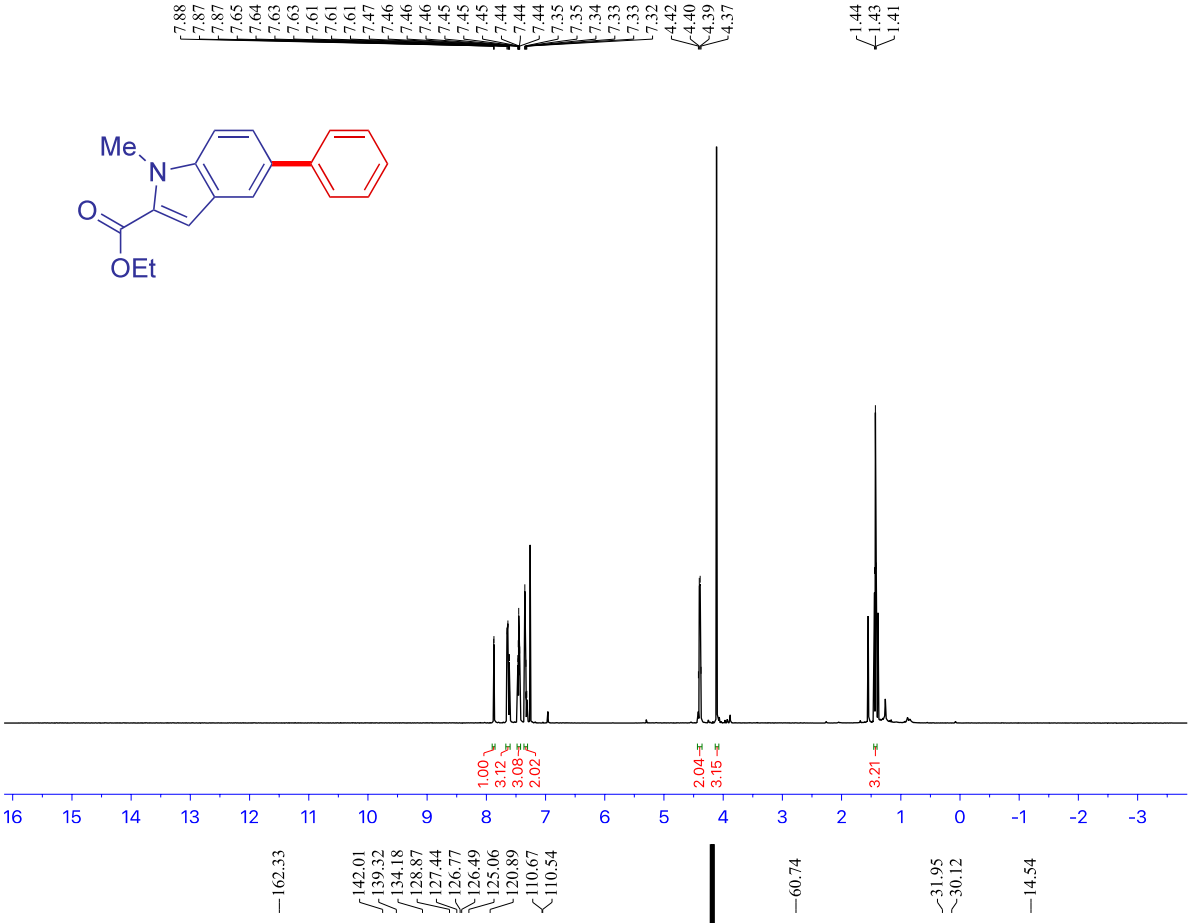

Figure S90. ^{13}C NMR spectrum of ethyl 1-methyl-5-phenyl-1*H*-indole-2-carboxylate, related to **Scheme 3**

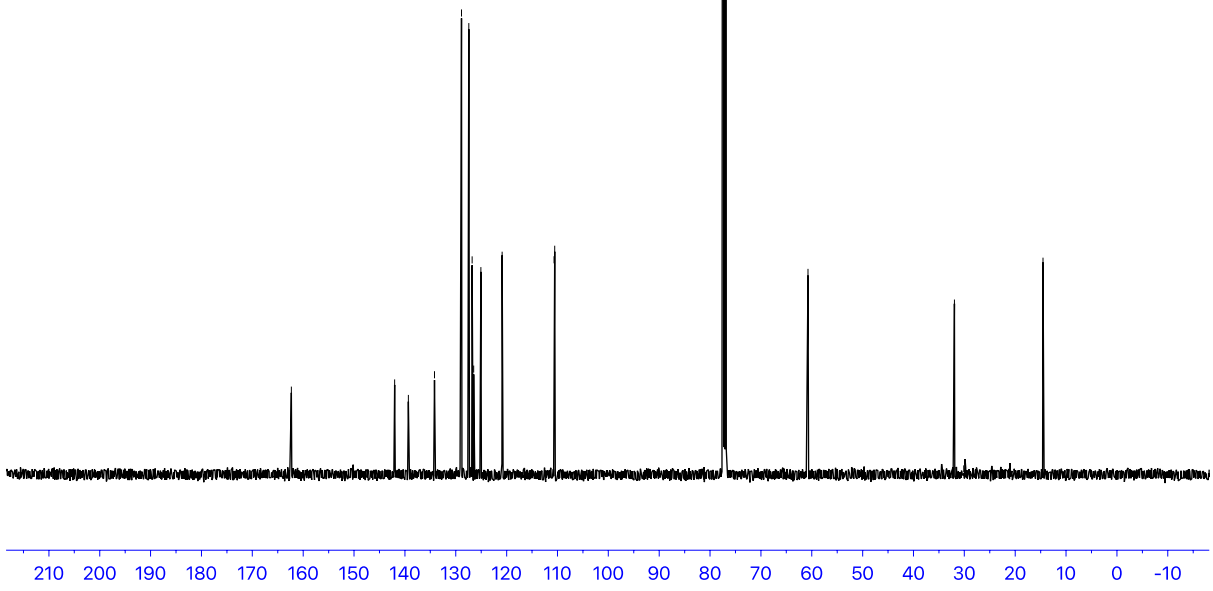

Figure S91. ^{1}H NMR spectrum of 2,4-di-*tert*-butyl-6-(5-(4-(trifluoromethyl)phenyl)-2*H*-benzo[*d*][1,2,3]triazol-2-yl)phenol, related to **Scheme 3**

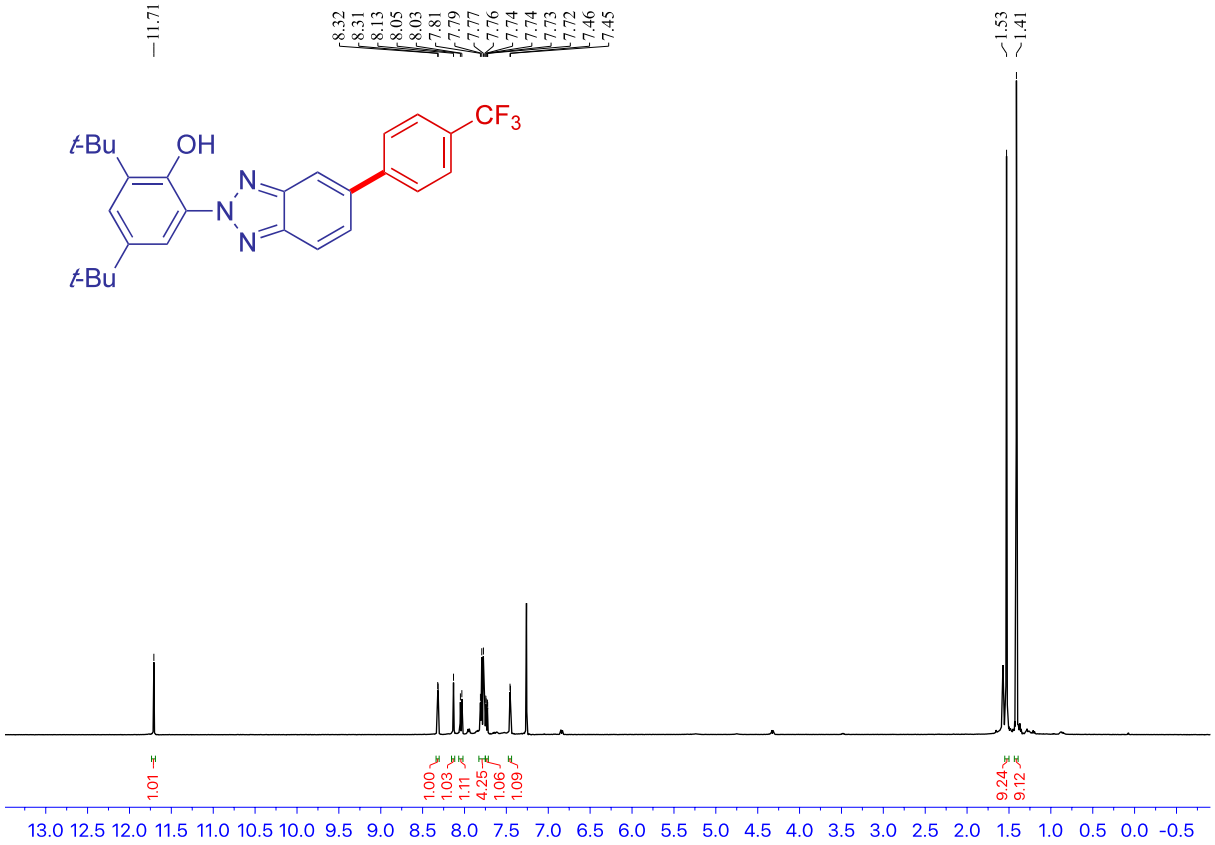

Figure S92. ^{13}C NMR spectrum of 2,4-di-*tert*-butyl-6-(5-(4-(trifluoromethyl)phenyl)-2*H*-benzo[*d*][1,2,3]triazol-2-yl)phenol, related to **Scheme 3**

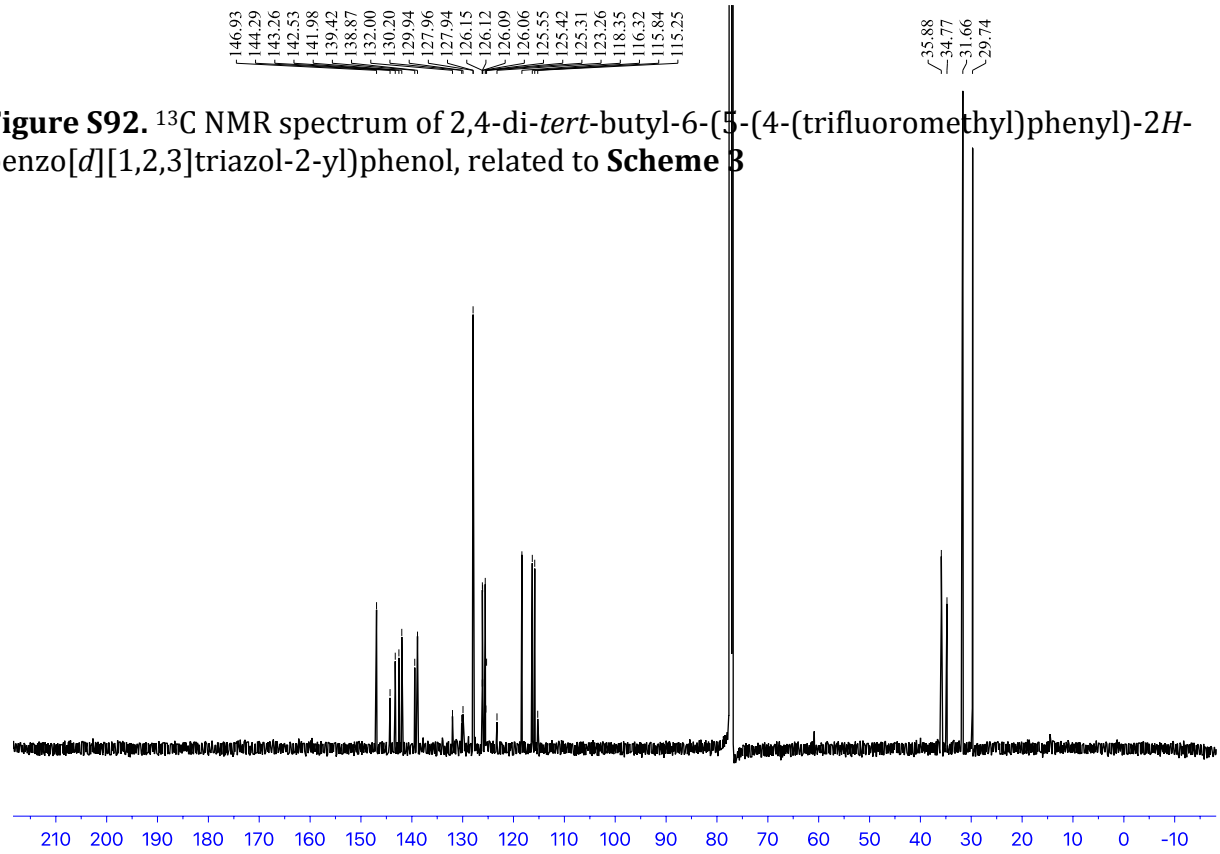

Figure S93. ^{19}F NMR spectrum of 2,4-di-*tert*-butyl-6-(5-(4-(trifluoromethyl)phenyl)-2*H*-benzo[*d*][1,2,3]triazol-2-yl)phenol, related to **Scheme 3**

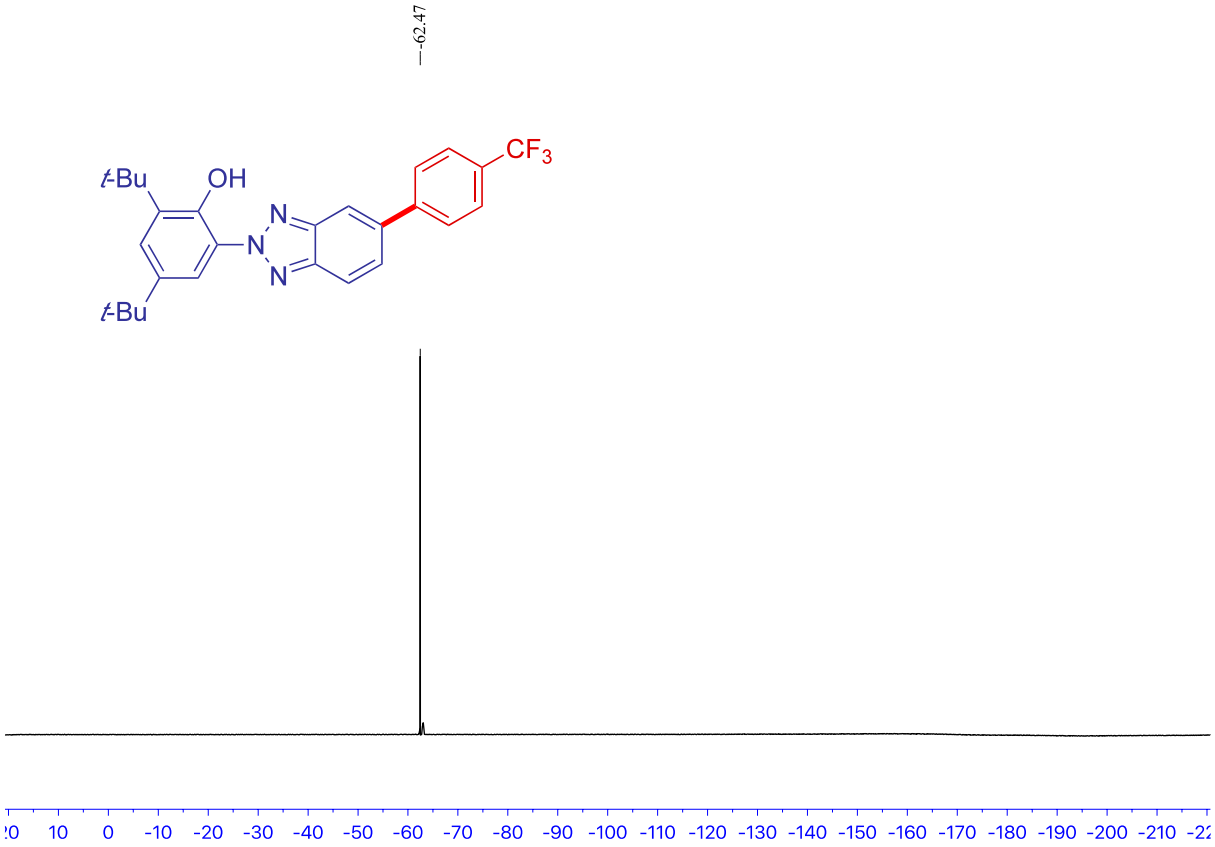

Figure S94. ^{1}H NMR spectrum of 4'-methoxy-3,5-bis(trifluoromethyl)biphenyl, related to **Scheme 3**

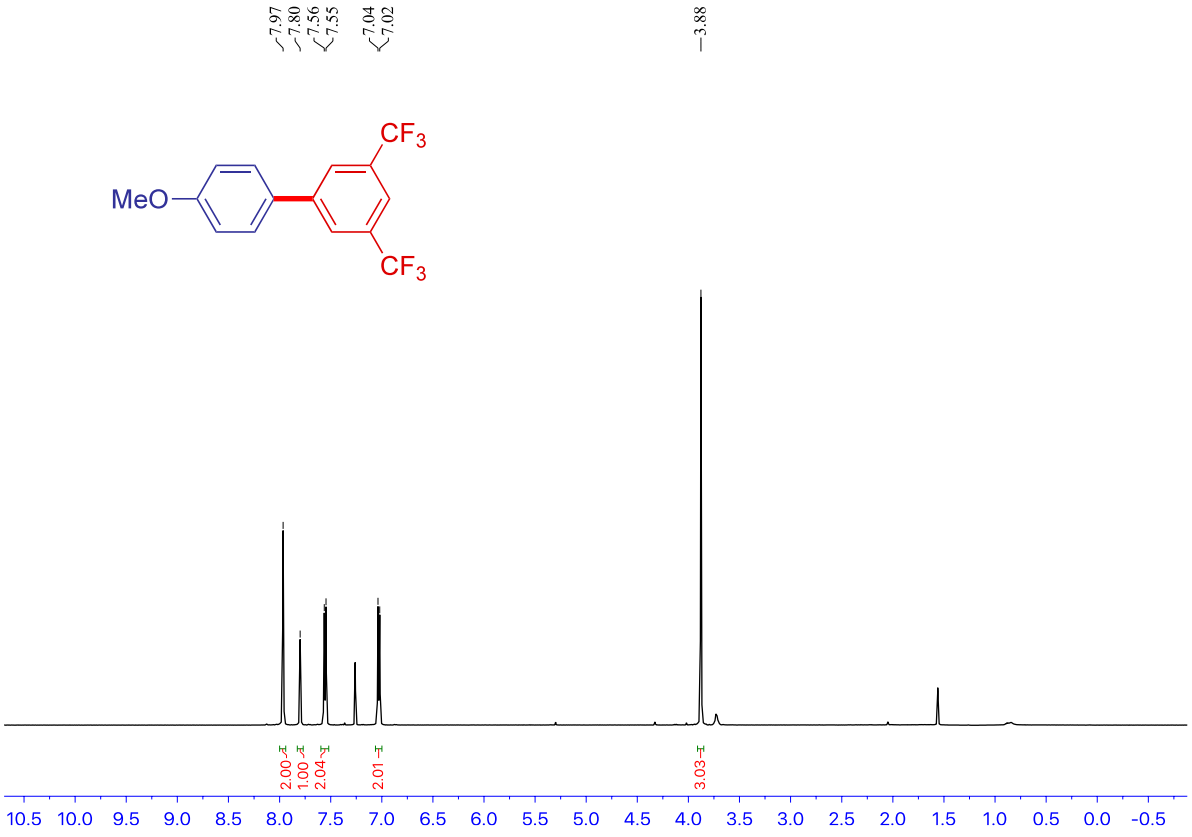

Figure S95. ^{13}C NMR spectrum of 4'-methoxy-3,5-bis(trifluoromethyl)biphenyl, related to **Scheme 3**

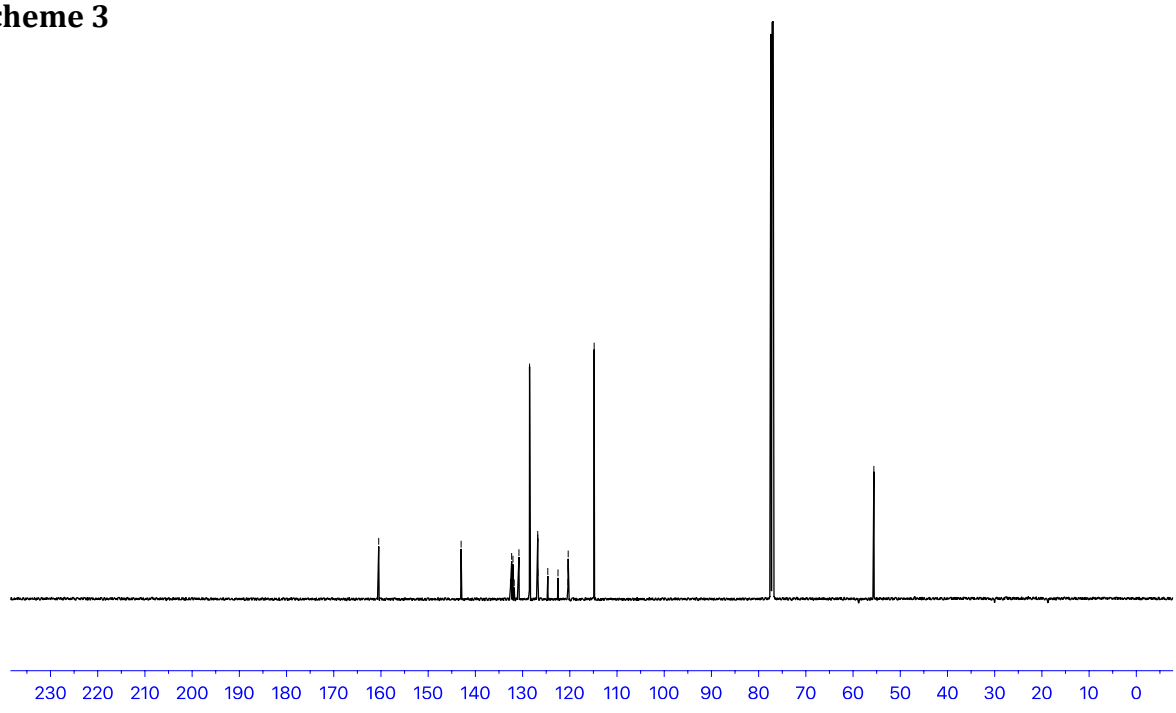

Figure S96. ^{19}F NMR spectrum of 4'-Methoxy-3,5-bis(trifluoromethyl)biphenyl, related to **Scheme 3**

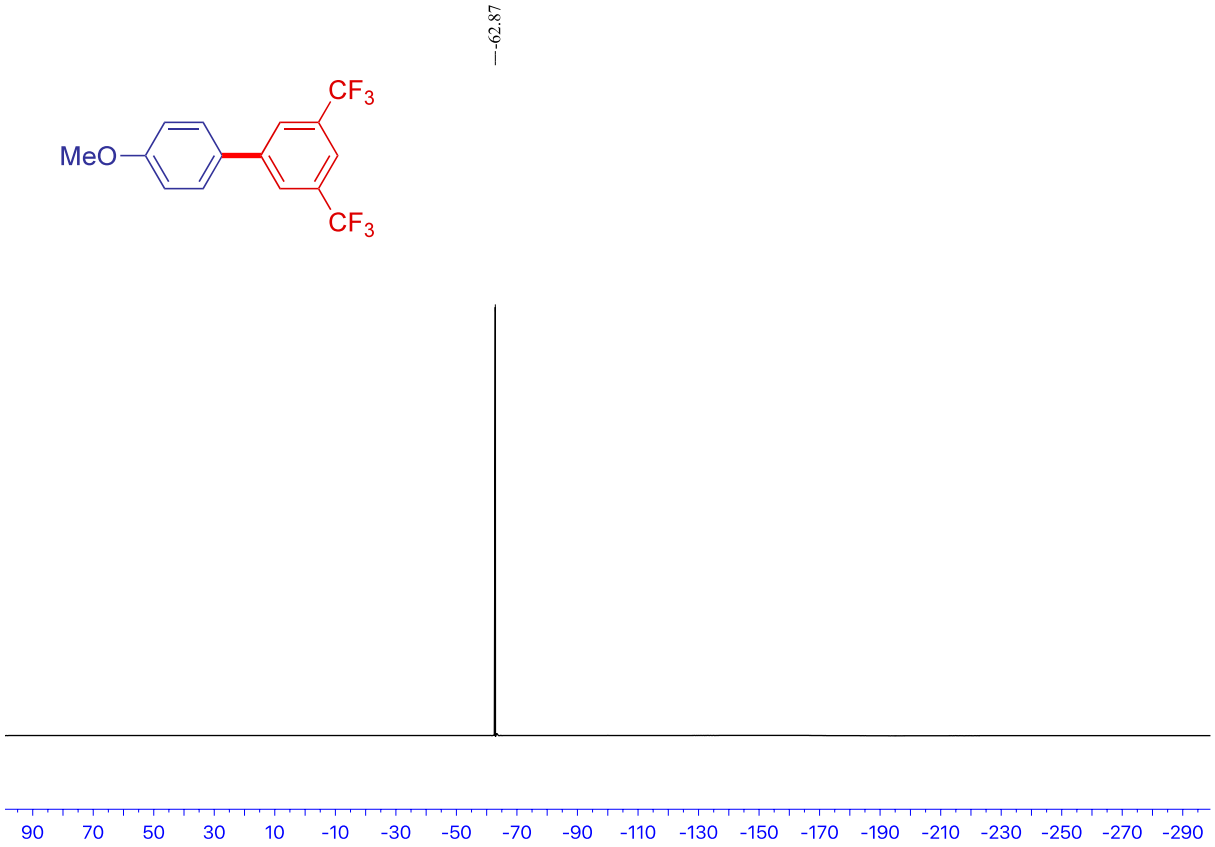

Figure S97. ^{1}H NMR spectrum of *tert*-butyl 2-(4,6-dimethoxypyrimidin-2-yl)-1*H*-pyrrole-1-carboxylate, related to **Scheme 3**

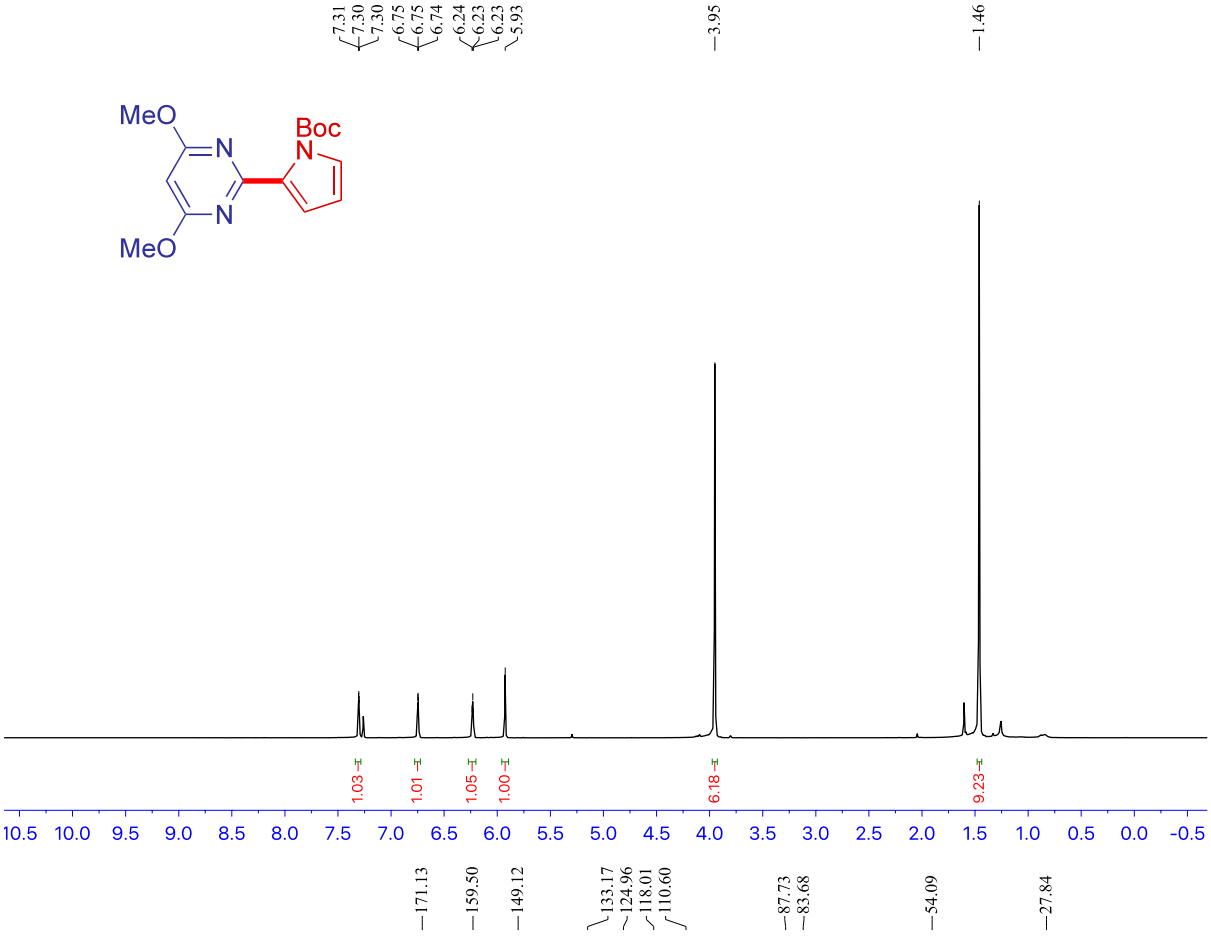

Figure S98. ^{13}C NMR spectrum of *tert*-butyl 2-(4,6-dimethoxypyrimidin-2-yl)-1*H*-pyrrole-1-carboxylate, related to **Scheme 3**

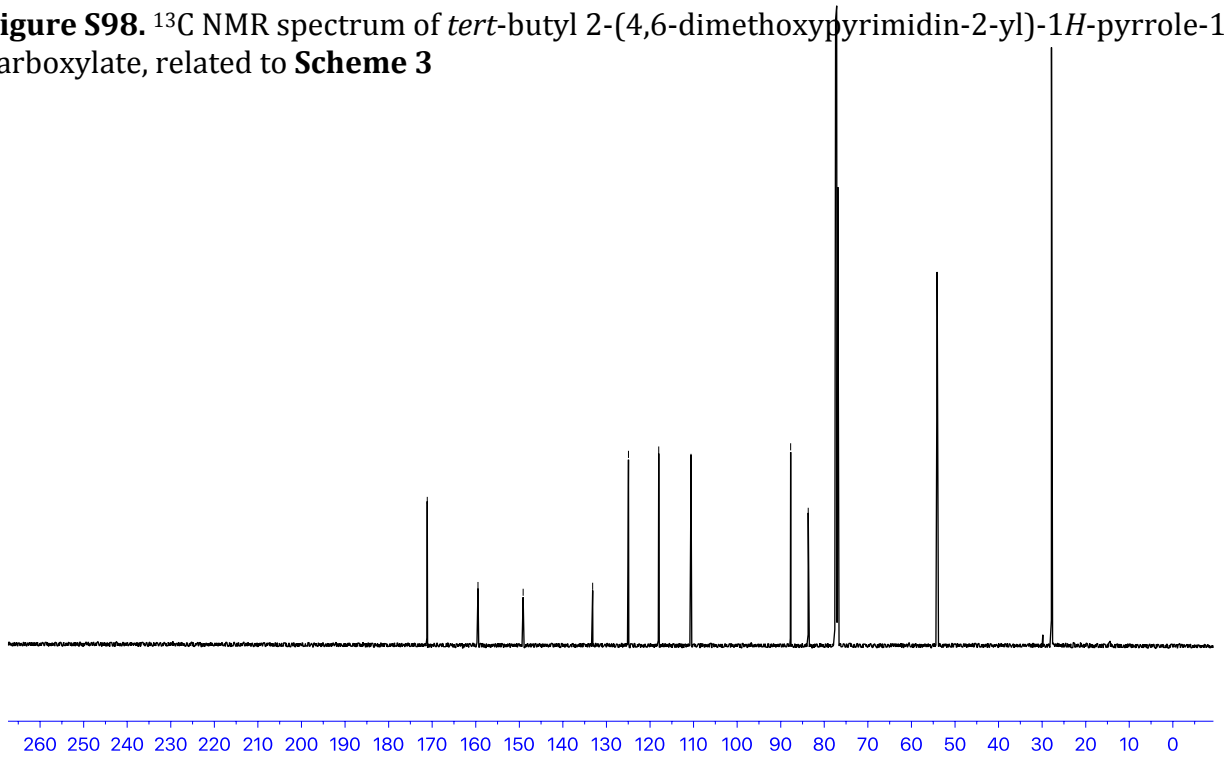

Figure S99. ^{1}H NMR spectrum of isopropyl 2-(4-([1,1'-biphenyl]-4-carbonyl)phenoxy)-2-methylpropanoate, related to **Scheme 4**

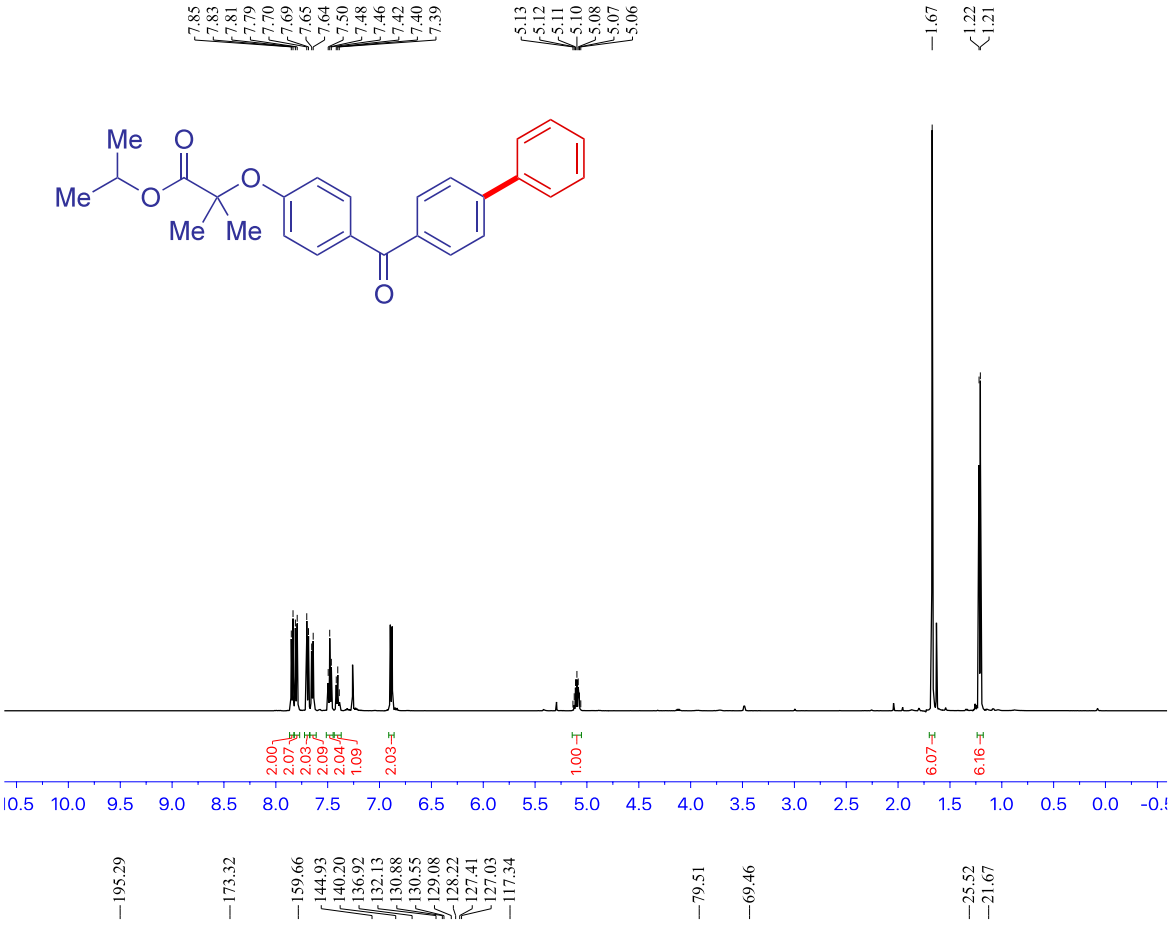

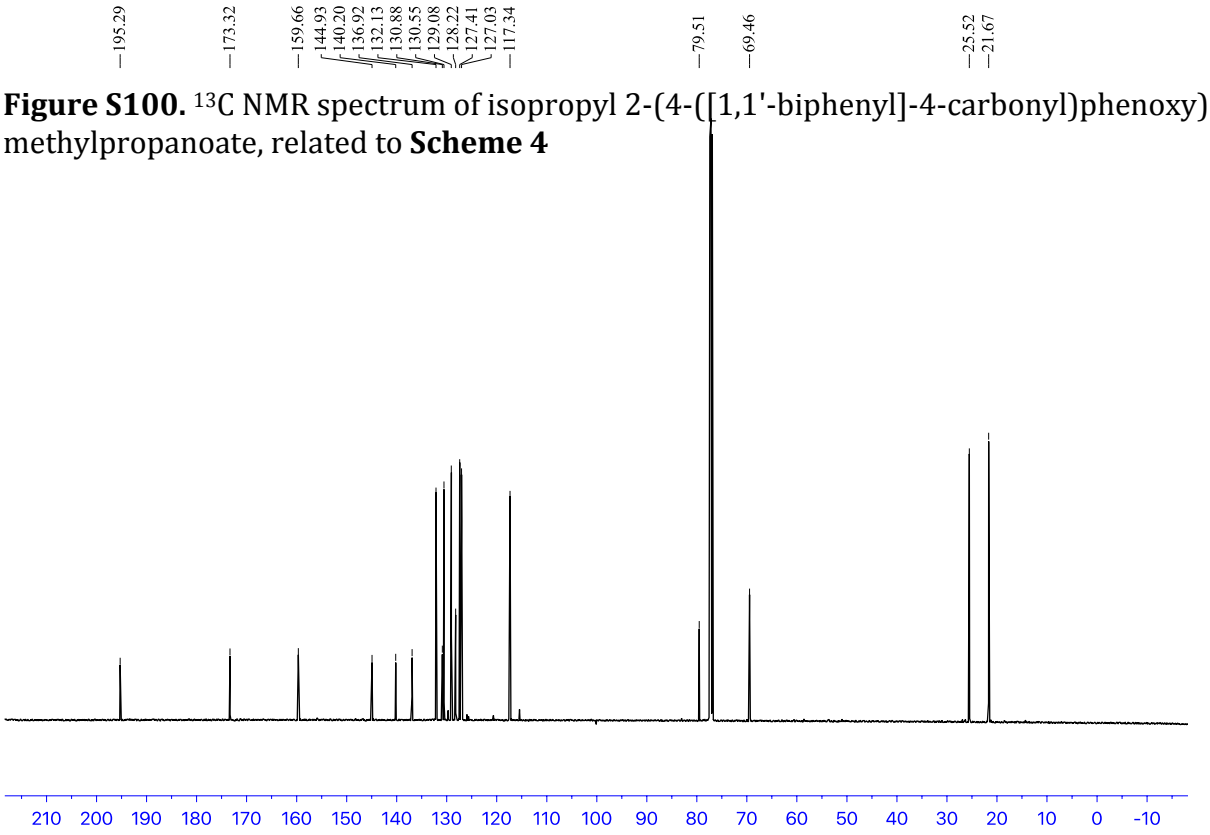

Figure S100. ^{13}C NMR spectrum of isopropyl 2-(4-([1,1'-biphenyl]-4-carbonyl)phenoxy)-2-methylpropanoate, related to **Scheme 4**

Figure S101. ^{1}H NMR spectrum of 1-(4-fluorophenyl)-4-(4-hydroxy-4-(4'-methoxy-[1,1'-biphenyl]-4-yl)piperidin-1-yl)butan-1-one, related to **Scheme 4**

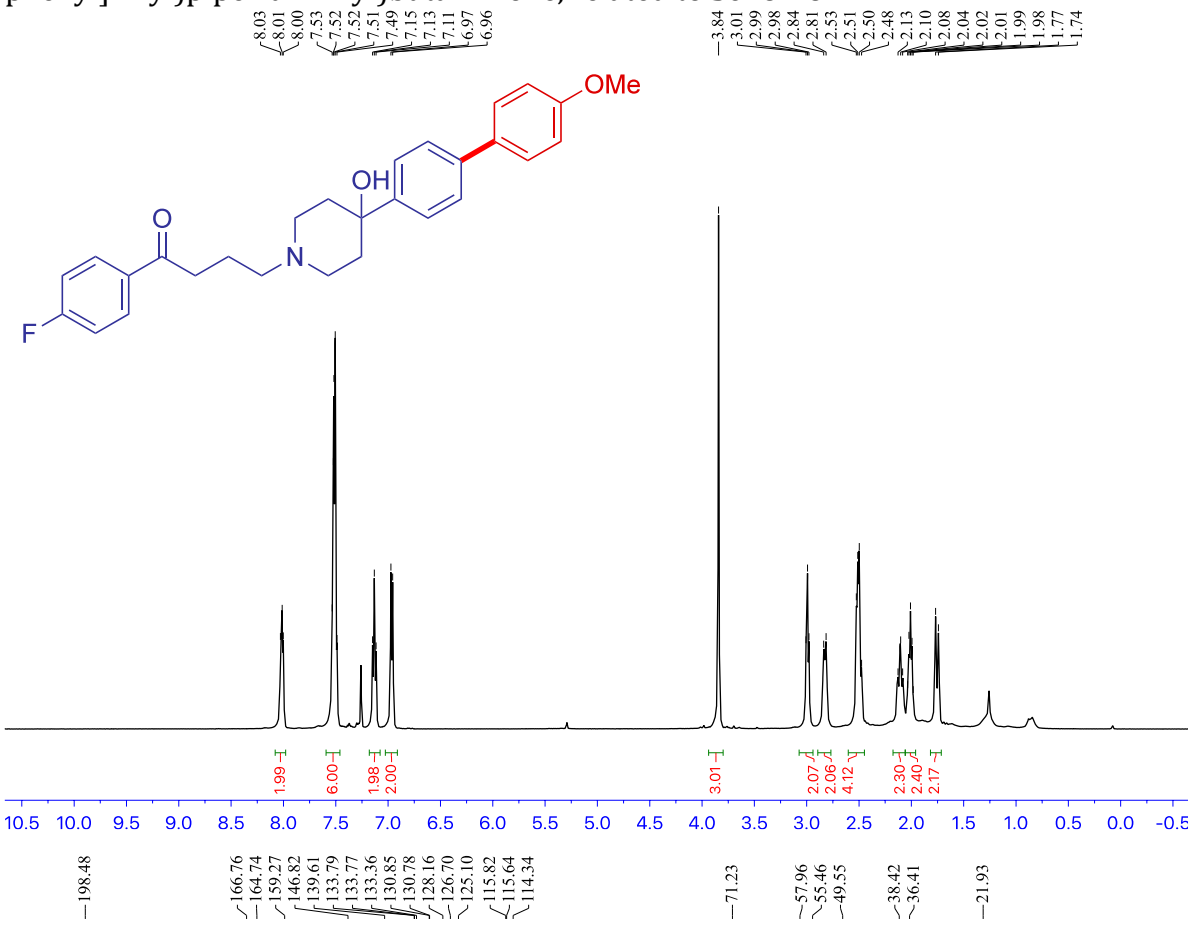

Figure S102. ^{13}C NMR spectrum of 1-(4-fluorophenyl)-4-(4-hydroxy-4-(4'-methoxy-[1,1'-biphenyl]-4-yl)piperidin-1-yl)butan-1-one, related to **Scheme 4**

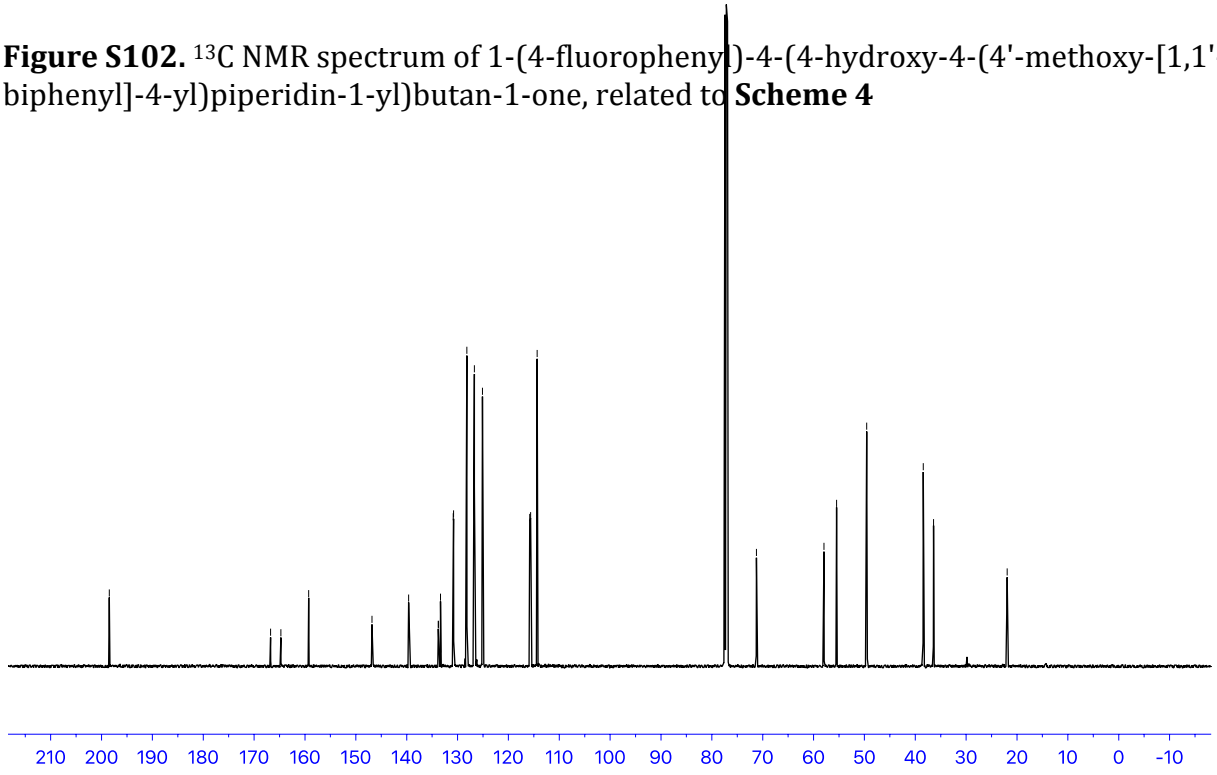

Figure S103. ^{19}F NMR spectrum of 1-(4-fluorophenyl)-4-(4-hydroxy-4-(4'-methoxy-[1,1'-biphenyl]-4-yl)piperidin-1-yl)butan-1-one, related to **Scheme 4**

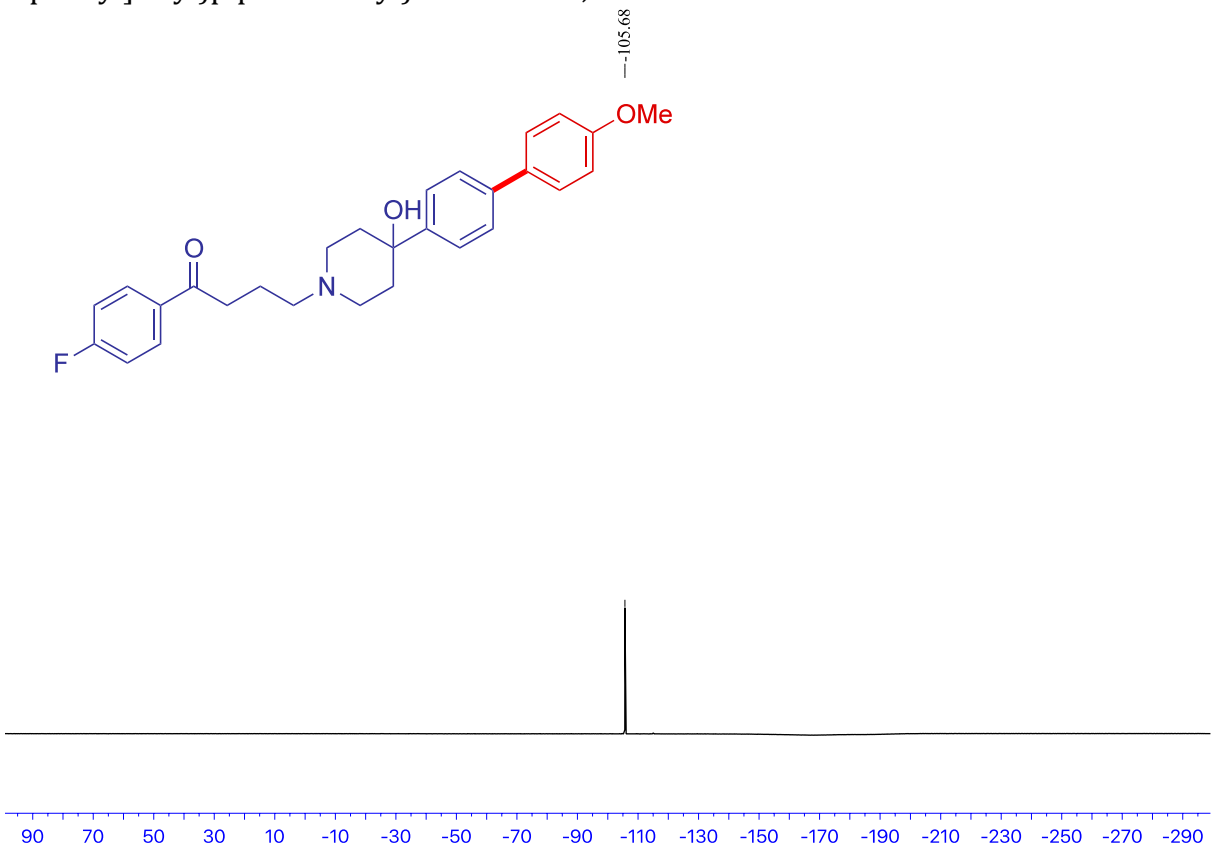

Figure S104. [1]H NMR spectrum of 2-(5-methoxy-2-methyl-1-(4'-methyl-[1,1'-biphenyl]-4-carbonyl)-1*H*-indol-3-yl)acetic acid, related to **Scheme 4**

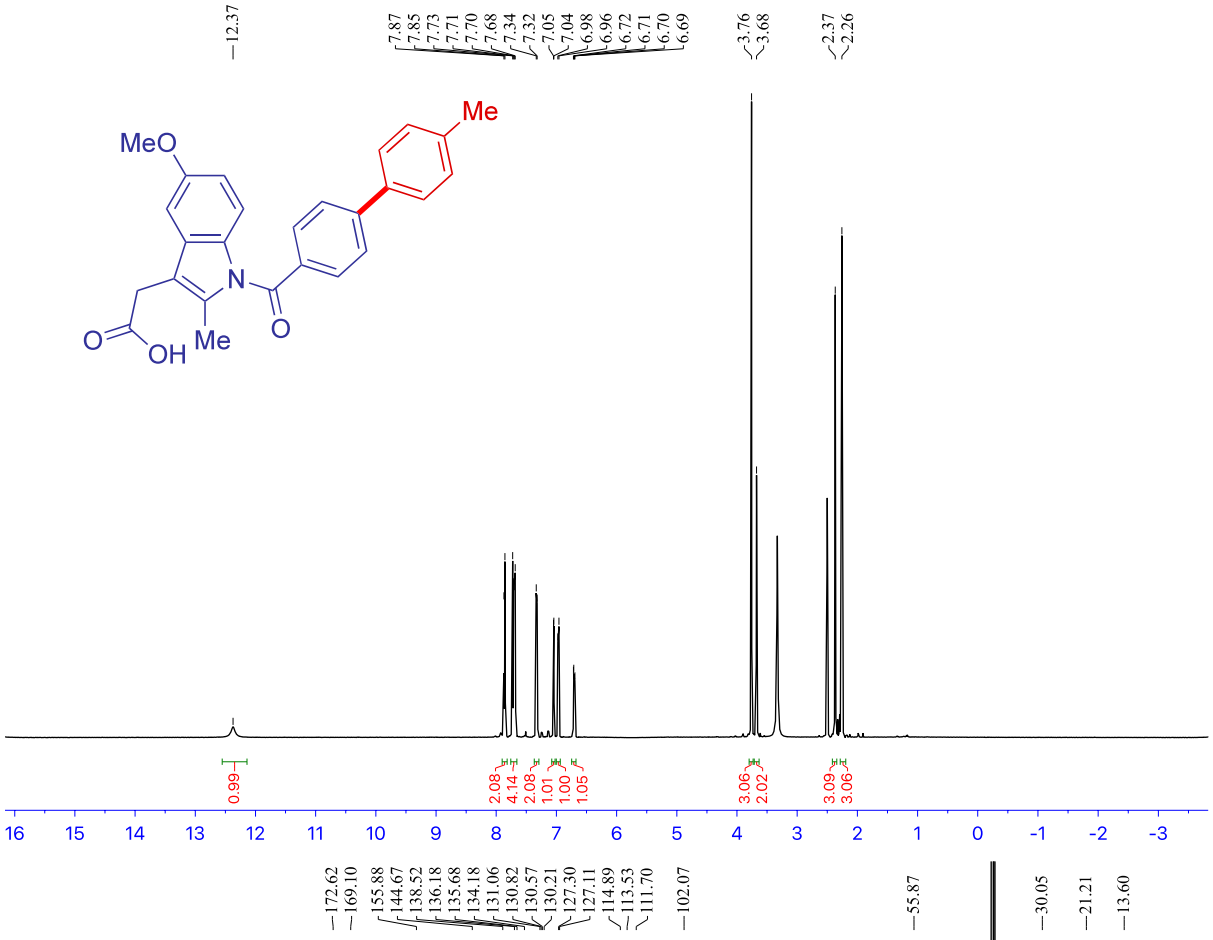

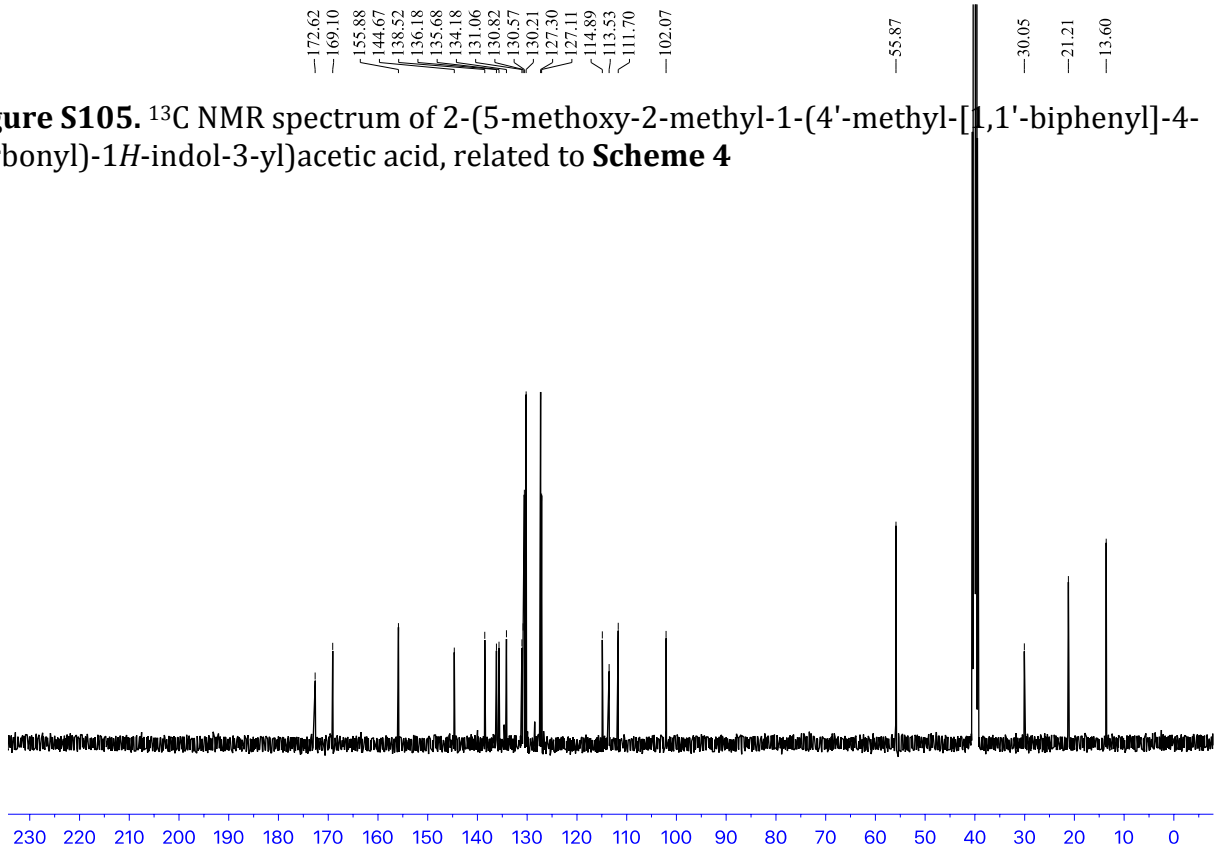

Figure S105. [13]C NMR spectrum of 2-(5-methoxy-2-methyl-1-(4'-methyl-[1,1'-biphenyl]-4-carbonyl)-1*H*-indol-3-yl)acetic acid, related to **Scheme 4**

Figure S106. ^{1}H NMR spectrum of *N,N*-dimethyl-3-(2-phenyl-10*H*-phenothiazin-10-yl)propan-1-amine, related to **Scheme 4**

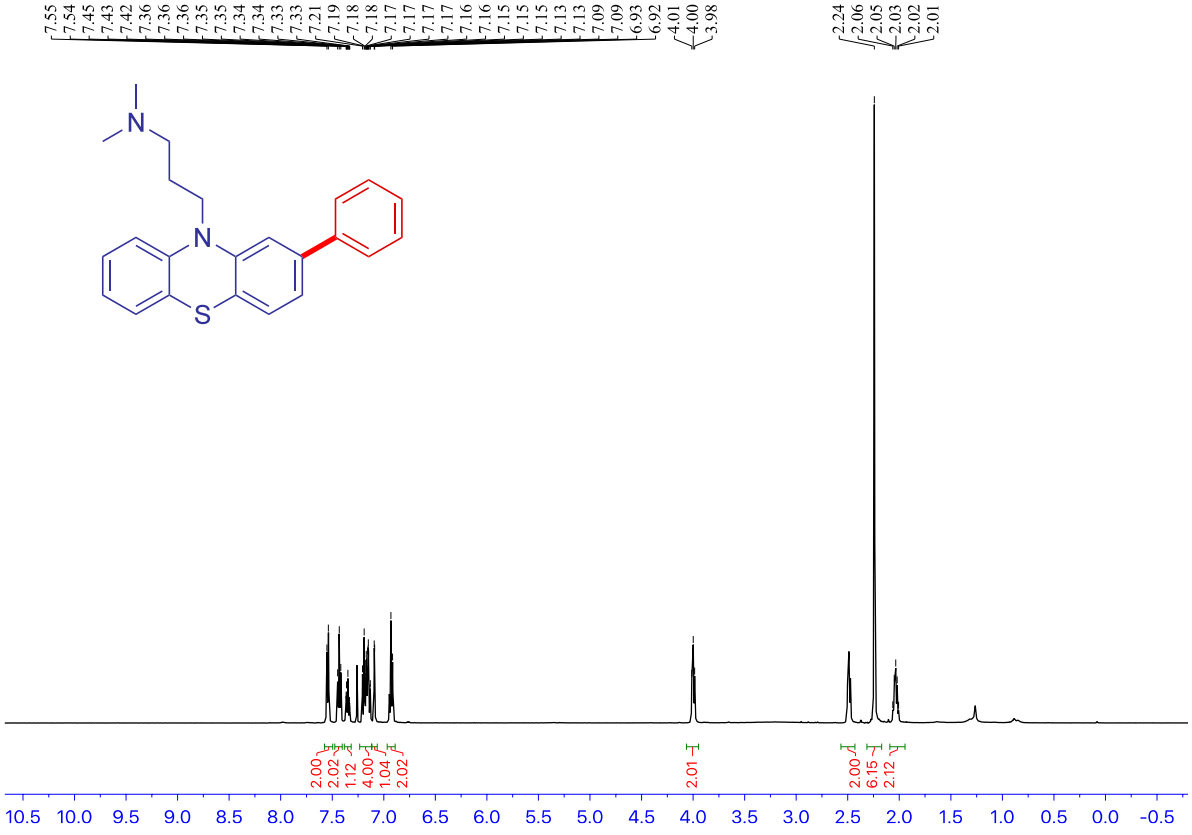

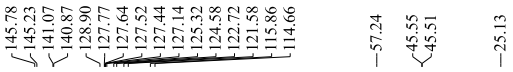

Figure S107. ^{13}C NMR spectrum of *N,N*-dimethyl-3-(2-phenyl-10*H*-phenothiazin-10-yl)propan-1-amine, related to **Scheme 4**

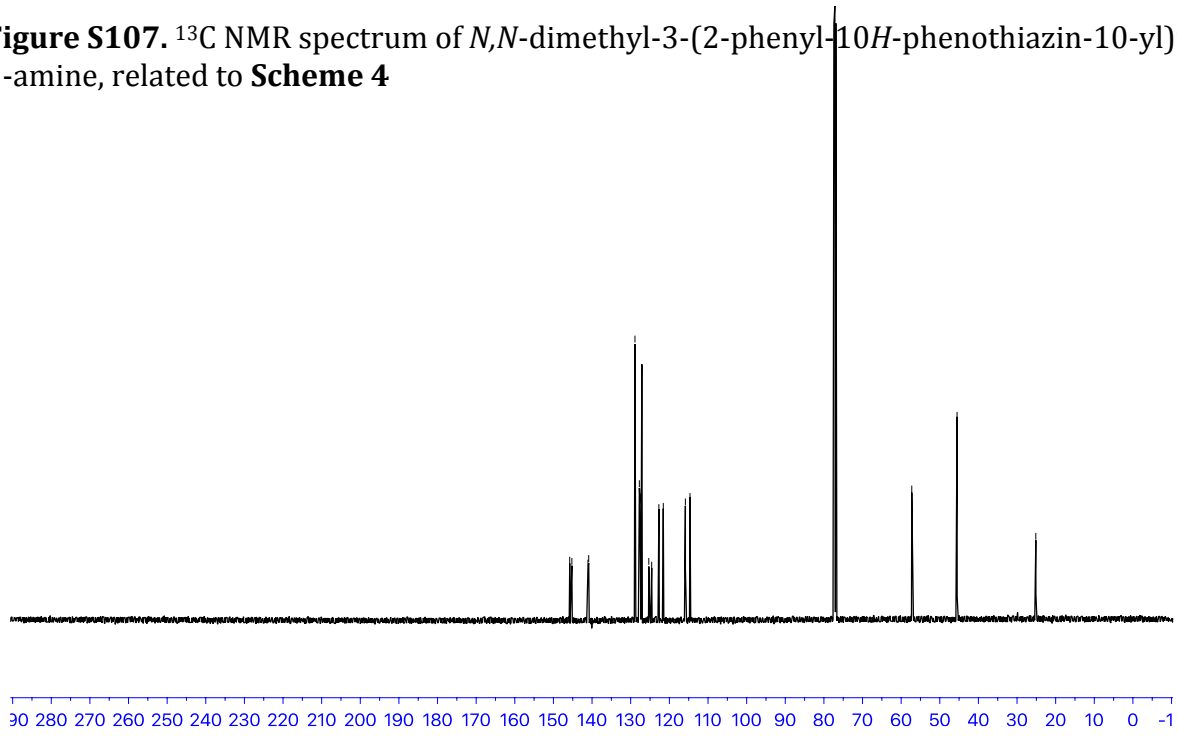

Figure S108. ^{1}H NMR spectrum of *N*-(4-(*N*-(cyclohexylcarbamoyl)sulfamoyl)phenethyl)-4-methoxy-4'-methyl-[1,1'-biphenyl]-3-carboxamide, related to **Scheme 4**

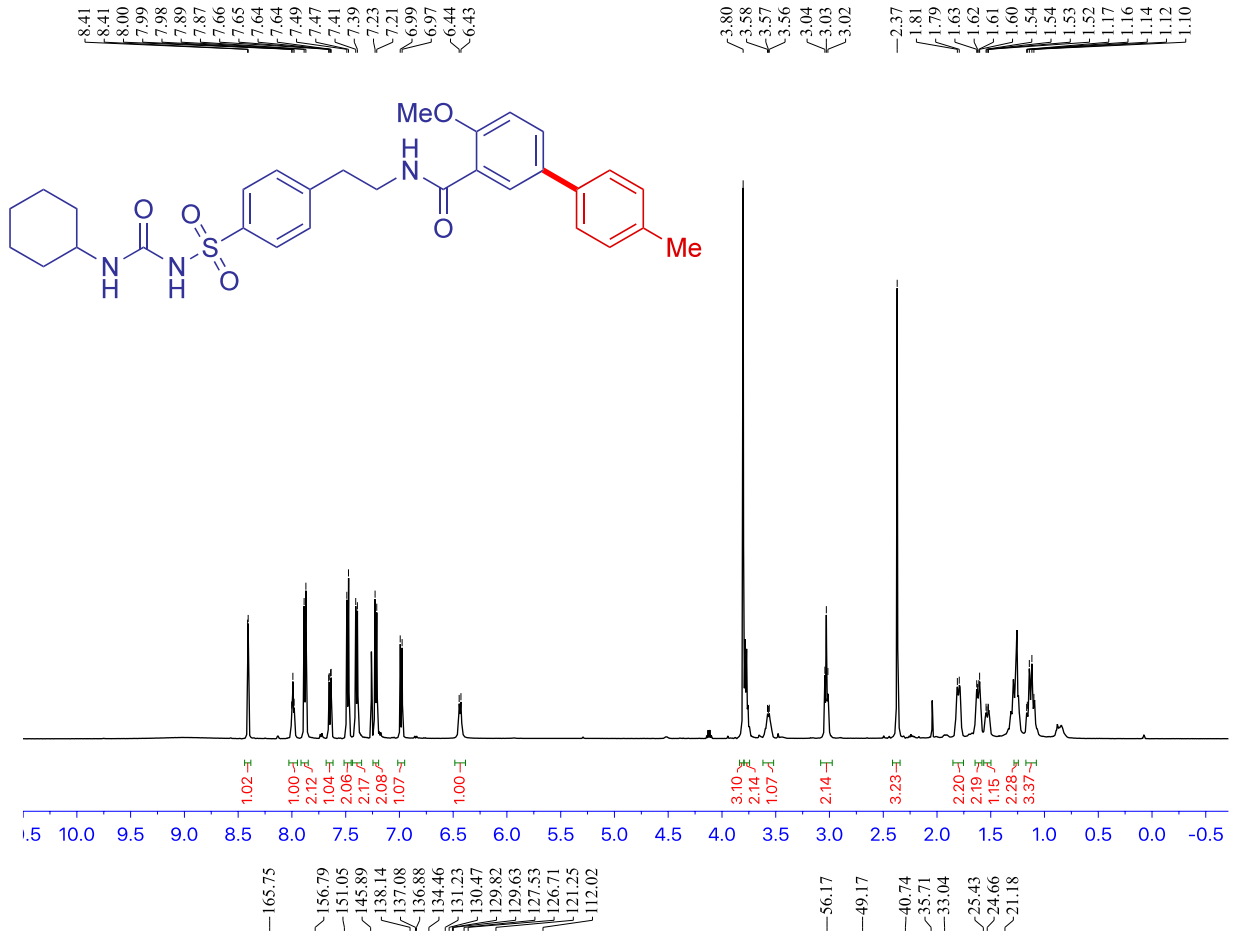

Figure S109. ^{13}C NMR spectrum of *N*-(4-(*N*-(cyclohexylcarbamoyl)sulfamoyl)phenethyl)-4-methoxy-4'-methyl-[1,1'-biphenyl]-3-carboxamide, related to **Scheme 4**

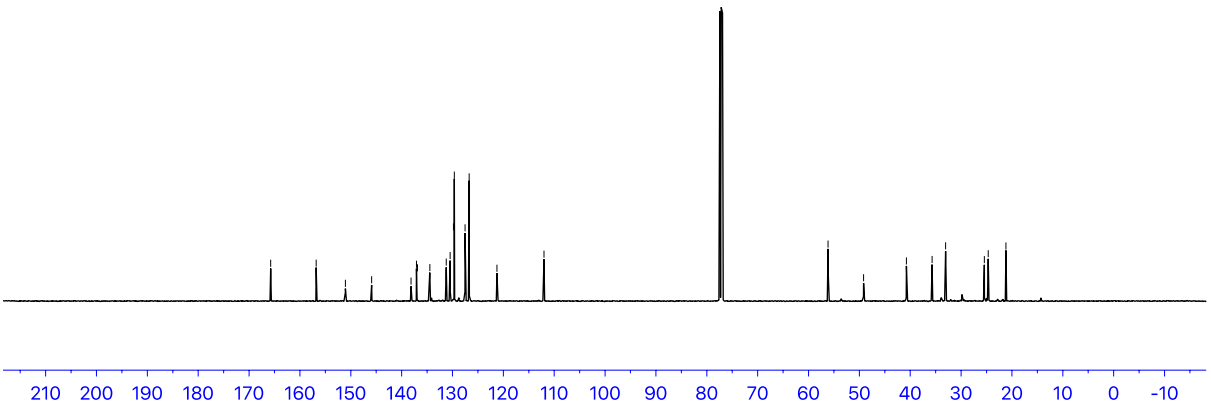

Figure S110. ^{1}H NMR spectrum of (2*S*,6'*R*)-2',4,6-trimethoxy-6'-methyl-7-(*p*-tolyl)-3*H*-spiro[benzofuran-2,1'-cyclohexan]-2'-ene-3,4'-dione, related to **Scheme 4**

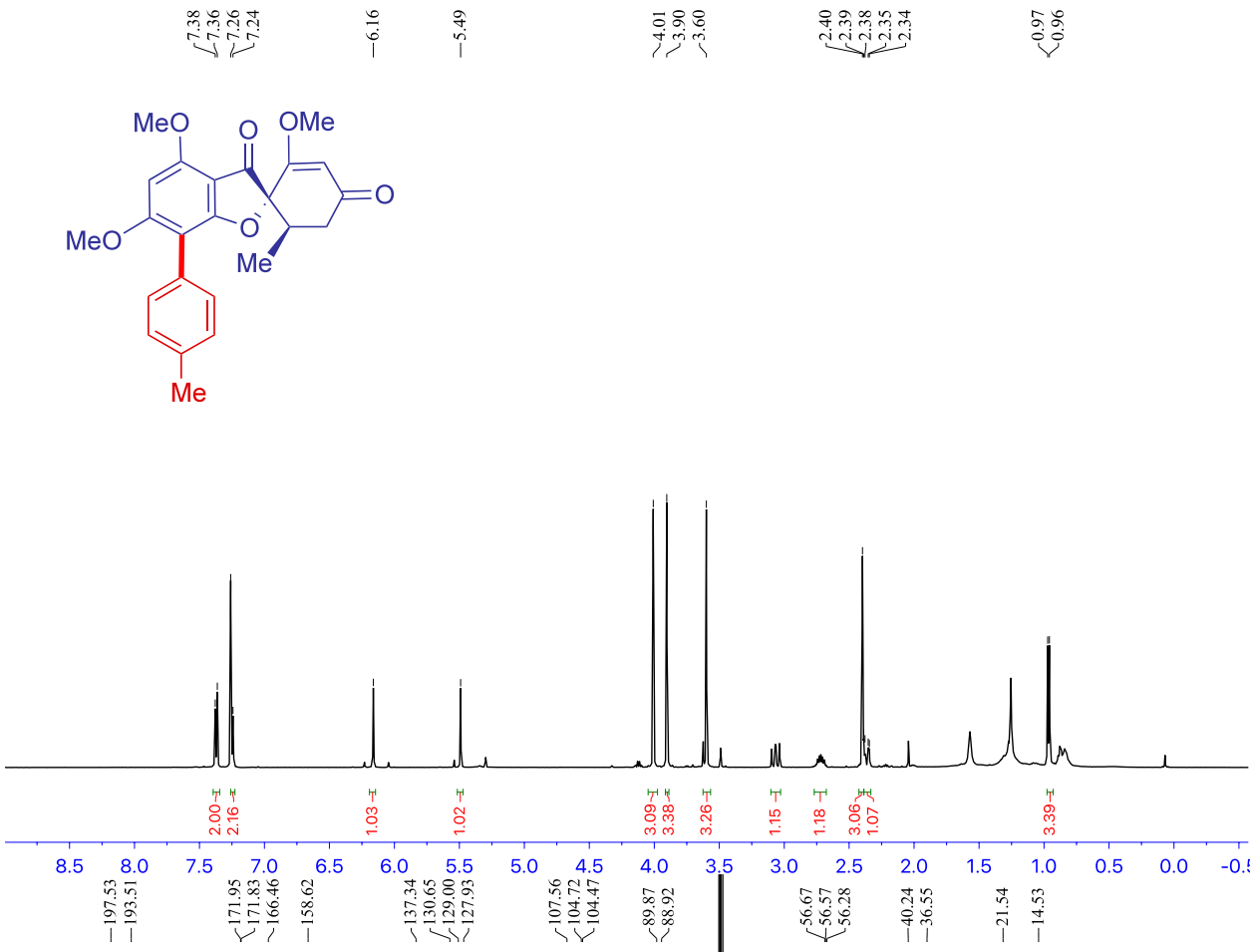

Figure S111. ^{13}C NMR spectrum of (2*S*,6'*R*)-2',4,6-trimethoxy-6'-methyl-7-(*p*-tolyl)-3*H*-spiro[benzofuran-2,1'-cyclohexan]-2'-ene-3,4'-dione, related to **Scheme 4**

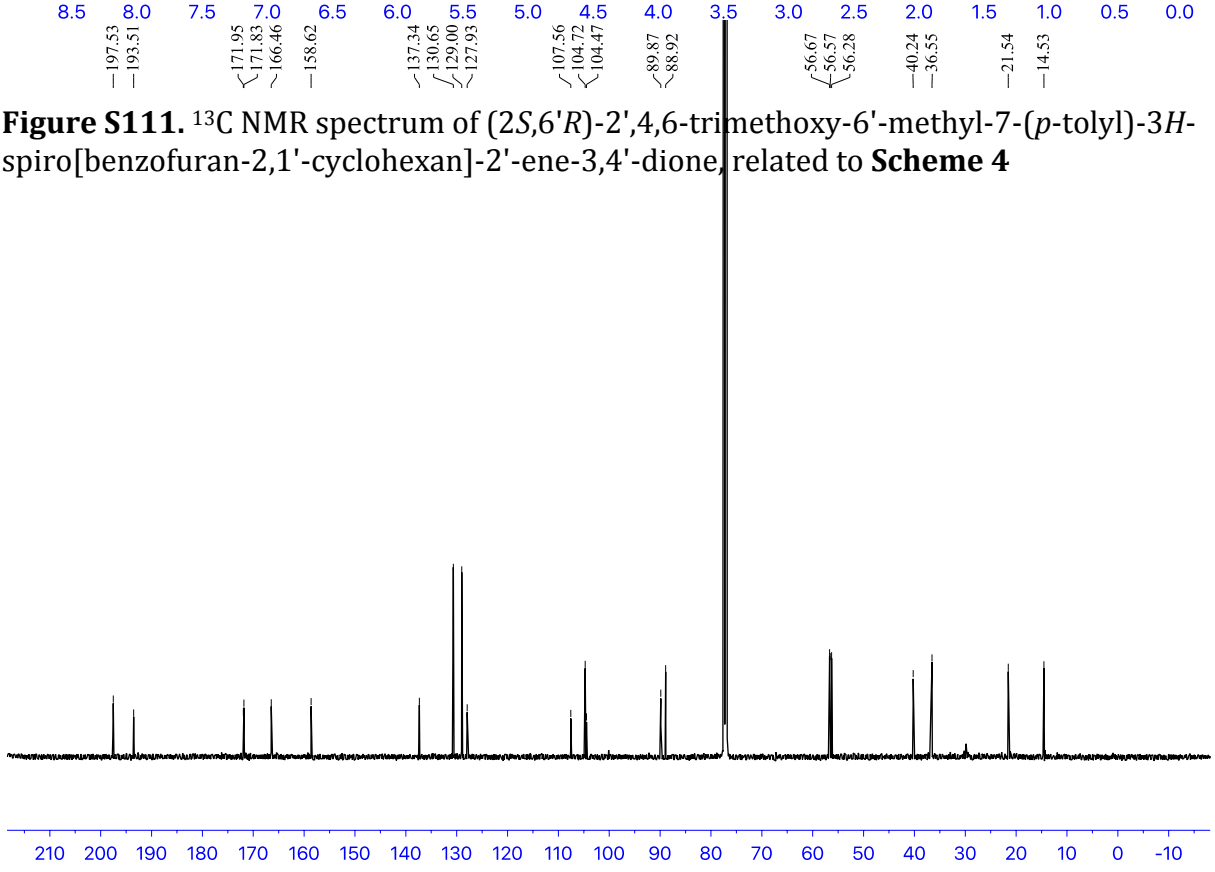

Figure S112. ^{1}H NMR spectrum of N^4-(7-(3,4-dimethoxyphenyl)quinolin-4-yl)-N^1,N^1-diethylpentane-1,4-diamine, related to **Scheme 4**

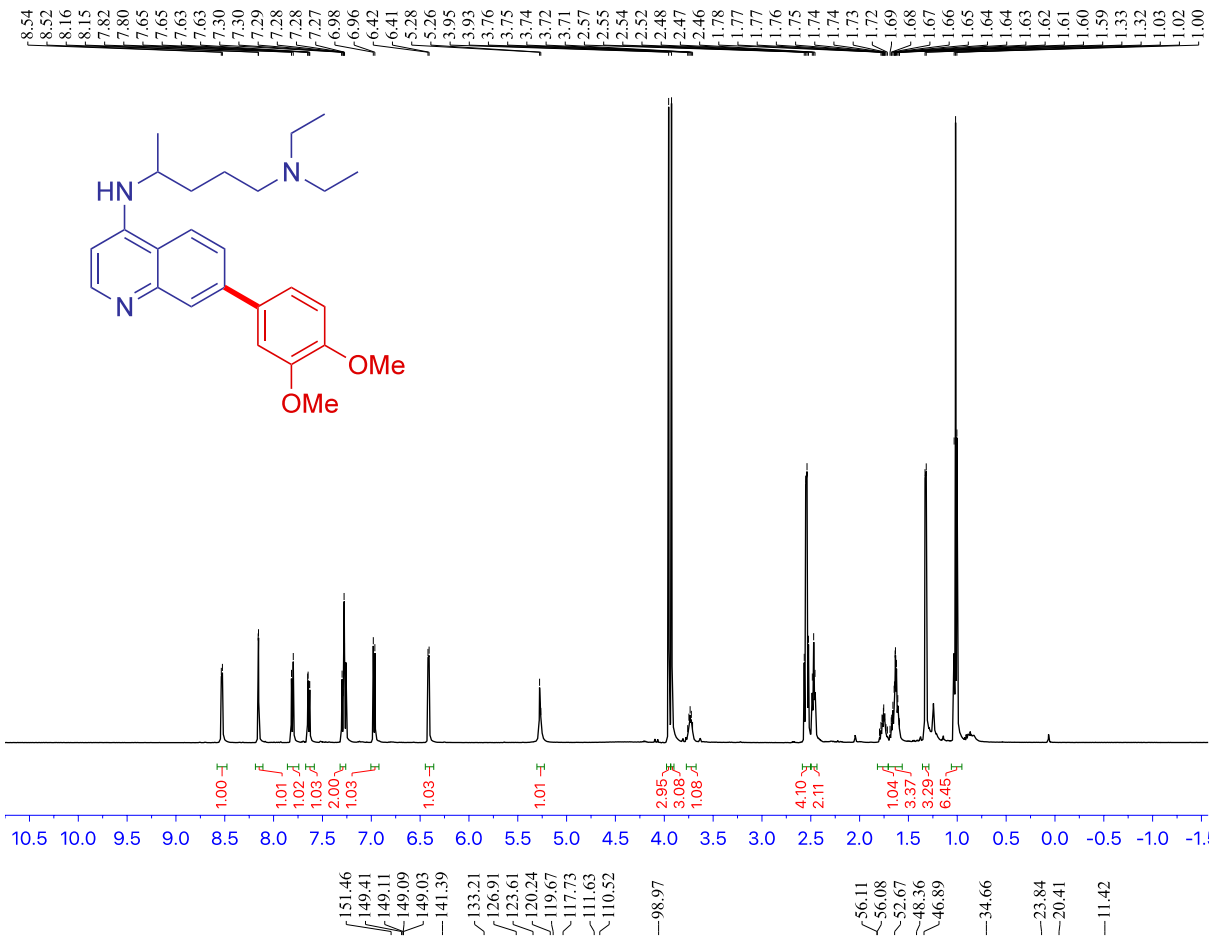

Figure S113. ^{13}C NMR spectrum of N^4-(7-(3,4-dimethoxyphenyl)quinolin-4-yl)-N^1,N^1-diethylpentane-1,4-diamine, related to **Scheme 4**

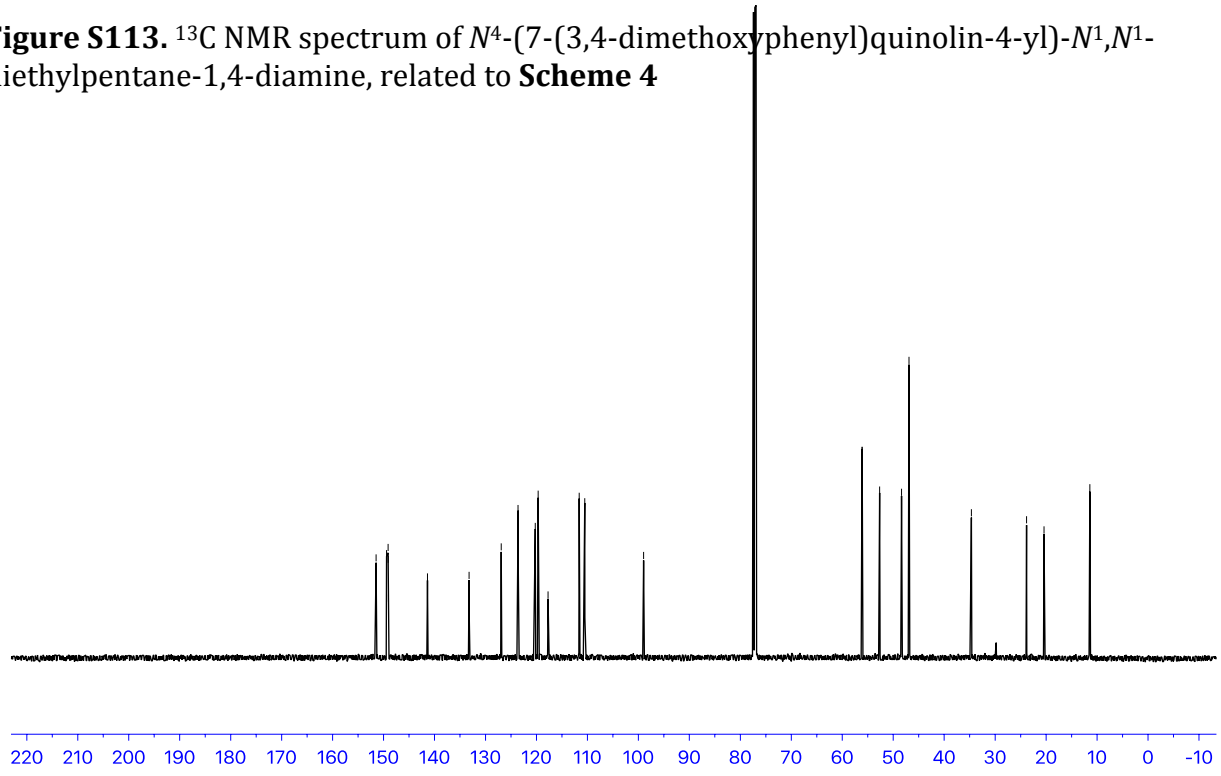

Scheme S1. Comparison of IPr, SIPr and IPr*, Related to **Table 1**.

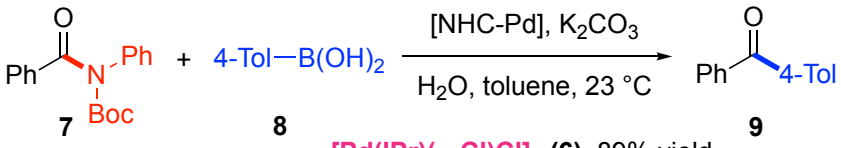

7 **8** **9**

[Pd(IPr)(μ-Cl)Cl]$_2$ (6), 89% yield
[Pd(SIPr)(μ-Cl)Cl]$_2$ (11), 74% yield
[Pd(IPr*)(μ-Cl)Cl]$_2$ (12), 24% yield

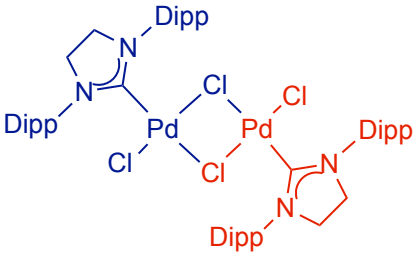

11, **[Pd(SIPr)(μ-Cl)Cl]$_2$**

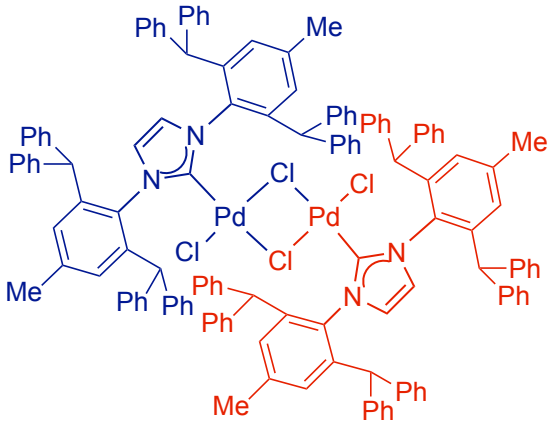

12, **[Pd(IPr*)(μ-Cl)Cl]$_2$**

Conditions: amide (1.0 equiv), 4-Tol-B(OH)$_2$ (2.0 equiv), catalyst ([Pd(NHC)(μ-Cl)Cl]$_2$, 0.05 mol%), K_2CO_3 (3.0 equiv), H_2O (5 equiv), toluene (0.50 M), 23 °C, 16 h.

Scheme S2. Determination of Relative Reaction Rates in the Suzuki-Miyaura Cross-Coupling Catalyzed by [Pd-NHC], Related to **Figure 2**.

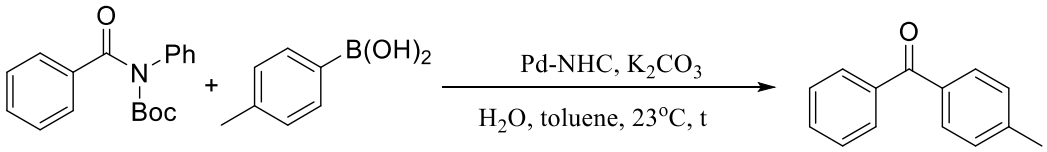

Conditions: amide (1.0 equiv), boronic acid (2 equiv), K_2CO_3 (3 equiv), H_2O (5.0 equiv), $[(IPr)Pd(\mu\text{-}Cl)Cl]_2$ (0.05 mol%), for other catalysts (0.1 mol%), toluene (0.5 M).

t/h	[(IPr)Pd(cin)Cl]	[(IPr)Pd(1-*t*Bu-ind)Cl]	Pd-PEPPSI-IPr	$[(IPr)Pd(\mu\text{-}Cl)Cl]_2$
0.167	0	0	0	4
0.5	0	0	0	9
1	1	2	1	35
2	21	9	9	60
4	42	25	21	89
6	62	48	29	94
8	76	67	36	97
12	77	90	48	99
20	80	92	59	100

Scheme S3. Determination of Turnover number (TON) in the Suzuki-Miyaura Cross-Coupling Catalyzed by $[(IPr)Pd(\mu\text{-}Cl)Cl]_2$, Related to **Scheme 1**.

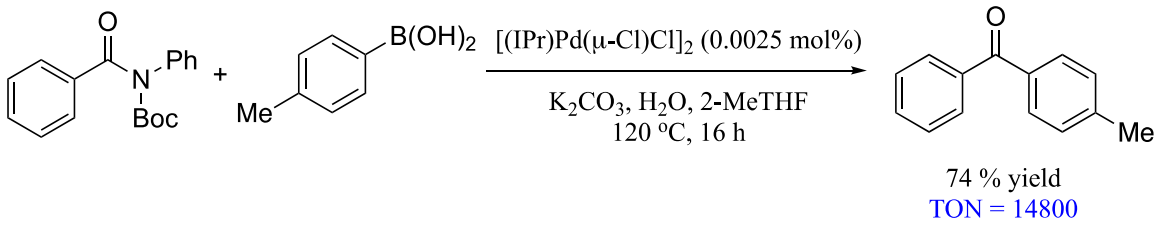

74 % yield
TON = 14800

Scheme S4. Determination of Relative Reaction Rates in the Suzuki-Miyaura Cross-Coupling Catalyzed by [Pd-NHC], Related to **Figure 3**.

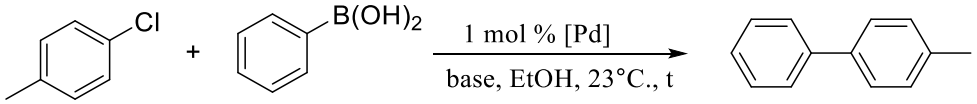

Conditions: ArCl (0.2 mmol), boronic acid (1.05 equiv), KO*t*Bu (1.1 equiv) or K_2CO_3 (2.2 equiv), [(IPr)Pd(μ-Cl)Cl]$_2$ (0.5 mol%), (IPr)Pd(1-*t*Bu-ind)Cl (1 mol%), EtOH (0.5 M), 23 °C.

t/min	[(IPr)Pd(μ-Cl)Cl]$_2$		[(IPr)Pd(1-*t*Bu-ind)Cl]	
	KO*t*Bu	K_2CO_3	KO*t*Bu	K_2CO_3
5	0	2	6	0
10	24	28	5	4
15	79	67	81	43
30	83	82	83	60
60	85	91	84	68

Scheme S5. Suzuki-Miyaura Cross-Coupling of 4-Chloroanisole, Related to **Figure 3**.

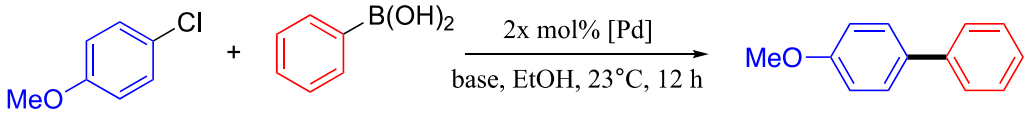

Conditions: ArCl (0.2 mmol), boronic acid (1.05 equiv), KO*t*Bu (1.1 equiv) or K_2CO_3 (2.2 equiv), [(IPr)Pd(μ-Cl)Cl]$_2$ (x mol %), [(IPr)Pd(1-*t*Bu-ind)Cl] (2x mol%), EtOH (0.5 M), 23 °C, 12 h; GC/^{1}H NMR yields.

Entry	**Base**	**x**	**Yield %**	
			[(IPr)Pd(μ-Cl)Cl]$_2$	[(IPr)Pd(1-*t*Bu-ind)Cl]
1		0.5	93	82
2	KO*t*Bu	0.1	94	78
3		0.05	68	65
4		0.5	99	95
5	K_2CO_3	0.1	99	95
6		0.05	83	81

Scheme S6. Suzuki-Miyaura Cross-Coupling of 2-Chloro-*m*-xylene, Related to **Figure 3**.

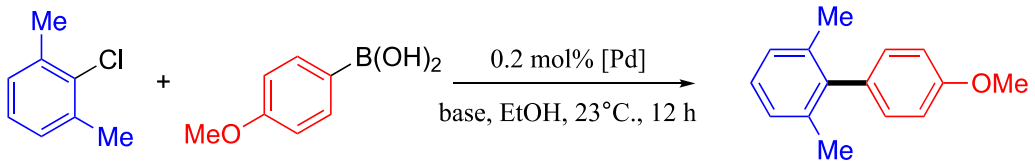

Conditions: ArCl (0.2 mmol), boronic acid (1.05 equiv), KO*t*Bu (1.1 equiv) or K_2CO_3 (2.2 equiv), [(IPr)Pd(μ-Cl)Cl]$_2$ (0.1 mol %)/[(IPr)Pd(1-*t*Bu-ind)Cl] (0.2 mol%), EtOH (0.5 M), 23 °C, 12 h; GC/^{1}H NMR yields.

Entry	**Base**	**Yield %**	
		[(IPr)Pd(μ-Cl)Cl]$_2$	[(IPr)Pd(1-*t*Bu-ind)Cl]
1	KO*t*Bu	76	63
2	K_2CO_3	99	99

Scheme S7. Suzuki-Miyaura of Aryl Chlorides at 50 ppm Pd Loading, Related to **Figure 3**.

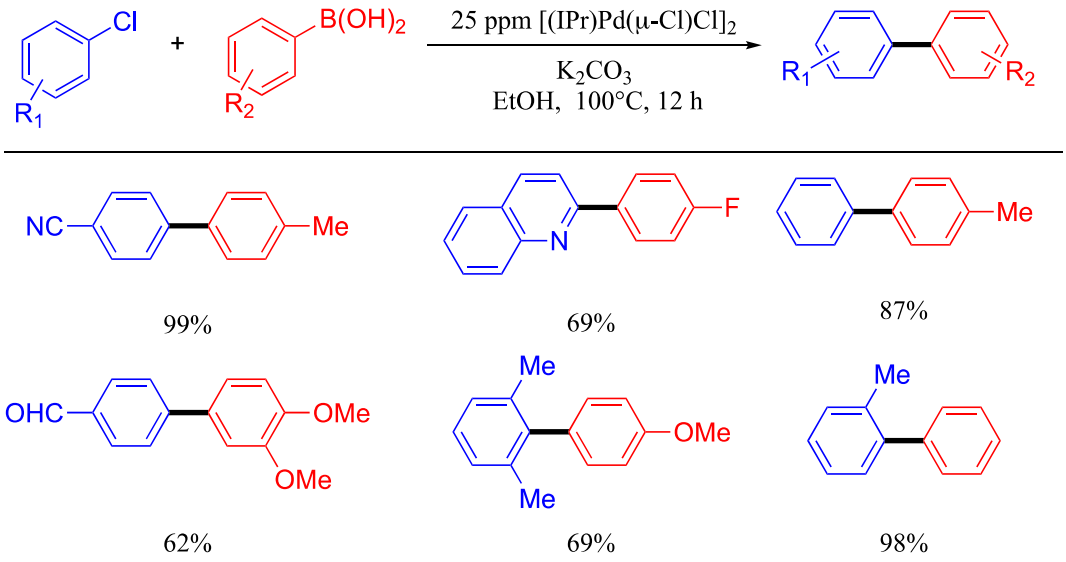

Conditions: ArCl (0.2 mmol), boronic acid (2 equiv), K_2CO_3 (3 equiv), $[(IPr)Pd(\mu\text{-}Cl)Cl]_2$ (0.0025 mol %), EtOH (0.5 M), 12 h. GC/^{1}H NMR yields.

Scheme S8. Plot of ln([Prod]end-[Prod]) versus time for a representative reaction involving catalyst, KOtBu and dvds in d_4-MeOH, Related to **Figure 3**.

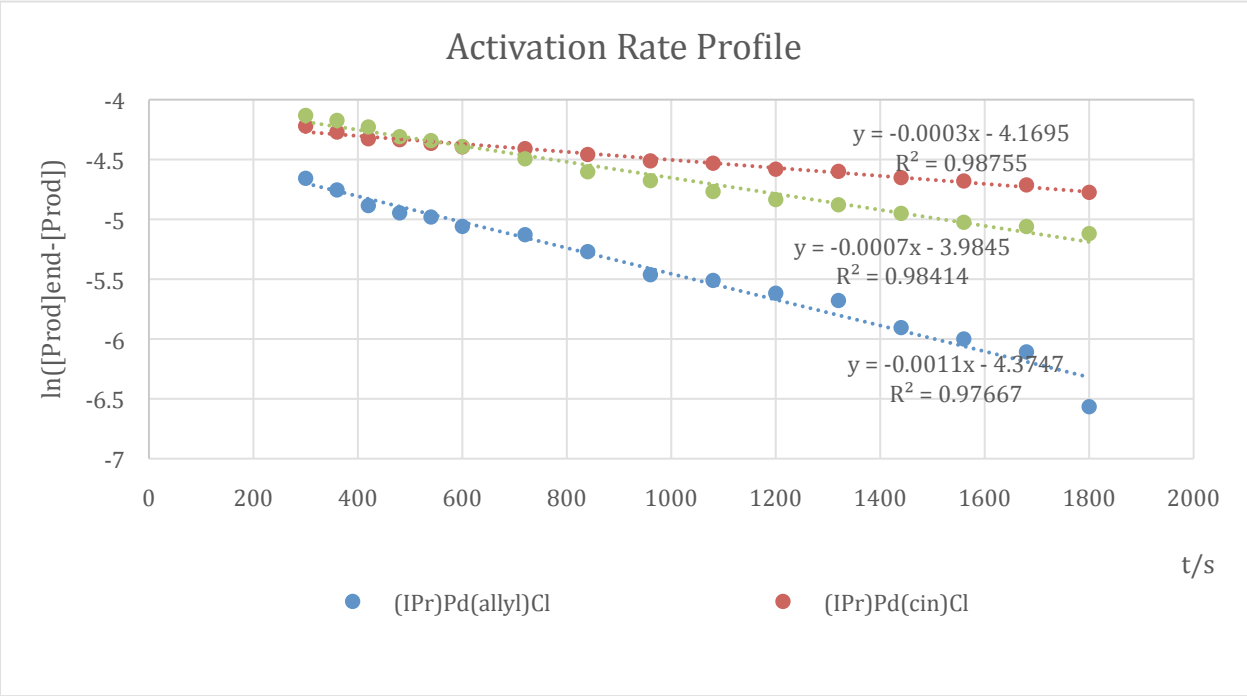

Table S1. Summary of Optimization of Pd-Catalyzed Biaryl Suzuki-Miyaura Cross-Coupling, Related to **Figure 3**.

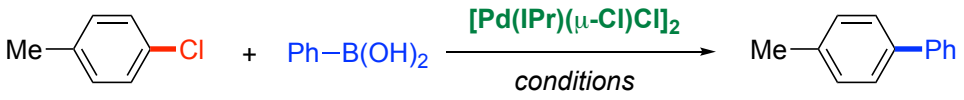

13 **8** **14**

entry	solvent	base	base (equiv)	*T* (°C)	yield[b] (%)
1	*i*-PrOH	KO*t*-Bu	1.1	23	32
2	EtOH	KO*t*-Bu	2.2	23	>98
3	EtOH	KO*t*-Bu	1.1	23	>98
4	dioxane	KO*t*-Bu	1.5	80	76
5	dioxane	Cs_2CO_3	1.5	80	63
6	DME	Cs_2CO_3	1.5	80	50
7	EtOH	K_2CO_3	2.2	23	>98
8	EtOH	K_2CO_3	1.5	23	93
9	EtOH	K_2CO_3	1.1	23	78
10	MeOH	KO*t*-Bu	1.1	23	91

Conditions: ArCl (1.0 equiv), catalyst (0.50 mol%), 4-Tol-$B(OH)_2$ (1.05), base (1.1-2.2 equiv), solvent (0.50 M), 23-80 °C, 12 h. [b]GC/^{1}H NMR yields.

Table S2. Pd-Catalyzed Biaryl Suzuki-Miyaura Cross-Coupling with Different [Pd(NHC)(μ-X)X]$_2$ Catalysts, Related to **Figure 3**.

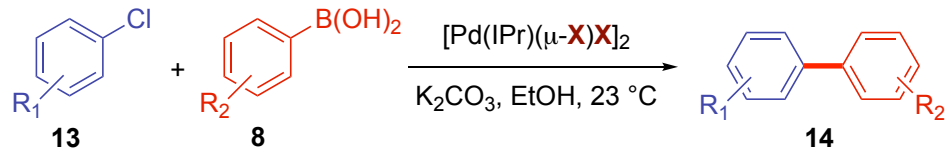

	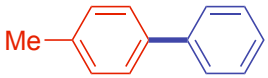	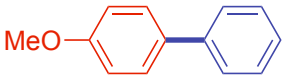	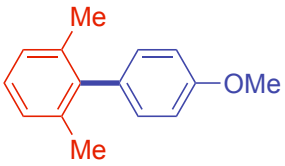
	yield (%)	yield (%)	yield (%)
X = Cl	>98	>98	>98
X = Br	85	87	82
X = I	<5	<5	<5
X = I	42[b]	33[b]	96[b]

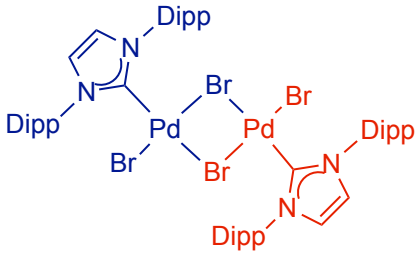

15, **[Pd(IPr)(μ-Br)Br]$_2$**

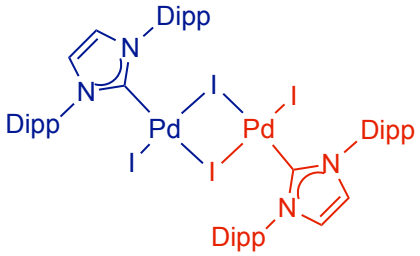

16, **[Pd(IPr)(μ-I)I]$_2$**

Conditions: ArCl (1.0 equiv), catalyst (0.05 mol%), Ar-B(OH)$_2$ (1.05), K_2CO_3 (2.2 equiv), EtOH (0.50 M), 23 °C, 12 h. [b]60 °C. Catalysts: X = Cl: [Pd(IPr)(μ-Cl)Cl]$_2$ (**6**); X = Br: [Pd(IPr)(μ-Br)Br]$_2$ (**15**); X = I: [Pd(IPr)(μ-I)I]$_2$ (**16**).

Transparent Methods

Computational Details

All DFT static calculations were performed at the GGA level with the Gaussian 09 set of programs (Frisch et al, 2016) using the BP86 functional of Becke and Perdew (Becke, 1988; Perdew, 1986; Perdew, 1986). The electronic configuration of the molecular systems was described with the standard split valence basis set with a polarization function of Ahlrichs and co-workers for H, C, B, N, O and Cl (SVP keyword in Gaussian) (Schafer et al., 1994) and Def2-QZVPP for K (Weigend, 2006). For Pd we used the quasi-relativistic Stuttgart/Dresden effective core potential (Kechle et al., 1994; Leininger et al., 1996) with an associated valence basis set (standard SDD keywords in Gaussian 09). Geometry optimizations were performed without symmetry constraints, and the characterization of the stationary points was performed by analytical frequency calculations. These frequencies were used to calculate unscaled zero-point energies (ZPEs) as well as thermal corrections and entropy effects at 298 K and 1 atm by using the standard statistical mechanics relationships for an ideal gas. Moreover, we also included the D3 Grimme pairwise scheme to account for dispersion corrections in the geometry optimizations (Grimme et al., 2010). Energies were obtained via single-point calculations on the BP86-optimized geometries using the M06 functional (Zhao et al., 2008). In these single-point energy calculations, H, C, B, N, O and Cl were described by using the Def2-TZVP basis set that includes polarization functions (Weigend, et al., 2005), Def2-QZVPP for K, whereas for the metal (Pd), the SDD basis set has been employed. On top of the M06/Def2-TZVP~sdd//BP86-D3/SVP~sdd energies, we added the ZPEs thermal and entropy corrections obtained at the BP86-D3/SVP~sdd level. In addition, to calculate the reported Gibbs energies, we included solvent effects of THF solution estimated with the polarizable continuous solvation model (PCM) as implemented in Gaussian 16 (Barone et al., 1998; Tomasi et al., 1994).

One-Step Synthesis of $[Pd(IPr)(m\text{-}Cl)Cl]_2$

In a glass vial, IPr·HCl (47.3 mg, 1 equiv.), $Pd(OAc)_2$ (30 mg, 1.2 equiv.) and K_2CO_3 (55 mg, 3.5 equiv.) were added, followed by dry toluene (0.5 mL). The reaction was heated at 80 °C overnight. The reaction was then filtered on celite and washed with DCM. 4M HCl in dioxane (0.4 mL) was added to the filtrate solution, and the mixture was stirred for 5 min. The solution was concentrated under vacuum. Pentane was added and the precipitate was filtered to yield 61 mg of a dark yellow powder (81% yield).

Large scale: In a glass vial, IPr·HCl (1.58 g, 1 equiv.), $Pd(OAc)_2$ (1 g, 1.2 equiv.) and K_2CO_3 (2.05 g, 4 equiv.) were added, followed by dry toluene (17 mL). The reaction was heated at 80 °C overnight. The reaction was then filtered on celite and washed with DCM. 4M HCl in dioxane (10 mL) was added to the filtrate solution, and the mixture was stirred for 10 min. The solution was concentrated under vacuum. Pentane was added and the precipitate was filtered to yield 1.69 g of a dark yellow powder (81% yield).

^1H NMR (400 MHz, $CDCl_3$) δ 7.54 (t, J = 7.7 Hz, 4H), 7.34-7.29 (m, 8H), 6.98 (s, 4H), 2.86 (br. s, 4H), 2.60 (br. s, 4H), 1.30 (d, J = 39.9 Hz, 24H), 0.99 (d, J = 27.5 Hz, 24H). Elemental analysis: Calcd for $C_{54}H_{72}N_4Cl_4Pd_2$ C: 57.30; H:6.41; N : 4.95. Found: C: 57.40; H: 6.50; N: 5.02.

List of Known Compounds/General Methods

All starting materials reported in the manuscript have been previously described in literature and prepared by the method reported previously unless stated otherwise. Amides were prepared by standard methods. All experiments involving palladium were performed using standard Schlenk techniques under nitrogen or argon unless stated otherwise. All solvents were purchased at the highest commercial grade and used as received or after purification by passing through activated alumina columns or distillation from sodium/benzophenone under nitrogen. All solvents were deoxygenated prior to use. All other chemicals were purchased at the highest commercial grade and used as received. Reaction glassware was oven-dried at 140 °C for at least 24 h or flame-dried prior to use, allowed to cool under vacuum and purged with argon (three cycles). All products were identified using ^{1}H NMR analysis and comparison with authentic samples. GC and/or GC/MS analysis was used for volatile products. All yields refer to yields determined by ^{1}H NMR and/or GC or GC/MS using an internal standard (optimization) and isolated yields (preparative runs) unless stated otherwise.^{1}H NMR and ^{13}C NMR spectra were recorded in $CDCl_3$ or DMSO on Bruker spectrometers at 500 (^{1}H NMR), 125 (^{13}C NMR) and 471 (^{19}F NMR) MHz. All shifts are reported in parts per million (ppm) relative to residual $CHCl_3$ peak (7.26 and 77.16 ppm, ^{1}H NMR and ^{13}C NMR, respectively). All coupling constants (*J*) are reported in hertz (Hz). Abbreviations are: s, singlet; d, doublet; t, triplet; q, quartet; brs, broad singlet. GC-MS chromatography was performed using Agilent HP6890 GC System and Agilent 5973A inert XL EI/CI MSD using helium as the carrier gas at a flow rate of 1 mL/min and an initial oven temperature of 50 °C. The injector temperature was 250 °C. The detector temperature was 250 °C. For runs with the initial oven temperature of 50 °C, temperature was increased with a 10 °C/min ramp after 50 °C hold for 3 min to a final temperature of 220 °C, then hold at 220 °C for 15 min (splitless mode of injection, total run time 22.0 min). High-resolution mass spectra were measured on a 7T Bruker Daltonics FT-MS instrument. All flash chromatography was performed using silica gel, 60 A, 300 mesh. TLC analysis was carried out on glass plates coated with silica gel 60 F254, 0.2 mm thickness. The plates were visualized using a 254 nm ultraviolet lamp or aqueous potassium permanganate. ^{1}H NMR and ^{13}C NMR data are given for all compounds in the SI for characterization purposes. ^{1}H NMR, ^{13}C NMR and HRMS data are given for all new compounds. All products have been previously reported unless stated otherwise.

Experimental Procedures and Characterization Data

General Procedure for the Synthesis of Starting Materials. All amides used in this study have been previously reported and prepared by reported methods (Zhou et al., 2019; Lei et al.; 2017; Liu et al., 2018; Monguchi et al., 2012; Lipshutz et al., 2008). Starting materials were synthesized according to general methods reported in the literature (Al-Huniti et al., 2018; Ackermann et al., 2011; Patel et al., 2012; Sun et al, 2016; Wang et al., 2017; Zhang et al., 2017). Catalysts **$[(IPr)Pd(\mu\text{-}Br)Br]_2$** and **$[(IPr)Pd(\mu\text{-}I)I]_2$** were prepared according to literature (Deska et al., 2010; Flahaut et al., 2009). ^{1}H NMR and ^{13}C NMR data are given for all starting materials in the section below for characterization purposes.

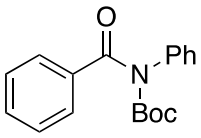

***tert*-Butyl benzoyl(phenyl)carbamate**. White solid. ^{1}H NMR (500 MHz, $CDCl_3$) δ 7.76 (d, *J* = 7.1 Hz, 2 H), 7.55 (t, *J* = 7.4 Hz, 1 H), 7.49-7.43 (m, 4 H), 7.37 (t, *J* = 7.4 Hz, 1 H), 7.30 (d, *J* = 7.4 Hz, 2 H), 1.26 (s, 9 H). ^{13}C NMR (125 MHz, $CDCl_3$) δ 172.78, 153.30, 139.10, 136.98, 131.72, 129.21, 128.28, 128.14, 127.96, 127.80, 83.50, 27.49. (Zhou et al., 2019)

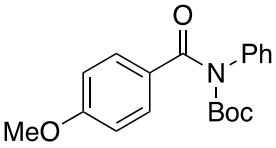

***tert*-Butyl (4-methoxybenzoyl)(phenyl)carbamate**. White solid. ^{1}H NMR (500 MHz, $CDCl_3$) δ 7.77 (d, *J* = 7.6 Hz, 2 H), 7.43 (t, *J* = 7.2 Hz, 2 H), 7.33 (t, *J* = 7.3 Hz, 1 H), 7.28 (d, *J* = 7.9 Hz, 2 H), 6.95 (d, *J* = 7.7 Hz, 2H), 3.88 (s, 3 H), 1.32 (s, 9 H). ^{13}C NMR (125 MHz, $CDCl_3$) δ 172.07, 162.78, 153.53, 139.48, 130.86, 129.12, 128.72, 127.75, 127.48, 113.56, 83.10, 55.49, 27.65. (Zhou et al., 2019)

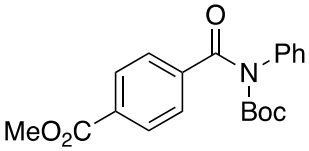

***tert*-Butyl phenyl((4-(methoxycarbonyl)benzoyl)carbamate.** White solid. ^{1}H NMR (500 MHz, $CDCl_3$) δ 8.14 (d, *J* = 8.1 Hz, 2 H), 7.78 (d, *J* = 8.1 Hz, 2 H), 7.46 (t, *J* = 7.6 Hz, 2 H), 7.38 (t, *J* = 7.3 Hz, 1 H), 7.28 (d, *J* = 7.8 Hz, 2 H), 3.97 (s, 3 H), 1.26 (s, 9 H). ^{13}C NMR (125 MHz, $CDCl_3$) δ 171.83, 166.21, 152.93, 141.01, 138.62, 132.53, 129.52, 129.27, 128.07, 127.99, 127.78, 84.01, 52.42, 27.51. (Zhou et al., 2019)

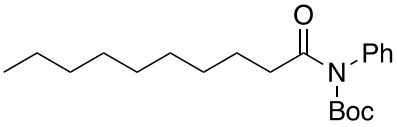

***tert*-Butyl decanoyl(phenyl)carbamate.** White solid. ^{1}H NMR (500 MHz, $CDCl_3$) δ 7.41(t, *J*=7.2 Hz, 2H), 7.34(t, *J*=7.3 Hz,1H), 7.09(d, *J*=7.7 Hz,2H), 2.92 (t, *J* = 7.4 Hz, 2 H), 1.70 (p, *J* = 7.3, 6.8 Hz, 2 H), 1.40 (s, 9 H), 1.29 (s, 12 H), 0.90 (t, *J* = 6.4 Hz, 3 H). ^{13}C NMR (125 MHz, $CDCl_3$) δ 176.0, 152.3, 139.2, 128.9, 128.2, 127.7, 82.9, 38.0, 31.9, 29.5, 29.3, 29.2, 27.8, 25.0, 22.7, 14.1. (Zhou et al., 2019)

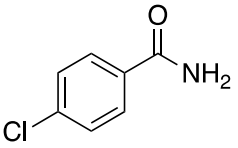

4-Chlorobenzamide. White solid. ^{1}H NMR (500 MHz, $CDCl_3$) δ 7.76 (d, *J* = 8.6 Hz, 2H), 7.43 (d, *J* = 8.5 Hz, 2H), 5.92 (brs, 2H). ^{13}C NMR (125 MHz, $CDCl_3$) δ 168.32, 138.51, 131.84, 129.07, 128.94. (Al-Huniti et al., 2018)

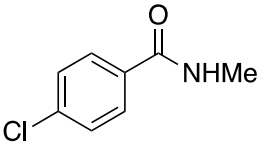

4-Chloro-*N*-methylbenzamide. White solid. ^{1}H NMR (500 MHz, $CDCl_3$) δ 7.70 (d, *J* = 8.1 Hz, 2H), 7.39 (d, *J* = 8.5 Hz, 2H), 6.24 (brs, 1H), 3.00 (d, *J* = 4.9 Hz, 3H). ^{13}C NMR (125 MHz, $CDCl_3$) δ 167.38, 137.75, 133.07, 128.95, 128.42, 27.06. (Ackermann et al., 2011)

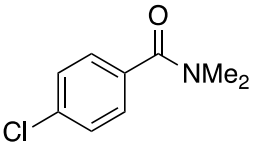

4-Chloro-*N*,*N*-dimethylbenzamide. White solid. ^{1}H NMR (500 MHz, $CDCl_3$) δ 7.36 (s, 4H), 3.09 (s, 3H), 2.96 (s, 3H). ^{13}C NMR (125 MHz, $CDCl_3$) δ 170.68, 135.70, 134.67, 131.44, 128.72, 39.68, 35.56. (Patel et al., 2012).

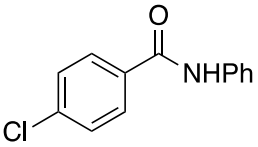

4-Chloro-*N*-phenylbenzamide. White solid. ^{1}H NMR (500 MHz, DMSO-d_6) δ 10.31 (s, 1H), 7.99 (d, *J* = 8.5 Hz, 2H), 7.77 (d, *J* = 7.6 Hz, 2H), 7.61 (d, *J* = 8.5 Hz, 2H), 7.36 (t, *J* = 7.9 Hz, 2H), 7.11 (t, *J* = 7.3 Hz, 1H). ^{13}C NMR (126 MHz, DMSO-d_6) δ 164.39, 138.94, 136.35, 133.63, 129.59, 128.59, 128.42, 123.79, 120.40. (Sun et al., 2016).

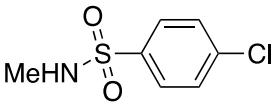

4-Chloro-*N*-methylbenzenesulfonamide. White solid. ^{1}H NMR (500 MHz, $CDCl_3$) δ 7.80 (d, *J* = 8.7 Hz, 2H), 7.50 (d, *J* = 8.6 Hz, 2H), 4.51 (d, *J* = 5.7 Hz, 1H), 2.67 (d, *J* = 5.4 Hz, 3H). ^{13}C NMR (125 MHz, $CDCl_3$) δ 139.42, 137.55, 129.58, 128.83, 29.45. (Wang et al., 2017)

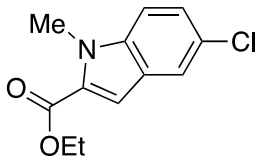

Ethyl 5-chloro-1-methyl-1*H*-indole-2-carboxylate. White solid. ^{1}H NMR (500 MHz, $CDCl_3$) δ 7.65 – 7.60 (m, 1H), 7.30 – 7.28 (m, 2H), 7.21 (s, 1H), 4.38 (q, *J* = 7.1 Hz, 2H), 4.06 (s, 4H), 1.41 (t, *J* = 7.1 Hz, 3H). ^{13}C NMR (125 MHz, $CDCl_3$) δ 162.05, 138.03, 129.30, 126.77, 126.30, 125.45, 121.72, 111.50, 109.41, 60.88, 31.96, 14.49. (Zhang et al., 2017)

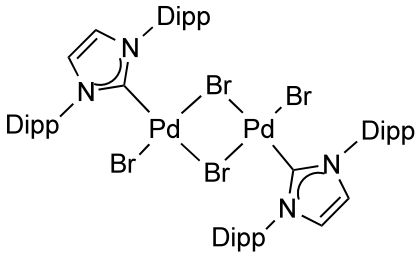

[(IPr)Pd(μ-Br)Br]$_2$. Brown solid. ^{1}H NMR (500 MHz, $CDCl_3$) δ 7.54 (t, *J* = 7.7 Hz, 4H), 7.34 (d, *J* = 7.7 Hz, 4H), 7.28 – 7.26 (m, 4H), 7.01 (s, 4H), 3.11 – 2.95 (m, 4H), 2.71 – 2.58 (m, 4H), 1.41 (d, *J* = 6.5 Hz, 12H), 1.23 (d, *J* = 7.8 Hz, 12H), 1.05 (d, *J* = 6.8 Hz, 12H), 0.94 (d, *J* = 6.8 Hz, 12H). ^{13}C NMR (126 MHz, $CDCl_3$) δ 153.13, 146.72, 146.31, 134.79, 130.49, 125.59, 124.52, 124.41, 28.96, 26.55, 26.52, 23.67, 23.62. (Deska et al., 2010)

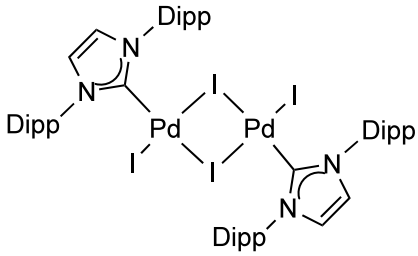

[(IPr)Pd(μ-I)I]$_2$. Red solid. ^{1}H NMR (500 MHz, $CDCl_3$) δ 7.51 (t, *J* = 7.8 Hz, 4H), 7.34 (d, *J* = 7.4 Hz, 4H), 7.27 – 7.22 (m, 4H), 7.09 (s, 4H), 3.34 – 3.24 (m, 4H), 2.89 – 2.62 (m, 4H), 1.47 (d, *J* = 6.6 Hz, 12H), 1.25 (d, *J* = 6.7 Hz, 12H), 1.08 (d, *J* = 6.9 Hz, 12H), 0.94 (d, *J* = 6.8 Hz, 12H). ^{13}C NMR (126 MHz, $CDCl_3$) δ 165.65, 146.53, 146.10, 135.53, 130.42, 125.54, 124.83, 124.42, 29.23, 26.67, 26.63, 24.19, 24.14. (Flahaut et al., 2009)

General Procedure for the Suzuki-Miyaura Cross-Coupling of Amides. An oven-dried vial equipped with a stir bar was charged with an amide substrate (neat, 1.0 equiv), potassium carbonate (typically, 3.0 equiv), boronic acid (typically, 2.0 equiv), Pd-NHC catalyst (typically, 0.5 mol%), water (typically, 5 equiv) placed under a positive pressure of argon, and subjected to three evacuation/backfilling cycles under high vacuum. Toluene (typically, 0.5 M) was added with vigorous stirring at room temperature, the reaction mixture was placed in a preheated oil bath and stirred for the indicated time. After the indicated time, the reaction mixture was cooled down to room temperature, diluted with CH_2Cl_2 (10 mL), filtered, and concentrated. A sample was analyzed by ^{1}H NMR ($CDCl_3$, 500 MHz) and GC-MS to obtain conversion, selectivity and

yield using internal standard and comparison with authentic samples. Purification by chromatography on silica gel (EtOAc/hexanes) afforded the tile product.

Phenyl(*p*-tolyl)methanone (Scheme 1, 9a)

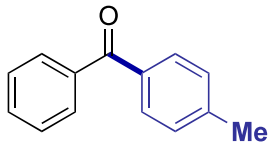

According to the general procedure, the reaction of *tert*-butyl benzoyl(phenyl)carbamate (0.20 mmol), 4-methylphenylboronic acid (2 equiv), K_2CO_3 (3 equiv), H_2O (5 equiv) and $[(IPr)Pd(\mu\text{-}Cl)Cl]_2$ (0.05 mol%) in toluene (0.5 M) for 16 h at room temperature, afforded after work-up and chromatography the title compound in 89 % yield (34.9 mg). White solid. ^1H NMR (500 MHz, $CDCl_3$) δ 7.79 (d, *J* = 6.9 Hz, 2H), 7.73 (d, *J* = 8.2 Hz, 2H), 7.58 (t, *J* = 7.4 Hz, 1H), 7.47 (t, *J* = 7.7 Hz, 2H), 7.28 (d, *J* = 7.9 Hz, 2H), 2.44 (s, 3H). ^{13}C NMR (125 MHz, $CDCl_3$) δ 196.64, 143.37, 138.09, 135.01, 132.29, 130.44, 130.06, 129.10, 128.34, 21.80. NMR spectroscopic data agreed with literature values (Zhou et al., 2019).

(4-Methoxyphenyl)(phenyl)methanone (Scheme 1, 9b)

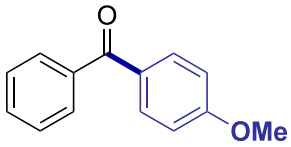

According to the general procedure, the reaction of *tert*-butyl benzoyl(phenyl)carbamate (0.20 mmol), phenylboronic acid (2 equiv), K_2CO_3 (3 equiv), H_2O (5 equiv) and $[(IPr)Pd(\mu\text{-}Cl)Cl]_2$ (0.25 mol%) in toluene (1 M) for 12 h at room temperature, afforded after work-up and chromatography the title compound in 98 % yield (41.6 mg). White solid. ^1H NMR (500 MHz, $CDCl_3$) δ 7.83 (d, *J* = 8.8 Hz, 2H), 7.76 (d, *J* = 6.8 Hz, 2H), 7.57 (t, *J* = 7.4 Hz, 1H), 7.47 (t, *J* = 7.7 Hz, 2H), 6.97 (d, *J* = 8.9 Hz, 2H), 3.89 (s, 3H). ^{13}C NMR (125 MHz, $CDCl_3$) δ 195.71, 163.36, 138.43, 132.70, 132.03, 130.31, 129.87, 128.33, 113.69, 55.65. NMR spectroscopic data agreed with literature values (Zhou et al., 2019).

Phenyl(4-(trifluoromethyl)phenyl)methanone (Scheme 1, 9c)

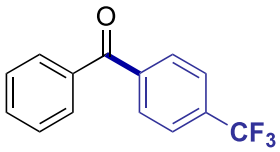

According to the general procedure, the reaction of *tert*-butyl benzoyl(phenyl)carbamate (0.20 mmol), (4-trifluoromethyl)phenylboronic acid (2 equiv), K_2CO_3 (3 equiv), H_2O (5 equiv) and $[(IPr)Pd(\mu\text{-}Cl)Cl]_2$ (0.25 mol%) in toluene (1 M) for 12 h at room temperature, afforded after work-up and chromatography the title compound in 82 % yield (41.1 mg). ^1H NMR (500 MHz, $CDCl_3$) δ 7.89 (d, *J* = 8.0 Hz, 2H), 7.81 (d, *J* = 6.9 Hz, 2H), 7.76 (d, *J* = 8.1 Hz, 2H), 7.63 (t, *J* = 7.5 Hz, 1H), 7.51 (t, *J* = 7.8 Hz, 2H). ^{13}C NMR (125 MHz, $CDCl_3$) δ 195.65, 140.86, 136.86, 133.85 (q, J^F = 32.7 Hz), 133.22, 130.27, 130.24, 128.66, 125.48 (q, J^F = 3.6 Hz), 123.81 (q, J^F = 272.7 Hz). ^{19}F NMR (471 MHz, $CDCl_3$) δ -63.01. NMR spectroscopic data agreed with literature values (Zhou et al., 2019).

1-Phenyldecan-1-one (Scheme 1, 9d)

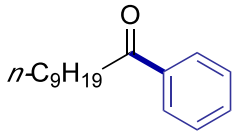

According to the general procedure, the reaction of *tert*-butyl decanoyl(phenyl)carbamate (0.20 mmol), phenylboronic acid (2 equiv), K_2CO_3 (3 equiv), H_2O (5 equiv) and $[(IPr)Pd(\mu\text{-}Cl)Cl]_2$ (0.5 mol%) in toluene (1 M) for 12 h at room temperature, afforded after work-up and chromatography the title compound in 91 % yield (42.3 mg). White solid. ^1H NMR (500 MHz, $CDCl_3$) δ 7.96 (d, *J* = 7.3 Hz, 2H), 7.55 (t, *J* = 7.4 Hz, 1H), 7.46 (t, *J* = 7.6 Hz, 2H), 2.96 (t, *J* = 7.4 Hz, 2H), 1.73 (p, *J* = 7.4 Hz, 2H), 1.41 – 1.25 (m, 12H), 0.88 (t, *J* = 6.8 Hz, 3H). ^{13}C NMR (125 MHz, $CDCl_3$) δ 200.77, 137.25, 132.98, 128.68, 128.20, 38.79, 32.03, 29.64, 29.62, 29.54, 29.43, 24.55, 22.82, 14.26. NMR spectroscopic data agreed with literature values (Lei et al., 2017).

(4-Methoxyphenyl)(phenyl)methanone (Scheme 1, 9b')

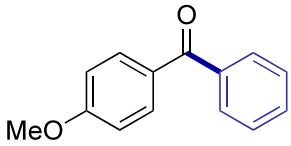

According to the general procedure, the reaction of *tert*-butyl (4-methoxybenzoyl)(phenyl)carbamate (0.20 mmol), phenylboronic acid (2 equiv), K_2CO_3 (3 equiv), H_2O (5 equiv) and $[(IPr)Pd(\mu\text{-}Cl)Cl]_2$ (0.5 mol%) in toluene (0.5 M) for 12 h at room temperature, afforded after work-up and chromatography the title compound in 93 % yield (39.5 mg). White solid. ^1H NMR (500 MHz, $CDCl_3$) δ 7.83 (d, *J* = 8.8 Hz, 2H), 7.76 (d, *J* = 6.8 Hz, 2H), 7.57 (t, *J* = 7.4 Hz, 1H), 7.47 (t, *J* = 7.7 Hz, 2H), 6.97 (d, *J* = 8.9 Hz, 2H), 3.89 (s, 3H). ^{13}C NMR (125 MHz, $CDCl_3$) δ 195.71, 163.36, 138.43, 132.70, 132.03, 130.31, 129.87, 128.33, 113.69, 55.65. NMR spectroscopic data agreed with literature values (Zhou et al., 2019).

Methyl 4-benzoylbenzoate (Scheme 1, 9e)

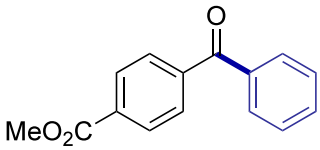

According to the general procedure, the reaction of *tert*-butyl phenyl((4-(methoxycarbonyl)benzoyl)carbamate (0.20 mmol), phenylboronic acid (2 equiv), K_2CO_3 (3 equiv), H_2O (5 equiv) and $[(IPr)Pd(\mu\text{-}Cl)Cl]_2$ (0.5 mol%) in toluene (1 M) for 12 h at room temperature, afforded after work-up and chromatography the title compound in 99 % yield (47.5 mg). White solid. ^1H NMR (500 MHz, $CDCl_3$) δ 8.15 (d, *J* = 8.4 Hz, 2H), 7.84 (d, *J* = 8.4 Hz, 2H), 7.81 (d, *J* = 6.9 Hz, 2H), 7.62 (t, *J* = 7.5 Hz, 1H), 7.50 (t, *J* = 7.8 Hz, 2H), 3.97 (s, 3H). ^{13}C NMR (125 MHz, $CDCl_3$) δ 196.19, 166.47, 141.47, 137.10, 133.37, 133.09, 130.25, 129.92, 129.65, 128.61, 52.63. NMR spectroscopic data agreed with literature values (Zhou et al., 2019).

Phenyl(o-tolyl)methanone (Scheme 1, 9d)

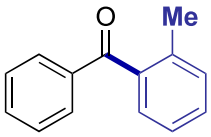

According to the general procedure, the reaction of *tert*-butyl benzoyl(phenyl)carbamate (0.20 mmol), 2-methylphenylboronic acid (2 equiv), K_2CO_3 (3 equiv), H_2O (5 equiv) and [(IPr*)Pd(μ-Cl)Cl]$_2$ (0.25 mol%) in toluene (1 M) for 12 h at room temperature, afforded after work-up and chromatography the title compound in 83 % yield (32.6 mg). ^{1}H NMR (500 MHz, $CDCl_3$) δ 7.80 (d, *J* = 6.8 Hz, 2H), 7.58 (t, *J* = 7.4 Hz, 1H), 7.46 (t, *J* = 7.7 Hz, 2H), 7.39 (t, *J* = 7.4 Hz, 1H), 7.34 – 7.28 (m, 2H), 7.24 (d, *J* = 7.5 Hz, 1H), 2.33 (s, 3H). ^{13}C NMR (125 MHz, $CDCl_3$) δ 198.78, 138.78, 137.90, 136.89, 133.26, 131.13, 130.37, 130.27, 128.66, 128.60, 125.33, 20.13. NMR spectroscopic data agreed with literature values (Zhou et al., 2019).

Determination of Kinetic Profiles Amides

General Procedure. An oven-dried vial equipped with a stir bar was charged with *tert*-butyl benzoyl(phenyl)carbamate (neat, 0.20 mmol, 1.0 equiv), potassium carbonate (3.0 equiv), 4-Tolylboronic acid (2.0 equiv), water (5.0 equiv), NHC-Pd (0.05 mol% for [(IPr)Pd(μ-Cl)Cl]$_2$, 0.1 mol% for other catalysts), placed under a positive pressure of argon, and subjected to three evacuation/backfilling cycles under high vacuum. Toluene (0.5 M) was added with vigorous stirring and the reaction mixture was stirred at 23 °C for the indicated time. After the indicated time, the reaction mixture was diluted with CH_2Cl_2 (10 mL), filtered, and concentrated. The sample was analyzed by ^{1}H NMR ($CDCl_3$, 500 MHz) and/or GC- MS to obtain conversion, selectivity and yield using internal standard and comparison with authentic samples.

Determination of Turnover Number

General Procedure. An oven-dried vial equipped with a stir bar was charged with an amide substrate (neat, 1.0 equiv), potassium carbonate (3.0 equiv), boronic acid (2.0 equiv) placed under a positive pressure of argon, and subjected to three evacuation/backfilling cycles under high vacuum. A stock solution of [(IPr)Pd(μ-Cl)Cl]$_2$ (0.0025 mol %) in 2-Methyltetrahydrofuran (0.5 M) was added with vigorous stirring at room temperature, the

reaction mixture was placed in a preheated oil bath at 100 °C or 120 °C and stirred the same temperature for 16 h. After the indicated time, the reaction mixture was cooled down to room temperature, diluted with CH_2Cl_2 (10 mL), filtered, and concentrated. The sample was analyzed by ^{1}H NMR ($CDCl_3$, 500 MHz) and/or GC-MS to obtain conversion, selectivity and yield using internal standard and comparison with authentic samples.

General Procedure for the Suzuki-Miyaura Cross-Coupling of Aryl Chlorides. An oven-dried vial equipped with a stir bar was charged with an aryl chloride or bromide (neat, 1.0 equiv), potassium carbonate (typically, 3.0 equiv), boronic acid (typically, 2.0 equiv) placed under a positive pressure of argon, and subjected to three evacuation/backfilling cycles under high vacuum. Ethanol (typically, 0.5 M) containing Pd-NHC catalyst (typically, 0.25 mol %) was added with vigorous stirring at indicated temperature, the reaction mixture was placed in a preheated oil bath and stirred for the indicated time. After the indicated time, the reaction mixture was cooled down to room temperature, diluted with CH_2Cl_2 (10 mL), filtered, and concentrated. A sample was analyzed by ^{1}H NMR ($CDCl_3$, 500 MHz) and GC-MS to obtain conversion, selectivity and yield using internal standard and comparison with authentic samples. Purification by chromatography on silica gel (EtOAc/hexanes) afforded the title product.

Determination of Kinetic Profiles Aryl Chlorides

General Procedure. An oven-dried vial equipped with a stir bar was charged with 4-chlorotoluene (neat, 0.20 mmol, 1.0 equiv), KO*t*Bu (1.1 equiv) or K_2CO_3 (2.2 equiv), phenylboronic acid (1.05 equiv) placed under a positive pressure of argon, and subjected to three evacuation/backfilling cycles under high vacuum. EtOH (0.5 M) containing NHC-Pd (0.5 mol% for $[(IPr)Pd(\mu\text{-}Cl)Cl]_2$, 1 mol% for (IPr)Pd(1-*t*Bu-ind)Cl) was added with vigorous stirring and the reaction mixture was stirred at 23 °C for the indicated time. After the indicated time, the reaction mixture was diluted with CH_2Cl_2 (10 mL), filtered, and concentrated. The sample was analyzed by ^{1}H NMR ($CDCl_3$, 500 MHz) and/or GC- MS to obtain conversion, selectivity and yield using internal standard and comparison with authentic samples.

[(IPr)Pd(μ-Cl)Cl]$_2$ Catalyzed Suzuki-Miyaura Cross-Coupling at Low Palladium Loading

General Procedure. An oven-dried vial equipped with a stir bar was charged with an aryl chloride or bromide (neat, 1.0 equiv), potassium carbonate (typically, 3.0 equiv), boronic acid (typically, 2.0 equiv) placed under a positive pressure of argon, and subjected to three evacuation/backfilling cycles under high vacuum. Ethanol (typically, 0.5 M) containing [(IPr)Pd(μ-Cl)Cl]$_2$ (typically, 0.0025 mol %) was added with vigorous stirring at indicated temperature, the reaction mixture was placed in a preheated oil bath and stirred for the indicated time. After the indicated time, the reaction mixture was cooled down to room temperature, diluted with CH_2Cl_2 (10 mL), filtered, and concentrated. A sample was analyzed by ^{1}H NMR ($CDCl_3$, 500 MHz) and GC-MS to obtain conversion, selectivity and yield using internal standard and comparison with authentic samples.

Experiments on Activation of Pd(II) to Pd(0)

Rates of Activation of [(IPr)Pd(allyl)Cl], [(IPr)Pd(cin)Cl] and [(IPr)Pd(μ-Cl)Cl]$_2$ in the presence of dvds were determined according to the previous report (Melvin et al., 2015).

General Procedure. KO*t*Bu (9.8 mg, 0.087 mmol) was dissolved in 300 μL of d_4-MeOH along with 100 μL of a 0.87 M solution of dvds in d_4-MeOH. [(IPr)Pd(allyl)Cl] (5.0 mg, 0.0087 mmol), [(IPr)Pd(cin)Cl] (5.6 mg, 0.0087 mmol), or [(IPr)Pd(μ-Cl)Cl]$_2$ (4.9 mg, 0.00435 mmol) was dissolved in 100 μL of d_4-MeOH. These solutions were combined in a J. Young NMR tube at −78 °C. The reaction mixture was degassed on a Schlenk line, after which dinitrogen was introduced into the NMR tube. An array of ^{1}H NMR spectra was taken at 25 °C over the course of 3 h. During this time, the growth of the methyl protons of the (IPr)Pd(dvds) product were monitored.

4-Methylbiphenyl (Table S2)

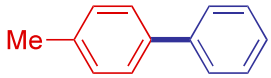

According to the general procedure, the reaction of 4-chlorotoluene (0.20 mmol), phenylboronic acid (1.05 equiv), K_2CO_3 (2.2 equiv) and $[(IPr)Pd(\mu\text{-}Cl)Cl]_2$ (0.05 mol%) in EtOH (0.5 M) for 12 h at 23 °C, afforded after work-up and chromatography the title compound in 98 % yield (33.1 mg). White solid. ^{1}H NMR (500 MHz, $CDCl_3$) δ 7.58 (d, *J* = 7.9 Hz, 2H), 7.50 (d, *J* = 7.8 Hz, 2H), 7.43 (t, *J* = 7.7 Hz, 2H), 7.34 (t, 1H), 7.26 (d, *J* = 7.7 Hz, 3H), 2.40 (s, 3H). ^{13}C NMR (125 MHz, $CDCl_3$) δ 141.30, 138.50, 137.16, 129.62, 128.85, 127.14, 127.12, 21.25. NMR spectroscopic data agreed with literature values (Liu et al., 2018).

4-Methoxybiphenyl (Table S2)

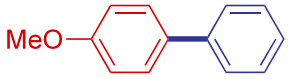

According to the general procedure, the reaction of 4-chloroanisole (0.20 mmol), phenylboronic acid (1.05 equiv), K_2CO_3 (2.2 equiv) and $[(IPr)Pd(\mu\text{-}Cl)Cl]_2$ (0.05 mol%) in EtOH (0.5 M) for 12 h at 23 °C, afforded after work-up and chromatography the title compound in 98 % yield (36.2 mg). White solid. ^{1}H NMR (500 MHz, $CDCl_3$) δ 7.59 – 7.49 (m, 4H), 7.42 (t, *J* = 7.8 Hz, 2H), 7.31 (t, *J* = 7.3 Hz, 1H), 6.98 (d, *J* = 8.7 Hz, 2H), 3.86 (s, 3H). ^{13}C NMR (125 MHz, $CDCl_3$) δ 159.39, 141.08, 134.04, 128.96, 128.40, 126.98, 126.90, 114.45, 55.60. NMR spectroscopic data agreed with literature values (Monguchi et al., 2012).

4'-Methoxy-2,6-dimethylbiphenyl (Table S2)

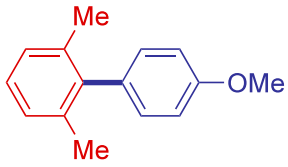

According to the general procedure, the reaction of 2-chloro-*m*-xylene (0.20 mmol), (4-methoxyl)phenylboronic acid (1.05 equiv), K_2CO_3 (2.2 equiv) and $[(IPr)Pd(\mu\text{-}Cl)Cl]_2$ (0.05 mol%) in EtOH (0.5 M) for 12 h at 23 °C, afforded after work-up and chromatography the

title compound in 98 % yield (41.7 mg). ^{1}H NMR (500 MHz, $CDCl_3$) δ 7.18 – 7.13 (m, 1H), 7.10 (d, *J* = 8.0 Hz, 2H), 7.06 (d, *J* = 8.7 Hz, 2H), 6.97 (d, *J* = 8.6 Hz, 2H), 3.86 (s, 3H), 2.04 (s, 6H). ^{13}C NMR (125 MHz, $CDCl_3$) δ 158.40, 141.66, 136.67, 133.47, 130.21, 127.38, 127.02, 113.95, 55.37, 21.05. NMR spectroscopic data agreed with literature values (Lipshutz et al, 2008).

4-Cyano-4'-methylbiphenyl (Scheme 2)

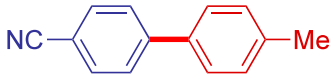

According to the general procedure, the reaction of 4-chlorobenzonitrile (0.20 mmol), 4-methylphenylboronic acid (2 equiv), K_2CO_3 (3 equiv) and $[(IPr)Pd(\mu\text{-}Cl)Cl]_2$ (0.25 mol%) in EtOH (0.5 M) for 12 h at 23 °C, afforded after work-up and chromatography the title compound in 97 % yield (37.5 mg). White solid. ^{1}H NMR (500 MHz, $CDCl_3$) δ 7.74 – 7.62 (m, 4H), 7.50 (d, *J* = 8.2 Hz, 2H), 7.29 (d, *J* = 7.9 Hz, 2H), 2.42 (s, 3H). ^{13}C NMR (125 MHz, $CDCl_3$) δ 145.71, 138.87, 136.37, 132.67, 129.95, 127.57, 127.17, 119.16, 110.65, 21.31. NMR spectroscopic data agreed with literature values (Liu et al., 2011).

4-Hydroxy-4'-methylbiphenyl (Scheme 2)

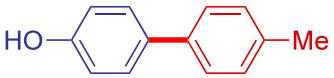

According to the general procedure, the reaction of 4-bromophenol (0.20 mmol), 4-methylphenylboronic acid (2 equiv), K_2CO_3 (3 equiv) and $[(IPr)Pd(\mu\text{-}Cl)Cl]_2$ (0.25 mol%) in EtOH (0.5 M) for 12 h at 60 °C, afforded after work-up and chromatography the title compound in 95 % yield (35.1 mg). White solid. ^{1}H NMR (500 MHz, $CDCl_3$) δ 7.46 (d, *J* = 8.4 Hz, 2H), 7.44 (d, *J* = 7.9 Hz, 2H), 7.22 (d, *J* = 7.8 Hz, 2H), 6.89 (d, *J* = 8.5 Hz, 2H), 4.80 (s, 1H), 2.38 (s, 3H). ^{13}C NMR (125 MHz, $CDCl_3$) δ 154.97, 138.03, 136.56, 134.14, 129.58, 128.33, 126.71, 115.72, 21.20. NMR spectroscopic data agreed with literature values (Edwards et al., 2014).

4-Amino-4'-methylbiphenyl (Scheme 2)

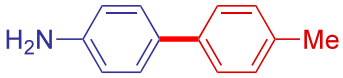

According to the general procedure, the reaction of 4-chloroaniline (0.20 mmol), 4-methylphenylboronic acid (2 equiv), K_2CO_3 (3 equiv) and $[(IPr)Pd(\mu\text{-}Cl)Cl]_2$ (0.25 mol%) in EtOH (0.5 M) for 12 h at 60 °C, afforded after work-up and chromatography the title compound in 78 % yield (28.6 mg). Yellow solid. ^{1}H NMR (500 MHz, $CDCl_3$) δ 7.43 (d, *J* = 8.2 Hz, 2H), 7.40 (d, *J* = 8.5 Hz, 2H), 7.21 (d, *J* = 7.9 Hz, 2H), 6.75 (d, *J* = 8.5 Hz, 2H), 3.70 (s, 2H), 2.37 (s, 3H). ^{13}C NMR (125 MHz, $CDCl_3$) δ 145.70, 138.46, 136.04, 131.76, 129.50, 127.96, 126.41, 115.53, 21.18. NMR spectroscopic data agreed with literature values (Kamio et al., 2019).

2-Amino-4'-methylbiphenyl (Scheme 2)

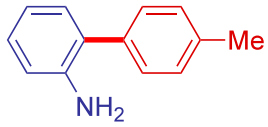

According to the general procedure, the reaction of 2-chloroaniline (0.20 mmol), 4-methylphenylboronic acid (2 equiv), K_2CO_3 (3 equiv) and $[(IPr)Pd(\mu\text{-}Cl)Cl]_2$ (0.25 mol%) in EtOH (0.5 M) for 12 h at 23 °C, afforded after work-up and chromatography the title compound in 92 % yield (33.7 mg). Yellow oil. ^{1}H NMR (500 MHz, $CDCl_3$) δ 7.35 (d, *J* = 8.1 Hz, 2H), 7.25 (d, *J* = 7.2 Hz, 2H), 7.17 – 7.09 (m, 2H), 6.82 (dt, *J* = 7.4, 1.2 Hz, 1H), 6.76 (dd, *J* = 8.0, 1.2 Hz, 1H), 3.73 (s, 2H), 2.40 (s, 3H). ^{13}C NMR (125 MHz, $CDCl_3$) δ 143.66, 136.96, 136.64, 130.58, 129.62, 129.07, 128.42, 127.77, 118.76, 115.68, 21.33. NMR spectroscopic data agreed with literature values (Ke et al., 2014).

2-(*p*-Tolyl)pyridine (Scheme 2)

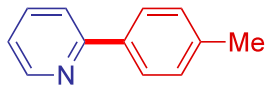

According to the general procedure, the reaction of 2-chloropyridine (0.20 mmol), 4-methylphenylboronic acid (2 equiv), K_2CO_3 (3 equiv) and $[(IPr)Pd(\mu\text{-}Cl)Cl]_2$ (0.25 mol%) in EtOH (0.5 M) for 12 h at 60 °C, afforded after work-up and chromatography the title compound in 82 % yield (27.7 mg). Yellow oil. ^{1}H NMR (500 MHz, $CDCl_3$) δ 8.68 (d, *J* = 4.7

Hz, 1H), 7.89 (d, *J* = 7.9 Hz, 2H), 7.76 – 7.68 (m, 2H), 7.28 (d, *J* = 7.9 Hz, 2H), 7.20 (t, *J* = 4.7 Hz, 1H), 2.41 (s, 3H). ^{13}C NMR (125 MHz, $CDCl_3$) δ 157.49, 149.61, 138.94, 136.66, 136.63, 129.48, 126.77, 121.79, 120.26, 21.28. NMR spectroscopic data agreed with literature values (Iglesias et al., 2012).

3-(6-Methoxynaphthalen-2-yl)pyridine (Scheme 2)

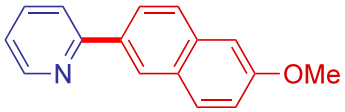

According to the general procedure, the reaction of 2-chloropyridine (0.20 mmol), 6-methoxy-2-naphthaleneboronic acid (2 equiv), K_2CO_3 (3 equiv) and $[(IPr)Pd(\mu\text{-}Cl)Cl]_2$ (0.25 mol%) in EtOH (0.5 M) for 12 h at 60 °C, afforded after work-up and chromatography the title compound in 97 % yield (45.6 mg). Yellow solid. ^{1}H NMR (500 MHz, $CDCl_3$) δ 8.73 (d, *J* = 4.4 Hz, 1H), 8.42 (s, 1H), 8.11 (dd, *J* = 8.6, 1.6 Hz, 1H), 7.87 – 7.82 (m, 3H), 7.78 (td, *J* = 7.7, 1.6 Hz, 1H), 7.25 – 7.22 (m, 1H), 7.21 – 7.15 (m, 2H), 3.95 (s, 3H). ^{13}C NMR (125 MHz, $CDCl_3$) δ 158.38, 157.61, 149.86, 136.90, 135.07, 134.74, 130.39, 129.15, 127.41, 126.28, 125.20, 122.00, 120.63, 119.33, 105.78, 55.49. NMR spectroscopic data agreed with literature values (Zhang et al., 2015).

Methyl 2-(*p*-tolyl)nicotinate (Scheme 2)

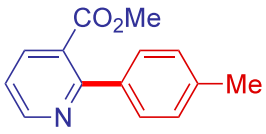

According to the general procedure, the reaction of methyl 2-chloronicotinate (0.20 mmol), 4-methylphenylboronic acid (2 equiv), K_2CO_3 (3 equiv) and $[(IPr)Pd(\mu\text{-}Cl)Cl]_2$ (0.25 mol%) in THF (0.5 M) for 12 h at 60 °C, afforded after work-up and chromatography the title compound in 75 % yield (34.1 mg). Colorless solid. ^{1}H NMR (500 MHz, $CDCl_3$) δ 8.76 (dd, *J* = 4.7, 1.5 Hz, 1H), 8.06 (dd, *J* = 7.8, 1.6 Hz, 1H), 7.45 (d, *J* = 8.0 Hz, 2H), 7.30 (dd, *J* = 7.8, 4.8 Hz, 1H), 7.24 (d, *J* = 7.8 Hz, 2H), 3.72 (s, 3H), 2.40 (s, 3H). ^{13}C NMR (125 MHz, $CDCl_3$) δ 168.92, 158.86, 151.40, 138.83, 137.92, 137.21, 129.07, 128.56, 126.96, 121.38, 52.52, 21.49. **HRMS** calcd for

$C_{14}H_{14}NO_2$ (M^+ + H) 228.0986, found 228.1019. NMR spectroscopic data agreed with literature values (Galenko et al., 2017).

3-(*p*-Tolyl)pyridine (Scheme 2)

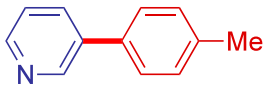

According to the general procedure, the reaction of 3-chloropyridine (0.20 mmol), 4-methylphenylboronic acid (2 equiv), K_2CO_3 (3 equiv) and $[(IPr)Pd(\mu\text{-}Cl)Cl]_2$ (0.25 mol%) in EtOH (0.5 M) for 12 h at 60 °C, afforded after work-up and chromatography the title compound in 89 % yield (30.1 mg). Yellow oil. ^{1}H NMR (500 MHz, $CDCl_3$) δ 8.84 (s, 1H), 8.57 (d, J = 4.9 Hz, 1H), 7.86 (d, J = 7.9 Hz, 1H), 7.49 (d, J = 8.1 Hz, 2H), 7.35 (dd, J = 7.9, 4.8 Hz, 1H), 7.29 (d, J = 7.8 Hz, 2H), 2.41 (s, 3H). ^{13}C NMR (125 MHz, $CDCl_3$) δ 148.36, 148.34, 138.18, 136.71, 135.09, 134.27, 129.94, 127.13, 123.65, 21.31. NMR spectroscopic data agreed with literature values (Iglesias et al., 2012).

3-(6-Methoxynaphthalen-2-yl)pyridine (Scheme 2)

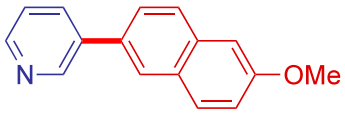

According to the general procedure, the reaction of 3-chloropyridine (0.20 mmol), 6-methoxy-2-naphthaleneboronic acid (2 equiv), K_2CO_3 (3 equiv) and $[(IPr)Pd(\mu\text{-}Cl)Cl]_2$ (0.25 mol%) in EtOH (0.5 M) for 12 h at 60 °C, afforded after work-up and chromatography the title compound in 96 % yield (45.1 mg). White solid. ^{1}H NMR (500 MHz, $CDCl_3$) δ 8.97 (d, J = 2.2 Hz, 1H), 8.61 (dd, J = 4.9, 1.6 Hz, 1H), 8.02 – 7.95 (m, 2H), 7.85 (d, J = 8.6 Hz, 1H), 7.81 (d, J = 8.9 Hz, 1H), 7.68 (dd, J = 8.5, 1.8 Hz, 1H), 7.43 – 7.37 (m, 1H), 7.20 (dd, J = 8.9, 2.5 Hz, 1H), 7.18 (s, 1H), 3.95 (s, 3H). ^{13}C NMR (125 MHz, $CDCl_3$) δ 158.27, 148.44, 148.24, 136.87, 134.59, 134.29, 133.00, 129.90, 129.23, 127.85, 126.11, 125.62, 123.77, 119.67, 105.73, 55.52. NMR spectroscopic data agreed with literature values (Voets et al., 2005).

5-(3,4-Dimethoxyphenyl)-1*H*-indole (Scheme 2)

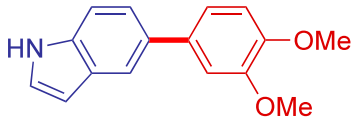

According to the general procedure, the reaction of 5-chloro-1*H*-indole (0.20 mmol), 3,4-dimethoxyphenylboronic acid (2 equiv), K_2CO_3 (3 equiv) and $[(IPr)Pd(\mu\text{-}Cl)Cl]_2$ (0.25 mol%) in EtOH (0.5 M) for 12 h at 60 °C, afforded after work-up and chromatography the title compound in 89 % yield (45.1 mg). White solid. ^{1}H NMR (500 MHz, $CDCl_3$) δ 8.18 (brs, 1H), 7.82 (s, 1H), 7.43 (q, *J* = 8.4 Hz, 2H), 7.26 – 7.23 (m, 1H), 7.22 – 7.15 (m, 2H), 6.96 (d, *J* = 8.0 Hz, 1H), 6.61 (s, 1H), 3.97 (s, 3H), 3.93 (s, 3H). ^{13}C NMR (125 MHz, $CDCl_3$) δ 149.20, 148.09, 135.89, 135.25, 133.50, 128.54, 124.97, 121.94, 119.61, 119.01, 111.68, 111.30, 111.07, 103.10, 56.17, 56.09. NMR spectroscopic data agreed with literature values (Jakab et al., 2015).

2-(4-Fluorophenyl)quinoline (Scheme 2)

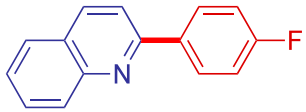

According to the general procedure, the reaction of 2-chloroquinoline (0.20 mmol), 4-fluorophenylboronic acid (2 equiv), K_2CO_3 (3 equiv) and $[(IPr)Pd(\mu\text{-}Cl)Cl]_2$ (0.25 mol%) in EtOH (0.5 M) for 12 h at 60 °C, afforded after work-up and chromatography the title compound in 97 % yield (43.3 mg).White solid. ^{1}H NMR (500 MHz, $CDCl_3$) δ 8.22 (d, *J* = 8.6 Hz, 1H), 8.20 – 8.10 (m, 3H), 7.83 (d, *J* = 8.6 Hz, 2H), 7.74 (t, *J* = 7.8 Hz, 1H), 7.53 (t, *J* = 7.6 Hz, 1H), 7.21 (t, *J* = 8.1 Hz, 2H). ^{13}C NMR (125 MHz, $CDCl_3$) δ 163.94 (d, J^F = 249.1 Hz), 156.37, 148.37, 137.04, 135.96 (d, J^F = 3.1 Hz), 129.92, 129.79, 129.54 (d, J^F = 8.4 Hz), 127.61, 127.22, 126.48, 118.76, 115.91 (d, J^F = 21.5 Hz). ^{19}F NMR (471 MHz, $CDCl_3$) δ -112.52. NMR spectroscopic data agreed with literature values (Wu et al., 2015).

2,4-Dimethoxy-6-(*p*-tolyl)-1,3,5-triazine (Scheme 2)

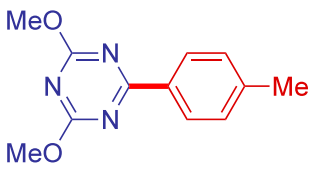

According to the general procedure, the reaction of 2-chloro-4,6-dimethoxy-1,3,5-triazine (0.20 mmol), 4-methylphenylboronic acid (2 equiv), K_2CO_3 (3 equiv) and $[(IPr)Pd(\mu\text{-}Cl)Cl]_2$ (0.25 mol%) in EtOH (0.5 M) for 12 h at 23 °C, afforded after work-up and chromatography the title compound in 98 % yield (45.3 mg). White solid. ^{1}H NMR (500 MHz, $CDCl_3$) δ 8.39 (d, J = 8.2 Hz, 2H), 7.29 (d, J = 8.0 Hz, 2H), 4.12 (s, 6H), 2.43 (s, 3H). ^{13}C NMR (125 MHz, $CDCl_3$) δ 175.05, 172.98, 143.69, 132.49, 129.40, 129.18, 55.29, 21.84. NMR spectroscopic data agreed with literature values (Li et al., 2013).

4-(4-(*tert*-Butyl)phenyl)-7-nitrobenzo[*c*][1,2,5]oxadiazole (Scheme 2)

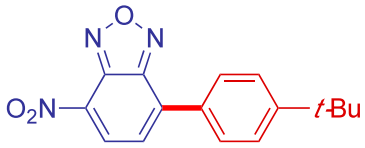

According to the general procedure, the reaction of 4-chloro-7-nitrobenzofurazan (0.20 mmol), 4-*tert*-butylphenylboronic acid (2 equiv), K_2CO_3 (3 equiv) and $[(IPr)Pd(\mu\text{-}Cl)Cl]_2$ (0.25 mol%) in EtOH (0.5 M) for 12 h at 23 °C, afforded after work-up and chromatography the title compound in 57 % yield (33.9 mg). Yellow solid. ^{1}H NMR (500 MHz, $CDCl_3$) δ 8.59 (d, J = 7.7 Hz, 1H), 8.02 (d, J = 8.6 Hz, 2H), 7.74 (d, J = 7.7 Hz, 1H), 7.62 (d, J = 8.6 Hz, 2H), 1.40 (s, 9H). ^{13}C NMR (125 MHz, $CDCl_3$) δ 155.27, 149.83, 143.52, 139.00, 135.01, 131.18, 130.95, 129.09, 126.61, 125.42, 35.21, 31.29. NMR spectroscopic data agreed with literature values (Singh et al., 2008).

3',4'-Dimethoxy-4-formylbiphenyl (Scheme 2)

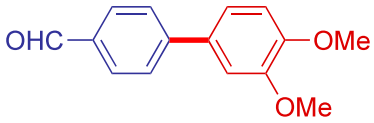

According to the general procedure, the reaction of 4-chlorobenzaldehyde (0.20 mmol), 3,4-dimethoxyphenylboronic acid (2 equiv), K_2CO_3 (3 equiv) and $[(IPr)Pd(\mu\text{-}Cl)Cl]_2$ (0.25 mol%) in EtOH (0.5 M) for 12 h at 60 °C, afforded after work-up and chromatography the title compound in 97 % yield (46.9 mg). Yellow solid. ^{1}H NMR (500 MHz, $CDCl_3$) δ 10.04 (s, 1H), 7.93 (d, J = 8.2 Hz, 2H), 7.72 (d, J = 8.2 Hz, 2H), 7.22 (d, J = 9.0 Hz, 1H), 7.15 (s, 1H), 6.98 (d, J = 8.4 Hz, 1H), 3.97 (s, 3H), 3.95 (s, 3H). ^{13}C NMR (125 MHz, $CDCl_3$) δ 192.00, 149.78, 149.51, 147.13,

134.95, 132.65, 130.44, 127.37, 120.13, 111.68, 110.54, 56.18. NMR spectroscopic data agreed with literature values (Wang et al., 2015).

4'-Methyl-[1,1'-biphenyl]-4-carboxylic acid (Scheme 2)

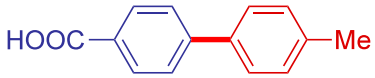

According to the general procedure, the reaction of 4-chlorobenzoic acid (0.20 mmol), 4-methylphenylboronic acid (2 equiv), KOH (3 equiv) and $[(IPr)Pd(\mu\text{-}Cl)Cl]_2$ (0.25 mol%) in EtOH (0.5 M) for 12 h at 100 °C, afforded after work-up and chromatography the title compound in 90 % yield (38.2 mg). White solid. ^{1}H NMR (500 MHz, DMSO-d_6) δ 12.93 (s, 1H), 8.00 (d, J = 8.6 Hz, 2H), 7.77 (d, J = 8.4 Hz, 2H), 7.63 (d, J = 8.2 Hz, 2H), 7.30 (d, J = 7.9 Hz, 2H), 2.35 (s, 3H). ^{13}C NMR (125 MHz, DMSO-d_6) δ 167.15, 144.22, 137.78, 136.10, 129.93, 129.67, 129.29, 126.77, 126.47, 20.71. NMR spectroscopic data agreed with literature values (Edwards et al., 2014).

5-(*p*-Tolyl)benzo[*d*][1,3]dioxole (Scheme 2)

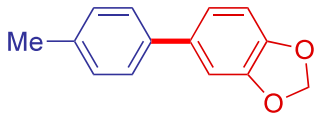

According to the general procedure, the reaction of 4-chlorotoluene (0.20 mmol), 3,4-(methylenedioxy)phenylboronic acid (2 equiv), K_2CO_3 (3 equiv) and $[(IPr)Pd(\mu\text{-}Cl)Cl]_2$ (0.25 mol%) in EtOH (0.5 M) for 12 h at 60 °C, afforded after work-up and chromatography the title compound in 86 % yield (36.5 mg). White solid. ^{1}H NMR (500 MHz, $CDCl_3$) δ 7.41 (d, J = 8.1 Hz, 2H), 7.22 (d, J = 7.8 Hz, 2H), 7.10 – 7.02 (m, 2H), 6.87 (d, J = 7.9 Hz, 1H), 5.99 (s, 2H), 2.38 (s, 3H). ^{13}C NMR (125 MHz, $CDCl_3$) δ 148.19, 146.95, 138.22, 136.81, 135.73, 129.58, 126.87, 120.50, 108.67, 107.69, 101.22, 21.20. NMR spectroscopic data agreed with literature values (Kamio et al, 2019).

4-Hydroxy-4'-methylbiphenyl (Scheme 2)

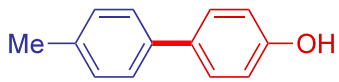

According to the general procedure, the reaction of 4-chlorotoluene (0.20 mmol), 4-hydroxyphenylboronic acid (2 equiv), K_2CO_3 (3 equiv) and $[(IPr)Pd(\mu\text{-}Cl)Cl]_2$ (0.25 mol%) in EtOH (0.5 M) for 12 h at 60 °C, afforded after work-up and chromatography the title compound in 89 % yield (32.8 mg). White solid. ^{1}H NMR (500 MHz, $CDCl_3$) δ 7.46 (d, J = 8.4 Hz, 2H), 7.44 (d, J = 7.9 Hz, 2H), 7.22 (d, J = 7.8 Hz, 2H), 6.89 (d, J = 8.5 Hz, 2H), 4.80 (s, 1H), 2.38 (s, 3H). ^{13}C NMR (125 MHz, $CDCl_3$) δ 154.97, 138.03, 136.56, 134.14, 129.58, 128.33, 126.71, 115.72, 21.20. NMR spectroscopic data agreed with literature values (Edwards et al., 2014).

2-(2,4-Difluorophenyl)pyridine (Scheme 2)

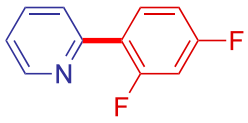

According to the general procedure, the reaction of 2-chloropyridine (0.20 mmol), 2,4-difluorophenylboronic acid (2 equiv), K_2CO_3 (3 equiv) and $[(IPr)Pd(\mu\text{-}Cl)Cl]_2$ (0.25 mol%) in EtOH (0.5 M) for 12 h at 60 °C, afforded after work-up and chromatography the title compound in 99 % yield (37.8 mg). Yellow oil. ^{1}H NMR (500 MHz, $CDCl_3$) δ 8.76 – 8.66 (m, 1H), 8.06 – 7.95 (m, 1H), 7.84 – 7.69 (m, 2H), 7.24 – 7.21 (m, 1H), 7.07 – 6.86 (m, 2H). ^{13}C NMR (125 MHz, $CDCl_3$) δ 163.34 (dd, J^F = 251.2, 11.6 Hz), 160.72 (dd, J^F = 252.2, 12.0 Hz), 152.70, 149.93, 136.61, 132.27 (dd, J^F = 9.6, 4.4 Hz), 124.36 (d, J^F = 9.1 Hz), 123.95 (d, J^F = 12.8 Hz), 122.57, 112.03 (dd, J^F = 21.3, 2.5 Hz), 104.50 (t, J^F = 26.5 Hz). ^{19}F NMR (471 MHz, $CDCl_3$) δ -109.36, -112.97. NMR spectroscopic data agreed with literature values (Bergmann et al, 2018).

2,4-Dimethoxy-6-(thiophen-3-yl)-1,3,5-triazine (Scheme 2)

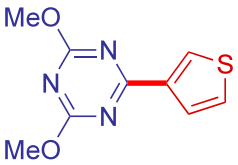

According to the general procedure, the reaction of 2-chloro-4,6-dimethoxy-1,3,5-triazine (0.20 mmol), 3-thienylboronic acid (2 equiv), K_2CO_3 (3 equiv) and $[(IPr)Pd(\mu\text{-}Cl)Cl]_2$ (0.25 mol%) in MeOH (0.5 M) for 12 h at 60 °C, afforded after work-up and chromatography the title compound in 87 % yield (38.8 mg). ^{1}H NMR (500 MHz, $CDCl_3$) δ 8.45 (dd, J = 3.0, 1.0 Hz, 1H), 7.87 (dd,

J = 5.1, 1.0 Hz, 1H), 7.34 (dd, *J* = 5.1, 3.1 Hz, 1H), 4.07 (s, 6H). ^{13}C NMR (126 MHz, $CDCl_3$) δ 172.89, 171.14, 139.44, 131.72, 127.64, 126.26, 55.22. NMR spectroscopic data agreed with literature values (Li et al., 2019).

3-(4,6-Dimethoxy-1,3,5-triazin-2-yl)benzonitrile (Scheme 2)

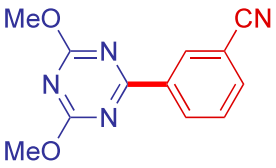

According to the general procedure, the reaction of 2-chloro-4,6-dimethoxy-1,3,5-triazine (0.20 mmol), 3-cyanophenylboronic acid (2 equiv), K_2CO_3 (3 equiv) and $[(IPr)Pd(\mu\text{-}Cl)Cl]_2$ (0.25 mol%) in EtOH (0.5 M) for 12 h at 60 °C, afforded after work-up and chromatography the title compound in 84 % yield (40.7 mg). White solid. ^{1}H NMR (500 MHz, $CDCl_3$) δ 8.80 (t, *J* = 1.4 Hz, 1H), 8.72 (dt, *J* = 8.0, 1.4 Hz, 1H), 7.84 (dt, *J* = 7.7, 1.4 Hz, 1H), 7.62 (t, *J* = 7.9 Hz, 1H), 4.15 (s, 6H). ^{13}C NMR (125 MHz, $CDCl_3$) δ 173.18, 173.04, 136.49, 135.79, 133.09, 132.84, 129.60, 118.40, 113.14, 55.66. HRMS calcd for $C_{12}H_{11}N4O_2$ (M^+ + H) 243.0877, found 243.0851.

2-Methoxy-5-(*p*-tolyl)pyridine (Scheme 3)

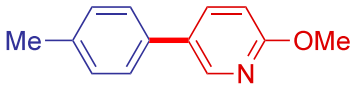

According to the general procedure, the reaction of 4-chlorotoluene (0.20 mmol), 6-methoxy-3-pyridinylboronic acid (2 equiv), K_2CO_3 (3 equiv) and $[(IPr)Pd(\mu\text{-}Cl)Cl]_2$ (0.25 mol%) in EtOH (0.5 M) for 12 h at 60 °C, afforded after work-up and chromatography the title compound in 97 % yield (38.6 mg). Colorless oil. ^{1}H NMR (500 MHz, $CDCl_3$) δ 8.37 (d, *J* = 2.5 Hz, 1H), 7.77 (dd, *J* = 8.6, 2.6 Hz, 1H), 7.42 (d, *J* = 8.1 Hz, 2H), 7.26 – 7.23 (m, 2H), 6.81 (d, *J* = 8.6 Hz, 1H), 3.98 (s, 3H), 2.40 (s, 3H). ^{13}C NMR (125 MHz, $CDCl_3$) δ 163.58, 144.92, 137.49, 137.27, 135.18, 130.21, 129.82, 126.68, 110.88, 53.66, 21.24. NMR spectroscopic data agreed with literature values (Liu et al., 2011).

***tert*-Butyl (4-(quinolin-2-yl)phenyl)carbamate (Scheme 3)**

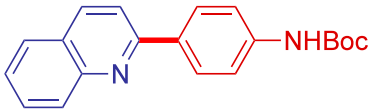

According to the general procedure, the reaction of 2-chloroquinoline (0.20 mmol), 4-(*N*-Boc-amino)phenylboronic acid (2 equiv), K_2CO_3 (3 equiv) and $[(IPr)Pd(\mu\text{-}Cl)Cl]_2$ (0.25 mol%) in EtOH (0.5 M) for 12 h at 60 °C, afforded after work-up and chromatography the title compound in 98 % yield (62.8 mg).White solid. ^1H NMR (500 MHz, $CDCl_3$) δ 8.19 (d, *J* = 8.6 Hz, 1H), 8.14 (d, *J* = 8.8 Hz, 3H), 7.85 (d, *J* = 8.6 Hz, 1H), 7.81 (d, *J* = 8.1 Hz, 1H), 7.71 (td, *J* = 7.3, 1.5 Hz, 1H), 7.57 – 7.47 (m, 3H), 6.61 (brs, 1H), 1.55 (s, 10H). ^{13}C NMR (125 MHz, $CDCl_3$) δ 156.84, 152.65, 148.44, 139.73, 136.81, 134.37, 129.74, 128.44, 127.58, 127.37, 127.19, 126.18, 118.75, 118.56, 29.86, 28.52. NMR spectroscopic data agreed with literature values (Cashion et al., 2011).

4'-Methyl-*N*-phenyl-[1,1'-biphenyl]-4-carboxamide (Scheme 3)

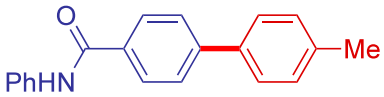

According to the general procedure, the reaction of 4-chloro-*N*-phenylbenzamide (0.20 mmol), 4-methylphenylboronic acid (2 equiv), K_2CO_3 (3 equiv) and $[(IPr)Pd(\mu\text{-}Cl)Cl]_2$ (0.25 mol%) in EtOH (0.5 M) for 12 h at 100 °C, afforded after work-up and chromatography the title compound in 93 % yield (53.4 mg). White solid. ^1H NMR (500 MHz, DMSO-d_6) δ 10.27 (s, 1H), 8.05 (d, *J* = 8.4 Hz, 2H), 7.84 – 7.78 (m, 4H), 7.66 (d, *J* = 8.2 Hz, 2H), 7.36 (t, *J* = 7.4 Hz, 2H), 7.32 (d, *J* = 7.9 Hz, 2H), 7.11 (t, *J* = 7.3 Hz, 1H), 2.36 (s, 3H). ^{13}C NMR (126 MHz, DMSO-d_6) δ 165.13, 142.98, 139.19, 137.58, 136.17, 133.37, 129.63, 128.58, 128.31, 126.71, 126.22, 123.61, 120.34, 20.70. HRMS calcd for $C_{20}H_{17}ON$ (M^+ + H) 288.1383, found 288.1378.

3-Methoxy-6-phenylpyridazine (Scheme 3)

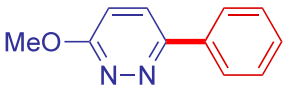

According to the general procedure, the reaction of 3-chloro-6-methoxypyridazine (0.20 mmol), phenylboronic acid (2 equiv), K_2CO_3 (3 equiv) and $[(IPr)Pd(\mu\text{-}Cl)Cl]_2$ (0.25 mol%) in EtOH (0.5 M) for 12 h at 60 °C, afforded after work-up and chromatography the title compound in 89 % yield (33.1 mg). White solid. ^1H NMR (500 MHz, $CDCl_3$) δ 8.01 (d, *J* = 8.3 Hz, 2H), 7.79 (d, *J* = 9.3 Hz, 1H), 7.54 – 7.43 (m, 3H), 7.05 (d, *J* = 9.2 Hz, 1H), 4.19 (s, 3H). ^{13}C NMR (125 MHz, $CDCl_3$) δ 164.44, 155.38, 136.39, 129.56, 129.07, 127.25, 126.67, 117.83, 55.04. NMR spectroscopic data agreed with literature values (Clapham et al., 2008).

4'-Methyl-[1,1'-biphenyl]-4-carboxamide (Scheme 3)

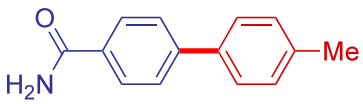

According to the general procedure, the reaction of 4-chlorobenzamide (0.20 mmol), 4-methylphenylboronic acid (2 equiv), KOH (3 equiv) and $[(IPr)Pd(\mu\text{-}Cl)Cl]_2$ (0.25 mol%) in EtOH (0.5 M) for 12 h at 100 °C, afforded after work-up and chromatography the title compound in 95 % yield (40.1 mg). White solid. ^1H NMR (500 MHz, DMSO-d_6) δ 8.00 (s, 1H), 7.95 (d, *J* = 8.4 Hz, 2H), 7.72 (d, *J* = 8.4 Hz, 2H), 7.62 (d, *J* = 8.2 Hz, 2H), 7.37 (s, 1H), 7.29 (d, *J* = 7.9 Hz, 2H), 2.35 (s, 3H). ^{13}C NMR (126 MHz, $CDCl_3$) δ 167.53, 142.64, 137.41, 136.30, 132.76, 129.58 (d, *J* = 9.3 Hz), 128.11, 126.66 (d, *J* = 8.5 Hz), 126.09, 20.68. NMR spectroscopic data agreed with literature values (Asghar et al., 2017).

***N*-Methyl-[1,1'-biphenyl]-4-carboxamide (Scheme 3)**

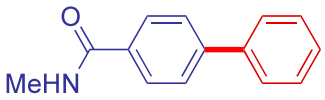

According to the general procedure, the reaction of 4-chloro-*N*-methylbenzamide (0.20 mmol), phenylboronic acid (2 equiv), K_2CO_3 (3 equiv) and $[(IPr)Pd(\mu\text{-}Cl)Cl]_2$ (0.25 mol%) in EtOH (0.5 M) for 12 h at 60 °C, afforded after work-up and chromatography the title compound in 93 % yield (39.2 mg). White solid. ^1H NMR (500 MHz, $CDCl_3$) δ 7.84 (d, *J* = 8.4 Hz, 2H), 7.63 (d, *J* = 8.3 Hz, 2H), 7.59 (d, *J* = 7.0 Hz, 2H), 7.45 (t, *J* = 7.6 Hz, 2H), 7.38 (t, *J* = 7.3 Hz, 1H), 6.38 (s, 1H), 3.03 (d, *J* = 4.8 Hz, 3H). ^{13}C NMR (125 MHz, $CDCl_3$) δ 168.10, 144.24,

140.13, 133.41, 129.02, 128.07, 127.50, 127.31, 127.29, 27.00. NMR spectroscopic data agreed with literature values (Rao et al., 2017).

_N,N_-Dimethyl-[1,1'-biphenyl]-4-carboxamide (Scheme 3)

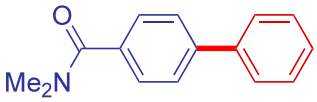

According to the general procedure, the reaction of 4-chloro-*N,N*-dimethylbenzamide (0.20 mmol), phenylboronic acid (2 equiv), K_2CO_3 (3 equiv) and $[(IPr)Pd(\mu\text{-}Cl)Cl]_2$ (0.25 mol%) in EtOH (0.5 M) for 12 h at 60 °C, afforded after work-up and chromatography the title compound in 88 % yield (39.6 mg). White solid.^{1}H NMR (500 MHz, $CDCl_3$) δ 7.62 (d, *J* = 8.2 Hz, 2H), 7.60 (d, *J* = 7.4 Hz, 2H), 7.50 (d, *J* = 8.2 Hz, 2H), 7.45 (t, *J* = 7.7 Hz, 2H), 7.37 (t, *J* = 7.3 Hz, 1H), 3.14 (s, 3H), 3.04 (s, 3H). ^{13}C NMR (125 MHz, $CDCl_3$) δ 171.59, 142.56, 140.46, 135.19, 128.99, 127.85, 127.78, 127.27, 127.17, 39.79, 35.56. NMR spectroscopic data agreed with literature values (Asghar et al., 2017).

4-Hydroxy-4'-methylbiphenyl (Scheme 3)

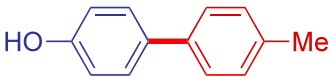

According to the general procedure, the reaction of 4-chlorophenol (0.20 mmol), 4-methylphenylboronic acid (2 equiv), K_2CO_3 (3 equiv) and $[(IPr)Pd(\mu\text{-}Cl)Cl]_2$ (0.25 mol%) in EtOH (0.5 M) for 12 h at 60 °C, afforded after work-up and chromatography the title compound in 82 % yield (30.2 mg). White solid. ^{1}H NMR (500 MHz, $CDCl_3$) δ 7.46 (d, *J* = 8.4 Hz, 2H), 7.44 (d, *J* = 7.9 Hz, 2H), 7.22 (d, *J* = 7.8 Hz, 2H), 6.89 (d, *J* = 8.5 Hz, 2H), 4.80 (s, 1H), 2.38 (s, 3H). ^{13}C NMR (125 MHz, $CDCl_3$) δ 154.97, 138.03, 136.56, 134.14, 129.58, 128.33, 126.71, 115.72, 21.20. NMR spectroscopic data agreed with literature values (Edwards et al., 2014).

***N*-Methyl-[1,1'-biphenyl]-4-sulfonamide (Scheme 3)**

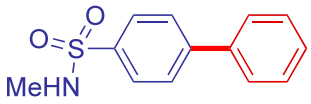

According to the general procedure, the reaction of 4-chloro-*N*-methylbenzenesulfonamide (0.20 mmol), phenylboronic acid (2 equiv), K_2CO_3 (3 equiv) and $[(IPr)Pd(\mu\text{-}Cl)Cl]_2$ (0.05 mol%) in EtOH (0.5 M) for 12 h at 100 °C, afforded after work-up and chromatography the title compound in 98 % yield (48.4 mg). White solid.^{1}H NMR (500 MHz, $CDCl_3$) δ 7.94 (d, *J* = 8.5 Hz, 2H), 7.73 (d, *J* = 8.4 Hz, 2H), 7.61 (d, *J* = 7.4 Hz, 2H), 7.48 (t, *J* = 7.6 Hz, 2H), 7.42 (t, *J* = 7.3 Hz, 1H), 4.64 (q, *J* = 5.4 Hz, 1H), 2.71 (d, *J* = 5.4 Hz, 3H). ^{13}C NMR (125 MHz, $CDCl_3$) δ 145.81, 139.42, 137.51, 129.19, 128.62, 127.89, 127.45, 29.52. NMR spectroscopic data agreed with literature values (Nordvall et al., 2007).

4,7-Di(thiophen-2-yl)benzo[*c*][1,2,5]thiadiazole (Scheme 3)

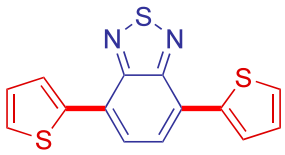

According to the general procedure, the reaction of 4,7-dibromobenzo[c][1,2,5]thiadiazole (0.20 mmol), 2-thienylboronic acid (3 equiv), K_2CO_3 (3 equiv) and $[(IPr)Pd(\mu\text{-}Cl)Cl]_2$ (0.025 mol%) in EtOH (0.5 M) for 12 h at 100 °C, afforded after work-up and chromatography the title compound in 98 % yield (58.9 mg). Red solid. ^{1}H NMR (500 MHz, $CDCl_3$) δ 8.10 (dd, *J* = 3.7, 1.2 Hz, 2H), 7.84 (s, 2H), 7.45 (dd, *J* = 5.0, 1.2 Hz, 2H), 7.21 (dd, *J* = 5.1, 3.7 Hz, 2H). ^{13}C NMR (125 MHz, $CDCl_3$) δ 152.82, 139.57, 128.23, 127.72, 127.01, 126.18, 125.96. NMR spectroscopic data agreed with literature values (Chen et al., 2015).

2-(3,4,5-Trifluorophenyl)pyrazine (Scheme 3)

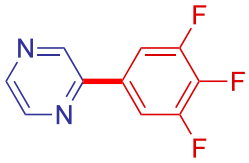

According to the general procedure, the reaction of 2-chloropyrazine (0.20 mmol), (3,4,5-trifluorophenyl)boronic acid (2 equiv), K_2CO_3 (3 equiv) and $[(IPr)Pd(\mu\text{-}Cl)Cl]_2$ (0.0025 mol%) in EtOH (0.5 M) for 12 h at 100 °C, afforded after work-up and chromatography the title compound in 84 % yield (35.3 mg). White solid. ^{1}H NMR (500 MHz, $CDCl_3$) δ 8.97 (d, *J* =

1.1 Hz, 1H), 8.63 (t, *J* = 2.0 Hz, 1H), 8.56 (d, *J* = 2.3 Hz, 1H), 7.75 – 7.65 (m, 2H). ^{13}C NMR (125 MHz, $CDCl_3$) δ 151.88 (ddd, *J* = 250.7, 10.3, 4.0 Hz), 149.62 (q, *J* = 2.5 Hz), 144.40, 144.09, 141.72, 141.09 (dt, *J* = 255.6, 15.3 Hz), 132.47 (td, *J* = 7.5, 4.5 Hz), 111.19 (dd, *J* = 17.2, 5.6 Hz). ^{19}F NMR (471 MHz, $CDCl_3$) δ -132.84 (d, *J* = 23.6 Hz, 2F), -158.00 (t, *J* = 21.2 Hz, 1F). NMR spectroscopic data agreed with literature values (Chen et al., 2015).

2-(6-Methoxypyridin-3-yl)pyrazine (Scheme 3)

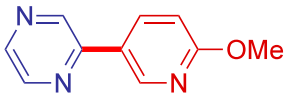

According to the general procedure, the reaction of 2-chloropyrazine (0.20 mmol), 6-methoxy-3-pyridinylboronic acid (2 equiv), K_2CO_3 (3 equiv) and $[(IPr)Pd(\mu\text{-}Cl)Cl]_2$ (0.05 mol%) in EtOH (0.5 M) for 12 h at 100 °C, afforded after work-up and chromatography the title compound in 98 % yield (36.7 mg). White solid. ^{1}H NMR (500 MHz, $CDCl_3$) δ 8.99 (s, 1H), 8.81 (s, 1H), 8.61 (s, 1H), 8.50 (s, 1H), 8.25 (d, *J* = 8.7 Hz, 1H), 6.88 (d, *J* = 8.1 Hz, 1H), 4.01 (s, 3H). ^{13}C NMR (125 MHz, $CDCl_3$) δ 165.38, 150.87, 145.88, 144.42, 142.96, 141.54, 137.30, 125.81, 111.55, 53.96. NMR spectroscopic data agreed with literature values (Chen et al., 2015).

3-(Pyridin-2-yl)quinoline (Scheme 3)

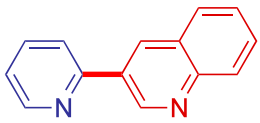

According to the general procedure, the reaction of 2-chloropyridine (0.20 mmol), 3-quinolineboronic acid (2 equiv), K_2CO_3 (3 equiv) and $[(IPr)Pd(\mu\text{-}Cl)Cl]_2$ (0.25 mol%) in EtOH (0.5 M) for 12 h at 60 °C, afforded after work-up and chromatography the title compound in 72 % yield (29.7 mg). White solid. ^{1}H NMR (500 MHz, $CDCl_3$) δ 9.55 (d, *J* = 2.2 Hz, 1H), 8.78 (d, *J* = 2.7 Hz, 2H), 8.16 (d, *J* = 8.4 Hz, 1H), 7.97 – 7.89 (m, 2H), 7.85 (td, *J* = 7.7, 1.8 Hz, 1H), 7.75 (t, *J* = 7.7 Hz, 1H), 7.59 (t, *J* = 7.5 Hz, 1H), 7.36 – 7.30 (m, 1H). ^{13}C NMR (125 MHz, $CDCl_3$) δ 155.04, 150.35, 149.45, 148.40, 137.22, 134.04, 132.07, 130.13, 129.45,

128.67, 128.03, 127.19, 122.97, 120.97. NMR spectroscopic data agreed with literature values (Chen et al., 2015).

4,6-Dimethoxy-2-(naphthalen-1-yl)pyrimidine (Scheme 3)

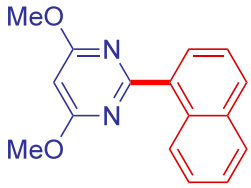

According to the general procedure, the reaction of 2-chloro-4,6-dimethoxypyrimidine (0.20 mmol), 1-naphthylboronic acid (2 equiv), K_2CO_3 (3 equiv) and $[(IPr)Pd(\mu\text{-}Cl)Cl]_2$ (0.025 mol%) in EtOH (0.5 M) for 12 h at 100 °C, afforded after work-up and chromatography the title compound in 95 % yield (50.6 mg). White solid. ^1H NMR (500 MHz, $CDCl_3$) δ 8.92 (d, *J* = 8.3 Hz, 1H), 8.19 (d, *J* = 6.5 Hz, 1H), 7.96 (d, *J* = 8.2 Hz, 1H), 7.91 (d, *J* = 7.5 Hz, 1H), 7.60 – 7.49 (m, 3H), 6.09 (s, 1H), 4.06 (s, 6H). ^{13}C NMR (125 MHz, $CDCl_3$) δ 171.44, 165.80, 135.66, 134.29, 131.25, 130.73, 129.46, 128.59, 126.58, 126.38, 125.82, 125.20, 88.10, 54.28. NMR spectroscopic data agreed with literature values (Chen et al., 2015).

Ethyl 1-methyl-5-phenyl-1*H*-indole-2-carboxylate (Scheme 3)

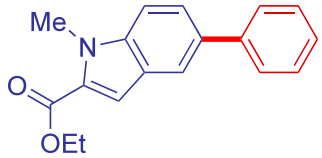

According to the general procedure, the reaction of ethyl 5-chloro-1-methyl-1H-indole-2-carboxylate (0.20 mmol), phenylboronic acid (2 equiv), K_2CO_3 (3 equiv) and $[(IPr)Pd(\mu\text{-}Cl)Cl]_2$ (0.25 mol%) in EtOH (0.5 M) for 12 h at 60 °C, afforded after work-up and chromatography the title compound in 92 % yield (51.4 mg). White solid. ^1H NMR (500 MHz, $CDCl_3$) δ 7.87 (d, *J* = 1.8 Hz, 1H), 7.67 – 7.59 (m, 3H), 7.48 – 7.42 (m, 3H), 7.37 – 7.31 (m, 2H), 4.39 (q, *J* = 7.1 Hz, 2H), 4.11 (s, 3H), 1.43 (t, *J* = 7.1 Hz, 3H). ^{13}C NMR (125 MHz, $CDCl_3$) δ 162.33, 142.02, 139.32, 134.19, 128.88, 128.82, 127.44, 126.77, 126.49, 125.07,

120.89, 110.67, 110.55, 60.74, 31.95, 14.54. NMR spectroscopic data agreed with literature values (Chikvaidze et al., 2012).

2,4-di-*tert*-Butyl-6-(5-(4-(trifluoromethyl)phenyl)-2*H*-benzo[*d*][1,2,3]triazol-2-yl)phenol (Scheme 3)

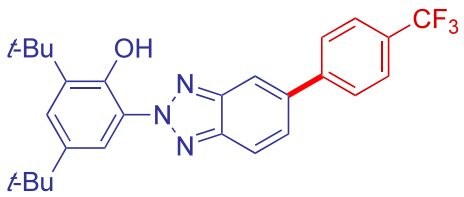

According to the general procedure, the reaction of 2,4-di-*tert*-butyl-6-(5-chloro-2H-benzo[d][1,2,3]triazol-2-yl)phenol (0.20 mmol), 4-(trifluoromethyl)phenylboronic acid (2 equiv), K_2CO_3 (3 equiv) and $[(IPr)Pd(\mu\text{-}Cl)Cl]_2$ (0.25 mol%) in EtOH (0.5 M) for 12 h at 60 °C, afforded after work-up and chromatography the title compound in 95 % yield (88.5 mg). White solid. ^{1}H NMR (500 MHz, $CDCl_3$) δ 11.71 (s, 1H), 8.32 (d, *J* = 2.3 Hz, 1H), 8.13 (s, 1H), 8.04 (d, *J* = 8.9 Hz, 1H), 7.83 – 7.75 (m, 4H), 7.73 (dd, *J* = 8.9, 1.6 Hz, 1H), 7.45 (d, *J* = 2.3 Hz, 1H), 1.53 (s, 9H), 1.41 (s, 9H). ^{13}C NMR (125 MHz, $CDCl_3$) δ 146.93, 144.29, 143.26, 142.53, 141.98, 139.42, 138.87, 130.07 (q, *J* = 32.8 Hz), 127.96, 127.94, 126.10 (q, *J* = 3.8 Hz), 125.55, 125.31, 124.34 (q, *J* = 272.0 Hz), 118.35, 116.32, 115.84, 35.88, 34.77, 31.66, 29.74. ^{19}F NMR (471 MHz, $CDCl_3$) δ -62.47. NMR spectroscopic data agreed with literature values (Chen et al., 2015).

4'-Methoxy-3,5-bis(trifluoromethyl)biphenyl (Scheme 3)

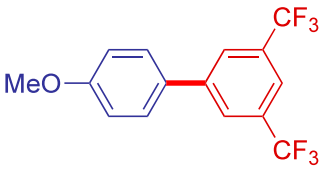

According to the general procedure, the reaction of 4-chloroanisole (0.20 mmol), (3,5-bis(trifluoromethyl)phenyl)boronic acid (2 equiv), K_2CO_3 (3 equiv) and $[(IPr)Pd(\mu\text{-}Cl)Cl]_2$ (0.05 mol%) in EtOH (0.5 M) for 12 h at 100 °C, afforded after work-up and chromatography the title compound in 76 % yield (48.7 mg). Colorless oil. ^{1}H NMR (500 MHz, $CDCl_3$) δ 7.97 (s, 2H), 7.80 (s, 1H), 7.55 (d, *J* = 8.5 Hz, 2H), 7.03 (d, *J* = 8.6 Hz, 2H), 3.88

(s, 3H). ^{13}C NMR (125 MHz, $CDCl_3$) δ 160.49, 143.04, 132.18 (q, *J* = 33.2 Hz), 130.77, 128.52, 126.79 (q, *J* = 3.9 Hz), 123.59 (q, *J* = 272.6 Hz), 120.34 (q, *J* = 3.7 Hz), 114.85, 55.59. ^{19}F NMR (471 MHz, $CDCl_3$) δ -62.87. NMR spectroscopic data agreed with literature values (Chen et al., 2015).

tert-Butyl 2-(4,6-dimethoxypyrimidin-2-yl)-1_H_-pyrrole-1-carboxylate (Scheme 3)

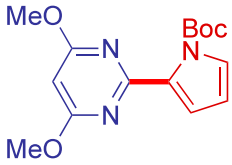

According to the general procedure, the reaction of 2-chloro-4,6-dimethoxypyrimidine (0.20 mmol), (1-(*tert*-butoxycarbonyl)-1H-pyrrol-2-yl)boronic acid (2 equiv), K_2CO_3 (3 equiv) and $[(IPr)Pd(\mu\text{-}Cl)Cl]_2$ (0.25 mol%) in EtOH (0.5 M) for 12 h at 60 °C, afforded after work-up and chromatography the title compound in 87 % yield (53.1 mg). Colorless oil. ^{1}H NMR (500 MHz, $CDCl_3$) δ 7.34 – 7.28 (m, 1H), 6.78 – 6.72 (m, 1H), 6.23 (t, *J* = 3.0 Hz, 1H), 5.93 (s, 1H), 3.95 (s, 6H), 1.46 (s, 9H). ^{13}C NMR (125 MHz, $CDCl_3$) δ 171.13, 159.50, 149.12, 133.17, 124.96, 118.01, 110.60, 87.73, 83.68, 54.09, 27.84. NMR spectroscopic data agreed with literature values (Chen et al., 2015).

Isopropyl 2-(4-([1,1'-biphenyl]-4-carbonyl)phenoxy)-2-methylpropanoate (Scheme 4)

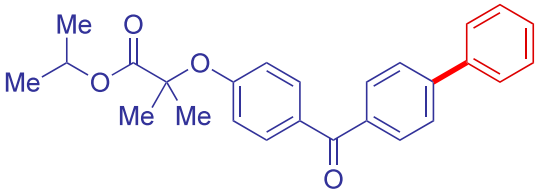

According to the general procedure, the reaction of Fenofibrate (0.20 mmol), phenylboronic acid (2 equiv), K_2CO_3 (3 equiv) and $[(IPr)Pd(\mu\text{-}Cl)Cl]_2$ (0.25 mol%) in *i*-PrOH (0.5 M) for 12 h at 60 °C, afforded after work-up and chromatography the title compound in 90 % yield (72.4 mg). White solid. ^{1}H NMR (500 MHz, $CDCl_3$) δ 7.84 (d, *J* = 8.2 Hz, 2H), 7.80 (d, *J* = 8.8 Hz, 2H), 7.69 (d, *J* = 8.4 Hz, 2H), 7.65 (d, *J* = 7.5 Hz, 2H), 7.48 (t, *J* = 7.7 Hz, 2H), 7.40 (t, *J* = 7.3 Hz, 1H), 6.89 (d, *J* = 8.8 Hz, 2H), 5.10 (hept, *J* = 6.3 Hz, 1H), 1.67 (s, 6H), 1.21

(d, *J* = 6.3 Hz, 6H). ^{13}C NMR (125 MHz, $CDCl_3$) δ 195.29, 173.32, 159.66, 144.93, 140.20, 136.92, 132.13, 130.88, 130.55, 129.08, 128.22, 127.41, 127.03, 117.34, 79.51, 69.46, 25.52, 21.67. HRMS calcd for $C_{26}H_{27}O_4$ (M^+ + H) 403.1904, found 403.1922.

1-(4-Fluorophenyl)-4-(4-hydroxy-4-(4'-methoxy-[1,1'-biphenyl]-4-yl)piperidin-1-yl)butan-1-one (Scheme 4)

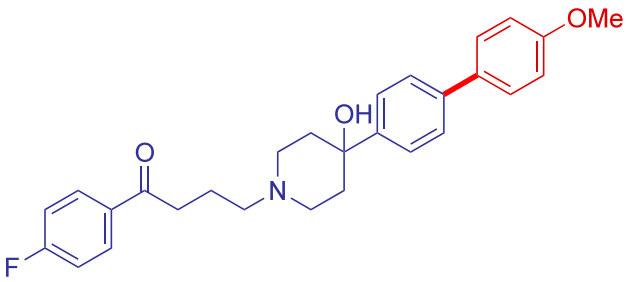

According to the general procedure, the reaction of Haloperidol (0.20 mmol), 4-methoxyphenylboronic acid (2 equiv), K_2CO_3 (5 equiv) and $[(IPr)Pd(\mu\text{-}Cl)Cl]_2$ (0.25 mol%) in EtOH (0.5 M) for 12 h at 60 °C, afforded after work-up and chromatography the title compound in 93 % yield (83.2 mg). Green solid. ^{1}H NMR (500 MHz, $CDCl_3$) δ 8.08 – 7.98 (m, 2H), 7.59 – 7.46 (m, 6H), 7.13 (t, *J* = 8.4 Hz, 2H), 6.96 (d, *J* = 8.3 Hz, 2H), 3.84 (s, 3H), 2.99 (t, *J* = 7.1 Hz, 2H), 2.83 (d, *J* = 11.2 Hz, 2H), 2.60 – 2.45 (m, 4H), 2.10 (t, *J* = 11.0 Hz, 2H), 2.01 (p, *J* = 6.1 Hz, 2H), 1.75 (d, *J* = 13.5 Hz, 2H). ^{13}C NMR (125 MHz, $CDCl_3$) δ 198.48, 165.75 (d, *J* = 254.4 Hz), 159.27, 146.82, 139.61, 133.78 (d, *J* = 3.0 Hz), 133.36, 130.82 (d, *J* = 9.2 Hz), 128.16, 126.70, 125.10, 115.73 (d, *J* = 21.8 Hz), 114.34, 71.23, 57.96, 55.46, 49.55, 38.42, 36.41, 21.93. ^{19}F NMR (471 MHz, $CDCl_3$) δ -105.68. HRMS calcd for $C_{28}H_{31}FNO_3$ (M^+ + H) 448.2282, found 448.2313.

2-(5-Methoxy-2-methyl-1-(4'-methyl-[1,1'-biphenyl]-4-carbonyl)-1H-indol-3-yl)acetic acid (Scheme 4)

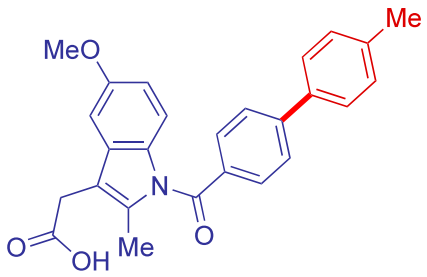

According to the general procedure, the reaction of Indomethacin (0.20 mmol), 4-methylphenylboronic acid (2 equiv), K_2CO_3 (5 equiv) and $[(IPr)Pd(\mu\text{-}Cl)Cl]_2$ (0.025 mol%) in EtOH (0.5 M) for 12 h at 100 °C, afforded after work-up and chromatography the title compound in 83 % yield (68.6 mg). White solid. ^{1}H NMR (500 MHz, DMSO-d_6) δ 12.37 (s, 1H), 7.86 (d, J = 8.3 Hz, 2H), 7.76 – 7.66 (m, 4H), 7.33 (d, J = 7.9 Hz, 2H), 7.05 (d, J = 2.5 Hz, 1H), 6.97 (d, J = 8.9 Hz, 1H), 6.70 (dd, J = 9.0, 2.5 Hz, 1H), 3.76 (s, 3H), 3.68 (s, 2H), 2.37 (s, 3H), 2.26 (s, 3H). ^{13}C NMR (125 MHz, DMSO-d_6) δ 172.62, 169.10, 155.88, 144.67, 138.52, 136.18, 135.68, 134.18, 131.06, 130.82, 130.57, 130.21, 127.30, 127.11, 114.89, 113.53, 111.70, 102.07, 55.87, 30.05, 21.21, 13.60. HRMS calcd for $C_{26}H_{24}NO_4$ (M^+ + H) 414.1700, found 414.1726.

_N,N_-Dimethyl-3-(2-phenyl-10_H_-phenothiazin-10-yl)propan-1-amine (Scheme 4)

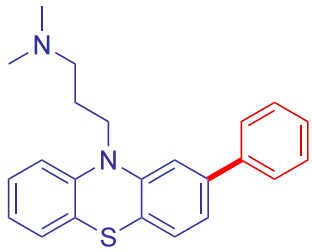

According to the general procedure, the reaction of Chlorpromazine hydrochloride (0.20 mmol), phenylboronic acid (2 equiv), K_2CO_3 (4 equiv) and $[(IPr)Pd(\mu\text{-}Cl)Cl]_2$ (0.25 mol%) in EtOH (0.5 M) for 12 h at 100 °C, afforded after work-up and chromatography the title compound in 95 % yield (68.5 mg). White solid. ^{1}H NMR (500 MHz, $CDCl_3$) δ 7.54 (d, J = 6.9 Hz, 1H), 7.43 (t, J = 7.7 Hz, 2H), 7.35 (t, J = 7.3 Hz, 1H), 7.23 – 7.11 (m, 4H), 7.09 (d, J = 1.8 Hz, 1H), 6.93 (t, J = 7.6 Hz, 2H), 4.00 (t, J = 6.9 Hz, 2H), 2.49 (t, J = 7.1 Hz, 2H), 2.24 (s, 6H), 2.03 (p, J = 7.0 Hz, 2H). ^{13}C NMR (125 MHz, $CDCl_3$) δ 145.78, 145.23, 141.07, 140.87, 128.90,

127.77, 127.64, 127.52, 127.44, 127.14, 125.32, 124.58, 122.72, 121.58, 115.86, 114.66, 57.24, 45.55, 45.51, 25.13. HRMS calcd for $C_{23}H_{25}N_2S$ (M^+ + H) 361.1738, found 361.1752.

_N_-(4-(_N_-(Cyclohexylcarbamoyl)sulfamoyl)phenethyl)-4-methoxy-4'-methyl-[1,1'-biphenyl]-3-carboxamide (Scheme 4)

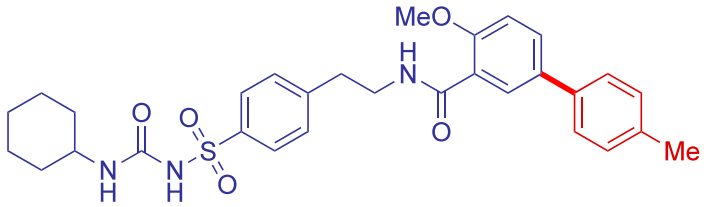

According to the general procedure, the reaction of Glibenclamide (0.20 mmol), 4-methylphenylboronic acid (2 equiv), K_2CO_3 (3 equiv) and $[(IPr)Pd(\mu\text{-}Cl)Cl]_2$ (0.25 mol%) in EtOH (0.5 M) for 12 h at 100 °C, afforded after work-up and chromatography the title compound in 76 % yield (83.6 mg). White solid. ^{1}H NMR (500 MHz, $CDCl_3$) δ 8.41 (d, *J* = 2.6 Hz, 1H), 7.99 (t, *J* = 5.8 Hz, 1H), 7.88 (d, *J* = 8.1 Hz, 2H), 7.65 (dd, *J* = 8.6, 2.6 Hz, 1H), 7.48 (d, *J* = 8.1 Hz, 2H), 7.40 (d, *J* = 8.1 Hz, 2H), 7.22 (d, *J* = 7.8 Hz, 2H), 6.98 (d, *J* = 8.6 Hz, 1H), 6.44 (d, *J* = 8.0 Hz, 1H), 3.80 (s, 3H), 3.79 – 3.74 (m, 2H), 3.62 – 3.52 (m, 1H), 3.03 (t, *J* = 6.9 Hz, 2H), 2.37 (s, 3H), 1.80 (d, *J* = 8.7 Hz, 2H), 1.65 – 1.58 (m, 2H), 1.57 – 1.50 (m, 1H), 1.28 – 1.24 (m, 2H), 1.17 – 1.08 (m, 3H). ^{13}C NMR (125 MHz, $CDCl_3$) δ 165.75, 156.79, 151.05, 145.89, 138.14, 137.08, 136.88, 134.46, 131.23, 130.47, 129.82, 129.63, 127.53, 126.71, 121.25, 112.02, 56.17, 49.17, 40.74, 35.71, 33.04, 25.43, 24.66, 21.18. HRMS calcd for $C_{30}H_{36}N_3O_5S$ (M^+ + H) 550.2370, found 550.2418.

(2_S_,6'_R_)-2',4,6-Trimethoxy-6'-methyl-7-(_p_-tolyl)-3_H_-spiro[benzofuran-2,1'-cyclohexan]-2'-ene-3,4'-dione (Scheme 4)

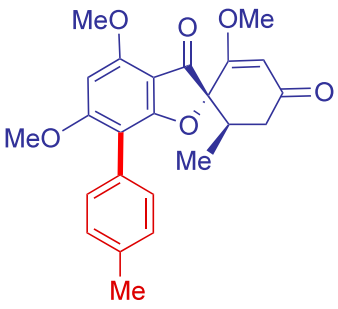

According to the general procedure, the reaction of (+)-Griseofulvin (0.20 mmol), 4-methylphenylboronic acid (2 equiv), K_2CO_3 (3 equiv) and $[(IPr)Pd(\mu\text{-}Cl)Cl]_2$ (1 mol%) in *t*-BuOH (0.5 M) for 12 h at 100 °C, afforded after work-up and chromatography the title compound in 62 % yield (50.6 mg). White solid. ^1H NMR (500 MHz, $CDCl_3$) δ 7.37 (d, *J* = 8.0 Hz, 2H), 7.24 (d, 2H), 6.16 (s, 1H), 5.49 (s, 1H), 4.01 (s, 3H), 3.90 (s, 3H), 3.60 (s, 3H), 3.10 – 3.03 (m, 1H), 2.77 – 2.68 (m, 1H), 2.39 (s, 3H), 2.39 – 2.33 (m, 1H), 0.97 (d, *J* = 6.7 Hz, 3H). ^{13}C NMR (125 MHz, $CDCl_3$) δ 197.53, 193.51, 171.95, 171.83, 166.46, 158.62, 137.34, 130.65, 129.00, 127.93, 107.56, 104.72, 104.47, 89.87, 88.92, 56.67, 56.57, 56.28, 40.24, 36.55, 21.54, 14.53. HRMS calcd for $C_{24}H_{25}O_6$ (M^+ + H) 409.1646, found 409.1668.

N^4-(7-(3,4-Dimethoxyphenyl)quinolin-4-yl)-N^1,N^1-diethylpentane-1,4-diamine (Scheme 4)

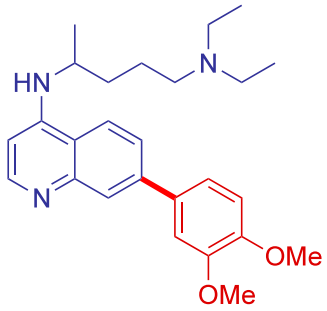

According to the general procedure, the reaction of Chloroquine diphosphate salt (0.20 mmol), 3,4-dimethoxyphenylboronic acid (2 equiv), K_2CO_3 (5 equiv) and $[(IPr)Pd(\mu\text{-}Cl)Cl]_2$ (0.025 mol%) in EtOH (0.5 M) for 12 h at 100 °C, afforded after work-up and chromatography the title compound in 89 % yield (75.1 mg). White solid. ^1H NMR (500 MHz, $CDCl_3$) δ 8.53 (d, *J* = 5.4 Hz, 1H), 8.16 (d, *J* = 1.9 Hz, 1H), 7.81 (d, *J* = 8.7 Hz, 1H), 7.64 (dd, *J* = 8.7, 1.9 Hz, 1H), 7.32 – 7.26 (m, 2H), 6.97 (d, *J* = 8.1 Hz, 1H), 6.41 (d, *J* = 5.4 Hz, 1H), 5.27 (d, *J* = 6.3 Hz, 1H), 3.95 (s, 3H), 3.93 (s, 3H), 3.74 (p, *J* = 6.3 Hz, 1H), 2.55 (q, *J* = 7.1 Hz, 4H), 2.47 (t, *J* = 6.8 Hz, 2H), 1.82 – 1.71 (m, 1H), 1.71 – 1.56 (m, 3H), 1.32 (d, *J* = 6.4 Hz, 3H), 1.02 (t, *J* = 7.1 Hz, 6H). ^{13}C NMR (125 MHz, $CDCl_3$) δ 151.46, 149.41, 149.11, 149.09, 149.03, 141.39, 133.21, 126.91, 123.61, 120.24, 119.67, 117.73, 111.63, 110.52, 98.97, 56.11, 56.08, 52.67, 48.36, 46.89, 34.66, 23.84, 20.41, 11.42. HRMS calcd for $C_{26}H_{36}N_3O_2$ (M^+ + H) 422.2802, found 422.2821.

Supplemental References

Frisch, M. J. et al. (2016). Gaussian 16, Revision C 01. (Gaussian Inc).

Becke, A. (1988). Density-functional exchange-energy approximation with correct asymptotic behavior. Phys. Rev. A *38*, 3098-3100.

Perdew, J. P. (1986). Density-functional approximation for the correlation energy of the inhomogeneous electron gas. Phys. Rev. B *33*, 8822-8824.

Perdew, J. P. (1986). Erratum: Density-functional approximation for the correlation energy of the inhomogeneous electron gas. Phys. Rev. B *34*, 7406.

Schäfer, A., Huber, C., and Ahlrichs, R. (1994). Fully optimized contracted Gaussian basis sets of triple zeta valence quality for atoms Li to Kr. J. Chem. Phys. *100*, 5829-5835.

Weigend, F. (2006). Accurate Coulomb-fitting basis sets for H to Rn. Phys. Chem. Chem. Phys. *8*, 1057-1065.

Kechle, W., Dolg, W., Stoll, M., and Preuss, H. (1994). Energy-adjusted pseudopotentials for the actinides. Parameter sets and test calculations for thorium and thorium monoxide. J. Chem. Phys. *100*, 7535-7542.

Leininger, T., Nicklass, A., Stoll, H., Dolg, M., and Schwerdtfeger, P. (1996). The accuracy of the pseudopotential approximation. II. A comparison of various core sizes for indium pseudopotentials in calculations for spectroscopic constants of InH, InF, and InCl. J. Chem. Phys. *105*, 1052-1059.

Grimme, S., Antony, J., Ehrlich, S., and Krieg, H. (2010). A consistent and accurate ab initio parametrization of density functional dispersion correction (DFT-D) for the 94 elements H-Pu. J. Chem. Phys. *132*, 154104-154119.

Zhao, Y., and Truhlar, D. G. (2008). Density functionals with broad applicability in chemistry. Acc. Chem. Res. *41*, 157-167.

Weigend, F., and Ahlrichs, R. (2005). Balanced basis sets of split valence, triple zeta valence and quadruple zeta valence quality for H to Rn: Design and assessment of accuracy. Phys. Chem. Chem. Phys. *7*, 3297–3305.

Barone, V., and Cossi, M. J. (1998). Quantum calculation of molecular energies and energy gradients in solution by a conductor solvent model. Phys. Chem. A *102*, 1995-2001.

Tomasi, J., and Persico, M. (1994). Molecular interactions in solution: an overview of methods based on continuous distributions of the solvent. Chem. Rev. *94*, 2027-2094.

Zhou, T., Li, G., Nolan, S. P., and Szostak, M. (2019). [Pd(NHC)(acac)Cl]: Well-Defined, Air-Stable, and Readily Available Precatalysts for Suzuki and Buchwald–Hartwig Cross-coupling (Transamidation) of Amides and Esters by N–C/O–C Activation. Org. Lett. *21*, 3304-3309.

Lei, P., Meng, G., Ling, Y., An, J., and Szostak, M. (2017). Pd-PEPPSI: Pd-NHC Precatalyst for Suzuki–Miyaura Cross-Coupling Reactions of Amides. J. Org. Chem. *82*, 6638-6646.

Liu, C., Li, G., Shi, S., Meng, G., Lalancette, R., Szostak, R., and Szostak, M. (2018). Acyl and Decarbonylative Suzuki Coupling of N-Acetyl Amides: Electronic Tuning of Twisted, Acyclic Amides in Catalytic Carbon-Nitrogen Bond Cleavage. ACS Catal. *8*, 9131-9139

Monguchi, Y., Hattori, T., Miyamoto, Y., Yanase, T., Sawama, Y., and Sajiki, H. (2012). Palladium on Carbon-Catalyzed Cross-Coupling using Triarylbismuths. Adv. Synth. Catal. *354*, 2561-2567.

Lipshutz, B. H., Petersen, T. B., and Abela, A. R. (2008). Room Temperature Suzuki-Miyaura Couplings in Water Facilitated by Nonionic Amphiphiles. Org. Lett. *10*, 1333-336.

Al-Huniti, M. H., Rivera-Chávez, J., Colón, K. L., Stanley, J. L., Burdette, J. E., Pearce, C. J., Oberlies, N. H., and Croatt, M. P. (2018). Development and Utilization of a Palladium-Catalyzed Dehydration of Primary Amides To Form Nitriles. Org. Lett. *20*, 6046-6050.

Ackermann, L., Lygin, A. V., and Hofmann, N. (2011). Ruthenium-catalyzed oxidative annulation by cleavage of C-H/N-H bonds. Angew. Chem. Int. Ed. *50*, 6379-6382.

Patel, B., Firkin, C. R., Snape, E. W., Jenkin, S. L., Brown, D., Chaffey, J. G. K., Hopes, P. A., Reens, C. D., Butters, M., and Moseley, J. D. (2012). Process Development and Scale-Up of AZD7545, a PDK Inhibitor. Org. Process Res. Dev. *16*, 447-460.

Sun, Y.-H., Sun, T.-Y., Wu, Y.-D., Zhang, X., and Rao, Y. (2016). A diversity-oriented synthesis of bioactive benzanilides via a regioselective C(sp^2)–H hydroxylation strategy. Chem. Sci. *7*, 2229-2238.

Wang, H., Sun, S., and Cheng, J. (2017). Copper-Catalyzed Arylsulfonylation and Cyclizative Carbonation of N-(Arylsulfonyl)acrylamides Involving Desulfonative Arrangement toward Sulfonated Oxindoles. Org. Lett. *19*, 5844-5847.

Zhang, K., Xu, X., Zheng, J., Yao, H., Huang, Y., and Lin, A. (2017). [3 + 3] Cycloaddition of in Situ Formed Azaoxyallyl Cations with 2-Alkenylindoles: An Approach to Tetrahydro-β-carbolinones. Org. Lett. *19*, 2596-2599.

Deska, J., del Pozo Ochoa, C., and Backvall, J.-E. (2010). Chemoenzymatic Dynamic Kinetic Resolution of Axially Chiral Allenes. Chem. Eur. J. *16*, 4447-4451.

Flahaut, A., Toutah, K., Mangeney, P., Roland, S. (2009). Diethylzinc−Mediated Allylation of Carbonyl Compounds Catalyzed by [(NHC)(PR_3)PdX_2] and [(NHC)Pd(η^3−allyl)Cl] Complexes. Eur. J. Inorg. Chem. *35*, 5422-5432.

Liu, N., Wang, L., and Wang, Z.-X. (2011). Room-temperature Nickel-Catalysed Cross-couplings of Aryl Chlorides with Arylzincs. Chem. Commun. *47*, 1598-1600.

Edwards, G. A., Trafford, M. A., Hamilton, A. E., Buxton, A. M., Bardeaux, M. C., and Chalker, J. M. (2014). Melamine and Melamine-Formaldehyde Polymers as Ligands for Palladium and Application to Suzuki-Miyaura Cross-Coupling Reactions in Sustainable Solvents. J. Org. Chem. *79*, 2094-2104.

Kamio, S., Kageyuki, I., Osaka, I., and Yoshida, H. (2019). Anthranilamide (aam)-Substituted Arylboranes in Direct Carbon–Carbon Bond Forming Reactions. Chem. Commun. *55*, 2624-2627.

Ke, H., Chen, X., and Zou, G. (2014). N-Heterocyclic Carbene-Assisted, Bis(phosphine)nickel-Catalyzed Cross-Couplings of Diarylborinic Acids with Aryl Chlorides, Tosylates, and Sulfamates. J. Org. Chem. *79*, 7132-7140.

Iglesias, M. J., Prieto, A., and Nicasio, M. C. (2012). Kumada-Tamao-Corriu Coupling of Heteroaromatic Chlorides and Aryl Ethers Catalyzed by (IPr)Ni(allyl)Cl. Org. Lett. *14*, 4318-4321.

Zhang, S.-S., Jiang, C.-Y., Wu, J.-Q., Liu, X.-G., Li, Q., Huang, Z.-S., Li, D., and Wang, H. (2015). Cp*Rh(iii) and Cp*Ir(iii)-catalysed Redox-neutral C–H Arylation with Quinone Diazides: Quick and Facile Synthesis of Arylated Phenols. Chem. Commun. *51*, 10240-10243.

Galenko, A. V., Shakirova, F. M., Galenko, E. E., Novikov, M. S., and Khlebnikov, A. F. (2017). Fe(II)/Au(I) Relay Catalyzed Propargylisoxazole to Pyridine Isomerization: Access to 6-Halonicotinates. J. Org. Chem. *82*, 5367-5379.

Voets, M., Antes, I., Scherer, C., Muller-Vieira, U., Biemel, K., Barassin, C., Marchais-Oberwinkler, S., and Hartmann, R. W. (2005). Heteroaryl-substituted Naphthalenes and Structurally Modified Derivatives: Selective Inhibitors of CYP11B2 for the Treatment of Congestive Heart Failure and Myocardial Fibrosis. J. Med. Chem. *48*, 6632-6642.

Jakab, A., Dalicsek, Z., Holczbauer, T., Hamza, A., Papai, I., Finta, Z., Timari, G., and Soos, T. ´(2015). Superstable Palladium(0) Complex as an Air- and Thermostable Catalyst for Suzuki Coupling Reactions. Eur. J. Org. Chem. 60-66.

Wu, K., Huang, Z., Liu, C., Zhang, H., and Lei, A. (2015). Aerobic C–N bond activation: a simple strategy to construct pyridines and quinolines. Chem. Commun. *51*, 2286-2289.

Li, X., Zhang, J., Geng, Y., and Jin, Z. (2013). Nickel-Catalyzed Suzuki-Miyaura Coupling of Heteroaryl Ethers with Arylboronic Acids. J. Org. Chem. *78*, 5078-5084.

Singh, R., Ramesh, U., Huang, J., Issakani, S., Tsvetkov, L., and Petroski, M. (2008). Ubiquitin Ligase Inhibitors. WO 2008115259, Sep 25, 2008.

Wang, M., Yuan, X., Li, H., Ren, L., Sun, Z., Hou, Y., and Chu, W. (2015). Nickel-catalysed Suzuki–Miyaura Cross-coupling Reactions of Aryl Halides with Arylboronic Acids in Ionic Liquids. Catal. Commun. *58*, 154-157.

Bergmann, A. M., Oldham, A. M., You, W., and Brown, M. K. (2018). Copper-catalyzed Cross-coupling of Aryl-, Primary Alkyl-, and Secondary Alkylboranes with Heteroaryl Bromides. Chem. Commun. *54*, 5381-5384.

Li, D., He, X., Xu, C., Huang, F., Liu, N., Shen, D., and Liu, F. (2019). N-Heterocarbene Palladium Complexes with Dianisole Backbones: Synthesis, Structure, and Catalysis. Organometallics *38*, 2539-2552.

Liu, C., Ni, Q., Bao, F., and Qiu, J. (2011). A Simple and Efficient Protocol for a Palladium-Catalyzed Ligand-Free Suzuki Reaction at Room Temperature in Aqueous DMF. Green Chem. *13*, 1260-1266.

Cashion, D. K., Chen, G., Kasi, D., Kolb, C., Liu, C., Sinha, A., Szardenings, A. K., Wang, E., Yu, C., Zhang, W., Gangadharmath, U. B., and Walsh, J. C. (2011). Imaging Agents for Detecting Neurological Disorders. WO 2011119565, Sep 29, 2011.

Clapham, K. M., Batsanov, A. S., Greenwood, R. D. R., Bryce, M. R., Smith, A. E., and Tarbit, B. (2008). Functionalized Heteroarylpyridazines and Pyridazin-3(2H)-one Derivatives via Palladium-Catalyzed Cross-Coupling Methodology. J. Org. Chem. *73*, 2176-2181.

Asghar, S., Tailor, S. B., Elorriaga, D., and Bedford, R. B. (2017). Cobalt-Catalyzed Suzuki Biaryl Coupling of Aryl Halides. Angew. Chem., Int. Ed. *56*, 16367-16370.

Rao, S. N., Reddy, N. N. K., Samanta, S., and Adimurthy, S. (2017). I_2-Catalyzed Oxidative Amidation of Benzyl Amines and Benzyl Cyanides under Mild Conditions. J. Org. Chem. *82*, 13632-13642.

Nordvall, G., and Yngve, U. (2007). Novel quinazolines as 5-ht6 modulators. WO 2007108744, Sep 27, 2007.

Chen, L., Ren, P., and Carrow, B. P. (2016). Tri(1-adamantyl)-phosphine: Expanding the Boundary of Electron-Releasing Character Available to Organophosphorus Compounds. J. Am. Chem. Soc. *138*, 6392-6395.

Chikvaidze, I., Barbakadze, N. N., and Samsoniya, S. A. (2012). Some New Derivatives of 5-Aryl-, 2,5-Diaryl- and 2-Ethoxycarbonyl-5-aryl-indoles. Arkivoc *6*, 143-154.

Melvin, P. R., Nova, A., Balcells, D., Dai, W., Hazari, N., Hruszkewycz, D. P., Shah, H. P., and Tudge, M. T. (2015). Design of a Versatile and Improved Precatalyst Scaffold for Palladium Catalyzed Cross-Coupling: $(\eta^3\text{-1-}t\text{Bu-indenyl})_2(\mu\text{-Cl})_2Pd_2$. ACS Catal. *5*, 3680-3688.